Regulation of TGFβ-superfamily signalling during early embryonic patterning

Bates, Thomas James David

Awarding institution:
King's College London

Regulation of TGFβ-superfamily signalling during early embryonic patterning

Thomas J. D. Bates

MRC Centre for Developmental Neurobiology

King's College London

Thesis submitted for the degree of Doctor of Philosophy (PhD)

September 2012

For Kenneth James Davey

The one person who should have seen this document finished

Abstract

One of the earliest steps in development is the specification of the germ layers, the embryonic subdivision into endoderm, mesoderm and ectoderm. Members of the Transforming Growth Factor β (TGFβ) family are required for endoderm and mesoderm induction, whilst inhibition of this pathway is vital for ectodermal specification. TGFβ inhibitors in the ectodermal region prevent the endoderm and mesoderm inducing signals from acting animally. Coco, an inhibitor of TGFβ, Bone Morphogenetic Protein (BMP) and Wnt signalling, is expressed throughout the animal half of the *Xenopus laevis* embryo up to gastrula stages. Loss-of-function experiments using morpholino oligonucleotides (MO) to Coco investigated whether Coco is required to inhibit these TGFβ ligands from signalling animally. Morphant embryos had clear germ layers defects: a loss of mesoderm and an expansion of endoderm. To investigate whether these defects were caused by an over activation of TGFβ signalling in the animal pole, Coco morphant embryos were coinjected with MOs to candidate TGFβ ligands (Vg1, Activin, Nodal). ActivinMO rescued the Coco knockdown phenotypes demonstrating that, in normal development, Coco prevents Activin signals from acting animally, ensuring correct ectoderm specification.

Coco overexpression induces ectopic heads that contain forebrain and midbrain, due to inhibition of both BMP and Wnt signalling. To investigate whether induction of heads by Coco is mediated via the induction of other factors, epistatic experiments were performed; Coco overexpression was combined with a knock down of BMP inhibitors. A reduction of BMP antagonism led to induction of ectopic heads that lacked anterior tissue, demonstrating a requirement for other BMP inhibitors downstream of Coco. To investigate downstream targets of genes involved in germ layer specification (Coco) and neural induction (Noggin1) a microarray screen was performed. Differences were found between the two signalling molecules confirming their different roles in early embryonic patterning.

Acknowledgements

I would firstly like to thank my first supervisor Dr. Esther Bell, who has offered boundless help, advice and support throughout my PhD. Her help has been invaluable, and I wouldn't have been able to write this thesis without it.

I also need to thank Dr. Clemens Kiecker, my second supervisor. His attention to detail and helpful guidance has, I think, endlessly improved my scientific and writing abilities.

Dr. David Chambers and Dr. Eric Blanc, performed and analysed the microarray section of this thesis, whilst also answering the numerous questions I had, making Chapter 5 possible. I have also received helpful tips during these past few months from Dr. Richard Wingate and Prof. Andrew Lumsden.

Throughout my time in the department I have been lucky to have the support of a great set of colleagues. Liam Henshaw has been a great person to work with in the lab helping with practical issues and offering advice and help when required. I would like to also thank all of the my friends that have made my time here so enjoyable; Megan O'Hare, Öniz Suleyman, Leigh Wilson, Mary Green, Kate Sellers, Ellen Robertshaw, Florent Campo-Paysaa, Peter Levy, Emma Broom, Mark Evans and Ali Walker. It is important to also mention some of the 'best' Post-docs in the department, Tom Butts, Sam Barnes, Paul Hunter and Phil Suetterlin.

Lastly, I would like to thank my parents for their support and allowing me to move home to write up, and importantly my girlfriend Carly who has been there for me throughout my writing up period and always offered a relaxing environment for me to forget about my thesis.

This work was funded by a studentship provided by the MRC.

Table of Contents

Table of Figures

Table of Tables

Chapter 1 Introduction

One of the most important aspects of developmental biology is the production of the correct cells in appropriate positions in the embryo. An example of this in vertebrates is germ layer specification, the correct organization of the three germ layers, tissues that give rise to all mature embryonic parts. The endoderm forms the gut and associated organs; the mesoderm becomes skeletal muscle, cardiac muscle, bone and blood and the ectoderm forms the skin, brain and spinal cord. Much is known about the factors involved in formation of the endoderm and mesoderm, however less is known about the specification of ectoderm.

1.1 Early divisions and fate maps

The early cleavages, or early cell divisions, during *Xenopus laevis* (African claw-toed frog) development are important for correct patterning at later stages. The fertilized egg usually divides for the first time about 1.5 hours after fertilisation; with the egg being split bilaterally and having an animal (top) to vegetal (bottom) axis. The subsequent twelve cleavages occur in concert every 20-30 minutes. The second division is a perpendicular cleavage that leads to a 4-cell embryo in which, for the first time, the darker pigmented ventral blastomeres allow the dorsal (future back) to ventral (future belly) axis to be seen. Three further divisions produce a 32-cell embryo with 4 tiers of 8 cells.

The specification of germ layers is the subdivision of the embryo into ectoderm, mesoderm and endoderm, and lineage-tracing studies have shown that at the 32-cell stage cells are loosely spatially linked to their future germ layer fate because of the signals they will receive. During the next 7 divisions that take the 32-cell stage up to a ≈4000 cell embryo, there are no major visible changes in embryo shape. However, a cavity called the blastocoel forms in the animal portion of the embryo that separates cells of the animal pole from those of the vegetal mass. At blastula stage there is a stringent fate map for the three germ layers (Figure 1.1).

When looking at a cross section, the cells from the animal pole become the ectoderm, which gives rise to epidermis ventrally (light blue) and neural tissue dorsally (dark blue), whilst the vegetal pole forms the endoderm (yellow). The mesoderm arises from the marginal zone (red). The epidermis forms the skin, whilst neural tissue becomes the central and peripheral nervous systems. The endoderm becomes the gut and associated organs, whilst the mesoderm becomes skeletal muscle, cardiac muscle and blood.

During later stages of development two other axes become morphologically relevant. The anterior-posterior axis describes the embryo in relation to the head and tail. The medio-lateral axis describes structures at, or away from the midline. Figure 1.2 summarises the different axes that are relevant for *Xenopus* development and how they are used.

1.2 Factors involved in the formation of the dorso-ventral axis, preceding germ layer specification

Maternal signalling that contributes to the specification of the future dorsal side of the embryo precedes the inductive processes involved in the formation of the germ layers. Cellular rearrangements occur as soon as embryogenesis has begun. When the sperm fertilizes the egg, a combination of microtubule rearrangement and cytoplasmic movement moves vegetally localized molecules towards the future dorsal side. One of the maternal pathways involved in specification of dorsal tissue is the Wnt signalling pathway. Wnts are secreted lipid-modified proteins that can induce cell fate changes by binding to receptors on target cells, resulting in the activation of an intracellular signalling cascade.

The first suggestion of an involvement for Wnt signalling in dorsal specification came from overexpression studies, where ventral injection of either Wnt1 or Xwnt8 mRNAs induced complete secondary body axes (Sokol et al., 1991). The Wnt intracellular component β-Catenin and downstream factors Lef/Tcf were

Figure 1.1 – Fate map of a blastula *Xenopus laevis* embryo. A diagrammatic representation of a sectioned blastula embryo, orientated with animal up, vegetal down, dorsal right and ventral left. Cells in the dorsal portion of the animal pole give rise to the neural plate (dark blue), whilst those more ventrally give rise to the epidermis (light blue). Cells from the marginal zone give rise to the mesoderm (red) and the most vegetal cells form the endoderm (yellow) of the embryo. Light blue = epidermis, Dark blue = neural plate, red = mesoderm and yellow = endoderm.

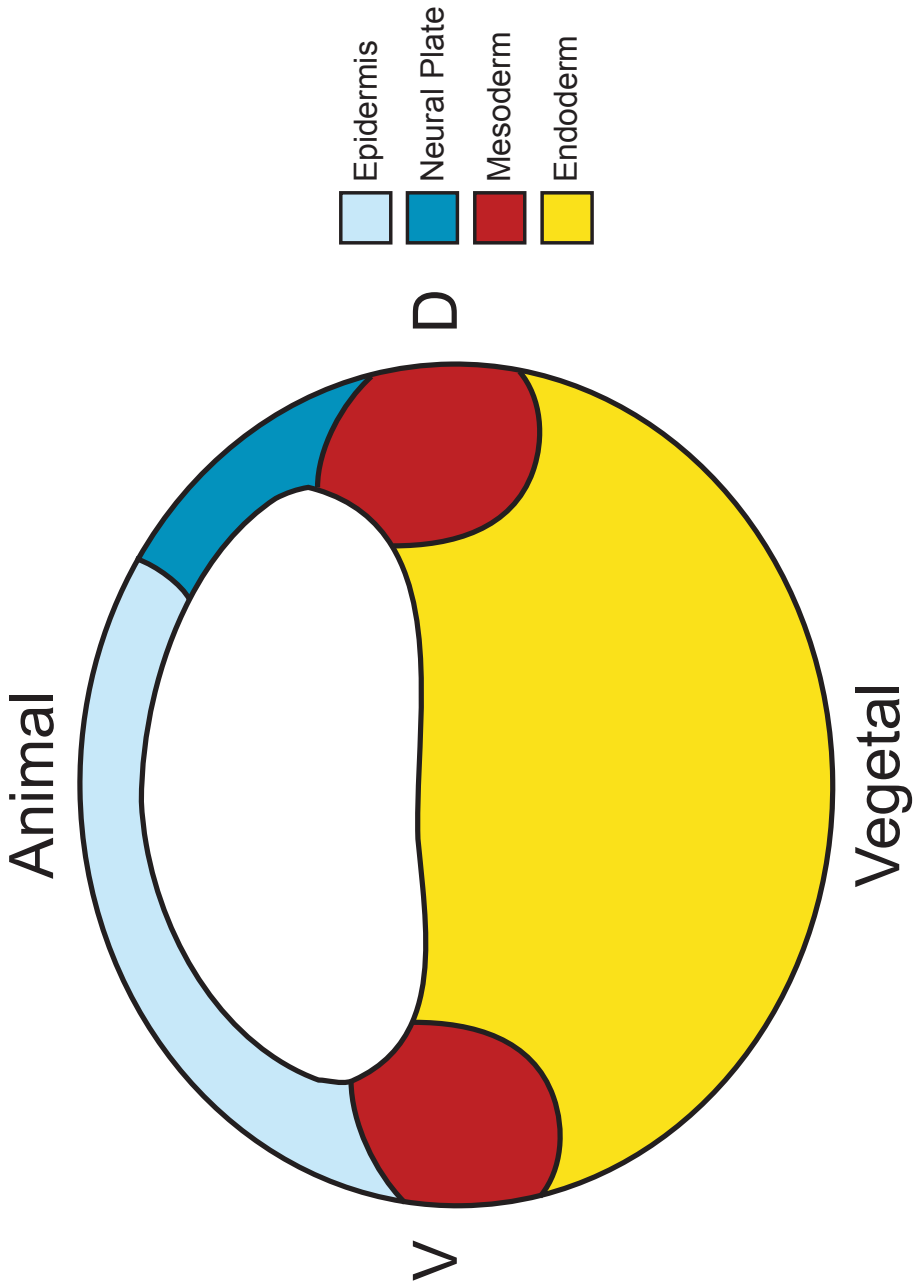

Figure 1.1 - Fate map of a blastula *Xenopus laevis* embryo

Figure 1.2 – Axes used to describe Xenopus development. A) 4-cell *Xenopus laevis* embryo, which has an animal (top) to vegetal (bottom) axis, and a dorsal (back) to ventral (front) axis. B) Neurula and tailbuds have an anterior (head) to posterior (end of tail) axis and also a dorsal (back) to ventral (front) axis. C) When looking dorsally, they also have medial (midline) to lateral (away from midline) axes.

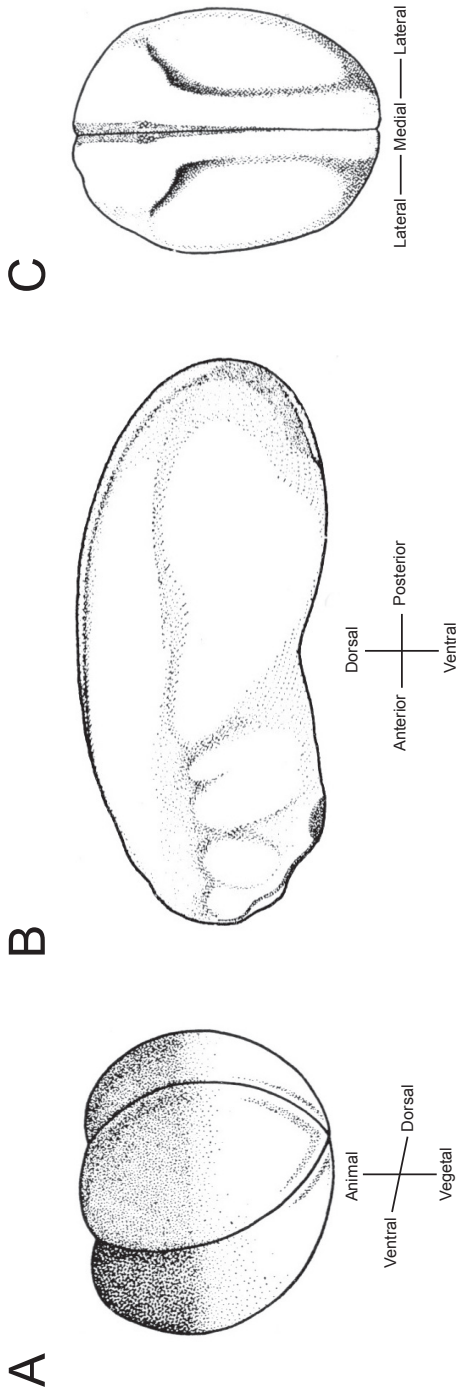

Figure 1.2 - Axes used to describe Xenopus development

also implicated in dorsal development, following loss of function studies (Heasman et al., 2000; Molenaar et al., 1996; Larabell et al., 1997).

Neither *Wnt1* nor *Wnt8* are expressed early enough to be involved in the early specification of the dorsal-ventral axis (Christian et al., 1991), however three lines of evidence supported a requirement for Wnt11 in this process. Firstly, *Wnt11* is expressed maternally, with a dorsal bias at 8-cell stage. Secondly, Wnt11 is required for the expression of other dorsally enriched genes, and thirdly, overexpression of Wnt11 caused dorsalization (Tao et al., 2005).
It was later shown that Wnt5a is also involved in dorsal specification, with evidence showing that Wnt5a and Wnt11 work together to activate the Wnt pathway (Cha et al., 2008; Cha et al., 2009).

1.3 Germ layer specification

The specification of the germ layers, the subdivision of the embryo into ectoderm, mesoderm and endoderm, has occurred by the late blastula stage (preceding gastrulation). It is a process that involves multiple inductive factors and is vital for correct axial development.

The transcription factor Veg-T (Zhang et al., 1998), the TGFβ ligands Vg1 (Joseph and Melton, 1998) and the Nodal-related genes Xnr1, Xnr2, Xnr5 and Xnr6, (Yasuo and Lemaire, 1999; Luxardi et al., 2010) are all involved in aspects of both endoderm and mesoderm formation. These factors, and their roles will be introduced in relevance to both processes.

1.3.1 Endoderm formation

The endodermal cells become the gut and associated organs of the embryo and are found in the vegetal portion of the early frog embryo, the factors involved will be introduced here (Figure 1.3).

Figure 1.3 - Endodermal gene network. Veg-T sits at the top of the endodermal hierarchy and induces *Sox7*. Sox7 and Vg1 are involved in the induction of maternal *Xnr5* and *Xnr6*. Sox7 also thought to play a role in inhibiting Sox3 negative regulation of *Xnr5*. Veg-T, Xnr5 and Xnr6 contribute to the induction of *Xnr1* and *Xnr2*, and zygotic expression of *Xnr5* and *Xnr6*. Veg-T and zygotic Xnr activity induces the *Mix* family of transcription factors. Zygotic Xnr activity also induces *GATA* binding proteins. *Sox17* genes are induced by a combination of Veg-T, Mix genes and GATA proteins. Sox17 and Activin induce early endodermal markers. *Sox17* genes induce late endodermal markers.

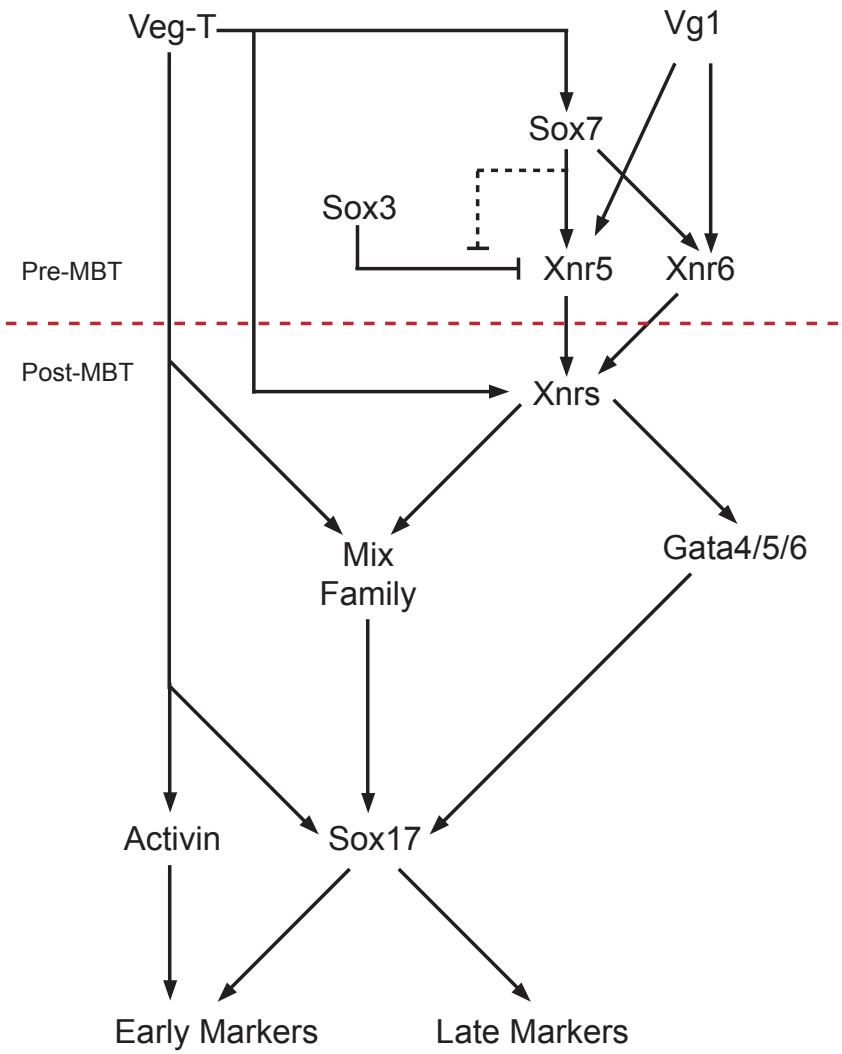

Figure 1.3 - Endodermal gene network

Veg-T, a transcription factor vital for mesoderm and endoderm formation (Zhang et al., 1998), is present maternally. Transcripts are localized at the vegetal pole of the *Xenopus* oocyte and, following fertilisation, *Veg-T* mRNA diffuses throughout the vegetal portion of the one-cell embryo. Importantly for correct specification of the germ layers, the horizontal third cell division ensures that *Veg-T* transcripts remain in the vegetal portion of the embryo. It is these vegetal cells that will become, the future endodermal cells of the embryo.

Nodal signalling is vital for endoderm formation in *Xenopus*, fish and mouse (Kimelman, 2006; Shen, 2007). Five of the six Nodal-related genes are involved in *Xenopus* endoderm and mesoderm development (Xnr1, -2, -4, -5, -6); Xnr5, Xnr6, Xnr1 and Xnr2 are involved in endoderm specification and gastrulation movements later in development (Yasuo and Lemaire, 1999; Luxardi et al., 2010).

Sox7 is one of the earliest targets of Veg-T, within the vegetal region of the embryo. Sox7 was shown to induce endodermal markers in whole embryos and in ectodermal explants when overexpressed, and is thought to mediate the Veg-T activation of endodermal differentiation. Sox7 facilitates the induction of *Xnr5* and *Xnr6* by Veg-T, but is also thought to inhibit the inhibitory effects of Sox3 on Xnr5 (Zhang, 2003; Zhang et al., 2005).

Before the onset of zygotic transcription (mid-blastula transition – MBT), Veg-T has been shown to induce the TGFβ factors *Xnr5* and *Xnr6* in the dorsal portion of the vegetal pole, with their pre-MBT expression being dependent on the presence of β-Catenin (Takahashi et al., 2000; Yang et al., 2002). Xnr5 and Xnr6 act redundantly to induce endoderm and mesoderm formation, with both pharmacological inhibition (of the ALK4/5/7 receptors prior to MBT) and morpholino knockdown causing drastic loss of markers for both tissue types (Luxardi et al., 2010).

Following the initiation of zygotic transcription at MBT, Veg-T further induces *Xnr5* and *Xnr6* throughout the vegetal zone, leading to a dorsal-ventral gradient of expression of these molecules. Veg-T in concert with Vg1, a maternal vegetally localized TGFβ ligand, induces the *Xenopus* Nodal-related genes *Xnr1* and *Xnr2*, genes involved in the determination of endodermal cell fate (Yasuo and Lemaire, 1999). In addition, Xnr5 and Xnr6, increase the levels of *Xnr1* and *Xnr2*, whilst also inducing *Xnr4* (Zhang et al., 1998; Sun et al., 1999).

Other important factors for endoderm specification are members of the Mix family (homeodomain transcription factors) and the GATA DNA binding proteins (zinc finger transcription factors). These genes are induced by Veg-T and Xnr signals, and act upstream of Sox17α/β, SRY (sex determining region Y) HMG-box transcription factors involved in endodermal development (Hudson et al., 1997; Sinner, 2006). Ectopic expression of the Mix family members *Mixer*, *Milk*, *Bix1*, *Bix4* and the GATA DNA binding proteins *GATA4/6* was shown to induce endodermal differentiation in animal caps (Ecochard et al., 1998; Tada et al., 1998; Henry and Melton, 1998; Casey et al., 1999; Weber et al., 2000). Their importance was confirmed with loss of function experiments that showed that Mixer and GATA4/6 were vital for the expression of endodermal markers (Henry and Melton, 1998; Kofron, 2004; Afouda, 2005).

Mix1 can induce ectopic expression of the endodermal markers in animal caps when cooperating with Siamois, a downstream Wnt target (Carnac et al., 1996). Additionally, when activity of Mix1 was reduced with an engrailed repressor form (inhibits the endogenous protein), there was a reduction in endodermal differentiation (Lemaire et al., 1998). Mixer is able to impose endodermal fate when overexpressed, whilst loss of function with a DN (dominant negative) form caused disruptions to endodermal formation and the expression of the downstream endodermal effectors *Sox17α/β* (Henry and Melton, 1998). Bix1, a target of Veg-T, caused the induction of endoderm when overexpressed at high levels (Tada et al., 1998). The closely related Bix4, another direct target of Veg-T, has the ability to rescue the expression of endodermal markers, in embryos with depleted Veg-T levels. Interestingly, Bix4 cannot restore the ability for the

cells to induce mesoderm, demonstrating a specific role in endoderm formation downstream of Veg-T (Casey et al., 1999). *Milk* is expressed in the prospective endoderm, and promotes endoderm at the expense of mesoderm. Overexpression of Milk in the marginal zone, blocked mesodermal cell involution and repressed expression of the mesodermal markers *Xbra* and *Gsc*. Expression of the endodermal marker *Endodermin* was increased, whilst Milk can also induce ectopic expression of endodermal markers in the animal region (Ecochard et al., 1998). Three zygotically expressed GATA DNA binding proteins (*GATA4, GATA5 and GATA6*) are also required for endoderm development; all three are able to induce endodermal markers in animal caps. It is thought that GATA6 is the predominant factor for maintaining endodermal gene expression, as it is a direct activator of *Sox17α* and *HNF3β*. GATA5 plays a later role in the formation of the developing gut and liver (Afouda, 2005).

Downstream of the Mix family and GATA binding proteins are Sox17α and Sox17β, transcription factors that have been shown to be required for endodermal development (Hudson et al., 1997) and are the only endodermal specific factors, induced by Veg-T, that are expressed pan-endodermally. In animal cap assays Sox17α and Sox17β were shown to induce both of the early endodermal markers *Endodermin* (Sasai et al., 1996) and *HNF1β* (Demartis et al., 1994), and there was also evidence that Sox17α and Sox17β were required for later endodermal development with the induction of the late endodermal markers *IFABP*, Intestinal Fatty Acid Binding Protein, (Shi and Hayes, 1994) and *Xlhbox8* (Wright et al., 1989). Importantly, neither Sox17α nor Sox17β are able to induce neural or mesodermal tissue. A dominant negative form of Sox17β inhibited Activin mediated induction of endodermal markers and confirmed that the factors were both necessary and sufficient for endodermal development (Hudson et al., 1997).

Activin, originally isolated from mammalian gonadal fluid as a stimulator of pituitary FSH (Follicle Stimulating Hormone) release (Vale et al., 1986), is a TGFβ ligand important for the induction of endoderm. Purified Activin was shown to be able to induce endodermal markers in *Xenopus* animal cap assays

(Jones et al., 1993; Ninomiya et al., 1999). In vitro studies have also shown that Activin is required for endodermal differentiation. Differentiation of endodermal cells was seen following Activin treatment of mouse embryonic stem cells (mESCs) (Kubo, 2004; Yasunaga et al., 2005; Gadue et al., 2006). In addition Activin caused the endodermal differentiation of human embryonic stem cells (hESCs) (D'Amour et al., 2006). However, having confirmed that Activin induced endodermal differentiation, it was shown that Activin and another TGFβ family member Bone Morphogenetic Protein 4 (BMP4) act synergistically when causing endodermal differentiation in hESCs (Teo et al., 2012).

1.3.2 3 steps of mesoderm formation

The mesodermal tissue is found in the marginal zone of blastula stage *Xenopus laevis* embryos and is induced by vegetal cells. Induction of mesodermal tissue is thought to occur in three steps (Figure 1.4): firstly all vegetal cells produce a general mesoderm inducing signal (arrows, Fig 1.4A), then whilst this general signal continues (grey arrows, Fig 1.4B), a second signal is derived from the dorso-vegetal cells (Nieuwkoop Centre) to induce the organizer (black arrows, Fig 1.4B). Lastly, opposing dorsal (Spemann Organizer) and ventral signals pattern the marginal zones (Fig 1.4C). These signalling centres will be introduced throughout this section (Figure 1.5).

1.3.2.1 First step of mesoderm induction: Vegetal mesoderm-inducing signal

The first step in mesoderm induction involves a general vegetal signal. The two main factors involved are the vegetally localized transcription factor Veg-T and the TGFβ ligand Vg1. Veg-T has been shown to induce mesodermal markers in cells that would normally become ectoderm (Stennard et al., 1996; Zhang and King, 1996) and importantly a DN version of Veg-T inhibits mesoderm induction (Horb and Thomsen, 1997), presumably because Veg-T is required by the vegetal cells in order for them to induce mesoderm. The maternally expressed, vegetally localized Vg1 is inherited by the vegetal most cells

Figure 1.4 - 3 steps of mesoderm formation. A) At early blastula stages pan-vegetal signals act as general mesoderm inducers. B) At later blastula stages, whilst general mesoderm signal continue, there is a dorsal mesoderm inducer from the Neiuwkoop centre. C) Lastly the marginzal zone acquires pattern from opposing dorsal and ventral inducing signals, causing two differing and opposing gradients (shaded areas). In all panels arrows indicate signals.

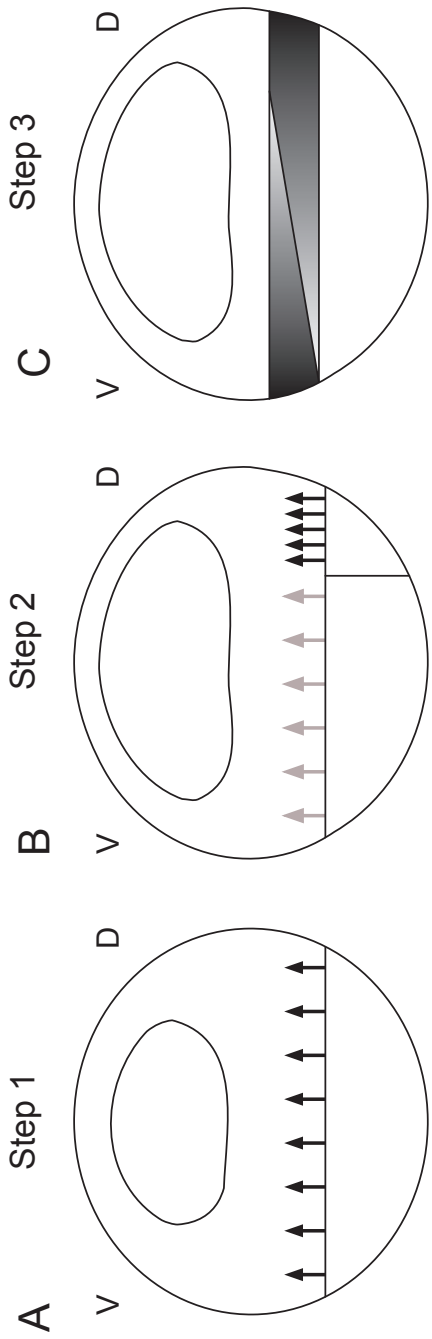

Figure 1.4 - 3 steps of mesoderm formation

Figure 1.5 – Mesodermal gene network. Veg-T sits at the top of the mesodermal hierarchy and induces *Vg1* and the *Xnr* genes. Vg1 is also involved in induction of Nodal related signals. On the dorsal side of the embryo a combination of Veg-T, Vg1 and β-Catenin leads to high levels of Nodal-related signals. On the ventral side of the embryo Veg-T and Vg1 induce lower levels of Nodal-related signals. In the dorsal half of the marginal zone high levels of *Activin* are induced and in turn induce dorsal mesoderm markers. In the ventral part of the marginal zone lower levels of Activin and high levels of Bmp4 and Xwnt8 induce ventral mesoderm. Expression of *Xbra* and *Fgf* occurs as a consequence of mesoderm induction.

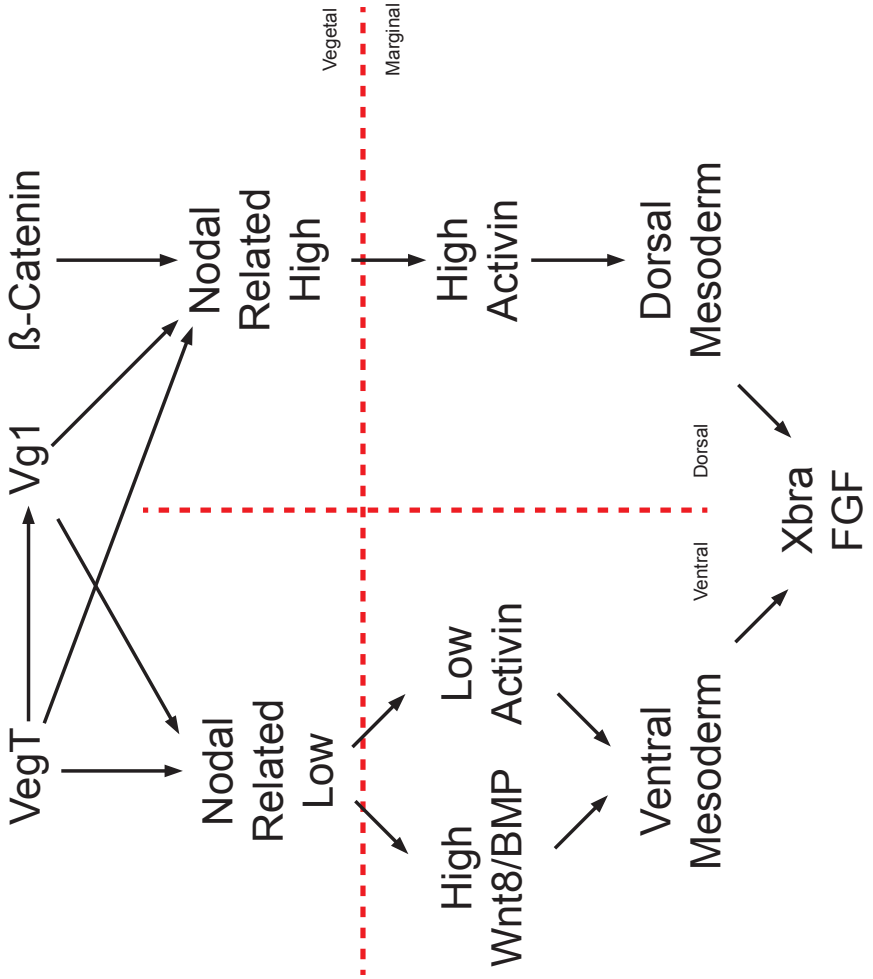

Figure 1.5 - Mesodermal gene network

(Rebagliati et al., 1985). Its vegetal localization and the ability to induce *Xnr* genes confirm that Vg1 can act as a vegetal signal working with Veg-T to start general mesoderm induction (Birsoy, 2006). Veg-T is required as a vegetal inducer of mesoderm development. Importantly, Veg-T is able to distinguish endoderm and mesoderm specification, by varying not only its downstream targets, but also by altering the levels of them. For example, a target of Veg-T, Bix1, induces endodermal markers at high levels, whilst it induces mesodermal markers at lower levels (Tada et al., 1998). However, Bix4, a member of the Mix family of endodermal transcription factors, is able to rescue the expression of endodermal genes in embryos where Veg-T is depleted, but is unable to rescue Veg-T's ability to induce mesoderm (Casey et al., 1999).

1.3.2.2 Second step in mesoderm formation: Nieuwkoop Centre

The second step in mesoderm induction is the formation of a dorsalizing signal that will induce the Spemann organizer in overlying mesodermally fated tissue. The Nieuwkoop centre is a group of dorso-vegetal cells, defined as those producing both mesoderm-inducing and dorsalizing signals. When transplanted ventrally, Nieuwkoop centre transplants induce an embryonic axis containing dorsal mesoderm, while retaining their endodermal fate. The cells are therefore inducing an organizer in adjacent mesoderm-fated host cells (Gimlich and Gerhart, 1984).

The TGFβ ligand Vg1 is not only involved in mesoderm induction, but has also been linked to a role in the formation of the Nieuwkoop centre. When high levels of Vg1 are used in gain of function studies, dorsal mesoderm is induced (Thomsen and Melton, 1993), whilst depletion of Vg1 using a DN form of the ligand blocked dorsal mesoderm formation (Joseph and Melton, 1998). Morpholino knock down further confirmed a requirement for Vg1 as part of the Nieuwkoop centre, with loss of function reducing the expression of organizer genes (Birsoy, 2006).

The maternal Wnt pathway has also been linked to the Nieuwkoop centre. It was shown that vegetal explants require Wnt signalling to be able to induce dorsal mesodermal markers in Nieuwkoop conjugates (Wylie et al., 1996) and that injection of Wnt mRNA could induce a secondary axis; presumably inducing an organizer (Sokol et al., 1991). However, Wnt loss of function does not block the induction of dorsal mesoderm markers in animal caps (Wylie et al., 1996). It is likely that Wnt signalling plays a role in regulation of the Nieuwkoop signal by allowing nuclear accumulation of β-Catenin and therefore the activation of downstream signals required for dorsal development.

As described, the Nodal-related genes play a vital role in endoderm specification in *Xenopus*, but are also required for different aspects of mesoderm development. In mice, the Nodal gene is a dose-dependent inducer of axial muscle (Jones et al., 1995).

Xnr5 and Xnr6 are important for initial mesoderm induction, and are the earliest expressed Nodal-related genes (Takahashi et al., 2000). A dorso-ventrally biased expression pattern in the marginal zone highlighted Xnr5 and Xnr6 as factors that could be involved in not only inducing mesoderm, but also in producing the Nieuwkoop centre (Takahashi et al., 2000). Combinatorial morpholino knockdown of Xnr5 and Xnr6 (to overcome the genes acting redundantly) caused a drastic reduction in expression of the mesoderm marker *Xbra* (Luxardi et al., 2010). As the maternally expressed *Xnr5/6* levels reduce towards gastrula stages, the zygotic *Xnr1* and *Xnr2* become expressed in circumblastoporal tissue (Jones et al., 1995; Takahashi et al., 2000), and Xnr1 is able to rescue the mesoderm-inducing ability of Veg-T depleted vegetal masses (Kofron et al., 1999). Xnr1/2 are required for convergent-extension, the migration of rostral mesoderm and the activation of movement effector genes (Luxardi et al., 2010). The other Nodal-related signal involved in mesoderm formation, *Xnr4*, is expressed in the Spemann organizer, and later in the notochord, and is thought to play a maintenance role in Nodal-related signalling (Joseph, 1997).

1.3.2.3 Step 3 of mesoderm formation: Dorsal patterning

During mesoderm induction, there are different markers expressed along the dorso-ventral axis, and Activin signalling has been shown to be important for this. A huge amount of work was performed to investigate the role Activin plays in mesoderm induction.

In 1987, a potent mesoderm-inducing factor (MIF) was purified from a Xenopus cell line (Cooke et al., 1987). Ectodermal explants cultured in MIF formed mesoderm and injection of MIF into the blastocoel caused the entire blastocoel roof, normally fated to become epidermis, to become mesodermal (Cooke et al., 1987; Green and Smith, 1990). Further extensive work confirmed that the mesoderm-inducing factor XTC-MIF was in fact Activin (Albano et al., 1990).

The expression of *Activin* was first analysed by real-time (RT) PCR. mRNA transcripts of *Activin* were shown to be present in the unfertilized egg and at blastula stages (Thomsen et al., 1990; Asashima et al., 1991). Remarkably, the Xenopus egg extract has mesoderm inducing ability (Asashima et al., 1991). However, only at neurula stages were *Activin* levels detectable by ISH (Dohrmann et al., 1993). Two reports from 1991 investigated the role of Activin receptors. ActR2 was cloned from a mouse cell line, and when the cDNA was expressed in cell culture it caused high affinity Activin binding (Mathews, 1991). In addition, XAR7, a *Xenopus* Activin receptor was also cloned and mRNA was expressed, like Activin, in the unfertilized egg and throughout subsequent development up until blastula stages (Kondo et al., 1991).

Induction by Activin was shown to involve threshold limits that led to the induction of different cell types at different concentrations (Thomsen et al., 1990; Green et al., 1992). The highest levels of Activin induced endoderm, whilst intermediate levels induce dorsal mesoderm, with the lowest levels inducing ventral mesoderm; epidermis forms in the absence of Activin (Thomsen et al., 1990; Green et al., 1992; Faure et al., 2000). In addition, overexpression of a truncated Activin receptor, acting as a dominant negative, inhibited the elongation of animal caps by Activin, also preventing the induction of the dorsal,

and pan-mesodermal markers *Xbra* and *Gsc* (Hemmati-Brivanlou et al., 1992). A role for Activin in specifying dorsal mesodermal fate was confirmed with the cell autonomous induction of the dorsally expressed organizer genes *Gsc* and *Noggin* (Green et al., 1994).

With the highest mesoderm-inducing concentration of Activin leading to dorsal fate and lower concentrations inducing ventral mesoderm, it was thought that a dorso-ventral gradient of Activin could be the basis of mesoderm patterning. Two reports – one biochemical, one immunohistolgical – addressed this and both showed that there are higher levels of Activin/TGFβ signalling on the dorsal side at the time of mesoderm induction (Faure et al., 2000; Schohl and Fagotto, 2002). Differing concentrations of an *Activin* morpholino caused a concentration dependent disruption to mesoderm formation and reduced the expression of other mesoderm inducing factors, further confirming the major role Activin plays in mesoderm induction and patterning (Piepenburg, 2004).

1.3.2.4 Step 3 of mesoderm formation: Ventral patterning

Patterning of the mesoderm in the marginal zone involves a dorsal specifier, and the same is true for ventral patterning.

Work using a truncated BMP receptor (*tBR*) showed that a lack of BMP signal converts ventral mesoderm to a dorsal fate (Graff et al., 1994), suggesting that ventral tissue specification also requires an active signal, and that it is not the default state for mesoderm. Since then, both Wnt and BMP signalling have been implicated in ventro-lateral mesoderm formation.

The BMP ligands *Bmp2* and *Bmp4* both have maternal transcripts, and whilst *Bmp2* is expressed zygotically throughout the ectoderm and mesoderm, *Bmp4* expression is restricted to the ventro-lateral marginal zone during gastrulation (Brivanlou, 1995). Both ligands were shown to induce *Xhox3*, an early ventro-lateral mesoderm marker. In addition, Bmp4 is able to ventralize the dorsal marginal zone when overexpressed, inhibiting the dorsal mesoderm marker *Gsc*

(Brivanlou, 1995). In later work, it was shown that heterodimers between Bmp4/7 directly induce ventral mesoderm, however Bmp2 and Bmp4 homodimers were unable to induce mesoderm alone, instead acting to ventralize Activin-induced mesoderm (Nishimatsu and Thomsen, 1998). Bmp2/4 was also shown to positively regulate ventrally expressed genes such as *Xvent1* (V Gawantka, 1995).

Wnt8 is expressed zygotically in the ventro-lateral mesoderm, a pattern that suggested a role for Wnt signalling in ventro-lateral mesoderm specification (Christian et al., 1991). Loss of function studies using a DNWnt8 ligand (that inhibits the response to Wnt signalling) caused the inhibition of the ventral mesoderm markers *XMyoD* and *Xpost* (Hoppler et al., 1996). *Wnt8* expression is regulated by Bmp2/4, confirming that BMP and Wnt signalling work together to specify ventral fate, whilst additionally inhibiting dorsal mesoderm development. Misexpression of Wnt8 in the dorsal marginal zone inhibits the expression of the notochord marker *Xnot*, causing a replacement of notochord by somitic muscle. In addition, Wnt8 was shown to positively regulate the expression of *MyoD*, a lateral mesoderm marker, highlighting a role for Wnt8 in patterning the dorsal mesoderm remotely via control of downstream targets (Hoppler and Moon, 1998). More recently, it was shown that the downstream Wnt activator Lef1 was required for ventral specification, with DNLef overexpression interfering with normal ventral and axial development (Roël et al., 2002).

These results suggest that BMP signalling actively promotes ventral fate, in cooperation with zygotic Wnt signalling. BMP signalling can also act to inhibit dorsal fate, with Wnt signalling playing a remote role in patterning of dorso-lateral mesoderm.

1.3.2.5 Genes required for mesoderm maintenance

Fibroblast Growth Factor (FGF) signalling (including intracellular activators) is required for Activin-induced ventral mesoderm (Cornell and Kimelman, 1994; LaBonne and Whitman, 1994). A dominant negative FGF receptor, which

inhibits mesoderm induction by FGF, causes defects in gastrulation and posterior development (Amaya et al., 1991). In accordance with this, FGF signalling is required throughout gastrulation, a time after mesoderm induction has occurred (Kroll and Amaya, 1996).

One of the targets of FGF signalling during mesoderm formation is Xbra, the *Xenopus* homologue of the mouse Brachyury gene (Smith et al., 1991). Brachyury is required for mesoderm formation in mouse, with loss of function causing gastrulation defects due to insufficient mesoderm cell numbers (Wilkinson et al., 1990). *Xbra* is expressed in the mesodermal cells, during *Xenopus* development (Smith et al., 1991). Disruption of *Xbra* expression can cause defects of gastrulation and mesodermal patterning, highlighting an important role after mesoderm induction. (Conlon et al., 1996).

1.3.2.6 Spatial organisation of the factors involved in endoderm and mesoderm formation

The formation of endoderm and mesoderm, as described requires many factors with overlapping functions (Figure 1.6). During this chapter these processes were introduced as distinct occurrences, whilst shared factors suggest that these processes happen in concert.

At the earliest stages, maternal signalling pathways initiate the dorso-ventral axis, endoderm formation and mesoderm induction. Maternal Veg-T signals induce maternal *Xnr* signalling that is involved in a vegetal mesoderm-inducing signal and initiation of downstream endodermal signalling. An overlap of dorsally localized β-Catenin, Vg1 and Xnr genes mark the site of the Nieuwkoop, a dorsal mesoderm-inducing signal (Figure 1.6A).

At later stages zygotically expressed factors are involved. Maternal Veg-T and Xnr signals have induced downstream members of the *Mix* and *GATA* families of transcription factors. In addition, Activin that has a dorso-ventral gradient, acts

Figure 1.6 - Schematic of factors involved in the formation of endoderm and induction of mesoderm. A) Zygotic *Veg-T*, *Vg1*, *Xnr* and *Wnt* signalling is involved in endoderm formation and in both global and dorsal mesoderm induction. Following the initiation of zygotic transcription, vegetal *Mix* and *GATA* transcription factors are involved in endoderm specification, whilst dorsal *Activin* signalling and ventral *Bmp*/*Wnt* signalling patterns the mesoderm in the marginal zone.

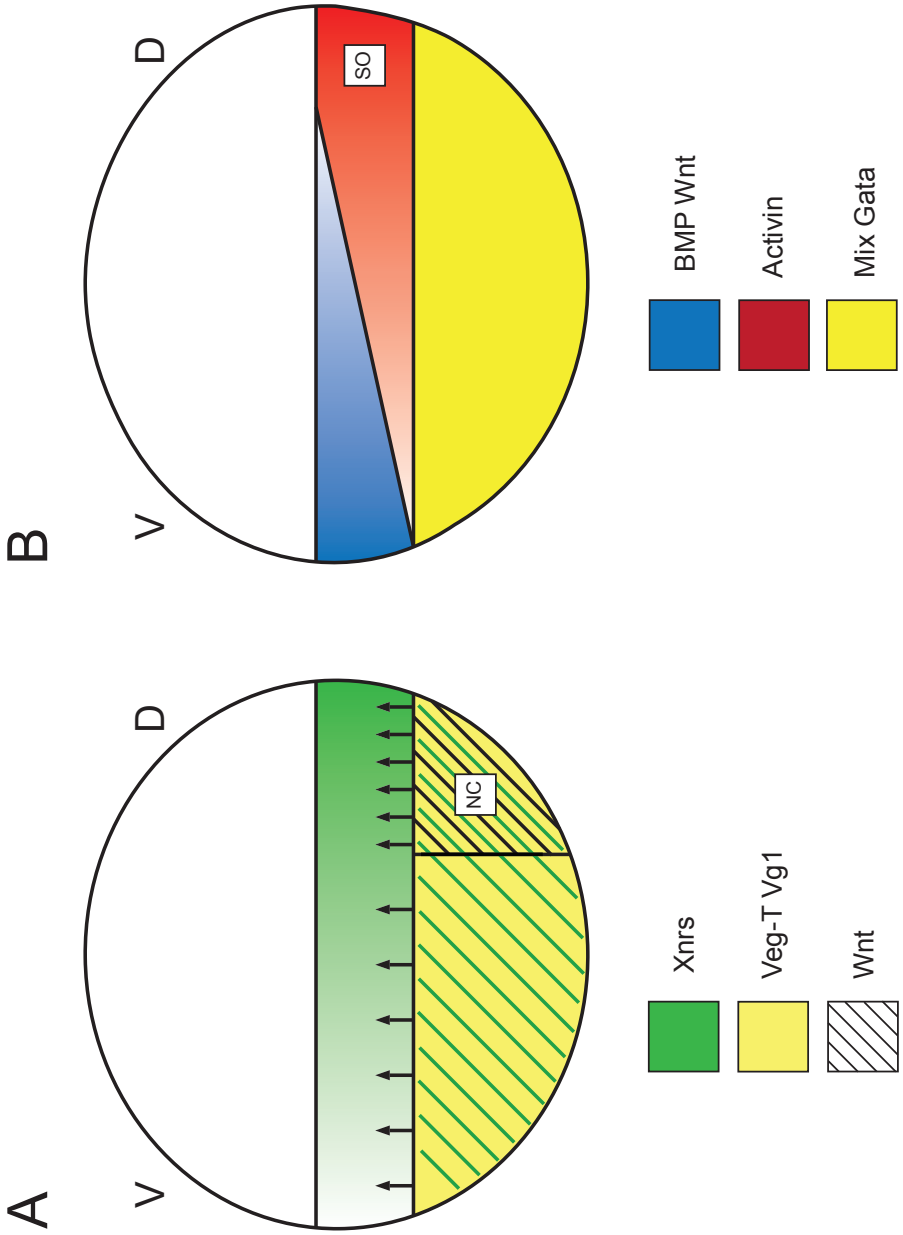

Figure 1.6 - Schematic of factors involved in the formation of endoderm and the induction of mesoderm

as a dorsal mesoderm-patterning signal, while BMP and Wnt signalling promote ventral fates (Figure 1.6B).

1.3.3 Ectoderm specification

The third germ layer, the ectoderm, arises from the animal most cells in the *Xenopus* blastula. It was originally thought that ectoderm might be a default state that does not receive any inductive signalling, however, studies into Veg-T have suggested otherwise. A depletion of Veg-T caused ectodermal markers to be expressed in the marginal zone (Zhang and King, 1996) suggesting that there is an animal 'ectoderm inducing' signal. Animally expressed factors have been described that both impose and protect ectodermal fate. Xema, the most important of these, is a transcription factor involved in both specifying and protecting ectodermal fate (Suri, 2005; Mir et al., 2007; Mir et al., 2008). Ectodermin, an inhibitor of TGFβ signalling, acts to inhibit mesoderm-inducing signals from the marginal zone (Dupont et al., 2005). Lastly, Norrin, a recently discovered BMP/TGFβ inhibitor and Wnt agonist, also inhibits mesoderm-inducing signals from the marginal zone but additionally plays a role in the specification of the neurectoderm (Xu et al., 2012).

Xema (*Xenopus* Ectodermally-Expressed Mesendoderm Antagonist) is a member of the Foxi family of transcription factors that is expressed zygotically in the animal region of blastula and gastrula *Xenopus* embryos (Suri, 2005). Further investigation into its expression pattern showed it to be very dynamic: expression begins dorsally at early blastula stage and then becomes expressed throughout the animal region by mid-blastula. In addition, expression is mosaic at all stages (Mir et al., 2008). One important aspect of ectoderm development is the inhibition of mesoderm inducing signal from the marginal zone, and Xema was shown to inhibit both Nodal-related and FGF mesoderm signals. Overexpression of Xema inhibited mesoderm formation, whilst MO knockdown stimulated ectopic expression of the mesodermal markers *Xbra*, *xWnt8* and *Chordin* and the endodermal marker *Sox17β* in the ectoderm (Suri, 2005). Although shown to be important for the inhibition of mesodermal fate in the animal pole, Xema plays a more significant, vital role in ectodermal specification. *Xema* is upregulated in

Veg-T depleted caps, suggesting a mutual repression between animal and vegetal determinants, and has been shown to be an activator of ectodermal differentiation. Xema overexpression in vegetal cells caused the induction of both ectodermal and epidermal markers, whilst repressing *Sox17α* and *Endodermin* expression. In addition XemaMO injections caused a reduction of ectodermal marker and problems with cell adhesion in the animal pole. In summary, Xema is the first gene that has been shown to play a role in specification of ectodermal fate and inhibition of mesoderm inducing signals from the marginal zone (Mir et al., 2007). *Xema*'s zygotic expression implied the requirement of a maternal activator whose identity was, until recently, unknown. *Foxi2* is a maternal animally expressed factor that acts as an upstream activator of Xema (Pohl et al., 2005; Cha et al., 2012). Foxi2 acts specifically as an activator of ectodermal specification, as cells that have depleted levels are still able to respond to mesoderm inducing factors (Cha et al., 2012).

TGFβ signals from the marginal zone are involved in mesoderm induction during germ layer specification, and it is important for the ectoderm maintenance, that these signals are unable to act in the animal portion of the embryo. *Ectodermin* is expressed maternally in the animal pole during *Xenopus* development, and was discovered in a screen for factors that could induce an ectodermal fate in prospective mesoderm. Ectodermin inhibits *Veg-T* induced TGFβ signalling via ubiquitination of Smad4, which indirectly reduces the transcription of downstream mesoderm genes (Dupont et al., 2005).

A recently reported gene, Norrin, was discovered in a search for secreted molecules involved in neurectoderm specification (Xu et al., 2012). Norrin is a maternal protein that can inhibit both Activin and Nodal-related signals by direct binding of the ligands in the extracellular space. Inhibition of BMP signalling is required for dorsal development, and there is reciprocal inhibition between Norrin and Bmp4 (Xu et al., 2012). Conversely activation of Wnt signalling is also vital for dorsal development (Heasman et al., 1994) and Norrin was shown to be an animally expressed Wnt agonist. A reduction of Norrin caused a reduction of dorsal gene expression (*Chordin*, *Noggin* and *Xnr3*) and it was

thought that it might play a role in Blastula Chordin and Noggin Expression (BCNE) Centre formation (Xu et al., 2012), a zygotically induced group of cells in the dorsal ectoderm, that specifies the presumptive anterior neural plate (Kuroda et al., 2004). Importantly, because of its promotion of Wnt signalling, it was proposed that Norrin is required for specification of the neurectoderm, with MO knockdown causing loss of eyes and other anterior neural structures (Xu et al., 2012).

Of the genes introduced here, Xema sits at the top of the hierarchy (Figure 1.7). It plays a role in inhibition of TGFβ signalling from the marginal zone, but most importantly actively promotes ectodermal differentiation. Both Ectodermin and Norrin act presumably before Xema to inhibit any maternal TGFβ signals and also are active following ectoderm specification to continue this inhibition of marginal mesoderm inducing signals.

1.4 Spemann organizer: Neural induction

At gastrula stages, ectodermal cells choose between a neural or epidermal fate. This fate choice, one of the earliest in development is an area of great controversy. It was shown by Mangold and Spemann that the dorsal blastopore lip (the cells that invaginate first during *Xenopus* gastrulation) induced an ectopic second axis when transplanted to the ventral side of a host embryo. Utilising darkly pigmented embryos of the newt *Triturus taeniatus* and the non-pigmented *Triturus cristatus* embryos, they were able to show that the ectopic axis was induced by the transplanted tissue, and importantly, that only a very small proportion of the induced tissue contributed to the secondary axis (Spemann and Mangold, 1924). These results suggested the existence of a 'neural inducer' released from the dorsal blastopore lip that is required for ectoderm to acquire a neural fate. Following a search for the elusive 'neural inducer', work in 1989 changed the understanding of neural induction: the dissociation of ectodermal cells into single cells, thereby inhibiting contact mediated cell signalling, was able to induce the expression of neural markers (Grunz and Tacke, 1989). These

Figure 1.7 - Ectodermal gene network. *Xema* inhibits Nodal-related signals from the marginal zone, but more importantly promotes ectodermal fates. *Ectodermin* inhibits Nodal-related signals and *Activin*. Norrin inhibits BMP and Activin signalling, but promotes Wnt signalling dorsally.

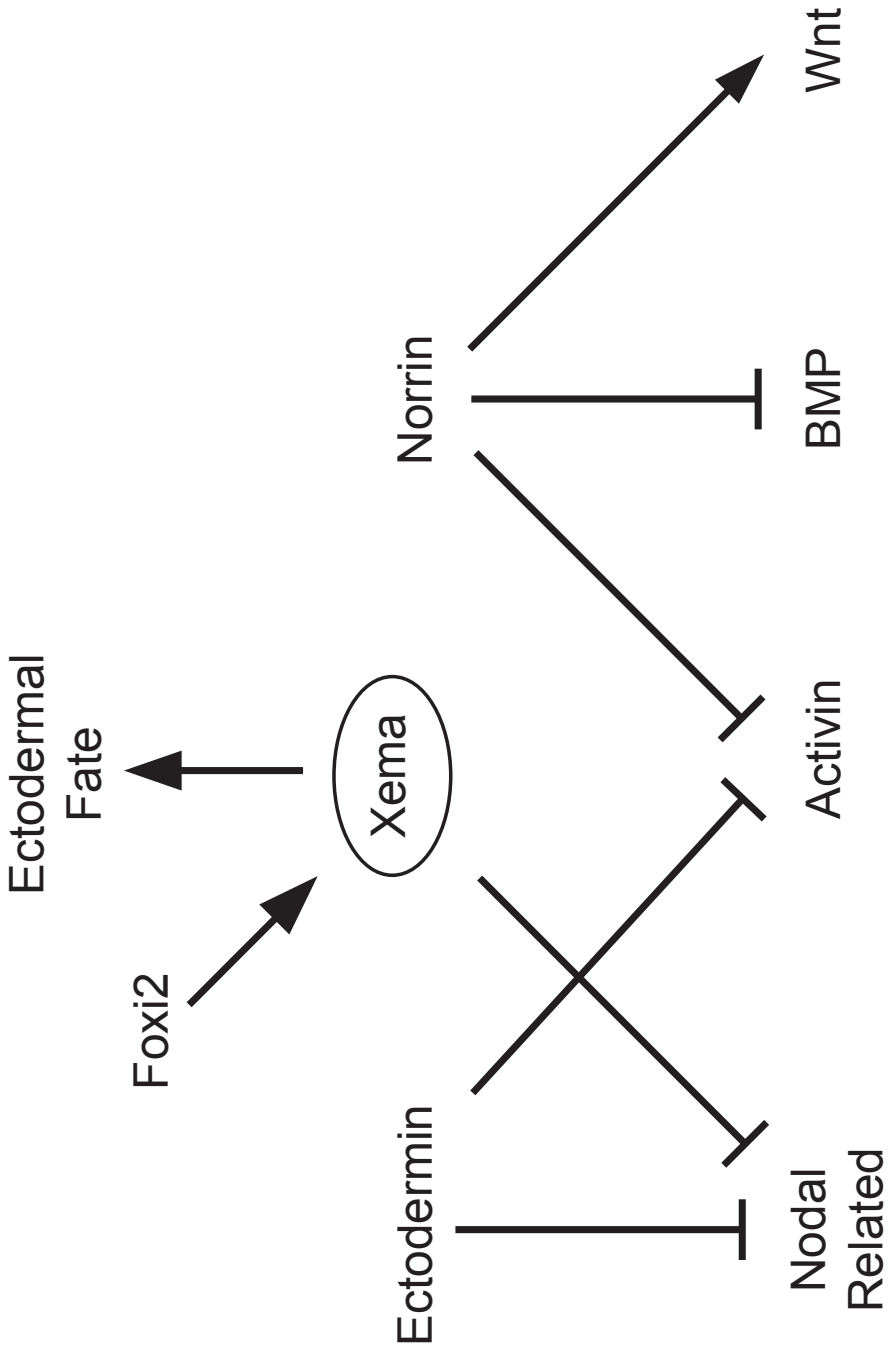

Figure 1.7 - Ectodermal gene network

results suggested that 'neural' tissue was the default state for ectodermal cells and that a signal was required for them to adopt an epidermal fate. BMPs, members of the TGFβ superfamily, had already been implicated in patterning: *Bmp2*, *Bmp4* and *Bmp7* were shown to be maternally expressed and involved in early development (Nishimatsu et al., 1992). BMP4 had been shown to be a ventralizing factor, and shown to induce ventral markers *in vitro* (Dale et al., 1992; Jones et al., 1992). Further work showed that overexpression of a BMP receptor was able to override dorsal signals (Graff et al., 1994) with defective BMP receptors disrupting normal dorso-ventral patterning (Maéno et al., 1994; Suzuki et al., 1994). In 1995, two studies showed inhibition of BMP to be the missing neural signal: firstly, a disruption of BMP signals in the ectoderm leads to direct neuralization (Hawley et al., 1995) and secondly, BMP ligands were shown to inhibit neural induction, and induce epidermal markers (Wilson and Hemmati-Brivanlou, 1995). These results led to the coining of the 'Default Model'. In this model, the Spemann organizer induces neural tissue by secreting an inhibitor of the inhibitor of neural tissue: with neural rather than epidermal fate being the default state of the ectoderm (Weinstein and Hemmati-Brivanlou, 1997).

1.4.1 Identification of BMP inhibitors expressed in the Spemann organizer

Neural tissues in *Xenopus laevis* are induced by BMP antagonists secreted from the Spemann organizer during early gastrulation (Muñoz-Sanjuán and Brivanlou, 2002). Three such factors, Noggin1, Chordin and Follistatin, bind BMP ligands in the extracellular space, preventing them from binding to their receptors and inhibiting activation of downstream signalling (Sasai et al., 1994; Sasai et al., 1995; Zimmerman et al., 1996; Fainsod et al., 1997; Iemura et al., 1998).

Noggin1 was isolated in a screen using UV irradiated embryos (that are ventralized due to lack of cortical rotation), with localized overexpression of Noggin1 causing the induction of ectopic partial axes (Smith et al., 1993). It was shown to be expressed in the organizer, and to directly bind to BMP4, and therefore inhibit BMP4 from binding to its own receptor (Zimmerman et al.,

1996). A new, related protein - Noggin2 – was recently cloned and is expressed during patterning of the neural plate. Results suggest that Noggin2 is, like Noggin1, able to inhibit BMP signalling, but in addition is also able to inhibit Nodal-related, Activin and Wnt signalling (Bayramov et al., 2011).

Chordin was discovered as a novel dorsalizing factor that was activated by the organizer specific transcription factors Gsc and Xnot. It too was shown to be an antagonist of BMP signalling (Sasai et al., 1994; Sasai et al., 1995). BMP inhibition was shown to be important from an evolutionary point of view; the antagonist relationship between BMPs and inhibitors was shown to be conserved amongst non-vertebrates, with the Drosophila genes Short Gastrulation (SOG) and Decapentaplegic (DPP) being homologues of the vertebrate genes Chordin and *BMP* (Holley et al., 1995). The third BMP inhibitor, Follistatin, was originally only described as an inhibitor of Activin (Nakamura et al., 1990), though its expression at blastula stages still suggested a role in the induction of mesoderm during development (Tashiro et al., 1991). It was later shown to be expressed specifically in the Spemann organizer (Hemmati-Brivanlou et al., 1994) and to have antagonistic effects on *Bmp* expression (Fainsod et al., 1997; Iemura et al., 1998).

1.4.2 Opposition to default model

The simplicity of the default model was called into question by more recent studies in both chick and Xenopus (Streit et al., 1998; Alvarez et al., 1998; Streit et al., 2000; Delaune, 2005). Streit and colleagues were investigating the role of BMP4 and its antagonist Chordin in both primitive streak (where cells involute during chick gastrulation) formation and neural induction in an amniote model system. Work showed that both *Bmp4* and *Chordin* are expressed prior to primitive streak formation, with *Bmp4* being downregulated as the streak forms. BMP4 overexpression in the posterior area pellucida (embryo forming tissue) inhibited primitive streak formation, whilst Chordin was able to induce an ectopic streak, expressing both mesoderm and organizer genes (Streit et al., 1998). However, Chordin was not sufficient to induce neural tissue, whilst

neither BMP4 nor BMP7 inhibited neural tissue formation. These results suggested that BMP inhibition by Chordin was required for primitive streak formation, but not for neural induction, presumably because the tissue in which ectopic tissue was not induced had received other fate inducing signals (Streit et al., 1998). Follow up work by the same group included a screen to find genes that were induced following the grafting of an ectopic organizer. Early Response to Neural Induction (ERNI) was isolated and is expressed at very early stages of development. The authors concluded that ERNI was the earliest known neural response gene (Streit et al., 2000). Further to this, when checking which tissues induced *ERNI* expression they found that they all corresponded to sites of FGF signalling. *ERNI* could be induced by FGF soaked beads, and inhibited by the pharmacological FGFR inhibitor SU5402, which also caused the loss of the early neural gene *Sox3*. It was therefore suggested that rather than BMP inhibition, FGF signals were required for neural induction in chick.

In response to the opposition to the default model, investigations were carried out that addressed the roles of BMP and FGF signalling in Xenopus neural induction (Khokha et al., 2005; Wills et al., 2010).

Firstly, Khokha and colleagues aimed to see if there was functional redundancy between BMP inhibitors expressed in the organizer; and if this redundancy was masking the endogenous requirement for BMP inhibition (Khokha et al., 2005). When using MOs against the BMP inhibitors Follistatin (FMO), Chordin (CMO) and Noggin (NMO), single and combinatorial double (FCMO, FNMO, CNMO) knockdowns resulted in very mild effects on neural induction. However, a triple (FCNMO) knockdown caused drastic loss of dorsal structures and expansions of ventral and posterior fates, results that confirmed the requirement of BMP inhibition throughout blastula and gastrula stages for neural induction (Khokha et al., 2005).

In addition, it was shown that anterior neural markers were most sensitive to increased concentrations of FCNMO, and therefore decreases in BMP inhibition (Wills et al., 2010). Additionally, BMP inhibition was able to neuralize ectodermal explants in the absence of FGF signalling, whilst FGF expression

was seen in the ventralized FCNMO injected embryos, highlighting a role for FGF in posterior and ventral development. FGF was required for the induction of Sox2 expression, which was then shown to be a marker of a pre-neural state (Wills et al., 2010). A mouse study provided further evidence that BMP inhibition is vital for neural development, but also that functional redundancy plays a role. In mice that lack the BMP inhibitor Chordin, neural development is normal, with mutants only displaying defective ear structures. In contrast, in mice that lack both Chordin and Noggin there is a dramatic loss of neural structures (Bachiller et al., 2000).

1.4.3 Head induction: are other signals required?

The Spemann organizer is widely regarded at the sole inducer of the dorsal axis, but experiments performed since its discovery suggested that there might be further complexity. Mice lacking the organizer genes Lim1 and Otx2 develop with no heads, but have normal trunks (Bally-Cuif and Boncinelli, 1997), meaning the posterior portion of the dorsal axis formed correctly, whilst head induction was impaired. In mice that lack the BMP inhibitors Chordin and Noggin, head formation is defective, whilst the rest of the embryo develops normally (Bachiller et al., 2000). These results suggested two different roles for the organizer, head induction and trunk induction.

Wnt signalling was implicated in head induction following the identification of Frzb-1, another gene expressed in the organizer. Frzb-1 overexpression inhibited dorsal mesoderm markers, instead causing embryos to develop large heads, effects that were later shown to be due to Wnt inhibition (Leyns et al., 1997; Wang et al., 1997). It was later shown that head induction requires inhibition of both BMP and Wnt signalling (Glinka et al., 1997). *tBR*, a truncated BMP receptor, had been shown to induce a partial second axis when overexpressed (Graff et al., 1994); however when coexpressed with a DNWnt8 construct, *tBR* induced a full axis with head, eyes and a notochord (Glinka et al., 1997). When using a plasmid that only allows overexpression to occur after the MBT, it was

clear that zygotically transcribed inhibition of both BMP and Wnt signalling conferred head inducing activity (Glinka et al., 1997).

The secreted antagonist Dickkopf-1 (*Dkk-1*) is expressed in the Spemann organizer during blastula and gastrula stages of *Xenopus* development and in the prechordal plate adjacent to the forebrain during later patterning of neural tissue (Glinka et al., 1998). In results similar to that of DNWnt8, coinjection of Dkk-1 and *tBR* induced a full second axis with head in *Xenopus*, a result that was mimicked by mDkk-1 and tBR (Glinka et al., 1998). Interestingly Dkk1 alone, could not dorsalize a DMZ explant, but in combination with *tBR* was able not only to dorsalize at the gastrula stage, but also to anteriorize when analysed at tailbud stage. Cerberus is a BMP/Wnt/TGFβ inhibitor expressed zygotically in the anterior endoderm of *Xenopus* that causes the induction of ectopic heads when overexpressed (Bouwmeester et al., 1996; Piccolo et al., 1999), further evidence that head induction required inhibition of BMP and Wnt signalling. It was suggested that a requirement for BMP and Wnt inhibition is conserved throughout the vertebrates. *Cerberus* is expressed in the anterior visceral endoderm (AVE), an extra-embryonic tissue equivalent to the anterior endoderm that is required for specifying an anterior pattern in the mouse embryo, however mutant mice develop normally, suggesting that other factors compensate during mouse development (Pearce et al., 1999; Simpson et al., 1999). *Dkk-1* is expressed in the prechordal plate in both mouse and fish, and in the mouse AVE and fish hypoblast (Pearce et al., 1999; Hashimoto, 2000), with null Dkk-1 mutants lacking head structures (Mukhopadhyay et al., 2001). Although BMP inhibition was shown to be vital for neural induction, the specification and induction of the head requires additional Wnt inhibition.

1.4.4 Competence: often overlooked

Although vitally important, inductive interactions are not governed only by the properties of the inducing cells, but also by the responsive capacity or

'competence' of the tissue receiving the signal. Competence of the ectoderm to both mesoderm-inducing and neural-inducing signals is important for correct neural specification (Chang and Harland, 2007).

Early work suggested dorso-ventral differences in the competence of the *Xenopus* ectoderm (Sharpe et al., 1987), whilst temporal changes in the ability of the *Xenopus* ectoderm to respond to neuralizing signals throughout gastrulation proposed a developmental timing mechanism that specifies a sequence of competencies (Servetnick and Grainger, 1991).

In chick, like in *Xenopus*, neural competency reduces throughout development. L5 is a carbohydrate epitope that was shown to be involved in neural specification (Streit and Stern, 1995). It is initially expressed in a domain that centred on the anterior primitive streak. At later stages expression starts to become restricted, so that by stage 6 it is only expressed in the neural plate. *L5* expression matches areas that are competent to Henson's Node (chick equivalent to Spemann organizer) grafts, and then only marks regions fated to become definitive neural tissue. Prolonged expression of *L5* can induce longer periods of competency, highlighting the possibility that it may not act cell autonomously, and that extrinsic cues could play an important role (Streit et al., 1997). The authors also thought that these results warranted a rethink of neural induction, separating three different aspects of this process. Firstly, competence of cells was specified; secondly, these cells were neuralized; and thirdly, neuralized cells were regionalized.

Molecular cues were also shown to be involved in the neural competency of *Xenopus* ectoderm. Ectopic expression of Protein Kinase C Alpha (PKCα) and the elongation factor eIF4AII enhanced neural induction (Otte and Moon, 1992). In later studies the effects of these genes as competence factors was investigated, with an enhancement of neural induction measured by the response to varying concentrations of Noggin protein (Morgan and Sargent, 1997). Ectopic expression of eIF4AII meant that the concentration of Noggin required to induce the neural marker *NCAM* in explants was 10% of that needed to get the same

response in uninjected control samples. The effect of PKCα overexpression was stronger, with only 1% of the original concentration required to induce *NCAM* (Morgan and Sargent, 1997). The *Xenopus* homolog of Lfc, is zygotically expressed throughout the ectoderm, is also able to increase neural competency when overexpressed (Morgan et al., 1999). RT-PCRs of whole embryos injected with Xlfc showed an increased the amount of neural tissue (*NCAM* and *Nrp1*) at the expense of epidermal (*EpiK*) and neural crest tissue (*Slug*), plus an increase of a neural competency factor (*PKCα*).

Remarkably, it was later shown that the neural ectoderm retains its competence to respond to Nodal/Smad2 signalling. Utilizing a hormone inducible Smad2 construct, and adding hormone during gastrulation inhibited expression of the neural markers *Sox3* and *Sox2*, whilst inducing ectopic expression of the mesoderm markers *MyoD* and *Chordin* (Chang and Harland, 2007). Importantly, if hormone was added after gastrulation the neural plate was not affected, highlighting an important role for the inhibition of TGFβ signals during gastrulation for neural development (Chang and Harland, 2007). Mesoderm-inducing factors were, in fact, shown to play a part in controlling the competence of neural tissue: a reduction in Veg-T expands the neurogenic region, whilst depletion of Veg-T in the vegetal most cells induces a neural fate (Yan and Moody, 2007).

In an investigation of intrinsic cues in neural induction, a novel role for Neuronatin (Nnat) was described. *Nnat* was shown to play a decisive role in mESC neural differentiation and also in *Xenopus* neural patterning. By increasing intracellular Ca^{2+} concentrations via antagonism of SERCA, a Ca2+ ATPase, Nnat was able to inhibit BMP signalling and promote a neural fate (Lin et al., 2010).

The competency of the ectoderm to respond to both neural and mesoderm inductive signals suggests that the competency of the ectoderm to both neural and mesoderm-inducing factors needs to be properly controlled for correct organisation.

1.5 The role of Coco during development

There have been numerous studies that investigated the TGFβ signals involved in germ layer specification. These secreted factors cause the formation of endoderm and the induction of mesoderm, and as a consequence of this; in order for tissue to gain an ectodermal fate TGFβ signalling must be inhibited. Relatively little is known about the genes that promote ectoderm by inhibiting TGFβ signalling.

Coco is a member of the Cerberus-DAN family of proteins, and was found in a screen of genes that were upregulated by the intracellular BMP/TGFβ inhibitor Smad7 (Muñoz-Sanjuán and Brivanlou, 2002). Coco is most closely related to Cerberus in *Xenopus* (Bouwmeester et al., 1996; Piccolo et al., 1999), and is the homologue of the mouse gene Cer-l2 (Marques et al., 2004), the chick gene Cerberus1 (Tavares et al., 2007) and the zebrafish gene Charon (Hashimoto, 2004).

Coco is a maternal BMP/Wnt/TGFβ inhibitor, expressed throughout the animal pole up until the end of gastrulation (Figure 1.8A). After stage 12, levels of Coco decline (Figure 1.8B). Lower levels of Coco persist and have been shown to play a role in L/R patterning (Vonica and Brivanlou, 2007).

In the egg, *Coco* is expressed in the animal half, presumably acting to inhibit maternal BMP4 (Bell et al., 2003), and interestingly its expression is complimentary to Veg-T (Figure 1.8C).

Injection of Coco mRNA into the vegetal pole at the two-cell stage caused a reduction in the expression of the pan-mesodermal markers *Xbra* and *FGF8* at gastrula stages. Additionally, overexpression at Coco in the animal pole caused large anterior expansions and posterior truncations (Bell et al., 2003). A localized ventral-vegetal injection of Coco mRNA at the four-cell stage induced ectopic

Figure 1.8 – Analysis of Coco in *Xenopus leavis.* A) *Coco* is expressed maternally in the animal pole up to gastrulation stages. B) RT-PCR showing strong expression from the egg up until stage 11, with weaker expression up until stage 19. Ornithine decarboxylase (ODC) is used here as a loading control. C) In the egg, *Coco* is coexpressed with *Bmp4* and opposes *Veg-T* expression. D) Coco reduces the competency of the ectoderm to Activin signals. Injection of Activin causes the induction of *Xnr1* and *Xwnt8* expression in animal caps until stage 11. Coinjection of Activin and Coco means that there is no induction at stage 10, earlier than normal.

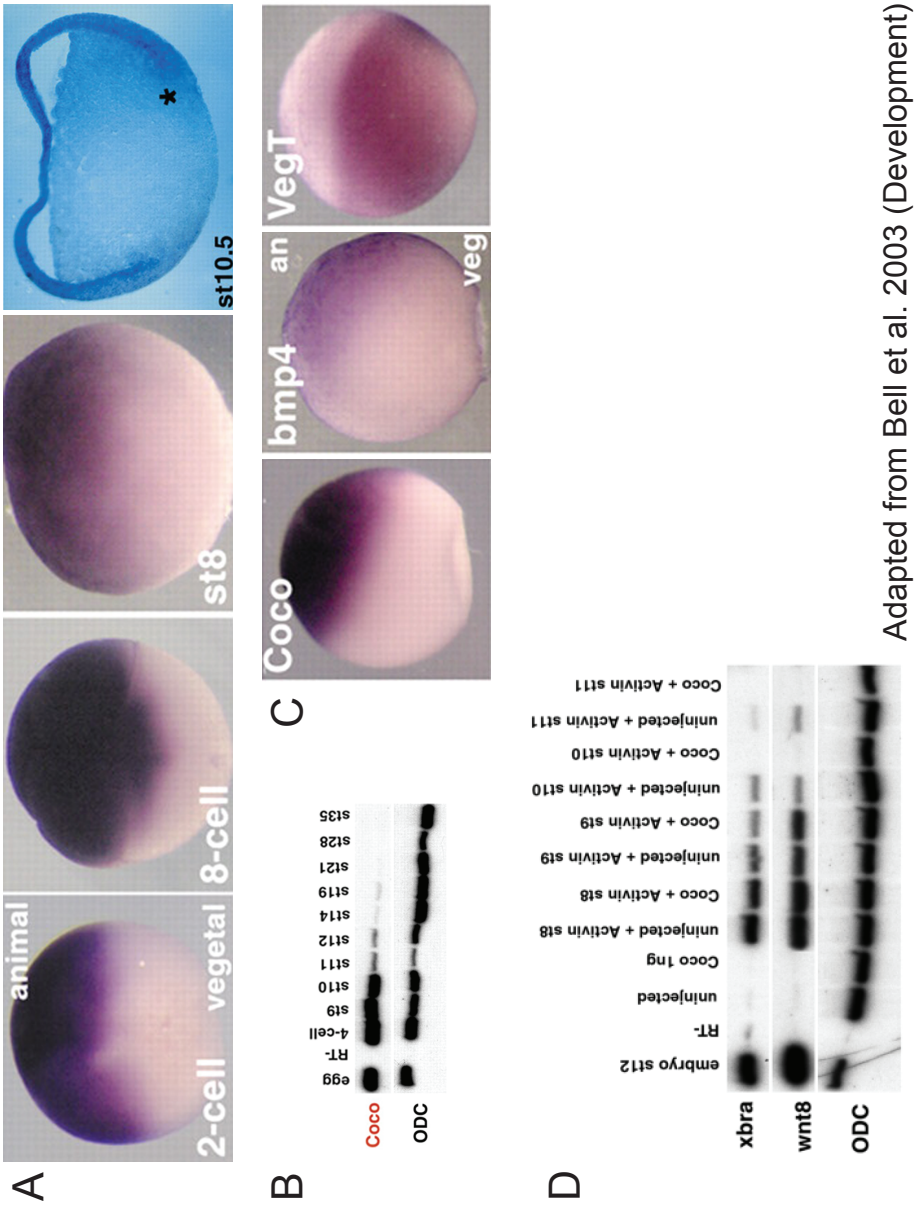

Figure 1.8 - Analysis of Coco in *Xenopus laevis*

heads containing forebrain and midbrain at tadpole stages, a result similar to overexpression of the closely related Cerberus (Piccolo et al., 1999).
The expression of *Coco* throughout the ectoderm falls sharply following gastrulation, coinciding with the loss of competency of ectoderm to respond to mesoderm-inducing signals (Green and Smith, 1990; Bell et al., 2003). Animal caps can respond to Activin, both morphologically and molecularly, but this ability reduces throughout time. Ectodermal explants cut from embryos injected with Coco mRNA had a reduced response to Activin. Activin was able to induce the expression of *Xbra* and *Xwnt8* in Control explants until stage 11, whilst Coco overexpression reduced the induction at stage 9 and completely inhibited the induction at stage 10 (Figure 1.8D), evidence that Coco was able to reduce the competency of the ectoderm to *Activin* signals (Bell et al., 2003).

1.5.1 Coco is also involved in left/right patterning

DAN domain proteins, members of the Cerberus/DAN family are inhibitors of TGFβ proteins and have been shown to be involved in L/R patterning in chick (Esteban et al., 1999), mouse (Marques et al., 2004) and zebrafish (Hashimoto, 2004).

Coco is expressed throughout the ectoderm during gastrulation, but in early neural stage embryos, expression shifts to posterior paraxial mesoderm where it overlaps with the TGFβ ligands *Xnr1* and *Derriere*. Injection of a Coco morpholino caused a lack of asymmetry to the internal organs (Vonica and Brivanlou, 2007), results that suggested that Coco was only required on one side (right) of the embryo, and that the TGFβ ligands Xnr1 and Derriere were required on the left side to initiate asymmetric gene activation (Vonica and Brivanlou, 2007). Later work further confirmed a role for Coco in L/R patterning. Left sided *Coco* expression is repressed by flow, movement of extracellular liquid through the gastrocoel roof plate, with both mechanical and genetic ablation of flow preventing unilateral Coco expression (Schweickert et al., 2010). These results suggest that unilateral expression of *Coco* is required to break embryonic symmetry.

Although Coco gain of function studies have been performed (Bell et al., 2003) and there is a clear role for Coco following gastrulation in L/R patterning (Vonica and Brivanlou, 2007; Schweickert et al., 2010), the early endogenous role of Coco remains unclear.

1.6 Aims of the thesis

Coco gain of function experiments highlight a possible role in head induction, whilst its spatio-temporal expression pattern is suggestive of a role in germ layer specification, leaving open questions about Coco's endogenous role.

BMP inhibition is vital for neural development (Khokha et al., 2005) with anterior fates being the most sensitive to a loss of BMP inhibition (Wills et al., 2010). Coco overexpression induces ectopic heads that contain forebrain and midbrain tissue, and it was hypothesised that Coco would ectopically induce BMP inhibitors in order to induce anterior neural tissue. In order to prove this hypothesis, and investigate a requirement for further BMP inhibition downstream of Coco, mRNA was coinjected with combinations of MOs against the BMP inhibitors Follistatin, Chordin and Noggin. The AP fate of the induced ectopic tissue was analysed by In Situ Hybridization (ISH).

As previously mentioned, the early endogenous role of Coco is unknown. Due to preliminary experiments and Coco's inhibition of TGFβ signal it was hypothesised that Coco plays a role germ layer specification (Vonica, Heasman, Brivanlou, Bell unpublished). In an attempt to prove this hypothesis Coco loss of function experiments were performed, with subsequent ISH analysis of known endodermal and mesodermal markers used to check any germ layer defects.

In an attempt to better understand Coco downstream signalling, a microarray was performed, comparing the overexpression of Coco, a BMP/Wnt/TGFβ inhibitor to Noggin1, a BMP inhibitor. It was hypothesised that a gene with a possible role in germ layer specification may have different downstream targets to that of a

gene involved in neural induction. To test this, the differential expression that occurred as a consequence of both Coco and Noggin overexpression was compared, whilst an ISH screen aimed to uncover novel genes involved in germ layer specification and neural induction.

Chapter 2 Materials & Methods

2.1 General Reagents and buffers

Solutions stored at room temperature (RT), unless otherwise stated.

α-DIG antibody	Sheep IgG antibody (Roche) for the detection of digoxigenin-labeled RNA probes.
1% Agarose Gel	1g agarose (Roche) in 100ml of 1x TBE, 10µl SYBR® Safe DNA Gel Stain (Invitrogen).
10% BBR	Boehringer Blocking Reagent (Roche); 10g in 100ml 1x MAB whilst heating at 65^{o}C until dissolved; autoclaved. Stored at -20^{o}C.
2% BBR Block	5ml 10% BBR up to 25ml with 1X MAB.
Bleaching Solution	44.25ml of ddH_2O, add 2.5ml Formamide (VWR), 2ml Hydrogen Peroxide (H_2O_2) (Sigma), 1.25ml 20x SSC (Sigma).
BM Purple	Spun for 5 mins at 4000rpm before addition to remove any sediment. (Roche)
10% CHAPS	3-[(3-Cholamidopropyl)dimethylammonio]-1-propanesulfonate (Sigma); 10g CHAPS dissolved in 100ml of ddH_2O. Stored at -20^{o}C.
Cysteine Solution	2% L-Cysteine Hydrochloride (Sigma), 1.2% Trizma Hydrochloride (Sigma), 1% NaOH (VWR) in ddH_2O.

50x Denhardts Solution	Blocking reagent that prevents probe binding non-specifically. Stored at -20^{o}C.
ddH_2O	MiliQ water autoclaved.
DIG	Digoxygenin label for In Situ Hybridization colour detection (Roche)
EDTA	Ethylenediaminetetraacetic acid 0.5M stock solution (Sigma)
Formaldehyde	36% stock solution (VWR)
Formamide	99.9% stock solution, molecular biology grade (VWR)
10% Ficoll	20g of Ficoll powder (Sigma) dissolved in 200ml of ddH_2O. Stored at 4^{o}C.
Ficoll Injection Solution	35ml of 10% Ficoll, 5ml 10x MMR up to 100ml with ddH_2O.
20% Gelatin	10g of Gelatin (Type B, Sigma) added to 50ml of PBS. Stored at -20^{o}C, used at 55^{o}C.
90% Glycerol	45ml of Glycerol (Sigma), 5ml of PBS. Mixed gently O/N to avoid bubbles.
Heparin Sodium Salt	Ensures denaturation of proteins in Hybridization Buffer, 100mg/ml stock solution. Stored at 4^{o}C.
Human Chorionic Gonadotropin (HGC)	Diluted in ddH_2O to make a 1unit/µl working concentration. Stored at 4^{o}C.
Hybridization Buffer (Hyb)	50ml Formamide, 25ml 20X SSC, 2ml 50 mg/ml Torula RNA, 100µl of 100mg/ml Heparin Sodium Salt, 2ml 50X Denharts, 100µl Tween20, 1ml of 10% CHAPS, 2ml of 0.5M EDTA. Stored at -20^{o}C.
Hydrogen Peroxide (H2O2)	Used for embryo bleaching. Stock kept at 4^{o}C.
Luria Broth (LB)	For 500ml. 10 tablets (Sigma) added to 500ml of H_2O, autoclaved.

Luria Broth (LB) Agar	For 500ml. 10 tablets (Sigma) added to 500ml of H_2O, autoclaved and set at RT.
5X MAB	For 1L. 58g Maleic Acid (Sigma), 43.65g NaCl (VWR), pH to 7.5 with NaOH (VWR). Autoclaved.
Magnesium Chloride (1M $MgCl_2$)	101.65g of $MgCl_2$ in 500ml of H_2O, autoclaved.
Methanol (MeOH)	98% Stock
10X MEM Salts	For 250ml. 52.33g of MOPS, 1.90g of EGTA, 0.30g of MGSO4. pH to 7.4 with NaOH (VWR).
MEMFA Fix	For 50ml. 5ml 10X MEMFA Salts, 5ml 37% Formaldehyde, 40ml ddH_2O.
10X MMR	58.440g NaCl, 1.491g KCl, 1.204g MgSO4, 2.940g $CaCl_2$, 11.915g HEPES, in 800ml ddH_2O, pH to 7.4 with NaOH, up to 1L with ddH_2O. Autoclave.
0.1X MMR	10ml of 10X MMR up to 1L with ddH_2O.
MOPS	3-(N-morpholino) propanesulfonic acid (Alfa Aesar)
5M NaCl	For 500 ml. 146.1 g NaCl up to 500ml with ddH_2O.
NTMT	1ml 5M NaCl, 2.5ml Tris-HCl, 2.5ml $MgCl_2$, 50µl Tween20 up to 50ml with ddH_2O.
PBS	10 Tablets (Oxoid) in 1L of H_2O. Autoclaved.
PBT	PBS with 0.1% Tween20 (Sigma)
4% Paraformaledhyde (PFA)	10ml 16% PFA up to 40ml with 30ml PBS. Stored at -20°C.
0.1M Potassium-3 Ferrocyanide Solution	1.65g of $K_3[Fe(CN)_6]$ (Sigma) powder in 50ml of ddH_2O.
0.1M Potassium-4 Ferrocyanide	2.11g of $K_4[Fe(CN)_6].3H_2O$ (Sigma)

Solution	powder in 50ml of ddH_2O.
Proteinase-K Enzyme	15µl aliquots of 10mg/ml of PBS stored at -20°C (Roche). Used at 1:1000 in PBT.
RNAse A	10mg/ml stock stored at -20°C (Sigma).
RNAse T	1000u/µl stored at -20°C.
2X Saline-Sodium Citrate (SSC) buffer	5ml 20X SSC Buffer (Sigma) up to 50ml with ddH_2O.
0.2X Saline-Sodium Citrate (SSC) buffer	500µl 20X SSC Buffer (Sigma) up to 50ml with ddH_2O.
SYBR Safe Gel Stain	Used at 1/10000 in 1% Agarose Gel (Invitrogen).
1X Tris/Borate/EDTA (TBE) Buffer	100ml of 10X TBE (Gibco) plus 900ml of ddH_2O.
2M Tris-HCl pH 9.5	121.1g Trizma-Base up 500ml with ddH_2O. pH to 9.5 with 2M HCl. Autoclaved.
0.1M Triethanolamine (TEA)	15.38ml of 100% TEA in 1L of ddH_2O. pH to 7.5 with HCl.
Torula mRNA	50mg/ml stored at -20°C (Sigma)
Tween20	100% solution (Sigma)
X-Gal	100mg/ml in Dimethylformamide (DMF) stored at -20°C (Bioline).
X-Gal Staining solution	500µl of 0.1M $K_3[Fe(CN)_6]$, 500µl of 0.1M $K_4[Fe(CN)_6].3H_2O$, 20µl of 1M $MgCl_2$ up to 10ml with PBT. Add 62.5µl of X-Gal/10ml of staining solution.

2.2 General Methods

2.2.1 Preparation of antibiotic plates

LB agar was melted in a microwave at 150W for 30 minutes (mins). When cooled to 55°C, ampicillin was added at 100µg/ml and the molten agar was

poured into sterile 90mm Petri dishes. After setting, plates were inverted and stored at 4°C.

2.2.2 Transformation Protocol

Day 1:
Sub Cloning Efficiency DH5α competent cells were stored in 50µl aliquots at -80°C. An aliquot of cells was thawed on ice for 15 mins. Once thawed 25ng of plasmid DNA/ 100ng ligation mix was added to the cells. The mixture was then carefully mixed and left on ice for a further 20 mins. The mixture was then heat shocked at 42°C for 45 seconds (secs), the optimal temperature for causing DNA to enter cells. After heat shock the cells were returned to ice for 2 mins. If the DNA added to the cells was a ligation product, a recovery step followed this. 400µl of LB was carefully added to the competent cells, and were tubes shaken in a 37°C incubator for 1 hour (hr) at 215 revolutions per minute (rpm). After this recovery the LB/cell mixture was plated onto ampicillin plates (see 2.2.1) using sterile glass beads. If only plasmid DNA was being transformed (and not a ligation) then the cells were plated without the recovery step. Plates were then incubated upside down in a 37°C incubator overnight (O/N) to form bacterial colonies.

Day 2:
On the following day single colonies were picked with sterile tips and added to 3ml of LB Amp (LB with Ampicillin 100µg/ml) for Mini-Prep/50ml for Midi-Pred/200ml for Maxi-Prep. Mini-Preps were incubated in sterile 15ml centrifuge tubes, Mid- and Maxi-Prep are incubated in autoclaved conical flasks.

2.2.3 Agarose Quantification of DNA/mRNA

2.2.3.1 Gel electrophoresis

Restriction digests and other DNA and RNA samples were analysed using agarose gel electrophoresis. 1% agarose gels were made by dissolving agarose (Sigma) in 1X TBE (Gibco) in a microwave at 750W. When molten, SYBR Safe

DNA stain was added (10µl in 100ml of gel) and the gel set in a mould. Gel electrophoresis was performed at 100V for 15-20mins and gels visualised using a UVP Benchtop UV Transilluminator and photographed. Approximate fragment sizes were determined using DNA ladders of known molecular weight (Hyperladder™, Bioline).

2.2.3.2 UV spectrophotometer

When checking the concentration of plasmid DNA and mRNA a GE Nanovue was used (followed manufacturers protocol).

2.2.4 Isolation of plasmid DNA

2.2.4.1 Mini-Prep isolation

The 5Prime Fast Plasmid® kit was used and the DNA was always eluted with ddH_2O. Plasmid DNA was obtained following the manufacturer's protocol. Products were always checked by gel electrophoresis.

2.2.4.2 Midi-/Maxi-Prep isolation

50ml (Midi) or 200ml (Maxi) of LB Amp culture was incubated O/N in a 37^{o}C incubator at 215 rpm. Cells were recovered by centrifugation at 10,000rpm for 15mins in a Sigma 4K15 centrifuge at 4^{o}C. The resultant bacterial pellet was resuspended in 6ml (Midi) or 10ml (Maxi) of chilled P1 buffer from Qiagen Hi-speed® Midi/Maxi plasmid kit (Qiagen) and plasmid DNA was obtained following the manufacturer's protocols.

2.2.5 Preparation of riboprobes for *in situ hybridization*

2.2.5.1 Linearisation of plasmid DNA

Each plasmid was linearised with specific enzymes and buffers (see Table 2.1). A 30µl reaction was made with the following parts: 4µg of DNA, 2µl of appropriate 10X enzyme buffer, 1µl of corresponding restriction enzyme, with the final volume being made up with ddH_2O. Reactions were incubated at 37°C for 2 hours. To check linearization, 2µl of cut plasmid DNA was run against 0.5 µl of un-cut plasmid DNA on a 1% agarose gel (linearised DNA runs as a single band, at a different speed than the un-cut plasmid DNA). Following successful linearisation the reaction was cleaned with a GFX DNA Purification Kit (followed manufacturers protocol) and eluted in 20µl of ddH_2O.

2.2.5.2 Transcription of DIG-Labelled RNA Probes

RNA probes were synthesised in RNAse-free conditions, with ddH_2O and sterile disposables always used. As for DNA linearisations each riboprobe has a specific RNA polymerase (see Table 2.1). Probes were transcribed using 1µg of linearised plasmid DNA in a total volume of 20µl. The reaction contained the following: 5µl of linearised plasmid DNA (=1µg), 2µl of 10X transcription buffer (Roche), 2µl of DIG RNA labelling mix (Roche), 0.5µl of RNAse Inhibitor (Roche), 1µl RNA polymerase (T7/T3/SP6) and 9.5µl ddH_2O. The reaction was incubated at 37°C for 3hr and following this incubation 1µl of DNAseI (RNAse free - Roche) was added and the reaction incubated for a further 15 mins at 37°C. 1µl of the riboprobe was then run on a 1% agarose gel to check transcription. Following successful transcription the reaction was cleaned using a GFX Probe-Quant G50 column (GE Healthcare). The probe was then added to Hyb buffer and stored at -20°C until needed (20µl reaction will make 5ml of Probe/Hyb mix).

2.2.6 Preparation of mRNA for micro-injection

mRNA was also always synthesised in RNAse-free conditions. The mMessage mMachine® SP6 Kit was used and a reaction with the following parts was made: 6µl (≈1.2µg) linearised DNA, 2µl 10X Reaction Buffer, 10µl 2X NTP/CAP

Solution, 2µl SP6 Enzyme Mix. The reaction was incubated at 37°C for 3 hours and cleaned as described in 2.2.5.2. The concentration of mRNA was determined and working concentrations prepared (see 2.2.3.2).

2.3 Frog embryos and embryo manipulation

Xenopus laevis were used for the experiments explained here, and were staged according to Nieuwkoop and Faber (1967).

2.3.1 Frog Husbandry

Female *Xenopus laevis* were primed the evening before use by an injection of 400-500units of HCG hormone into their lymph sac. Eggs were obtained by massaging the female frogs, and then fertilised using testes dissected from male *Xenopus laevis.* Fertilization causes cortical rotation (turning) to occur, and when 'turned', eggs were treated with Cysteine solution to remove their jelly coating. Embryos were raised in 0.1X MMR unless otherwise stated.

2.3.2 Microinjection of frog embryos

2.3.2.1 Preparation for injections

To ensure embryos didn't stick to the surface of Petri dishes injections were carried out on a 1% agarose dish. To reduce leaking of cell contents following needle puncture, embryos were injected in ficoll injection solution. Embryos were injected using glass micro-pipettes pulled on program 84 (Pressure=500, Heat=550, Pull=20, Vel=25, Time=25) on a Sutter P-97 needle puller. Needles were calibrated to inject 10nl per injection. mRNAs and MOs were back loaded into the glass micro-pipettes using loading tips (Eppendorf). Following injection embryos were kept in ficoll injection solution for at least 5 hours and transferred into 0.1X MMR before gastrulation.

2.3.2.2 Preparation of morpholinos for injection

Morpholino (MO) stocks were always kept sealed at 4°C, whilst working concentrations were kept at room temperature (RT) (see Table 2.3).

To ensure the MO was in solution before injection they were heated to 55^{o}C for 5 mins, before being kept at 37^{o}C until required.

2.3.2.3 mRNA and Morpholino co-injection

When co-injecting, 1μl of each solution was mixed together in a sterile 0.5ml eppendorf tube and kept on ice. It is important to note that when mixing mRNA and MO injection volume was doubled to ensure the originals concentrations were maintained.

2.3.2.4 Microinjection

Coco mRNA (and Coco + F,C,NMO combinations) was injected vegetally in one of the vegetal blastomeres at the 4 cell stage (Figure 2.1A). CocoMO and CocoMUT were both injected twice (half sized injections) at the one cell stage (Figure 2.1B). TGFβ MOs (ActMO, Xnr5/6MO, Vg1MO) were all injected animally in one of two blastomeres at the two-cell stage (Figure 2.1C). β-Gal mRNA was always co-injected with the TGFβ MOs (injection size doubled). For the mircroarray, mRNA for both Coco (1ng) and Noggin (40pg) was injected animally at the one-cell stage (Figure 2.1D).

2.3.2.5 Embryo Fixation

From stage 22, vitelline membranes were removed before fixation. Embryos were fixed in glass vials (Wheaton) for 1 hr in MEMFA fix at RT, being rocked at 60rpm on a Stuart orbital shaker. Following the incubation, MEMFA Fix was replaced with 100% MeOH and embryos were rocked for a further 5 mins at RT to equilibrate. One final wash of 100% MeOH was done before storing embryos at -20^{o}C.

Figure 2.1 - Microinjection sites in *Xenopus laevis* embryos. A) Sites for Coco mRNA (green) single/coinjections. Lateral view shows injection into vegetal portion if ventral blastomere. Vegetal view shows injection into middle of one blastomere. B) Sites for TGFβMO (blue) injections. Lateral view shows injection into the animal pole of one blastomere and the two-cell stage. Animal view shows injection into the centre of one blastomere at the two-cell stage. C-D) Sites for CocoMO (yellow) and Coco/Noggin mRNA injections (Red-Microarray). Lateral views show two injections into the animal pole at the one cell stage. Animal views show two injection sites that are spread evenly over the animal pole at the one-cell stage.

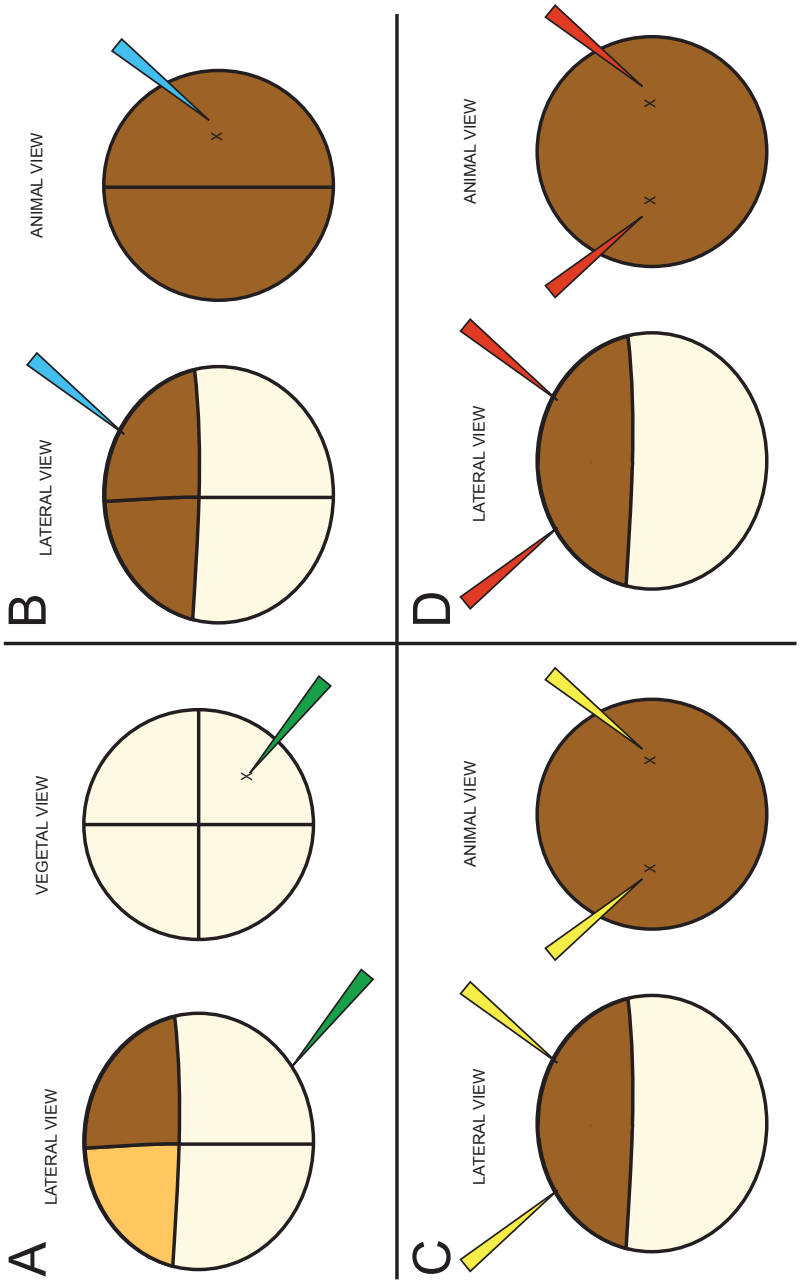

Figure 2.1 - Microinjection sites in Xenopus laevis embryos

2.3.2.6 X-Gal Staining

When β-Gal was injected into embryos, X-Gal staining (a substrate that is turned blue by β-Gal) was used to detect it. Initially embryos were fixed for 10mins in MEMFA Fix at RT (rocking) and were then washed for 5 mins in 100% PBT. X-Gal Staining solution (pre-heated to 37^{o}C) was added and embryos stained at 37^{o}C for 10-25 mins until the blue signal was strong. Following this colour reaction, a further 5 mins wash in 100% PBT was performed. Finally embryos were fixed for a further 50mins in MEMFA Fix at RT, and stored in 100% MeOH at -20^{o}C.

2.3.3 In Situ Hybridization (ISH)

For ISH reactions embryos were always fixed then stored in 100% MeOH at -20^{o}C for at least 24hr. All washes at RT were done on an orbital rocker at 60rpm. 37^{o}C washes were done in an incubator with no rocking. 60^{o}C washes were done in a water bath with no rocking. 4^{o}C ON incubations were done in a fridge on an orbital rocker at 60rpm.

Day 1:
Initially embryos were processed in glass vials. Embryos were first washed in 100% MeOH for 5mins at RT, followed by four 5mins rehydration washes (75% MeOH/ddH_2O, 50% MeOH/ddH_2O, 25% MeOH/PBT and 100% PBT). Following rehydration embryos were washed a further three times in 100% PBT. Embryos then had bleaching solution (see 2.1) added and were put under an artificial light source for 2 hours. Following bleaching, embryos were washed in 100% PBT for 5 mins at RT. The embryos were then treated with a Proteinase K/PBT wash for 5mins at RT. This step helps to permeabilize the embryo by removing some of the outer protein, allowing better probe penetration. It is important to ensure this step is only 5mins for optimal staining later in the protocol. Next, two 5mins washes with 0.1M TEA were performed at RT. Following this embryos were washed twice in TEA + acetic anhydride for 5mins at RT. The acetic anhydride acts to neutralize free amines within the embryos to

make sure the probe binds specifically to mRNA. This was followed by two 5mins 100% PBT washes at RT, before embryos were refixed in 4% PFA for 20mins at RT. This fixing step helps to ensure embryo integrity following Proteinase K treatment. After fixation embryos were washed five times in 100% PBT for 5mins at RT and were then put into Hyb buffer (without probe) for at least 1 hour at 60^{o}C. The ISH protocol can be paused at this stage, with embryos being stored in Hyb buffer at -20^{o}C. If this has been done the embryos must be warmed up to 60^{o}C for 30mins before addition of probe.
Having been processed in glass vials up this stage, they were then transferred into baskets for the next two days of the ISH protocol. Apparatus as shown in Figure 2.2 was set up in a 60^{o}C water bath. Embryos were hybridized O/N at 60^{o}C.

Day 2:
1ml (per basket) of pre-warmed Hyb buffer was added to a sterile eppendorf tube rack, here used as a modified rack for the first wash. Baskets were placed into the pre-warmed Hyb for 10mins at 60^{o}C. Following this wash baskets were placed in a modified rack that could be moved in and out of subsequent wash solutions. These washes were done in sterile tip boxes. The first three washes were in 2X SSC (pre-heated to 60^{o}C) for 20mins at 60^{o}C. Embryos were then washed in a 2X SSC RNAse wash (RNAse A- 20μg/ml, RNAse T_1-10μg/ml) for 30mins at 37^{o}C, to remove any mismatched double stranded RNA in the embryo. A 10min wash in 2X SSC at RT then removed excess RNAse. Following the 2X washes, embryos were washed in 0.2X SCC twice for 30mins at 60^{o}C. Next, two washes were done in 1X MAB at RT for 15mins. To prepare embryos for the addition of antibody, they were blocked for at least one hour at RT in 2% BBR block. α-DIG antibody was diluted at 1/2500 in 2% BBR block, and embryos were incubated O/N at 4^{o}C.

Day 3:
Embryos were removed from α-DIG/BBR block and were washed in 1X MAB for 1hr, five times. They were left in 1X MAB following the final wash rocking O/N at RT.

Figure 2.2 - Apparatus used for hybridization step during whole mount ISH. A) Sterile 14ml centrifuge tube with 2-position lid. Modified basket is placed into 0.5 ml of DIG probe for hybridization step. b) Embryos were hybridized in coloured modified baskets, and were washed in custom-made racks standing in sterile tip boxes.

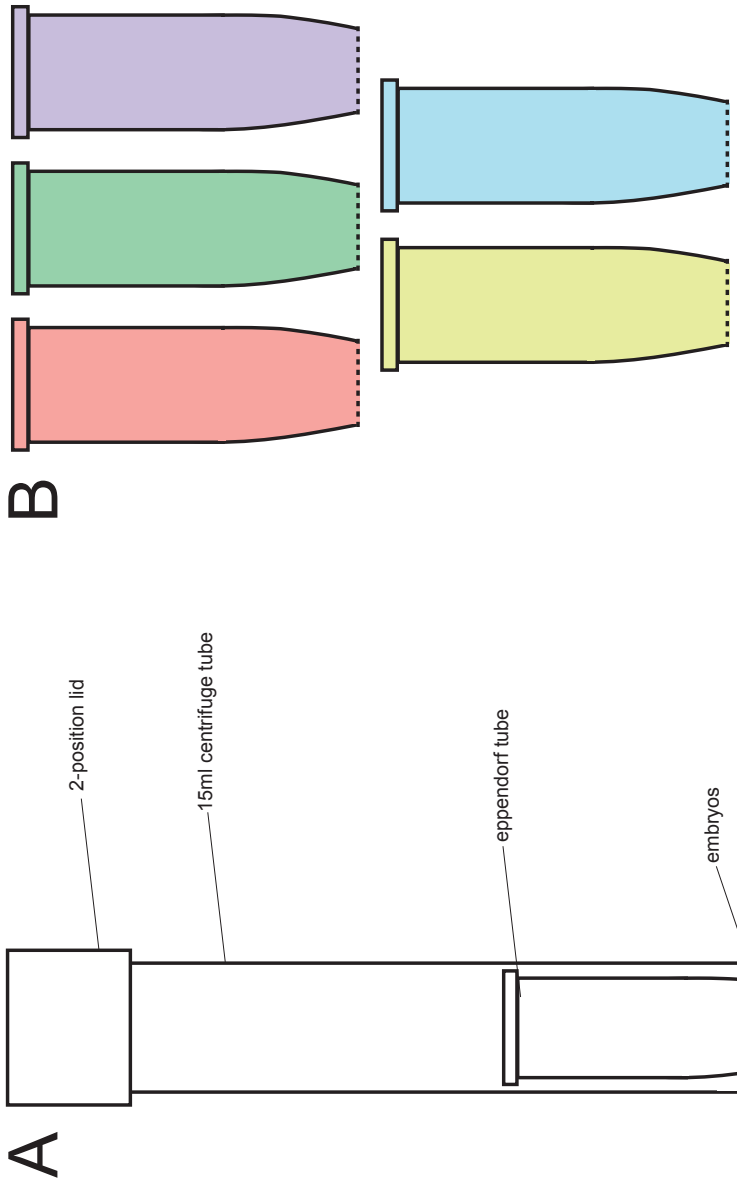

Figure 2.2 - Apparatus used for hybridization step during whole mount ISH

Day 4:

Embryos were removed from their baskets, transferred to sterile 24 well dishes (Nunc) and washed twice in NTMT (pH 9.5) at room temperature for 5mins. For detection of DIG signal, embryos were stained in BM Purple (Roche) in the dark at RT. If being stained over several days, embryos were washed thrice in NTMT for 5mins and stored O/N at 4^{o}C. Fresh BM purple was then added the day after.

Stopping Colour Reaction:

When the stain was strong enough, embryos were washed twice in 1X MAB for 5mins to stop the reaction. They were then washed three times in 100% PBT for 5mins, when photographs could be taken. To store embryos and also to prepare them for embedding in gelatin, embryos were fixed in 4% PFA at 4^{o}C O/N.

2.3.4 Embedding/Sectioning embryos following ISH

Following ISH embryos were post-fixed in 4% at least O/N at 4^{o}C. Embryos were embedded in 20% gelatin and sectioned on a vibratome. Prior to use 20% gelatin was melted at 55^{o}C for two hours. Embryos were left in 1ml of gelatin at 55^{o}C for at least 1hr to equilibrate. Following this step, embryos were put into 2ml of fresh molten gelatin in a mould on ice. Before the gelatin set, the embryo was orientated in relation to the sectioning requirements. The gelatin block was then left to set at 4^{o}C for 1-2 hours. When set, the block could be cut down in size ready for sectioning, continuing to ensure the correct orientation of embryo. Blocks were fixed in 4% PFA (that has been chilled on ice) at 4^{o}C O/N at least. Once fixed, blocks were sectioned on a LeicaVT1000S vibratome taking 50μm sections. Sections were mounted on glass slides in 90% glycerol and sealed prior to imaging.

2.3.5 Taking pictures of ISH/slides

Embryos were always pictured on agarose plates. Phenotype and ISH pictures were taken using a Zeiss StemiSV6 microscope with attached OlympusDP70 camera. Pictures from the same experiment were always taken at the same

magnification, so they could be directly compared. Slides were imaged on a Nikon Eclipse80*i* using a 4X objective.

Table 2-1 Plasmid information

Name	Type	Linearisation	Polymerase	Reference
Coco	mRNA	AscI	SP6	Bell et al. 2003
β-Gal	mRNA	NotI	SP6	Liu Lab KCL
Coco-5'	mRNA	AscI	SP6	Vonica & Brivanlou 2007
Noggin	mRNA	NotI	SP6	Zimmerman et al. 1996
Emx1	Probe	HindIII	T7	Pannese et al. 1998
Otx2	Probe	SalI	T3	Pannese et al. 1995
Krox20	Probe	SalI	T3	Nieto & Bradley 1991
Hoxb9	Probe	EcoRI	T7	Wright et al. 1990
Sox17β	Probe	EcoRI	T7	Hudson et al. 1997
Xbra	Probe	XhoI	SP6	Smith et al. 1991
Chordin	Probe	EcoRI	T7	Khokha et al. 2005
Cat2	Probe	EcoRI	T7	Unpublished
Tipin	Probe	EcoRI	T7	Unpublished
Crabp2	Probe	KpnI	T7	Delva et al. 1999
Atp13a4	Probe	SalI	T7	Unpublished
Tll2	Probe	SalI	T7	Unpublished
Nr13-l	Probe	SalI	T7	Unpublished
Cav2	Probe	SalI	T7	Unpublished
Cyp26c1	Probe	EcoRV	T7	Tanibe et al. 2008
Hpgds	Probe	SalI	T7	Unpublished
ZFP91-l	Probe	SalI	T7	Unpublished
Tcea3	Probe	SalI	T3	Unpublished

Table 2-2 – Morpholino sequences

Name	Sequence	Reference
CocoMO1	5'-CTGGTGGCCTGGAACAACAGCATGT-3'	Vonica & Brivanlou 2007
CocoMO2	5'-TGGTGGCCTGGAACAGCAGCATGTC-3'	Vonica & Brivanlou 2007
CocoMUT	5'-CTGCTGGCGTCCATCAAGAGCTTGT-3'	Bell Lab
FollistatinMO	5'-TCCTTTCATTTAACATCCTCAGTGC-3'	Bell Lab
ChordinMO	5'-GGACACTGCATTTTTGTGGTTCCAA-3'	del Barco Barrantes et al. 2003
NogginMO	5'-CACAAGGCACTGGGAATGATCACTG-3'	Bell Lab
Xnr5MO	5′-AGATAAAGCCTAGCACAGCCATATC-3′	Luxardi et al. 2010
Xnr6MO	5′-CAAGACTAAGTTCACTAGGGCCATC-3′	Luxardi et al. 2010
ActivinMO	5'-CGAGGGTCTCCAAGCGGAGAGGAGA-3'	Bell Lab
Vg1MO	5'-CCACAGTCTCAGCCACACCATACTG-3'	Birsoy et al. 2006

Table 2-3 - Morpholino injection concentrations

Name	Injection Total
CocoMO1+2	40ng
CocoMUT	40ng
FollistatinMO	20ng
ChordinMO	20ng
NogginMO	20ng
ControlMO	20ng
Xnr5/6MO	15ng
ActivinMO	50ng
Vg1MO	45ng

Chapter 3 Investigating the requirement for BMP inhibition downstream of Coco's activity

3.1 Background

The single BMP inhibitors Follistatin, Chordin and Noggin are expressed in the *Xenopus* organizer (Khokha et al., 2005), and single or double knockdown of the BMP inhibitors Follistatin, Chordin and Noggin in *Xenopus tropicalis* embryos caused no observable neural plate defects. However, simultaneous knockdown of all three factors resulted in drastic loss of anterior and dorsal tissue (Khokha et al., 2005). These results, further confirmed in *Xenopus laevis* (Wills et al., 2010), gave evidence that BMP inhibition is vital for neural development and that functional redundancy exists between these extracellular BMP antagonists.

Coco is a maternal BMP inhibitor, which also inhibits Wnt and other TGFβ signalling (Bell et al., 2003). It is expressed throughout the animal half of the embryo up to gastrulation (Bell et al., 2003). When overexpressed vegetally, Coco causes a loss of mesoderm (downregulation of the mesodermal markers *Fgf8* and *Xbra*) and increases the size of the organiser (both *Otx2* and *Gsc* upregulated) in gastrula embryos. At tadpole stages, ventro-vegetal Coco overexpression induces ectopic heads that contain forebrain (*Rx*/*Emx1*) and midbrain (*Otx2*/*En2*) tissues.

To investigate the possibility that Coco induces other BMP inhibitors, the phenotype of Coco mRNA injected embryos was compared to that of embryos coinjected with Coco mRNA and MOs against the BMP inhibitors Follistatin, Chordin and Noggin. In addition to see if there was functional redundancy downstream of Coco, combinatorial coinjections with two or three MOs were also performed.

3.2 Results

3.2.1 Investigating a requirement for BMP inhibition downstream of Coco –an experimental approach

To investigate whether or not Coco requires the BMP antagonists Follistatin, Chordin and Noggin for its induction of ectopic heads, a MO knockdown approach was undertaken. The phenotypic and molecular effects of Coco mRNA overexpression and the effects of Follistatin (FMO), Chordin (CMO) and Noggin (NMO) knockdown were confirmed (Bell et al., 2003; Khokha et al., 2005).

To directly investigate the requirement of BMP inhibition following Coco overexpression and to address possible functional redundancy, combinatorial microinjections were performed. Coco mRNA was coinjected with single (Coco+FMO, +CMO, +NMO), double (Coco+ FCMO, +FNMO, +CNMO) or triple (Coco+FCNMO) combinations of MO followed by a morphological and molecular assessment of the induced tissue.

3.2.2 Molecular analysis of Coco induced ectopic heads

Embryos injected with Coco mRNA displayed ectopic heads (compare arrowhead in Figure 3.1A to Figure 3.1B; n=326/434). To confirm whether the ectopic heads contained neural tissue, ISH analysis was performed. Antisense probes for *Emx1*, a marker of the dorsal telencephalon (Pannese et al., 1998), *Otx2*, a marker of the fore/midbrain (Pannese et al., 1995; Blitz and Cho, 1995), *Krox20*, a marker of rhombomeres 3 and 5 in the hindbrain (Nieto and Bradley, 1991) and *Hoxb9* a marker of the spinal cord, previously *XlHbox6* (Wright et al., 1990), were used to assess the expression characteristics of ectopic tissue.

Emx1 is expressed in the dorsal telencephalon (Figure 3.1C) and in the kidney of wild type embryos (asterisk, Figure 3.1C). Expression was also seen in ectopic heads (arrowhead, Figure 3.1D; n=76/78) highlighting the induction of ectopic

Figure 3.1 – ISH analysis of Coco overexpression in Stage 28 *Xenopus laevis* embryos. A), C), E), G) and I) are stage 28 uninjected control embryos. B), D), F), H) and J) are embryos injected with Coco mRNA ventro-vegetally at the 4 cell stage. A) Control uninjected embryo. B) Injection of Coco mRNA induces ectopic heads with cement glands, black arrowhead marks ectopic cement gland. C-J) ISH analysis of Coco overexpression. C) *Emx1* is expressed in the forebrain and kidney, D) *Emx1* is expressed in Coco induced ectopic heads, black arrowhead marks ectopic expression. E) *Otx2* is expressed in the forebrain and midbrain, F) *Otx2* is expressed in Coco induced ectopic heads, black arrowhead marks ectopic expression. G) *Krox20* is expressed in R3+5 of the hindbrain, H) *Krox20* was never expressed in Coco induced ectopic heads. I) *Hoxb9* is expressed in the spinal cord, J) *Hoxb9* expression was never seen in Coco induced ectopic heads.

All panels are lateral views of stage 28 embryos, and are orientated with anterior to the left and dorsal up. cg, cement gland,

fb, forebrain, hb, hindbrain, kd, kidney, mb, midbrain, sc, spinal cord, In C) and D) *= kidney.

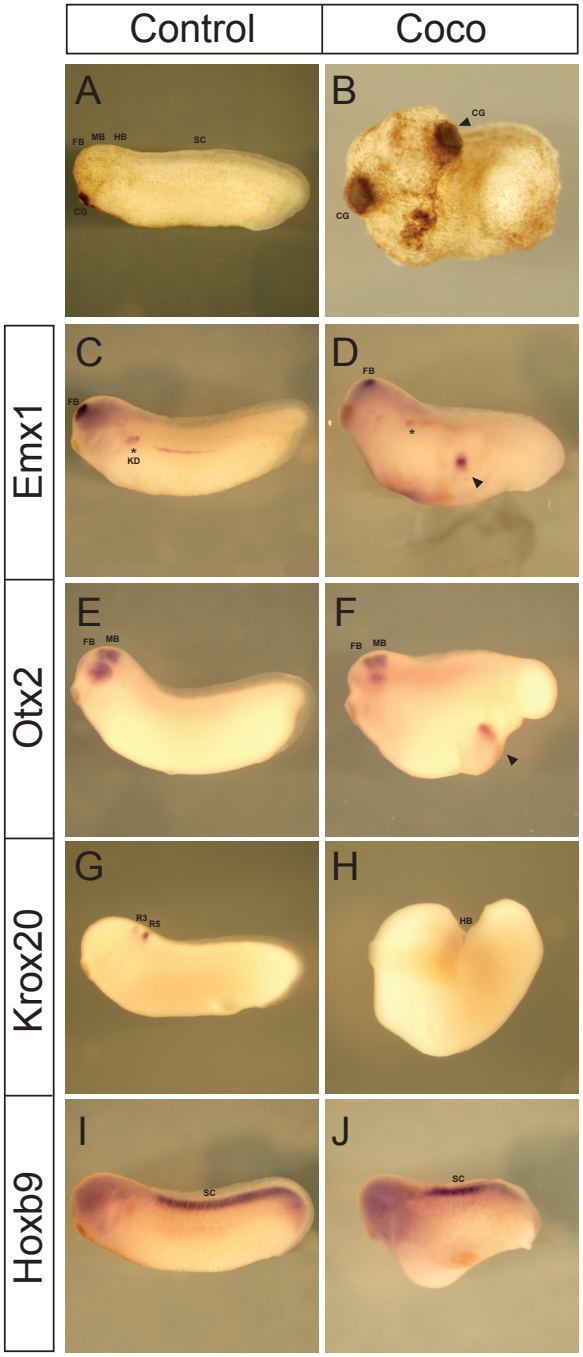

Figure 3.1 - ISH analysis of Coco overexpression in Stage 28 *Xenopus laevis* embryos

forebrain tissue. *Otx2* is expressed in the anterior neurectoderm in wild type embryos (Figure 3.1E). There was also expression in the ectopic heads (arrowhead, Figure 3.1F; n=83/83). Coco induced ectopic heads never expressed the hindbrain marker *Krox20* (compare Figure 3.1G to Figure 3.1H; n=0/45) or the spinal cord marker *Hoxb9* (compare Figure 3.1I; n=32/32 to Figure 3.1J; n=0/39).

Taken together these data confirm that the ectopic heads induced by Coco contain forebrain and midbrain tissue, but no posterior structures such as hindbrain or spinal cord.

3.2.3 A reduction of BMP inhibition alone caused mild anterior phenotypes

Before using MOs against Follistatin (FMO), Chordin (CMO) and Noggin (NMO) in combination with Coco mRNA confirmation of previously published effects were required (Khokha et al., 2005). Here wild type embryo length and the expression domains of *Otx2* (Figure 3.2A) and *Emx1* (Figure 3.2B-C) were compared to MO injected embryos (Figure 3.2D-L).

There was no obvious difference in embryo length or the expression of *Otx2* (Figure 3.2D; n=7/7) or *Emx1* (Figure 3.2E-F; n= 6/6) following injection of CMO (Figure 3.2B; n=7/7). However, when knocking down Follistatin or Noggin singularly, effects were detectable. Follistatin morphant embryos displayed a slight reduction in length and exhibited a slight reduction in *Emx1* expression, but no obvious change in *Otx2* expression (Figure 3.2G-I; n=5/5).

Noggin morphant embryos showed a similar phenotype; a reduction in embryo length and no obvious change in *Otx2* expression (Figure 3.2J; n=6/7). However, when looking at *Emx1* expression, there was a reduction of forebrain tissue (arrow heads, Figure 3.2K-L; n=6/7).

Figure 3.2 – ISH analysis following MO knockdown of BMP inhibitors in Stage 28 *Xenopus laevis* embryos. A-C) Stage 28 uninjected control embryos. D-F) ChordinMO injected embryos. G-I) FollistatinMO injected embryos. J-L) NogginMO injected embryos. A) *Otx2* is expressed in the forebrain and midbrain. B-C) *Emx1* is expressed in the forebrain and kidney, asterisk in B show expression in kidney, whilst black arrowhead in C shows forebrain expression in anterior view. D) *Otx2* expression is normal in CMO injected embryos, E-F) *Emx1* expression is normal in CMO injected embryos, asterisk in E show expression in kidney, whilst black arrowhead in F shows forebrain expression in anterior view. G) *Otx2* expression seems normal in shorter FMO injected embryos, H-I) *Emx1* expression is reduced in FMO injected embryos, asterisk in H show lighter expression in kidney, whilst black arrowhead in I shows lighter forebrain expression in anterior view. J) *Otx2* expression seems normal in shorter NMO injected embryos, K-L) *Emx1* expression is reduced in NMO injected embryos, asterisk in K shows faint expression in kidney, whilst arrowhead in L shows reduction of forebrain expression in anterior view.

A-B), D-E), G-H) and J-K) are lateral views orientated with anterior to the left and dorsal up. C), F), I) and L) are anterior views orientated with dorsal to the top.

fb, forebrain, hb, hindbrain, kd, kidney, mb, midbrain

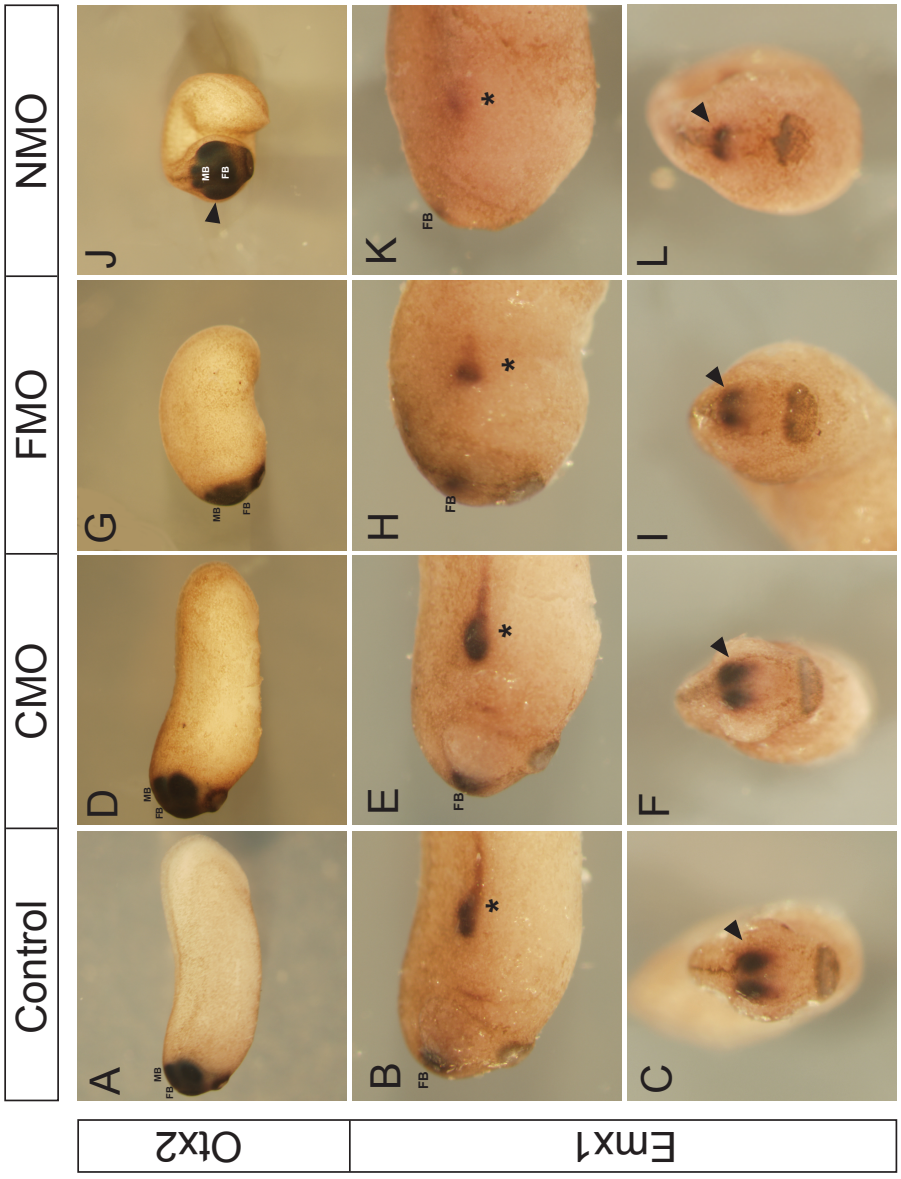

Figure 3.2 - ISH analysis following MO knockdown of BMP inhibitors in stage 28 *Xenopus laevis* embryos

Here a mild global effect on the embryo following single knockdown of Follistatin and Noggin was confirmed (Khokha et al., 2005). Next, a comparison of the phenotypes caused by coinjection of Coco mRNA and MOs against these factors was performed. The ectopic tissue induced by Coco (ectopic head with cement gland) was compared with the tissue induced following coinjection. Morphological assessment (presence of cement gland/structural integrity) highlighted a requirement for BMP inhibition in Coco overexpression.

3.2.4 A loss of BMP inhibition following Coco overexpression causes morphological changes to induced ectopic tissue

Embryos were coinjected with a combination of Coco mRNA and MOs against one (FMO, CMO, NMO), two (FCMO, FNMO, CNMO) or three (FCNMO) BMP inhibitors and ectopic tissue assessed. Injection of Coco mRNA induced ectopic heads with cement glands, pigmented structures that demarcates the anterior limit of the embryo (compare Figure 3.3A to Figure 3.3B; n=316/398).

Embryos coinjected with Coco mRNA and a single MO (CocoFMO/CMO/NMO) displayed ectopic tissue that did not always have a well-defined cement gland (arrowheads, Figure 3.3C, n=36/66; Figure 3.3D, n=58/82; Figure 3.3E, n=36/55).

Embryos coinjected with Coco mRNA and two MOs (CocoFCMO/FCMO/CNMO) displayed ectopic tissue, that also did not always have a well-defined cement gland (arrow heads, Figure 3.3F n=67/79; Figure 3.3G n=67/74; Figure 3.3H n=32/33) and looked less structurally integral than tissue induced following coinjection with one MO.

However, when coinjecting Coco mRNA with all three MOs, embryos exhibited ectopic tissue that resembled the induction of a partial axis (Nakayama et al., 1998) (arrow head, Figure 3.3I; n=38/45).

Figure 3.3 – Morphological analysis of embryos coinjected with Coco and MOs against BMP inhibitors. A) Stage 28 uninjected control embryo. B) Embryos injected with Coco mRNA exhibit ectopic heads (arrowhead) with cement gland. C-E) Coinjection of Coco and one MO ventro-vegetally induced ectopic tissue lacking cement glands. C) Coinjection of Coco and FMO, D) Coinjection of Coco and CMO, E) Coinjection of Coco and NMO. F-H) Coinjection of Coco and two MOs ventro-vegetally induced ectopic tissue lacking cement glands that showed a reduction structural integrity. F) Coinjection of Coco and FCMO. G) Coinjection of Coco and FNMO. H) Coinjection of Coco and CNMO. I) Coinjection of Coco and FCNMO induced ectopic tissue that lacked cement gland and resembled a partial axis. J) Coinjection of Coco and control MO induced ectopic head with a cement gland.

All panels are lateral views of stage 28 embryos, and are orientated with anterior to the left and dorsal up.

cg, cement gland, fb, forebrain, hb, hindbrain, mb, midbrain, sc, spinal cord.

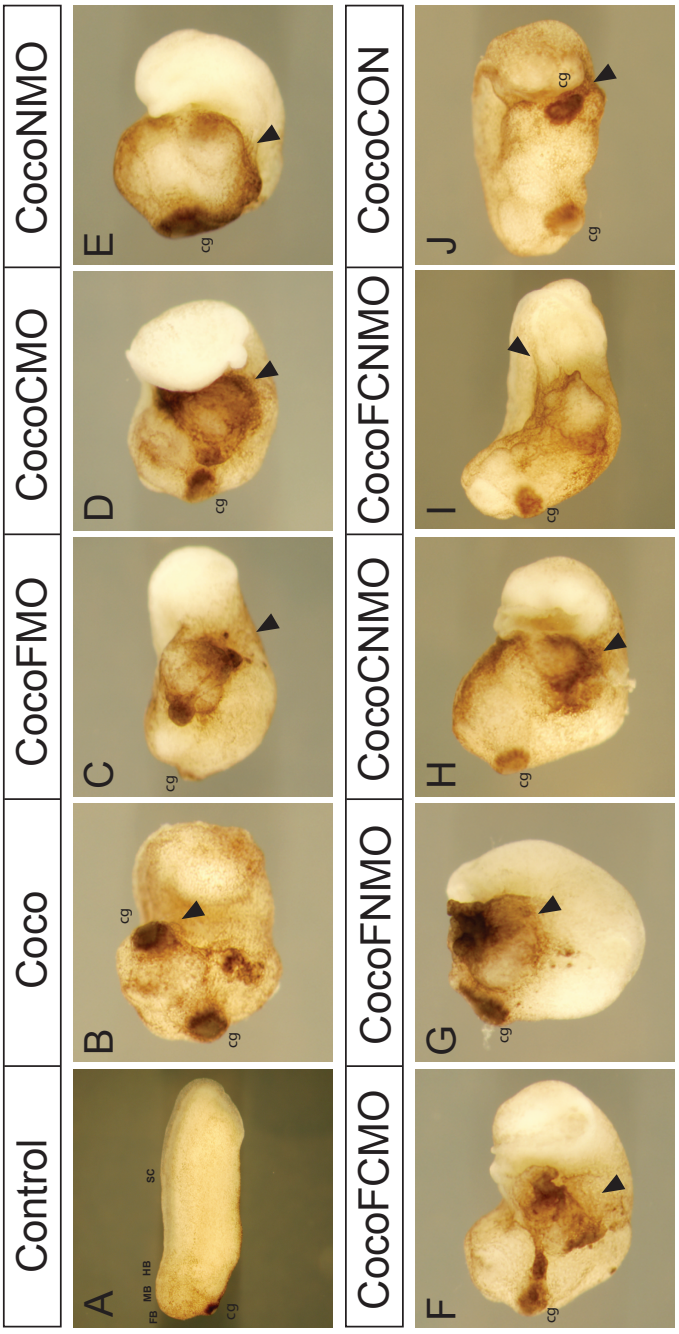

Figure 3.3 - Morphological analysis of embryos coinjected with Coco and MOs against BMP inhibitors

Coinjection of *Coco* mRNA and a control MO had no effect of the ectopic heads that were induced (arrow head, Figure 3.3J; n=86/128), demonstrating that the phenotypes seen following previous coinjections were caused by a loss of BMP inhibition.

The data shows that a reduction of BMP inhibition causes a reduction in ectopic head formation. (Figure 3.4; white=WT, red= ect. Heads, green = ect. tissue). Coinjection of Coco and a single MO caused induction of ectopic tissue that had no cement gland, whilst coinjection of Coco and two MOs also induced ectopic tissue that lacked a cement gland but that was also less structurally integral. Lastly coinjection of Coco and three MOs induced ectopic tissue that resembled a partial axis.

3.2.5 A reduction of BMP inhibition causes a fate change to Coco-induced ectopic tissue

To assess if there was a fate change in the tissues induced by coinjection of Coco and MOs against BMP inhibitors, ISH analysis was performed with a selection of markers of the AP axis.

Expression of *Emx1* was seen in the ectopic heads of Coco mRNA injected embryos (compare arrow heads arrow head Figure 3.5A to Figure 3.5B; n=11/11), however in a small number of embryos coinjected with Coco and a MO against a single BMP inhibitor there was no ectopic *Emx1* expression (Figure 3.5C-F; CocoFMO n= 3/40, CocoCMO n=3/22, CocoNMO n=2/18), suggesting that there was no forebrain tissue in the Coco induced heads.

There was also ectopic expression of *Otx2* in *Coco* induced heads (compare Figure 3.5G to Figure 3.5H; n=18/18), and when Coco and single MOs against BMP inhibitors were injected there was still ectopic expression (Figure 3.5I-L;

Figure 3.4 – Coinjection of Coco and increasing numbers of MOs against BMP inhibitors reduced ectopic head formation. In all cases, White = Wild type, Red = Ectopic head with cement gland and Green = ectopic tissue without a cement gland. (-)- n=78; Coco- n=398; CocoFMO- n=66, CocoCMO- n=82, CocoNMO- n=55; CocoFCMO- n=79, CocoFNMO- n=74, CocoCNMO- n=33; CocoFCNMO- n=45).

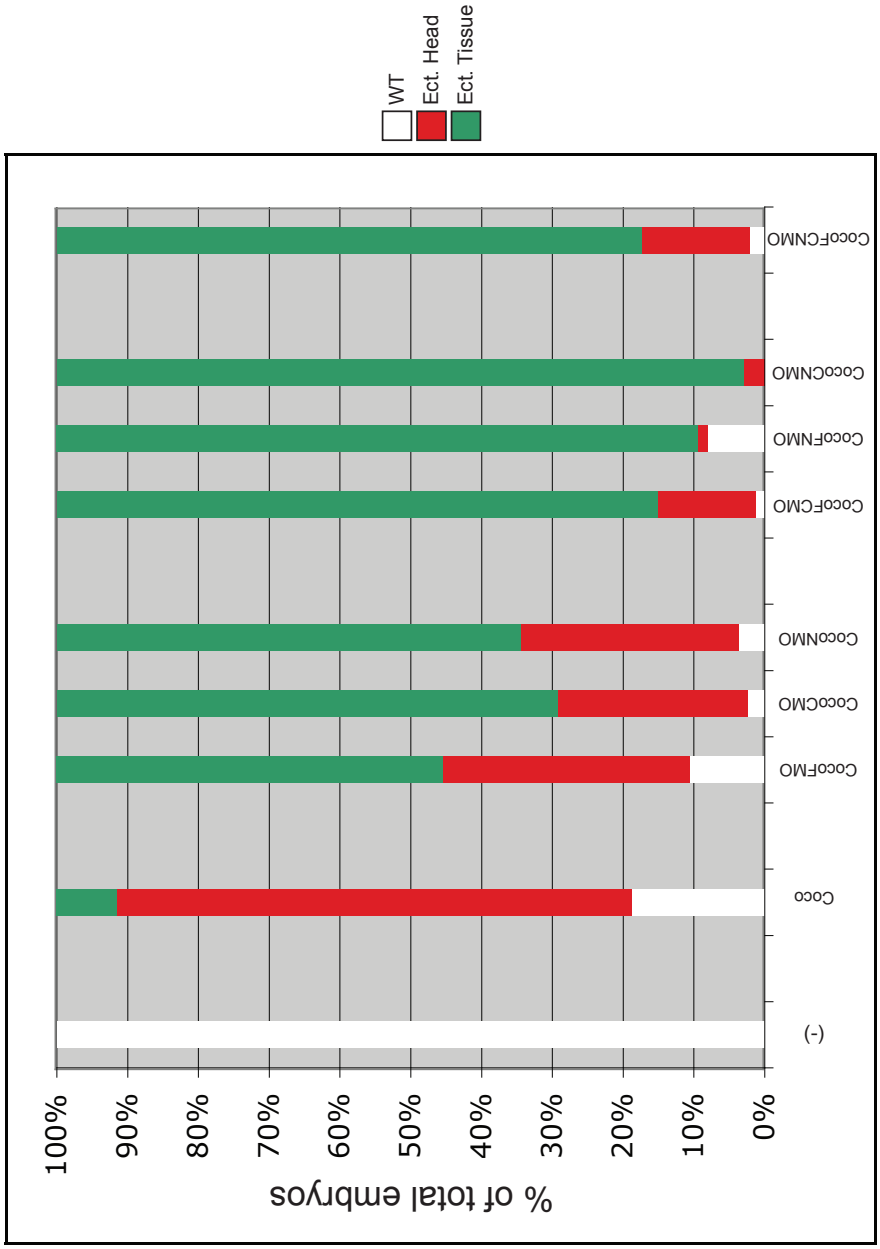

Figure 3.4 - Coinjection of Coco and increasing numbers of MOs against BMP inhibitors reduced ectopic head induction

Figure 3.5 – ISH analysis of phenotypes resulting from coinjection of Coco and single MOs against BMP inhibitors. A-E), G-K), M-Q) and S-W) ISH analysis of stage 28 tailbud embryos. F), L), R) and X) Graphical representation of ISH analyses. A) *Emx1* is expressed in the forebrain and kidney, black arrowhead marks forebrain expression and asterisk marks kidney expression. B) *Emx1* is expressed in Coco induced ectopic heads, black arrowhead marks ectopic expression. C-E) Embryos coinjected with Coco and single MOs lack ectopic *Emx1* expression in a small proportion of embryos (arrowheads). C) Coinjection of Coco and FMO. D) Coinjection of Coco and CMO. E) Coinjection of Coco and NMO. F) Graphical representation of results from B-E; Coco n=11, CocoFMO n=40, CocoCMO n=22, CocoNMO n=18. G) *Otx2* is expressed in forebrain and midbrain, black arrowhead marks expression. H) *Otx2* is expressed in Coco induced ectopic heads, black arrowhead marks expression. I-K) Embryos coinjected with Coco and single MOs always had ectopic *Otx2* expression, black arrowheads mark expression. I) Coinjection of Coco and FMO. J) Coinjection of Coco and CMO. K) Coinjection of Coco and NMO. L) Graphical representation of results from H-K; Coco n=18, CocoFMO n=33, CocoCMO n=34, CocoNMO n=34. M) *Krox20* is expressed in rhombomere 3+5 of the hindbrain, black arrowhead marks expression. N) *Krox20* was never expressed in Coco induced ectopic heads. O-Q) Coinjection of Coco and single MOs induced ectopic *Krox20* expression in a small proportion of embryos, black arrowheads mark ectopic expression. O) Coinjection of Coco and FMO. P) Coinjection of Coco and CMO. Q) Coinjection of Coco and NMO. R) Graphical representation of results from N-Q; Coco n=18, CocoFMO n=24, CocoCMO n=23, CocoNMO n=13. S) *Hoxb9* is expressed in the spinal cord of stage 28 uninjected control embryos, black arrowhead marks expression. T) *Hoxb9* was never expressed in Coco induced ectopic heads. U-W) Coinjection of Coco and single MOs never induced ectopic *Hoxb9* expression. U) Coinjection of Coco and FMO. V) Coinjection of Coco and CMO. W) Coinjection of Coco and NMO. X) Graphical representation of results from T-W; Coco n=13, CocoFMO n=19, CocoCMO n=24, CocoNMO n=29. A-E), G-K), M-Q) and S-W) are lateral views orientated with dorsal up, ventral down, anterior left and posterior right.

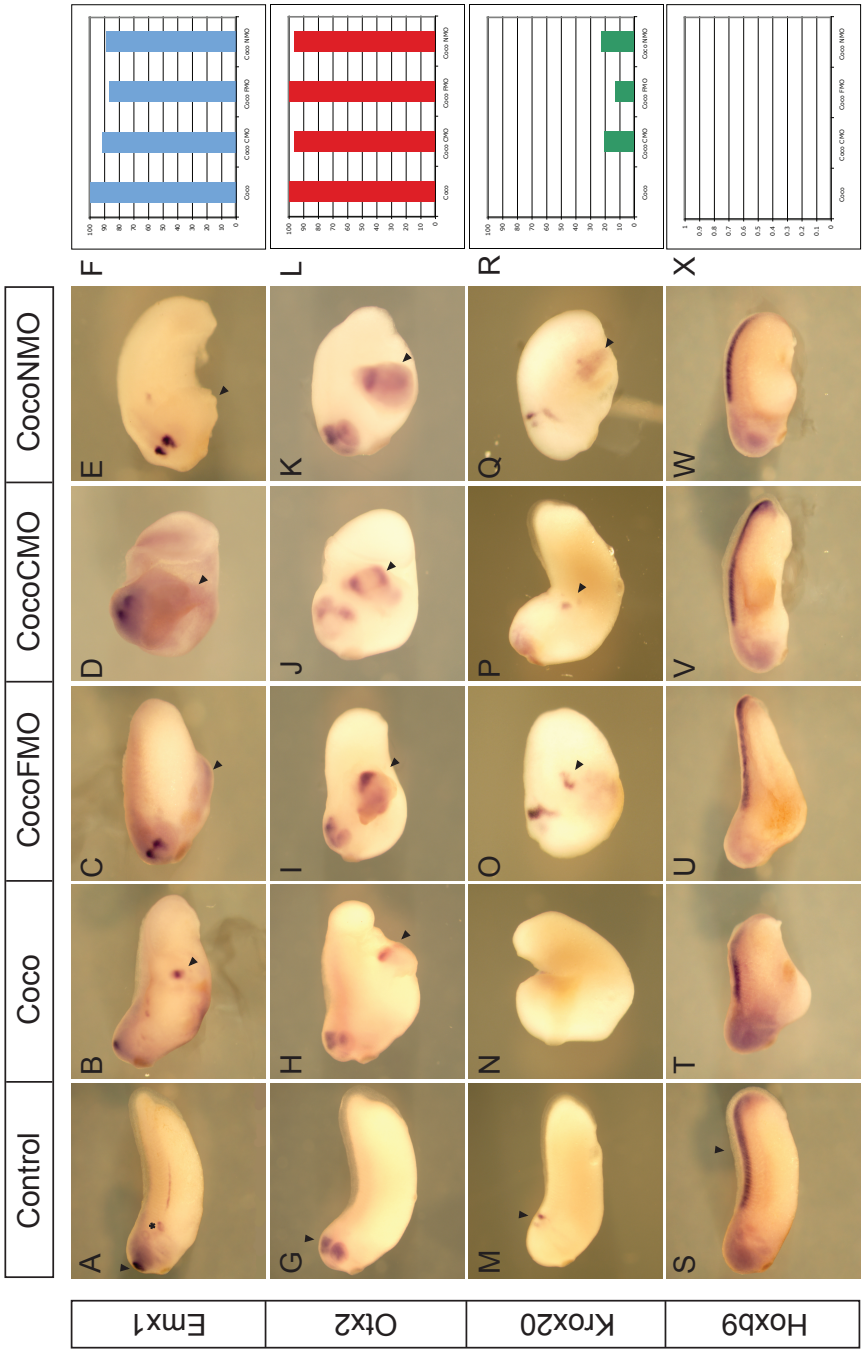

Figure 3.5 - ISH analysis of phenotypes resulting from coinjection of Coco and single MOs against BMP inhibitors

CocoFMO n=32/33, CocoCMO n= 34/34, CocoNMO n=33/34), possible evidence that midbrain tissue was present.

Krox20 (Figure 3.5M) was not expressed in Coco mRNA induced ectopic heads (Figure 3.5N; n=18/18). In a small proportion of embryos coinjected with Coco and a single MO there was ectopic Krox20 expression (arrowheads, Figure 3.5O-R; CocoFMO n= 5/24, CocoCMO n=3/23, CocoNMO n=3/13), indicating that ectopic hindbrain tissue was induced.

Hoxb9, expressed in the spinal cord of wild type embryos (Figure 3.5S) was not expressed in Coco-induced ectopic heads (Figure 3.5T; n=13/13). Ectopic *Hoxb9* was not observed in embryos coinjected with Coco and a MO against a single BMP inhibitor (Figure 3.5U-X; CocoFMO n=19/19, CocoCMO n=24/24, CocoNMO n=29/29), suggesting the absence of ectopic spinal cord tissue.

These results indicated that following reduction of a single BMP inhibitor there was an anterior to posterior fate change of Coco-induced tissue. These results differ from those of previously published work, with an effect observed following a loss of one single BMP inhibitors (Khokha et al., 2005; Wills et al., 2010). This was probably due to the induced axis having a heightened sensitivity to a reduction in BMP inhibition.

Having shown a fate change of induced tissue following coinjection of Coco and a single MO, combinations of two or three MOs against BMP inhibitors were coinjected with Coco mRNA, to see if further AP shifts were observed.

In embryos coinjected with Coco and combinations of two MOs against two different BMP inhibitors there was a lack of ectopic *Emx1* expression (Figure 3.6A-E; CocoCNMO n=7/21, CocoFNMO n=6/19, CocoFCMO n= 6/27) in the induced tissue in a higher proportion of embryos (compare Figure 3.6F to Figure 3.5F). When looking at the forebrain/midbrain marker *Otx2*, embryos coinjected with Coco and 2 MOs always had ectopic expression (Figure 3.6I-K; CocoCNMO n= 21/21, CocoFNMO n=24/25, CocoFCMO n=34/34).

Figure 3.6 – ISH analysis of phenotypes resulting from coinjection of Coco and double MOs against BMP inhibitors. A-E), G-K), M-Q) and S-W) ISH Analysis of tailbud embryos. F), L), R) and X) Graphical representation of ISH analyses. A) *Emx1* is expressed in the forebrain and kidney, black arrowhead marks forebrain expression and asterisk marks kidney expression. B) *Emx1* is expressed in Coco induced ectopic heads, black arrowhead marks ectopic expression. C-E) Emx1 expression in embryos coinjected with Coco and double MOs. C-E) Embryos coinjected with Coco and double MOs lack ectopic *Emx1* expression in a larger proportion of embryos (arrowheads). C) Coinjection of Coco and CNMO. D) Coinjection of Coco and FNMO. E) Coinjection of Coco and FCMO. F) Graphical representation of results from B-E; Coco n=11, CocoCNMO n=21, CocoFNMO n=19, CocoFCMO n=27. G) *Otx2* is expressed in forebrain and midbrain, black arrowhead marks expression. H) *Otx2* is expressed in Coco induced ectopic heads, black arrowhead marks expression. I-K) Embryos coinjected with Coco and single MOs always had ectopic *Otx2* expression, black arrowheads mark expression. I) Coinjection of Coco and CNMO. J) Coinjection of Coco and FNMO. K) Coinjection of Coco and FCMO. L) Graphical representation of results from H-K; Coco n=18, CocoCNMO n=21, CocoFNMO n=25, CocoFCMO n=34. M) *Krox20* is expressed in rhombomere 3+5 of the hindbrain, black arrowhead marks expression. N) *Krox20* was never expressed in Coco induced ectopic heads. O-Q) Coinjection of Coco and single MOs induced ectopic *Krox20* expression in a larger proportion of embryos, black arrowheads mark ectopic expression. O) Coinjection of Coco and CNMO. P) Coinjection of Coco and FNMO. Q) Coinjection of Coco and FCMO. R) Graphical representation of results from N-Q; Coco n=18, CocoCNMO n=19, CocoFNMO n=31, CocoFCMO n=12. S) *Hoxb9* is expressed in the spinal cord of stage 28 uninjected control embryos, black arrowhead marks expression. T) *Hoxb9* was never expressed in Coco induced ectopic heads. U-W) Coinjection of Coco and single MOs never induced ectopic *Hoxb9* expression. U) Coinjection of Coco and CNMO. V) Coinjection of Coco and FNMO. W) Coinjection of Coco and FCMO. X) Graphical representation of results from T-W); Coco n=13, CocoCNMO n=16, CocoFNMO n=21, CocoFCMO n=35. A-E), G-K), M-Q) and S-W) lateral views with dorsal up, ventral down, anterior left and posterior right.

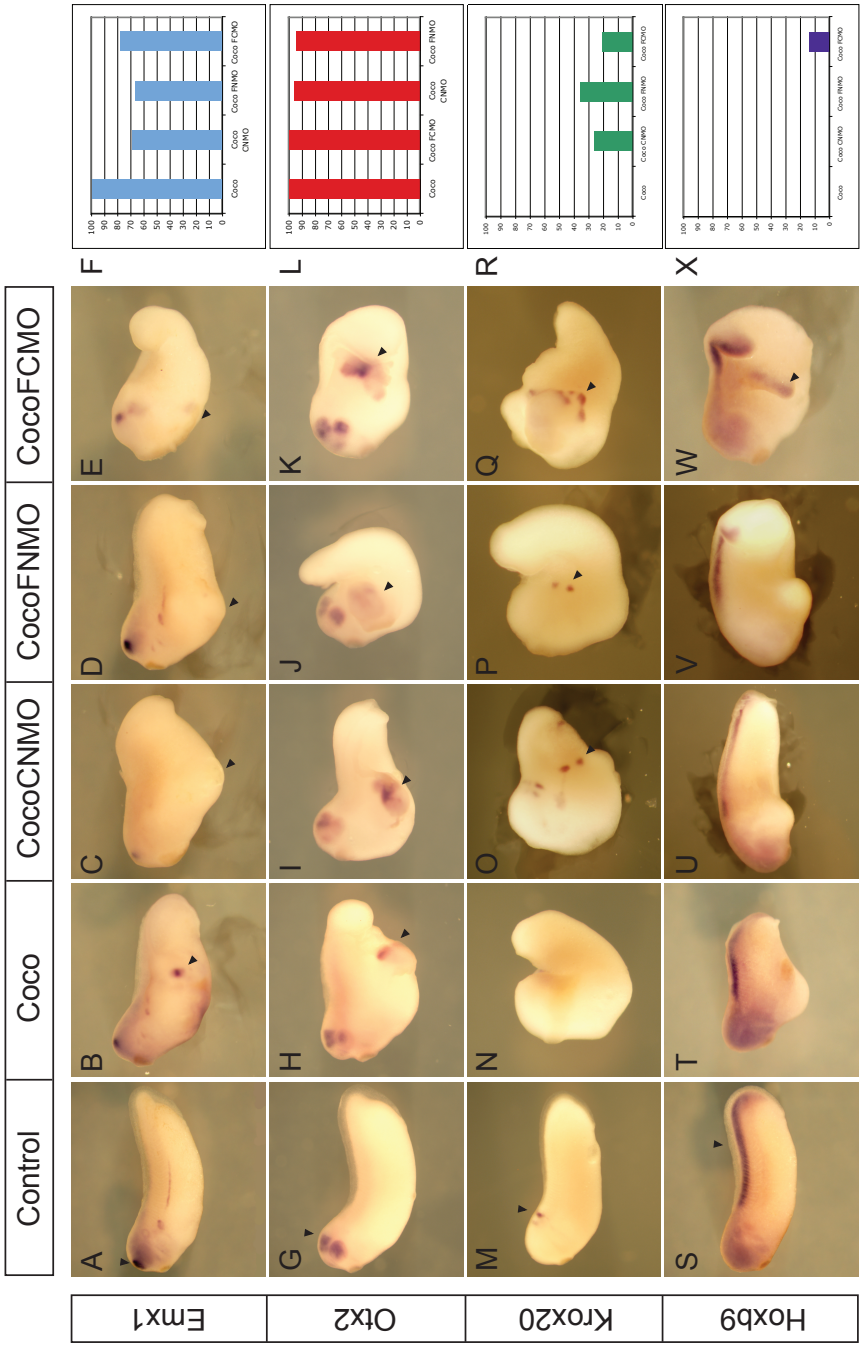

Figure 3.6 - ISH analysis of phenotypes resulting from coinjection of Coco and double MOs against BMP inhibitors.

In embryos coinjected with Coco and two MOs, ectopic Krox20 expression was seen (Figure 3.6O-Q; CocoCNMO n= 7/19, CocoFNMO n=8/31, CocoFCMO n=2/12) in a higher proportion of embryos (compare Figure 3.6R to Figure 3.5R). Ectopic *Hoxb9* expression was never seen in embryos injected with CocoCNMO or CocoFNMO (Figure 3.6S-V; CocoCNMO n=0/16, CocoFNMO n=0/21).

Interestingly however, in embryos injected with CocoFCMO ectopic *Hoxb9* expression was seen in a small proportion of embryos (Figure 3.6W-X; n=5/35), evidence that the induced tissue contained spinal cord tissue.

To see if a further reduction in BMP inhibition following Coco overexpression could cause more severe fate changes, embryos were lastly injected with Coco mRNA and a triple combination of BMP inhibitor MOs.

In half of the embryos coinjected with Coco and FCNMO there was a lack of ectopic *Emx1* expression (Figure 3.7A-C; n=12/24), a much larger proportion than those of single and double combinations (compare Figure 3.7D to Figure 3.6F and Figure 3.5F). However, ectopic *Otx2* expression was present in over 90% of the injected embryos (Figure 3.7E-H; n=21/23). Over 40% of Coco+FCNMO injected embryos exhibited ectopic *Krox20* expression (Figure 3.7I-L; n=9/22), and 25% of injected embryos had ectopic *Hoxb9* expression (Figure 3.7M-P; n=6/24).

These results provide evidence that a reduction in BMP inhibition caused a fate change of Coco-induced ectopic tissue. Overexpression of Coco induced ectopic tissue containing forebrain and midbrain markers (Figure 3.8A). Coinjection of Coco and single and double MOs induced ectopic tissue that also expressed a hindbrain marker at the expense of forebrain (Figure 3.8B). When Coco was coinjected with a triple combination of MOs there was induction of tissue that expressed hindbrain and spinal cord markers (Figure 3.8C).

Figure 3.7 – Molecular analysis of phenotypes resulting from coinjection of Coco and triple MOs against BMP inhibitors. A-C), E-G), I-K) and M-O) Analysis of tailbud embryos. D), H), L) and P) Graphical representation of ISH analysis. A) *Emx1* is expressed in the forebrain and kidney, black arrowhead marks forebrain expression, asterisk marks kidney. B) *Emx1* is expressed in Coco induced ectopic heads, black arrowhead marks ectopic expression. C) Coinjection of Coco and FCNMO caused half of the injected embryos to lack ectopic *Emx1* expression. D) Graphical representation of results from B-C; Coco n=11, CocoFCNMO n=24. E) *Otx2* is expressed in forebrain and midbrain of uninjected control embryos, black arrowhead marks expression. F) *Otx2* is expressed in Coco induced ectopic heads, black arrowhead marks ectopic expression. G) Embryos coinjected with Coco and FCNMO always had ectopic *Otx2* expression, black arrowhead marks ectopic expression. H) Graphical representation of results from F-G; Coco n=18, CocoFCNMO n=23. I) *Krox20* is expressed in rhombomeres 3+5 of the hindbrain, black arrowhead marks expression. J) *Krox20* was never expressed in Coco induced ectopic heads. K) Coinjection of Coco and two MOs induced ectopic *Krox20* expression in about 40% of embryos, black arrowhead marks ectopic expression. L) Graphical representation of results from J-K; Coco n=18, CocoFCNMO n=22. M) *Hoxb9* is expressed in the spinal cord, black arrowhead marks expression. N) *Hoxb9* was never expressed in Coco induced ectopic heads. O) Coinjection of Coco and FCNMO induced ectopic *Hoxb9* expression in a quarter of embryos, black arrowhead marks ectopic expression. P) Graphical representation of results from N-O; Coco n=13, CocoFCNMO n=24. A-C), E-G), I-K) and M-O) are lateral views orientated with dorsal up, ventral down, anterior left and posterior right.

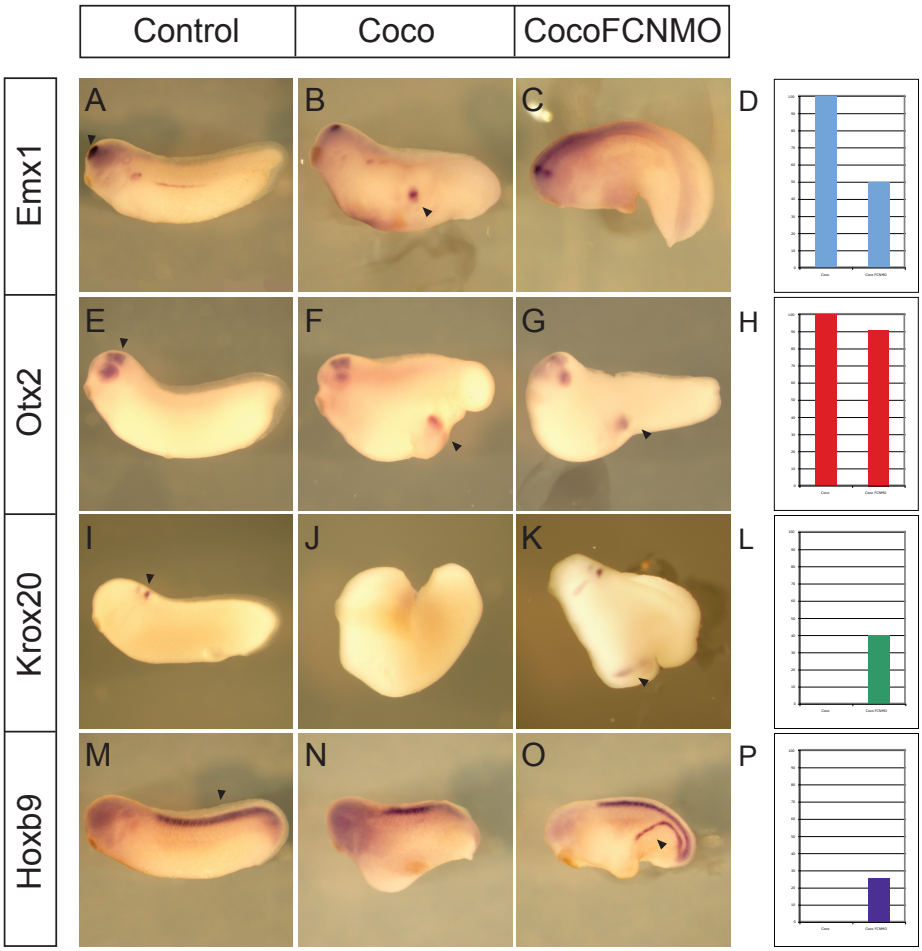

Figure 3.7 - Molecular analysis of phenotypes resulting from coinjection of Coco and triple MOs against BMP inhibitors

Figure 3.8 – Summary of results from Chapter 3. A) Representation of ectopic tissue induced by Coco overexpression, which contained forebrain (blue) and midbrain tissue (red). B) Representation of ectopic tissue induced following coinjection of Coco and single/double MOs, which contained forebrain (blue), midbrain tissue (red) and hindbrain tissue (yellow). C) Representation of ectopic tissue induced following coinjection of Coco and triple MOs, which contained midbrain tissue (red), hindbrain tissue (yellow) and spinal cord tissue (green).

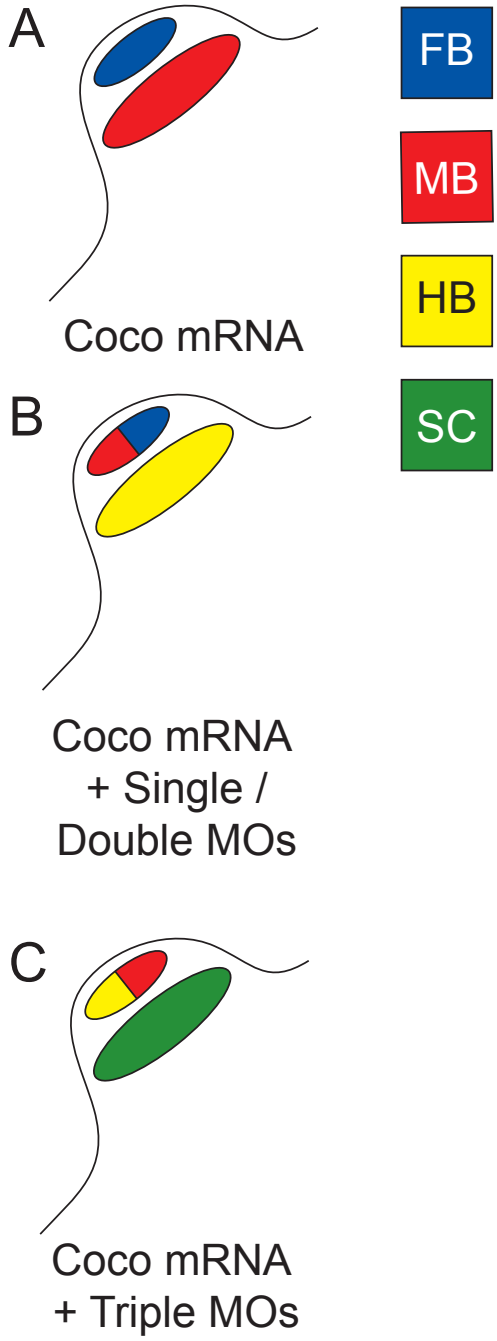

Figure 3.8 - Summary of results from Chapter 3

3.3 Discussion

3.3.1 Chapter summary

Published work reported that localized overexpression of Coco causes the induction of ectopic heads and discussed possible endogenous roles for Coco during early development (Bell et al., 2003). However, whether Coco requires other BMP inhibitors to produce its overexpression phenotype (ectopic fore/midbrain) has not been investigated. This chapter aimed to address this, specifically the requirements of the BMP inhibitors Follistatin, Chordin and Noggin.

Data obtained in this investigation suggests that Coco induces all three BMP inhibitors to induce ectopic heads. Combinatorial injection of Coco and increasing numbers of MOs against three BMP inhibitors showed a fate change of the induced tissue (Figure 3.8). Coinjections of Coco and single MOs very occasionally induced tissue that lacked ectopic *Emx1* (forebrain) expression but did express ectopic *Krox20* (hindbrain). For both double and triple MO combinations, these effects were enhanced; more embryos lacked ectopic forebrain but instead exhibited ectopic hindbrain. Ectopic spinal cord tissue was observed following coinjection with Coco+FCMO and Coco+FCNMO; evidence for possible functional redundancy of the BMP inhibitors induced following Coco overexpression.

Coco's overexpression being affected by FCNMO knockdown in an area where these genes are not normally expressed, suggests that *Chordin*, *Noggin* and *Follistatin* were induced by Coco, ventrally. Coco overexpression increased the expression domain of *Chordin* (data not shown), yet no ectopic staining was observed ventrally. However, overexpression of Coco in the VMZ has previously been shown to induce ectopic *Chordin* (Bell et al., 2003), presumably at levels that could not be detected by in situ hybridization. I propose that the same is true

of both Noggin and Follistatin, with Coco overexpression inducing an ectopic region of BMP inhibition ventrally.

In terms of technical considerations, it is important to remember that the findings from this chapter, the requirement for BMP inhibition, are in reference to Coco's ectopic overexpression activity. This chapter did not investigate the endogenous factors involved with Coco, this being the aim of the next chapter.

3.3.2 Functional redundancy downstream of Coco

When gauging the significance of these results, a loss of forebrain fate following a reduction of BMP signalling is not surprising. Studies in both mouse and frog have shown that inhibition of BMP signalling promotes forebrain specification (Bachiller et al., 2000; Anderson et al., 2002; Davis et al., 2004; Khokha et al., 2005; Wills et al., 2010) and within these studies functional redundancy of BMP inhibitors is often described. In such work, where these signalling molecules acted redundantly, no phenotypes were seen in single morphants/mutants (Bachiller et al., 2000; Khokha et al., 2005). Here, in contrast there was a phenotypic change following the coinjection of Coco and a single BMP inhibitor MO. When employing double and triple combinations of knockdown downstream of Coco, there was not only an increase in the proportion of embryos that displayed fate changes, but also increases in the severity of the fate change.

Though data suggests that other BMP inhibitors do act redundantly following induction by Coco overexpression, it was not clear why the coinjection of a single BMP inhibitor MO caused fate shifts. One possible reason is that Coco only induced the BMP inhibitors Follistatin, Chordin and Noggin ectopically, whilst other BMP inhibitors were missing. For example in a wild type situation Cerberus (Piccolo et al., 1999), Xnr3 (Hansen et al., 1997) and Twisted Gastrulation/TSG (Chang et al., 2001) could compensate for the loss of single BMP inhibitors. The lack of these cooperative factors could give the ectopic

tissue an increased sensitivity to a reduction in BMP inhibition, the most likely cause of fate shifts following coinjection of Coco and a single MO.

3.3.3 Contribution of Wnt and TGFβ inhibition

Coco acts as a multifunctional inhibitor of BMP, Wnt and TGFβ signalling. The phenotypes observed in this investigation have only addressed a reduction of BMP inhibition, as we only MOS blah blah XXXXYYYY . Studies have shown that an inhibition of both BMP and Wnt signalling is required for head induction (Glinka et al., 1997), and it would be conceivable that a reduction of Wnt inhibition in combination with Coco may well have an effect on the overexpression phenotype. Wnt signalling has been shown to be involved in neural induction, but seemingly indirectly by reducing BMP levels in the ectoderm (Baker et al., 1999; Gómez-Skarmeta et al., 2001). Future investigations within our lab will explore the contributions of Wnt and TGFβ inhibition to the Coco overexpression phenotype

These results demonstrate a requirement for BMP inhibition downstream of Coco's overexpression activity. Without BMP inhibitors downstream, Coco cannot induce ectopic heads containing fore- and midbrain, but instead induces more posterior tissues. To understand the endogenous requirement of Coco and whether it is a 'head inducer' (Bell et al., 2003) or whether it is involved in earlier specification (as suggested by its expression profile), MO knockdown was performed to reduce its activity.

Chapter 4 Coco controls germ layer specification via inhibition of TGFβ signalling

4.1 Background

Germ layer specification, the correct organisation of the three embryonic germ layers endoderm, mesoderm and ectoderm, precedes gastrulation and is vital for development.

Several TGFβ ligands are required for endoderm and mesoderm formation. Vg1 is a vegetally localised TGFβ ligand and is involved in endoderm development and dorso-ventral patterning of the marginal zone (Joseph and Melton, 1998), with the *Xenopus* Nodal-related genes Xnr5 and Xnr6 being involved in endoderm and mesoderm specification prior to gastrulation (Luxardi et al., 2010). Activin has been shown to play important roles in both mesoderm and endoderm formation (Hudson et al., 1997; Piepenburg, 2004).

Coco is maternally expressed in the animal pole and is an inhibitor of TGFβ signalling, suggestive of a role in germ layer specification.
Preliminary experiments from the Bell lab used Host Transfer (HT) knockdown to reduce Coco's activity. Oocytes were taken out of donor females and injected with anti-sense oligonucleotides to inhibit Coco RNA, and were matured for 24-48 hours *in vitro* before being placed into host females. HT knockdown of Coco suggested a role on germ layer specification; whilst at tadpole stages a loss of Coco caused a dose dependent loss of anterior structures. (unpublished Vonica, Heasman, Brivanlou, Bell).

I hypothesised that a reduction of Coco allowed one or several of the TGFβ ligands discussed above to become over-active animally, thereby causing a disruption of the germ layers. Importantly, Coco knockdown using specific MOs gave the same phenotype as HT knockdown. To test this hypothesis, rescue experiments were performed. Specific MOs against Coco were injected at the

one-cell stage and then MOs against TGFβs were injected at the two-cell stage. Expression of *Xbra* and *Sox17β* was used to assess mesoderm and endoderm tissue formation following coinjection, to see if there was a rescue of the germ layer defects.

4.2 Results

In order to investigate whether TGFβ ligands are involved downstream of Coco during development, it was initially important to better understand the loss of function phenotype. CocoMO was injected globally at the one-cell stage and mesoderm and endoderm phenotypes assessed at blastula stages.

4.2.1 Coco knockdown causes multiple germ layer defects

Xbra is expressed in the marginal zone of stage 9 *Xenopus laevis* embryos (red arrowheads in B; Fig. 4.1A-B). Following Coco knockdown there was reduction of *Xbra* staining (red arrowheads in D; Fig. 4.1C-D; n= 26/30). *Sox17β* is expressed in the vegetal pole of stage 10 embryos (Fig. 4.1E) throughout the presumptive endodermal cells, but not within the marginal zone or in the ectoderm (Dotted line; Fig. 4.1F). When Coco activity was knocked down there was a shift of the endoderm animally into the marginal zone (dotted line; Fig. 4.1G-H; n= 33/39). When taken together, these data confirm that MO knockdown of Coco phenocopied the loss of mesoderm and shift of endoderm following the HT experiments.

To confirm that the effects seen following CocoMO knockdown were specific, I performed a rescue experiment. Coco mRNA with a 5' mutation (that overcomes the inhibition by the MO) was able to rescue the shift of the endoderm when coinjected with CocoMO (Fig 4.2A-C; n= 14/22). This result suggests that the germ layer defects observed are due to a specific reduction in Coco activity.

I noticed that following Coco knockdown the loss of mesoderm and the shift of endoderm were asymmetric in most of the embryos. To assess whether this effect was specific or random further analysis of the phenotypes were performed.

Coco HT knockdown caused a reduction in antero-dorsal structures in tadpole embryos, so it was hypothesised that a reduction of Coco caused a disruption of

Figure 4.1 – ISH analysis of Stage 9 *Xenopus laevis* embryos injected with CocoMO. A) *Xbra* is expressed in the mesoderm in the marginal zone. B) *Xbra* expression in section, red arrowheads mark expression in the marginal zone. C) *Xbra* expression is lost on one side of embryo following CocoMO injection. D) *Xbra* expression lost on one side of embryo following injection of CocoMO, red arrowhead marks continued expression on one side. E) *Sox17β* is expressed in the endoderm of the vegetal region. F) *Sox17β* expression in section, dotted line marks limit of expression within vegetal region. G) *Sox17β* expression is shifted in embryos injected with CocoMO. H) *Sox17β* expression in section following CocoMO injection, dotted line shows limit of expression is into the marginal zone.

A), C), E) and G) lateral views of whole mount ISH, orientated with animal up and vegetal down. B), D), F) and H) Sections through whole mount ISH, orientated with animal up and vegetal down. Blue staining in C), D), G) and H) is a β-Gal tracer for global CocoMO injections.

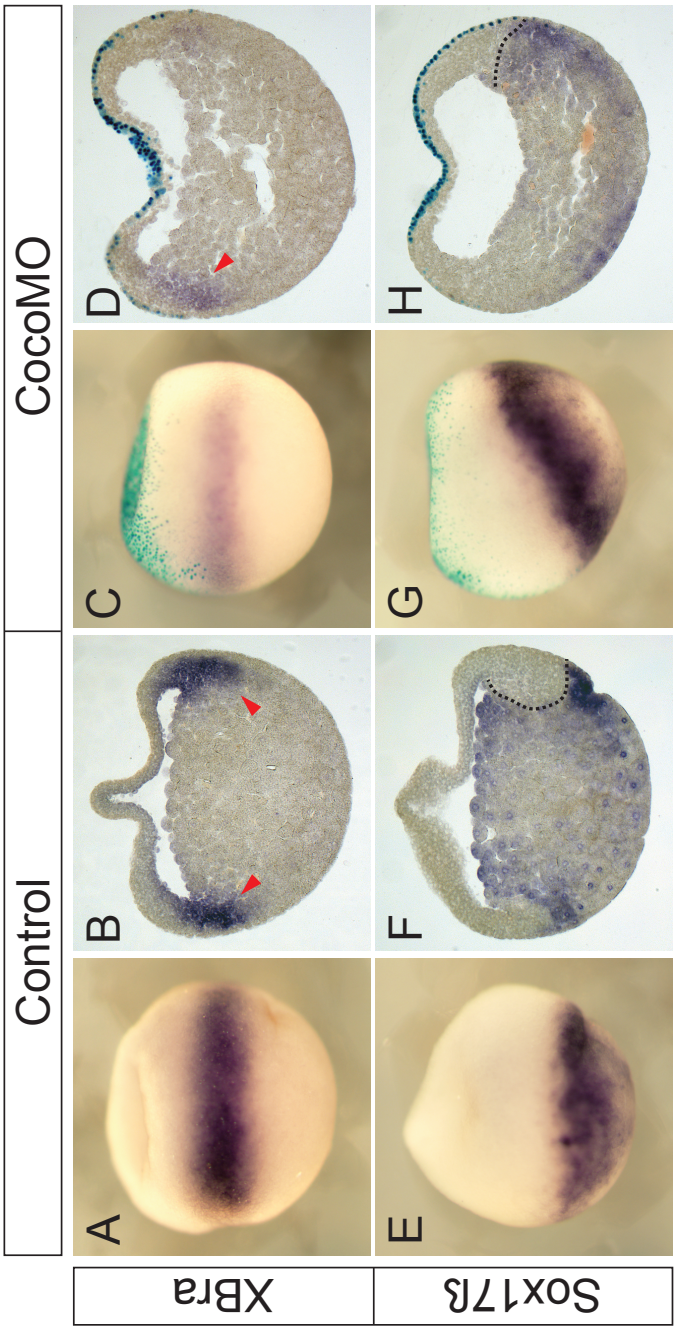

Figure 4.1 - ISH analysis of stage 9 *Xenopus laevis* embryos injected with CocoMO

dorsal tissues at earlier stages. Initially to address this idea, the asymmetry of the mesoderm loss was investigated to see if it was a specific dorsal or ventral effect.

4.2.2 Coco knockdown causes germ layer defects on the dorsal side of the embryo

The initial description of the Coco knockdown phenotype was performed at stage 9, when there is no visible dorso-ventral polarity to the embryo. To overcome this and in order to give the mesodermal defects positional information, phenotypes were assessed in older embryos. At stage 11, when the dorsal blastopore lip was clearly visible and therefore the dorso-ventral axis easily seen, *Xbra* was always expressed in the marginal zone (Fig. 4.3A), which can be seen in section (Fig. 4.3B). However, following Coco knockdown there was a severe reduction in *Xbra* expression, with expression localized to a far more animal domain (Fig. 4.3C; n =18/20). When compared to control expression, there was a reduction in mesoderm (opposite dorsal blastopore lip), an effect that was more severe on the dorsal side (same side as dorsal lip) of the embryo (red arrowhead, Fig. 4.3D). These results suggest that the loss of mesoderm seen at stage 9 was predominantly affecting the dorsal marginal zone. To further confirm this, expression of *Chordin*, a presumptive dorsal mesoderm marker (Fig. 4.3E) was analysed. Following CocoMO injection a reduction of Chordin expression was observed (Fig. 4.3F), further evidence that a loss of Coco caused a disruption to dorsal mesoderm.

Having shown that Coco knockdown caused a loss of dorsal mesoderm; it seemed likely that the endoderm phenotype would have similar asymmetry. When assessing endoderm phenotypes at later stages, gastrulation cell movements caused the endoderm to become internalised, making the shift of endoderm hard to observe via whole mount ISH (data not shown). Because of this, lineage tracing was utilised to analyse the endoderm shift in more detail. Coco was knocked down globally at the one cell stage, and then at the 4-cell stage, when the pigmentation allows dorso-ventral orientation, a β-Gal tracer was injected either ventrally or dorsally.

Figure 4.2 – Rescue of CocoMO endoderm shift with injection of Coco mRNA. A) *Sox17β* is expressed in the endoderm. B) *Sox17β* expression is shifted in embryos injected with CocoMO. C) Shift of *Sox17β* expression is rescued with embryos coinjected with CocoMO and Coco mRNA.

A-C) and are lateral views, orientated with animal up and vegetal down.

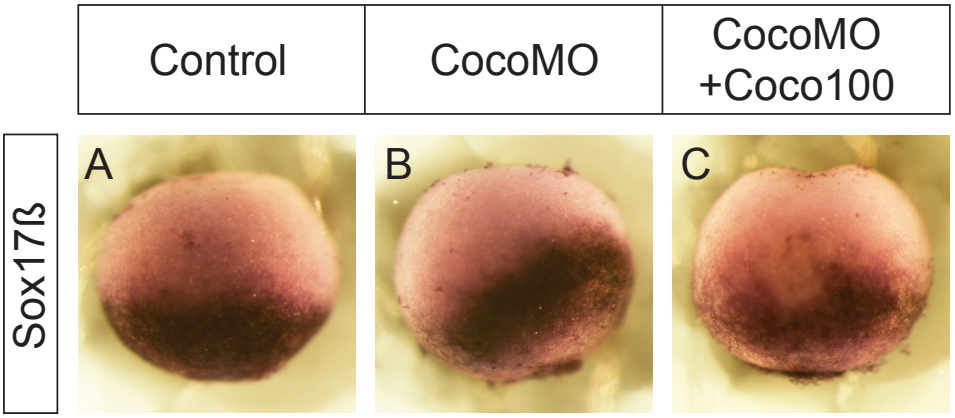

Figure 4.2 - Rescue of CocoMO endoderm shift with injection of Coco mRNA in stage 9 Xenopus laevis embryos.

Figure 4.3 - ISH analysis of mesoderm loss in *Xenopus laevis* embryos injected with CocoMO. Analysis of stage 11 embryos (A-D). Analysis of stage 9 embryos (E-F). A-B) *Xbra* is expressed in the mesoderm of the closing blastopore ring. C) *Xbra* expression is weaker and in a more animal domain following injection of CocoMO. D) *Xbra* expression in section following CocoMO injection, red arrowhead marks continued expression. E) *Chordin* is expressed in the presumptive dorsal mesoderm. F) *Chordin* expression in reduced in embryos injected with CocoMO.

A), C), E) and F) lateral views, orientated with animal up and vegetal down. B) and D) sections through stage 11 embryo orientated with animal up, vegetal down and dorsal right.

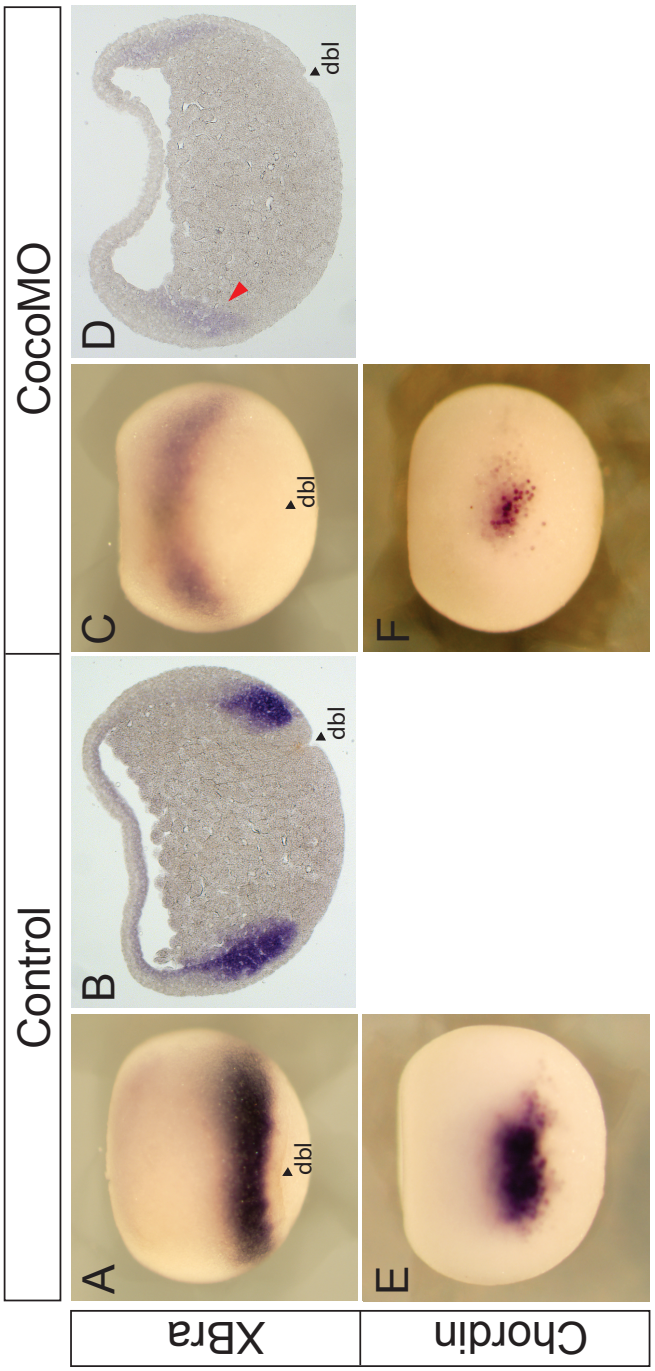

Figure 4.3 - ISH analysis of mesoderm loss in Xenopus laevis embryos injected with CocoMO

When Coco was knocked down and β-Gal injected dorsally, there was a shift of *Sox17β* expression on the same side as the tracer (compare Fig. 4.4A to Fig. 4.4B; n=8/11). Conversely, when β-Gal was injected ventrally, the shift of *Sox17β* expression occurred on the opposite side from the tracer (Fig. 4.4C; n=7/10). Figure 4.4 is a summary of the results from the first part of this chapter. These results confirm that both the loss of mesoderm (Fig 4.5A-B) was most severe and the shift of endoderm occurred on the dorsal side of the embryo (Fig. 4.5C-D).

Coco inhibits TGFβ ligands, factors that are essential for mesoderm and endoderm specification. I hypothesised that Coco protected ectodermal fate via inhibition of TGFβ signalling. It seemed possible that Coco knockdown allowed an animal over activation of a TGFβ ligand that caused a disruption of germ layers. To test this, rescue experiments were planned. CocoMO was injected at the one cell stage and then following the first cell division a TGFβMO (together with a β-Gal tracer) was injected in order to rescue correct germ layer formation.

4.2.3 A reduction of Vg1 following Coco knockdown is unable to rescue germ layer defects

Vg1 is a TGFβ ligand that is essential for endoderm and mesoderm specification (Joseph and Melton, 1998; Birsoy, 2006) so to test whether an excess of Vg1 signalling was causing the germ layer defect, CocoMO was coinjected with Vg1MO.

Coco knockdown caused a reduction in *Xbra* expression when compared to uninjected controls (compare Fig. 4.6A-A' with Fig. 4.6B-B'; n = 12/13). Following coinjection with Vg1MO no obvious rescue of mesoderm was observed (arrowhead, Fig. 4.6C-C'; n= 7/8), whilst injection of Vg1MO alone

Figure 4.4 – Analysis of endoderm shift phenotype resulting from CocoMO injection. A) *Sox17β* is expressed in the endoderm. B) *Sox17β* expression is shifted towards a dorsal β-Gal stain in embryos injected with CocoMO. B) *Sox17β* expression is shifted away from a ventral β-Gal stain in embryos injected with CocoMO.

A-C) Lateral views orientated with animal up and vegetal down.

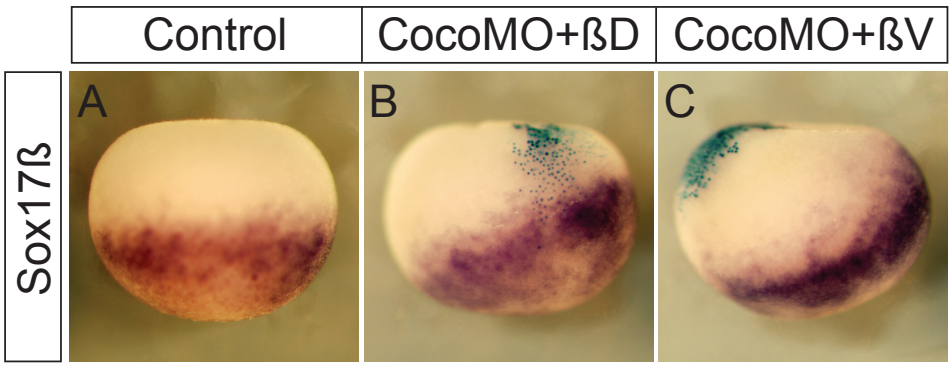

Figure 4.4 - Analysis of endoderm shift phenotype resulting from CocoMO injection

Figure 4.5 – Diagram of phenotypes resulting from Coco knockdown in *Xenopus laevis* embryos. A) Representation of wild type *Xbra* expression in the marginal zone. B) Representation of *Xbra* expression in an embryo injected with CocoMO globally at the one-cell stage, showing most severe loss of mesoderm dorsally. C) Representation of wild type *Sox17β* expression in the vegetal region. D) Representation of *Sox17β* expression in an embryo injected with CocoMO globally at the one-cell stage, showing an animal shift of endoderm dorsally.

All diagrams are representations of stage 9 embryos orientated with animal to the top, vegetal to the bottom, ventral to left and dorsal to the right.

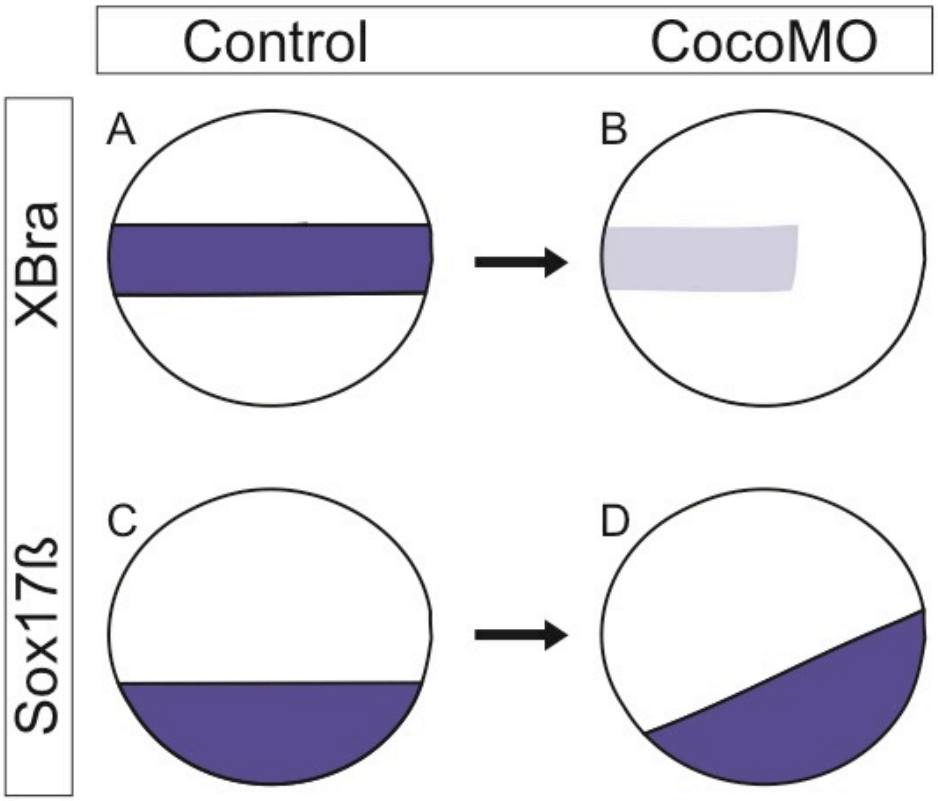

Figure 4.5 - Diagrammatic representation of phenotypes resulting from *Coco* knockdown in *Xenopus laevis* embryos

Figure 4.6 – Analysis of germ layer phenotypes resulting from coinjection of CocoMO and Vg1MO. A-A') *Xbra* is expressed in the mesoderm of the marginal zone. B) *Xbra* expression is reduced in embryos injected with CocoMO, B') *Xbra* expression is lost in the marginal zone. C-C') Lost *Xbra* expression is not rescued in embryos coinjected with CocoMO and Vg1MO* red arrowhead in C' marks continued lack of expression in marginal zone. D-D') *Xbra* is reduced in embryos injected with Vg1MO alone, red arrowhead in D' marks continued expression in marginal zone. E-E') *Sox17β* is expressed in the endoderm. F) *Sox17β* expression is shifted in embryos injected with. F') *Sox17β* expression shift is into the marginal zone, red arrowhead marks expression. G-G') *Sox17β* expression shift is not rescued in embryos coinjected with CocoMO and Vg1MO*, red arrowhead in G' shows continued expression in marginal zone. H-H') *Sox17β* expression ir reduced in embryos injected with Vg1MO alone.

A-D) and E-H) are lateral views, orientated with animal up and vegetal down. A'-D') and E'-H') are sections orientated with animal up and vegetal down. Blue staining in C-D') and G-H') is a β-Gal tracer for the injection of the Vg1MO.

*CocoMO/Vg1MO embryos are injected at the one-cell stage with CocoMO, and then injected with Vg1MO with β-Gal in one of the two blastomeres at the two-cell stage.

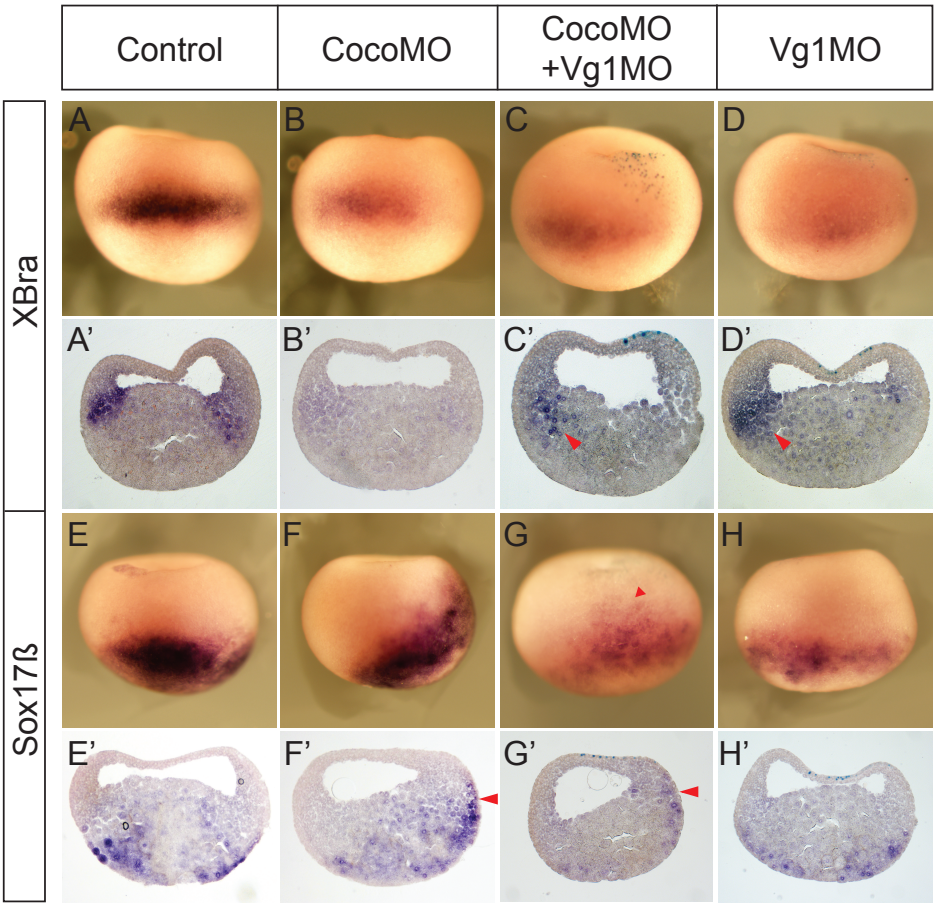

Figure 4.6 - Analysis of germ layer phenotypes resulting from coinjection of CocoMO and Vg1MO

caused a loss of mesoderm (Fig. 4.6D-D'; n = 6/8). Although a reduction of *Xbra* following Vg1MO injection has not been shown before, Vg1MO was shown to inhibit the induction of *Xbra* in animal-vegetal conjugate experiments (Birsoy, 2006). This would explain why Vg1MO was unable to rescue the loss of mesoderm.

To assess whether Vg1MO could rescue the endoderm shift, *Sox17β* expression was again analysed (Fig. 4.6E-F and E'-F'). There was no clear rescue of the endoderm shift following coinjection of CocoMO and Vg1MO (arrowhead, Fig 4.6G-G'; n=9/10) although there was a reduction in *Sox17β* intensity. Compared to CocoMO injection alone (Fig 4.6E-F') Vg1MO injection alone caused a similar reduction in *Sox17β* staining, which did not affect the domain of its expression (Fig. 4.6H-H'; n=8/10). The reduction in *Sox17β* staining (that had no effect on expression domain) following Vg1MO injection was probably the reason for the *Sox17β* shift to have a reduced intensity following coinjection.

These results provide evidence that reducing levels of Vg1 affected both mesoderm and endoderm but could not rescue Coco's knockdown phenotype. It is therefore unlikely that an over activation of Vg1 signalling was the cause of the Coco loss-of-function defects.

Xnr5 and Xnr6 are *Xenopus* Nodal-related genes that were shown to be essential for mesoderm and endoderm formation (Luxardi et al., 2010). To investigate whether a Nodal-related signal was increased following the reduction of Coco activity, coinjections of CocoMO and Xnr5/6MO were performed.

4.2.4 A reduction of both Xnr5 and Xnr6 following Coco knockdown is unable to rescue germ layer defects

Coco knockdown caused a loss of mesoderm (compare Fig. 4.7A-A' to Fig. 4.7B-B'), which coinjection of Xnr5/6 MO was unable to rescue, instead causing a more severe reduction in *Xbra* staining in the marginal zones (Fig. 4.7C-C';

Figure 4.7 – Analysis of germ layer phenotypes resulting from coinjection of CocoMO and Xnr5/6MO. A-A') *Xbra* is expressed in the mesoderm of the marginal zone. B) *Xbra* expression is reduced in embryos injected with CocoMO, B') *Xbra* expression is lost in the marginal zone. C-C') Lost *Xbra* expression is not rescued in embryos coinjected with CocoMO and Xnr5/6MO*. D-D') *Xbra* expression expands into the animal pole in embryos injected with Xnr5/6MO alone, red arrowhead in D' marks expansion of expression in marginal zone. E-E') *Sox17β* is expressed in the endoderm. F) *Sox17β* expression is shifted in embryos injected with. F') *Sox17β* expression shift is into the marginal zone, red arrowhead marks expression. G-G') *Sox17β* expression shift is partially rescued in embryos coinjected with CocoMO and Xnr5/6MO*, red arrowhead in G' shows expression in animal pole. H-H') *Sox17β* expression is reduced in embryos injected with Xnr5/6MO alone.

A-D) and E-H) are lateral views, orientated with animal up and vegetal down. A'-D') and E'-H') are sections orientated with animal up and vegetal down. Blue staining in C-D') and G-H') is a β-Gal tracer for the injection of Xnr5/6MO.

*CocoMO/Xnr5/6MO embryos are injected at the one-cell stage with CocoMO, and then injected with Xnr5/6MO with β-Gal in one of the two blastomeres at the two-cell stage.

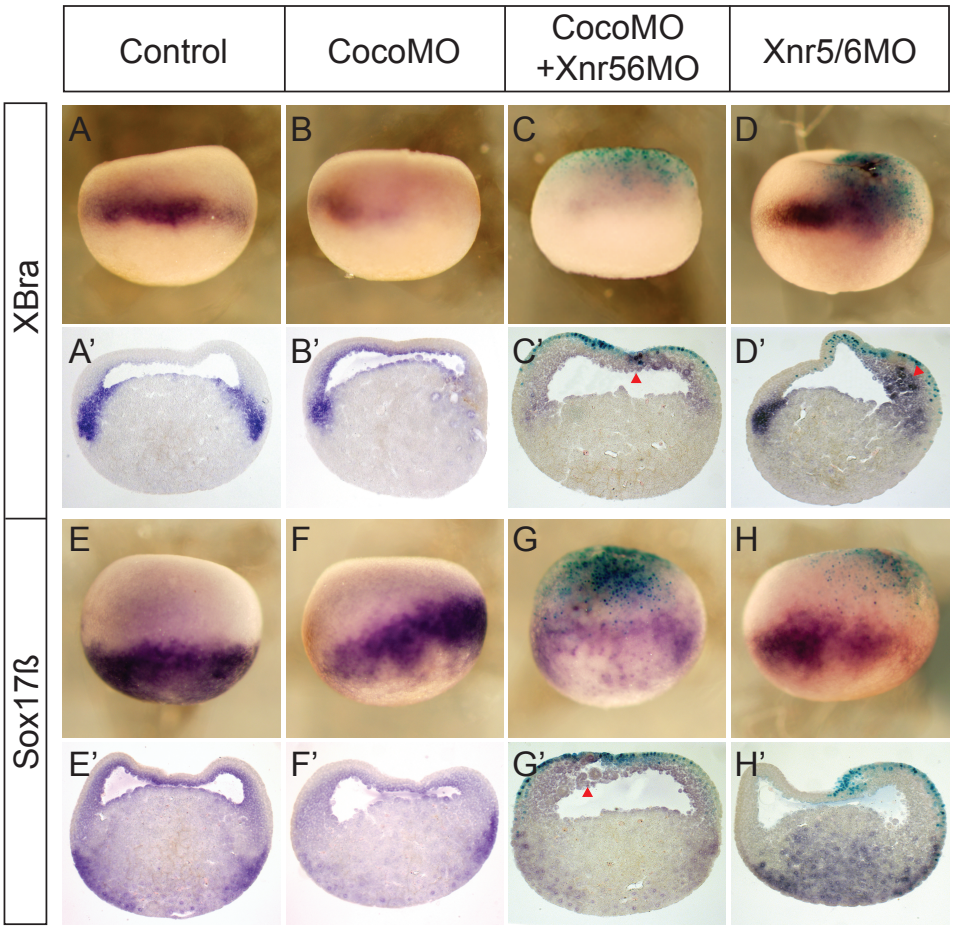

Figure 4.7 - Analysis of germ layer phenotypes resulting from coinjection of CocoMO and Xnr5/6MO

n=8/11). This further reduction in *Xbra* expression following coinjection of CocoMO and Xnr5/6MO, is a result that agrees with previously published loss of function of Xnr5/6 (Luxardi et al., 2010). Surprisingly, coinjection of CocoMO and Xnr5/6MO induced ectopic *Xbra* expression in the animal pole (arrowhead, Fig. 4.7C) in cells that would normally be ectodermal. When injecting Xnr5/6MO animally there was a clear expansion of *Xbra* expression into the animal pole (arrowhead, Fig. 4.7D-D'). High power images (data not shown) of Xnr5/6MO injected embryos show that the cells in the animal pole exhibit a mesodermal morphology, being larger and less tightly packed. Future experiments could investigate this further and explain this apparent change in cell fates.

In order to test the ability of Xnr5/6MO to rescue the change in *Sox17β* expression seen following Coco knockdown (compare Fig. 4.7E-E' to Fig. 4.7F-F'), endoderm phenotypes were assessed following coinjection. However, a reduction of Xnr5/6 downstream of Coco knockdown was only able to partially rescue the shift of endoderm (Fig. 4.7G; n= 6/9) and again seemed to induce ectopic *Sox17β* expression in the animal pole (arrowhead, Fig. 4.7G'). Injection of Xnr5/6MO alone in the animal region caused a reduction of *Sox17β* expression and also an expansion of the marginal zone (Fig. 4.7H-H'; n=6/10).

This data confirming that Xnr5/6MO was only to have a partial rescue of Coco's loss of function phenotype provided evidence that, like Vg1, Xnr5/6 was unlikely to have become over-activated following Coco knockdown, and therefore was not responsible for the germ layer defects. One interesting observation was the change to the animal region of the embryo following Xnr5/6 injection. Coinjection caused both *Xbra* and *Sox17β* expression in the animal pole whilst Xnr5/6MO alone caused an expansion of *Xbra*, but not *Sox17β* staining in the animal region, results that have not previously been described.

4.2.5 A reduction of Activin following Coco knockdown is able to rescue both germ layer phenotypes

Activin, a TGFβ ligand, was shown to be involved in both endoderm and mesoderm development (Hudson et al., 1997; Piepenburg, 2004) and to have a dorso-ventral bias during blastula and gastrula stages of *Xenopus laevis* development (Green et al., 1994; Schohl and Fagotto, 2002). Due to Activin's involvement in germ layer specification and a reported asymmetric activity pattern it seemed highly possible that its over-activation could be causing the mesoderm and endoderm phenotypes caused by Coco knockdown.

Importantly, coinjection of CocoMO and ActivinMO was able to rescue the loss of *Xbra* expression (Fig 4.8A) caused by Coco knockdown (compare Fig 4.8B and Fig 4.8C; n=12/16), a result that was confirmed when looking in sections (arrowhead, Fig. 4.8 C'). When injected alone, ActivinMO caused a reduction in *Xbra* (Fig. 4.8D; n=14/17), the severity of which became clearer in sections (arrowhead; Fig. 4.8D').

Next, the ability for ActivinMO to rescue the dorsal shift of endoderm was addressed (compare Fig. 4.8E-E' to Fig. 4.8F-F'; n=12/15). A reduction in Activin signalling following Coco knockdown was able to rescue the animal shift of *Sox17β* expression (Fig. 4.8G-G'; n= 16/26). ActivinMO alone caused a reduction in *Sox17β* staining, which did not affect the spatial pattern (Fig. 4.8H-H').

When taken together, these results confirm that ActivinMO was able to rescue both the loss of mesoderm and the shift of endoderm. This data suggests that following Coco knockdown (a reduction in Coco's activity), *Activin* becomes active more animally, thereby causing a disruption to the specification and spatial organisation of the germ layers.

4.2.6 Model

The experiments presented in this chapter provide evidence that in a wild type situation Coco (expressed in the animal pole) acts to inhibit Activin signals from the marginal zone from becoming active more animally (Fig. 4.9A). Following Coco knockdown and therefore a reduction in Activin inhibition, Activin signals are able to become over active animally, presumably with a dorsal bias (Figure 4.9B). It is the asymmetric increase in Activin that could be causing the asymmetric germ layers defect seen (Figure 4.9 C-F).

Figure 4.8 – Analysis of germ layer phenotypes resulting from coinjection of CocoMO and ActivinMO. A-A') *Xbra* is expressed in the mesoderm of the marginal zone. B) *Xbra* expression is reduced in embryos injected with CocoMO, B') *Xbra* expression is lost in the marginal zone. C) Lost *Xbra* expression is rescued in embryos coinjected with CocoMO and ActivinMO*, C') Xbra expression rescued in the marginal zone, red arrowhead marks expression. D-D') *Xbra* expression is reduced in embryos injected with ActivinMO alone, red arrowhead in D' marks weaker expression in marginal zone. E-E') *Sox17β* is expressed in the endoderm. F) *Sox17β* expression is shifted in embryos injected with. F') *Sox17β* expression shift is into the marginal zone, red arrowhead marks expression. G-G') *Sox17β* expression shift is rescued in embryos coinjected with CocoMO and ActivinMO*, red arrowhead in G' shows wild type expression limit. H-H') *Sox17β* expression is reduced in embryos injected with ActivinMO alone.

A-D) and E-H) are lateral views, orientated with animal up and vegetal down. A'-D') and E'-H') are sections orientated with animal up and vegetal down. Blue staining in C-D') and G-H') is a β-Gal tracer for the injection of ActivinMO.

*CocoMO/ActivinMO embryos are injected at the one-cell stage with CocoMO, and then injected with ActivinMO in one of the two blastomeres at the two-cell stage.

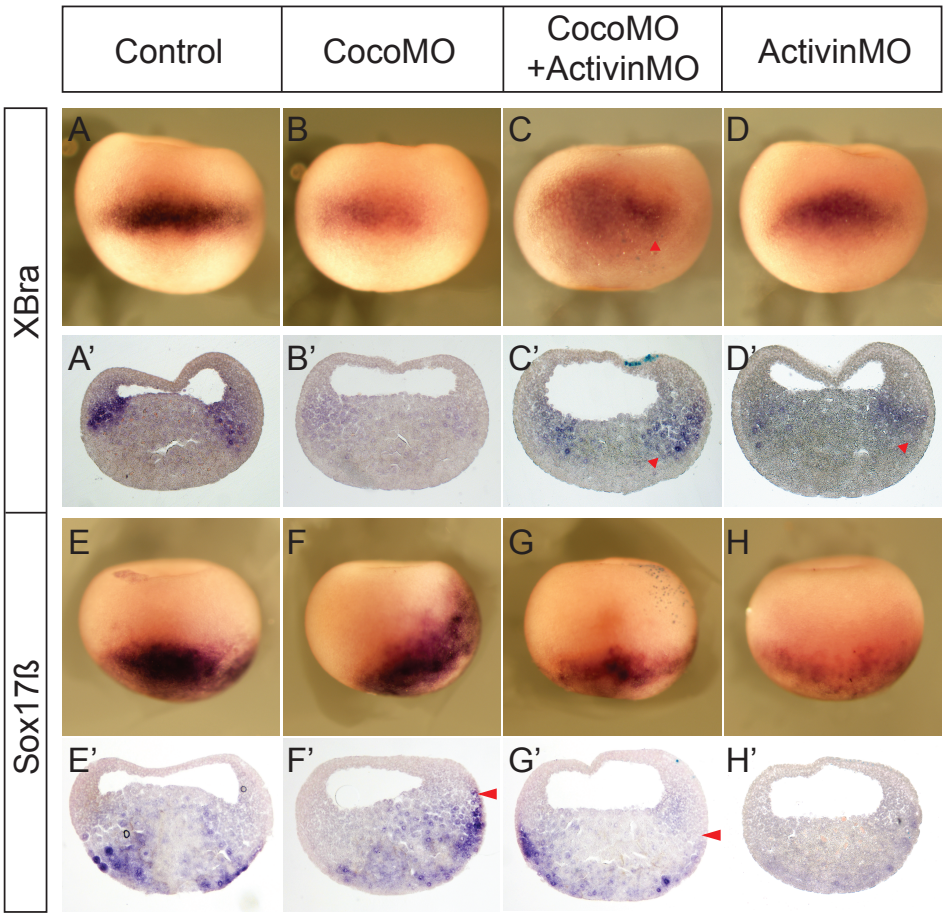

Figure 4.8 - Analysis of germ layer specification resulting from coinjection of CocoMO and ActivinMO

Figure 4.9 – Summary of phenotypes resulting from CocoMO injection in *Xenopus laevis*. A-B) Model of Coco inhibition of Activin in wild type and Coco MO injected embryos. C-F) Corresponding mesoderm and endoderm phenotypes in stage 9 embryos. A) In a wild type situation Coco (Blue) acts to inhibit the dorso-ventrally biased Activin signals from the marginal zone. B) Following knockdown of Coco there is an asymmetric over activation of the Activin signals dorsally. C) Representation of wild type *Xbra* expression (a marker of mesoderm), D) Representation of Xbra expression in embryo injected with CocoMO globally at the one-cell stage. CocoMO induced loss of *Xbra*, most severe dorsally. E) Representation of wild type *Sox17β* expression (a marker of endoderm), D) Representation of *Sox17β* expression in embryo injected with CocoMO globally at the one-cell stage, showing animal shift of endoderm dorsally.

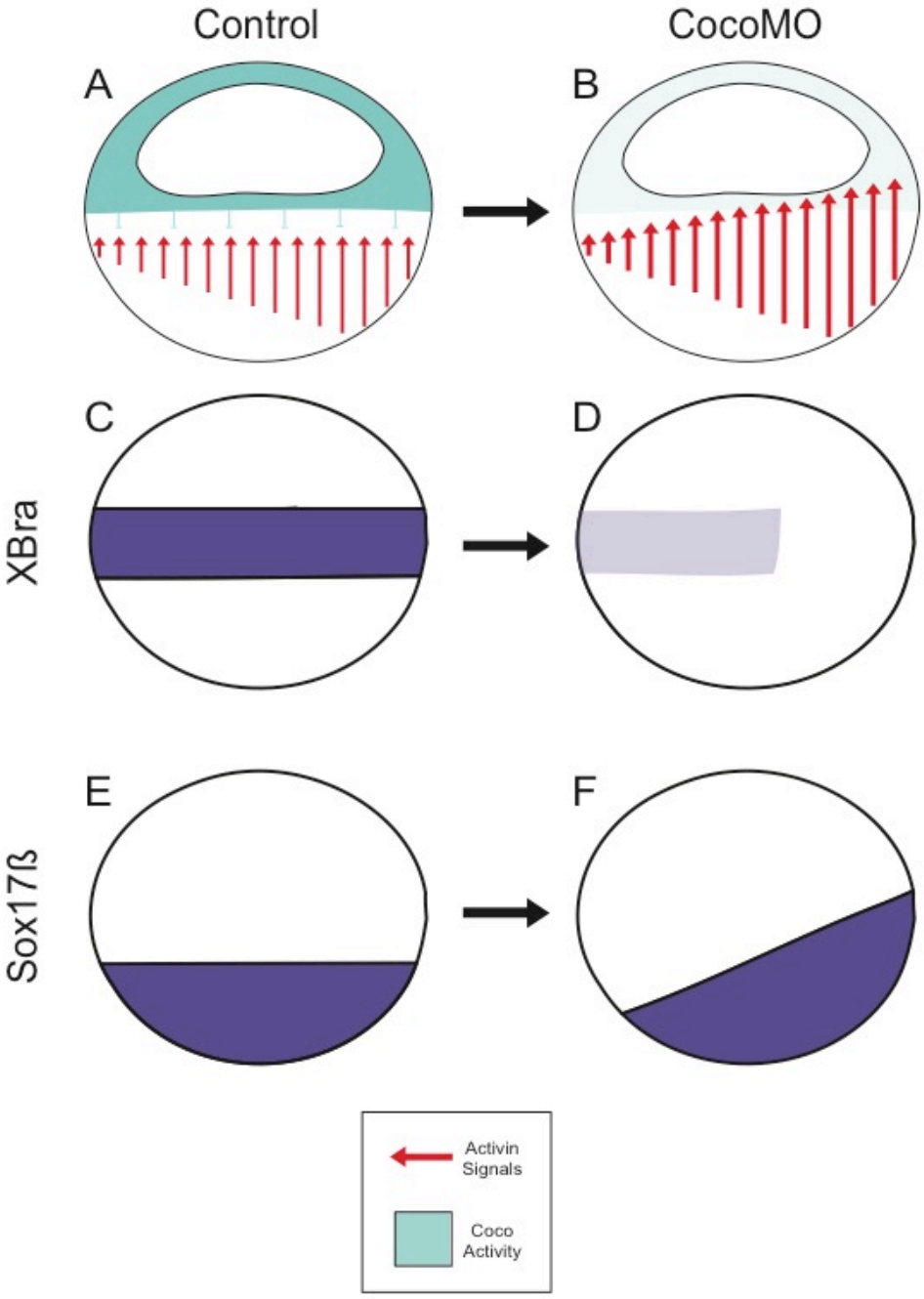

Figure 4.9 - Summary of phenotypes resulting from CocoMO injection in *Xenopus laevis*

4.3 Discussion

4.3.1 Chapter summary

Coco's overexpression phenotype, the induction of ectopic heads that contain forebrain and midbrain tissue, highlighted a possible role in neural induction. However preliminary loss of function data suggested instead that Coco's endogenous role was in germ layer specification. HT knockdown of Coco caused germ layer defects at gastrula stages and loss of anterior and dorsal structures at tadpole stages. This chapter aimed to better understand the knockdown phenotypes and identify any signalling molecules that could be involved.

Following knockdown of Coco, asymmetric phenotypes were seen. There was a reduction of mesoderm throughout the marginal zone, which was most severe dorsally, whilst the endoderm expanded into the animal region, dorsally. The effect of CocoMO on ectodermal specification was also investigated, however unfortunately ISH analysis using the ectodermally specific DIG probes against both *Xema* and *Ectodermin* was unsuccessful.

Due to Coco's ability to inhibit TGFβs and its expression pattern, it was hypothesised that an over activation of TGFβ signalling may have resulted in the germ layer defects. Experiments were performed where CocoMO was coinjected with TGFβ MOs in an attempt to rescue the shift of endoderm and loss of mesoderm. Knockdown of neither Vg1 nor Xnr5/6 were successful in rescuing the germ layer defects, however, knockdown of Activin was able to rescue both phenotypes. Data demonstrated that injection of CocoMO allowed an over activation of Activin that caused the germ layer defects, highlighting an endogenous requirement for Coco to inhibit Activin signals from becoming active animally.

When performing MO knockdowns, it is important to perform mRNA rescue to show that phenotypes are specific. Coinjection of CocoMO and Coco mRNA

with a 5' mutation was able to rescue the germ layer defects observed confirming that it was specifically a reduction of Coco that was causing the germ layer defects described here. In addition it was important to check that the Coco MOs do not have a non-specific affect. To address this CocoMUT (an 8-base change MO) morpholino was injected, which caused no germ layer disruption (data not shown).

4.3.2 What causes the shift of endoderm following CocoMO injection

TGFβ signalling has been shown to be involved in endoderm and mesoderm formation during development (Schier, 2003). I show that the TGFβ ligand Activin became overactive following Coco knockdown, causing germ layer defects following its increase in activity.

Evidence has shown that the highest levels of Activin signalling occur in the vegetal pole, specifying endodermal fate (Faure et al., 2000) while a gradient of Activin activity has also been reported in the developing marginal zone (Schohl and Fagotto, 2002). High levels of Activin induce mesoderm with dorsal characteristics, whilst lower levels induce more ventral cell types (Green et al., 1994). Further, pSmad2, the active mediator of Activin/TGFβ signalling, is enriched dorsally from stage 9 until stage 10 (Schohl and Fagotto, 2002), providing molecular evidence that Activin signalling has a dorso-ventral bias during blastula stages. Collating these results, three different Activin thresholds can be assumed (Fig 4.10A), with the highest level inducing endoderm, the next level inducing axial/dorsal mesoderm and the lowest level inducing ventral mesoderm. Following Coco knockdown Activin signals become asymmetrically over-active in the animal pole, suggesting that the endodermal threshold is reached through the dorsal portions of the marginal zones, at the expense of dorsal mesoderm (Fig 4.10B). Future experiments that highlight increased levels of pSmad2 in the animal region dorsally would further confirm that the observed germ layer defects were caused by an over activation of Activin signalling.

Figure 4.10 – Model: altered Activin levels affect germ layer specification following CocoMO injection. A) Diagrammatic representation of different Activin levels in a stage 9 *Xenopus laevis* embryo. 1) Lowest levels induce ventral mesoderm, 2) next highest induces dorsal mesoderm, 3) highest levels induce endoderm. B) Diagrammatic representation of Activin levels after CocoMO injection. The domain that normally induces dorsal mesoderm receives a higher signal and endoderm is induced instead.

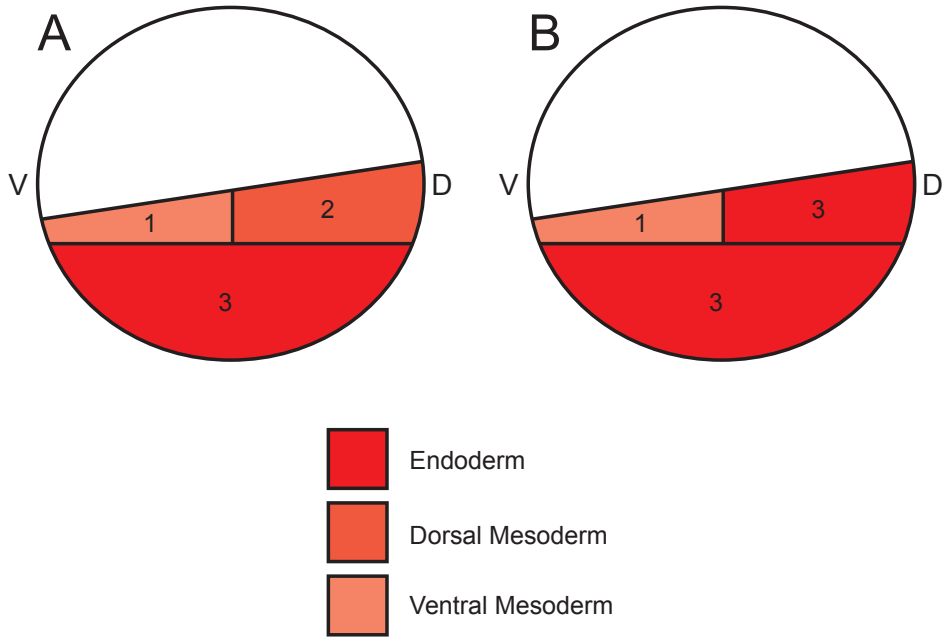

Figure 4.10 - Model: altered Activin levels affect germ layer specification following CocoMO injection

Table 4-1 Factors with a similar role to Coco in development

Gene Name	Expression	Domain	Role	Effect on BMP Signalling	Effect on TGFβ Signalling	Effect on Wnt Signalling
Coco	Maternal	Ectoderm	Extracellular Binding	Antagonist	Antagonist	Antagonist
Cerberus	Zygotic	Anterior Endoderm	Extracellular Binding	Antagonist	Antagonist	Antagonist
Xema	Zygotic	Ectoderm	Transcription Factor	-	-	-
Norrin	Maternal	Ectoderm	Extracellular Binding	Antagonist	Antagonist	Agonist
Ectodermin	Maternal	Ectoderm	Smad4 Ubiquitin Ligase	Antagonist	Antagonist	-

4.3.3 Coco seems to have a distinct role protecting ectodermal fate during development

Coco is a BMP, TGFβ and Wnt inhibitor expressed maternally in the ectoderm. Coco loss of function caused germ layer defects and a loss of anterior structures at tadpole stages. Cerberus, Xema, Norrin and Ectodermin are genes that share certain characteristics (Table 4.1), but are not identical to Coco.

Cerberus is more likely to be involved in head induction due to its expression domain (Bouwmeester et al., 1996; Piccolo et al., 1999) and although Norrin was able to inhibit Activin and BMP4 signalling in vitro, in contrast to Coco it is a Wnt agonist (Xu et al., 2012). Because of this Wnt activation it seems that Norrin is involved in neurectoderm specification rather than protecting ectodermal fate.

Ectodermin was shown to have a role very important role in ectoderm specification. It acts to restrict the activity of TGFβ signals to the mesoderm by restricting Smad4 distribution (Dupont et al., 2005). These results suggest that Ectodermin is essential for the specification of the ectoderm and is could be a maternal animal patterning factor in *Xenopus* opposing Nodal-related signals.

Xema (Foxi1e) was shown to inhibit mesodermal and endodermal fate, it does so via inhibition of FGF rather than TGFβ (Suri, 2005; Mir et al., 2007), but importantly is the only gene described that actively initiates ectodermal differentiation and therefore is currently the most important ectodermal factor. I propose that Coco works alongside Ectodermin and Norrin to inhibit Activin

signalling, becoming active in the animal pole of *Xenopus*. It could also play a role in inhibiting Wnt signalling in the animal pole to oppose Wnt agonists.

Chapter 5 Microarray analysis highlights mechanistic differences between the BMP/TGFβ/Wnt inhibitor Coco and the BMP inhibitor Noggin 1

5.1 Background

In the previous chapter I showed that the endogenous role of Coco is the control of germ layer specification via inhibition of the TGFβ ligand Activin. The next aim was to investigate the downstream differences between Coco, a maternal BMP/TGFβ/Wnt inhibitor (Bell et al., 2003) and Noggin1, a zygotically expressed BMP inhibitor (Smith and Harland, 1992; Smith et al., 1993; Zimmerman et al., 1996; Bayramov et al., 2011).

Coco is expressed throughout the animal half of the embryo up to gastrulation. It is able to induce ectopic heads when overexpressed (Bell et al., 2003), due to its ability to inhibit BMP and Wnt signalling (Glinka et al., 1997; Glinka et al., 1998; Piccolo et al., 1999). *Noggin1* is expressed in the Spemann organizer, and causes the induction of a partial axis when overexpressed (Smith et al., 1993; Zimmerman et al., 1996), indicative of being a single BMP inhibitor. There has been some controversy about the action of Noggin with a recent paper suggesting it can inhibit BMP, TGFβ and Wnt signalling (Bayramov et al., 2011). In this paper they found that Noggin2 (a closely related protein that is expressed later in development) could inhibit all three pathways. It is only when applying an artificial 5' UTR that the authors are able to elicit such a response from Noggin1. We therefore can assume that the Noggin mRNA used in the microarray, which caused the same overexpression phenotype as Noggin1, can still be thought of as only a BMP inhibitor.

To uncover downstream differences between Coco and Noggin, a microarray was performed (Chambers and Lumsden, 2008). Animal caps were cut from

embryos injected with both Coco and Noggin1 mRNA, and changes in gene expression were analysed. Genes were grouped firstly by whether they had been upregulated or downregulated, and secondly by whether it was as a consequence of Coco overexpression, Noggin overexpression or both. Bioinformatic analysis was performed to see any global changes in up- or downregulation, whilst genes were also classified by function. As a second means to understand potential differences between the factors an ISH screen was employed where the expression of genes up- and downregulated by Coco and Noggin was investigated.

5.2 Results – Microarray analysis

The mRNA samples were hybridized on Affymetrix GeneChip *Xenopus laevis* Genome 2.0 arrays by Dr David Chambers (KCL). The data were normalised using Variance Stabilisation Normalisation (Huber et al., 2002) and Robust Multi-array Averaging (Irizarry et al., 2003). Both normalisations gave essentially identical results. The differential expression statistics were computed with Limma (Smyth, 2004). Dr. Eric Blanc (KCL) performed all analysis of data.

Throughout this chapter, all microarray data described was performed in triplicate, and results from Coco and Noggin overexpression were compared to control conditions.

5.2.1 Analysis of Coco overexpression

To see if Coco overexpression caused changes to gene expression the data was compared to control uninjected animal caps on an MA scatter plot. The average expression of every recorded gene, in this case from the six different replicates (3x Control, 3xCoco) is plotted on the *x*-axis using a Log2 scale. The respective change in expression (or expression ratio) is plotted against the mean expression level (or expression product). The change of expression is also plotted on a Log2 scale so that genes that are upregulated as a consequence of Coco overexpression have a positive value, whilst those downregulated have a negative value. Simply put, mean gene expression goes up from left to right, with upregulated genes above 0 on the *y*-axis and those downregulated below 0. When analysing an MA plot, a Loess (Locally estimated scatterplot smoothing) line is used to check if differential expression has any trend towards intensity, hoping for a line that follows the *x*-axis.

Importantly, when an MA plot of the differential expression following Coco overexpression was made, the Loess line showed that the data had no trend

towards expression intensity (red line, Fig 5.1A). It was also clear that there were a large number of genes that had been upregulated as a consequence of Coco overexpression, whilst there were fewer genes that had been downregulated (Fig 5.1A).

Next in order to see if the observed readings matched the expected distribution of the population in question the differential expression following Coco overexpression was analysed statistically using a QQ plot. The *t*-value distribution of a normal population is plotted along the *x*-axis and represents the statistical outcome of an experiment if there had been no differential expression. The expected distribution is plotted against the *t*-value distribution of all the differential expression caused by the experimental condition being analysed. If expression levels in Coco injected caps had not been measurably different from the control, then all points would be expected to fall along the $x=y$ line. If however, more genes are upregulated than would be expected by chance then points are seen above the $x=y$ lines and if more genes are downregulated then points are seen below the $x=y$ line.

When the distribution of Coco's differentially expressed *t*-values were plotted against an expected population it was clear that there were more genes upregulated as a consequence of Coco overexpression than would be expected by chance. Interestingly there were far fewer genes that were downregulated as a consequence of Coco overexpression.

When imposing a *P*-value of $1e^{-03}$ cut off point for the Coco induced differential expression, 187 probe sets were above the cut off point (Fig 5.1C).

5.2.2 Analysis of Noggin overexpression

Analysis of the differential expression caused by Noggin overexpression, using the same three plots, offered different conclusions from those resulting from Coco overexpression.

Figure 5.1 – Bioinformatical analysis of Microarray data following Coco overexpression. A) An MA plot characterization of differential gene expression following Coco overexpression. There are a large number of genes with higher expression following Coco overexpression, with a smaller number of genes that had lower expression following Coco overexpression. Loess line (red) shows that the differential expression data shows no trend along the intensity axis. B) Is a QQ (Quantile-Quantile) plot that compares the distribution of the expected population (in this case the average expression) to the observed population (change in expression). The data shows a large number of genes that have higher expression than would be expected by chance and a smaller number of the gene where the opposite is true. C) A P-Value plot that is used as a cut off for the number of readings that are used in further analysis.

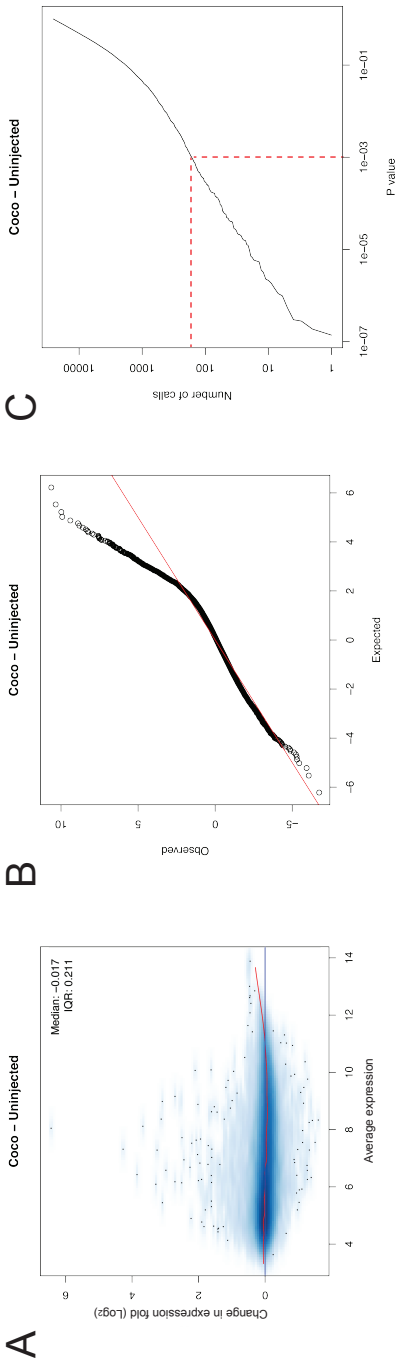

Figure 5.1 - Bioinformatical analysis of Microarray data following Coco overexpression

Importantly the Loess line showed that the differential expression data caused by Noggin overexpression showed no trend along the intensity axis (red line, Figure 5.2A). After analysis of an MA plot it was clear that there was a more even distribution of genes that were up- and downregulated as a consequence of Noggin overexpression (Fig 5.2A). There were a lot more genes downregulated that would be expected by chance when compared to those that were upregulated. This can be seen in an increased density of points below the $x=y$ line in the QQ plot (Fig 5.2B). Using the same *P*-value cut off point of $1e^{-03}$ for Noggin induced differential expression, 225 probe sets were above the cut off point (Fig 5.2C).

In conclusion, the use of these three plots highlighted possible differences between the downstream effects of Coco and Noggin overexpression. Importantly, in both cases it was shown that the data showed no trend towards intensity. Statistically, it seemed possible that Coco overexpression might cause more genes to be upregulated than downregulated. Whilst the converse seemed true of Noggin. Using standard a *P*-value cut off there were similar numbers of genes that were statistically differentially expressed. Next, in order to confirm the global changes caused by Coco and Noggin overexpression, genes were grouped by their up- or downregulation, and also by whether the changes were a consequence of Coco overexpression, Noggin overexpression, or both.

5.2.3 Coco and Noggin have different effects after overexpression

From initial observations of the microarray data, results suggested that there were differences in the number of genes that had increased or decreased expression following Coco and Noggin overexpression. In order to confirm this, tables were produced that grouped genes by their change of expression, and further divided them by which gene caused the expression change, Coco, Noggin or both (Table 5.1 and 5.2; Coco = Yellow, Noggin = Blue, Both = Red). When represented graphically, this was confirmed; Coco caused more genes to have higher expression, whilst Noggin on the other hand had the opposite effect, causing more genes to have reduced expression (Figure 5.3; Coco Up = 104;

Figure 5.2 - Bioinformatical analysis of Microarray data following Noggin1 overexpression. A) An MA plot characterization of differential gene expression following Noggin1 overexpression. There seems to be equal numbers of genes with higher and lower expression following Noggin1 overexpression. Loess line (red) shows that the differential expression data shows no trend along the intensity axis. B) A QQ (Quantile-Quantile) plot compares the distribution of the expected population (in this case the average expression) to the observed population (change in expression). The data shows that similar numbers of genes have higher and lower expression than would be expected by chance. C) A P-Value plot that is used as a cut off for the number of readings that are used in further analysis.

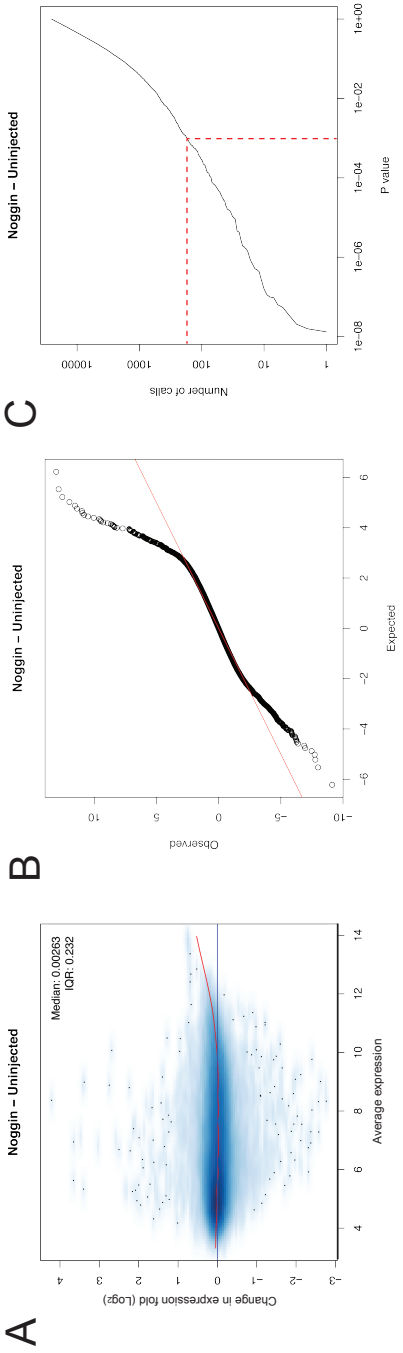

Figure 5.2 - Bioinformatical analysis of Microarray data following Noggin1 overexpression

Figure 5.3 - Different proportions of genes with increased and decreased expression following Coco and Noggin1 overexpression. A) Graphical plot using total lists of genes up and down regulated. Coco increased the expression of 104 genes (yellow), Noggin1 increased the expression of 46 genes (Blue) and 46 genes had their expression increased by both Coco and Noggin1 (Red). Coco only reduced the expression of 6 genes; Noggin1 reduced the expression of 104 with 31 genes having their expression reduced by both Coco and Noggin1.

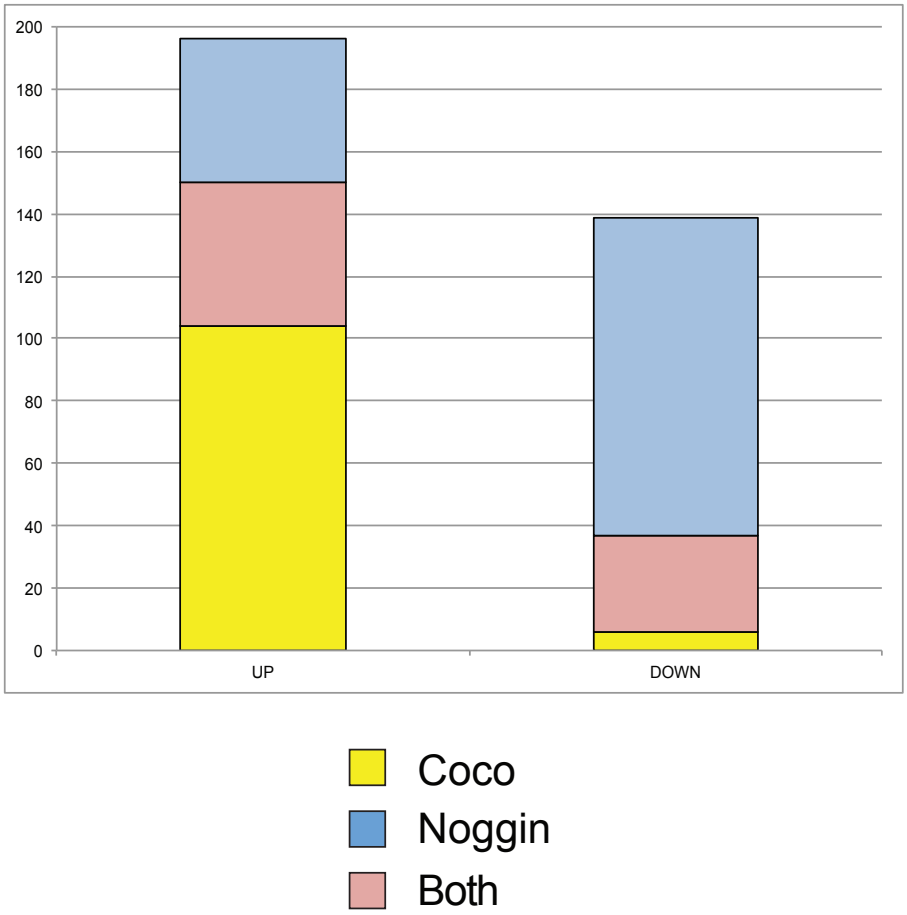

Figure 5.3 - Different proportions of genes with increased and decreased expression following Coco and Noggin1 overexpression

Coco Down = 6; Noggin Up = 46; Noggin Down = 102; Both Up = 46; Both Down = 31).

5.2.4 Classification of up- and down-regulated genes

The microarray analysis has shown that there are clear differences in the effect of Coco and Noggin overexpression. In order to gain an understanding of global differences between the lists, genes were grouped into one of 9 categories based on their general role using classifications similar to those outlined before (Altmann et al., 2001) (Figure 5.4 and 5.5). Genes were placed into one of the following groups; Amino Acid Biosynthesis, Cellular Processes, Transport/Binding, Transcription, Signal Transduction, Cell Structure, Nucleotide Metabolism, Hypothetical/Unknown or No Database Match. Genes places in 'Hypothetical/Unknown' were genes with full coding sequence that are yet to be functionally identified, whilst genes that were placed in 'No Database Match' gave no results when using the blastn algorithm of BLAST (Basic Local Alignment Search Tool) against the Nucleotide Collection (nr/nt) database (Altschul et al., 1990).

When looking at the 150 genes overexpressed by Coco the majority of the genes encoded proteins belonging to four main groups: (1) transcription (18.7%); (2) signal transduction (17.3%); (3) cellular processes (14.7%) and (4) cell structure (14.0%). It is important to note here that 20.7% were clones that were unknown and had no hits in the Nucleotide Collection database; presumably these are a mixture of partial cDNAs/UTRs and uncharacterised genes. Coco overexpression caused the subsequent downregulation of 37 genes. The majority of which belonged to two main groups: (1) transcription (48.6%), (2) signal transduction (13.5%), with 20.7% being hypothetical proteins with uncharacterised function. These results suggest a large number of genes upregulated due to overexpression Coco overexpression were involved in transcription and signal transduction, whilst nearly half of the genes that were downregulated by Coco overexpression were involved in transcription.

Figure 5.4 - Functional classification groupings of genes differentially expressed as a consequence of Coco overexpression. A) Functional classification groupings of genes upregulated as a consequence of Coco overexpression. B) Functional classification groupings of genes upregulated as a consequence of Coco overexpression. Dark Blue = Amino Acid Biosynthesis, Red = Cellular Processes, Green = Transport/Binding, Purple = Transcription, Light Blue = Signal Transduction, Orange = Cell Structure, Dark Pink = Nucleotide Metabolism, Yellow = Hypothetical/Unknown, Light Pink = No Database Match.

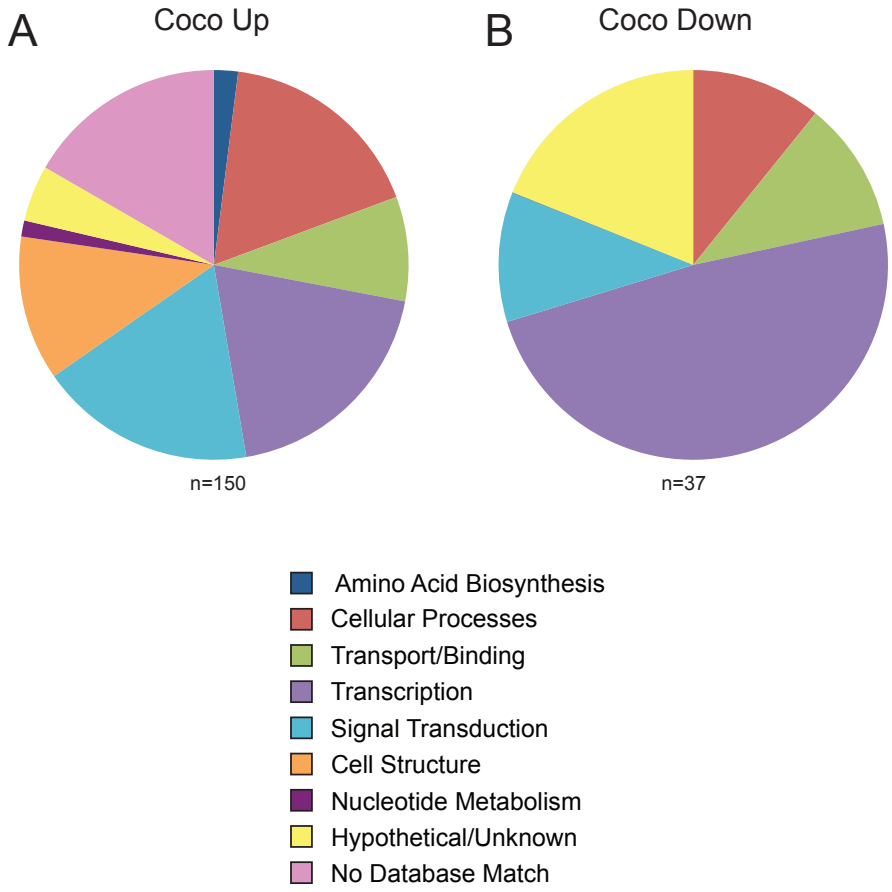

Figure 5.4 - Functional classification groupings of genes differentially expressed as a consequence of Coco overexpression

Figure 5.5 - Functional classification groupings of genes differentially expressed as a consequence of Noggin1 overexpression. Array targets showing increased and decreased RNA levels grouped into different categories. A) Functional classification groupings of genes upregulated as a consequence of Noggin1 overexpression. B) Functional classification groupings of genes upregulated as a consequence of Noggin1 overexpression. Dark Blue = Amino Acid Biosynthesis, Red = Cellular Processes, Green = Transport/Binding, Purple = Transcription, Light Blue = Signal Transduction, Orange = Cell Structure, Dark Pink = Nucleotide Metabolism, Yellow = Hypothetical/Unknown, Light Pink = No Database Match.

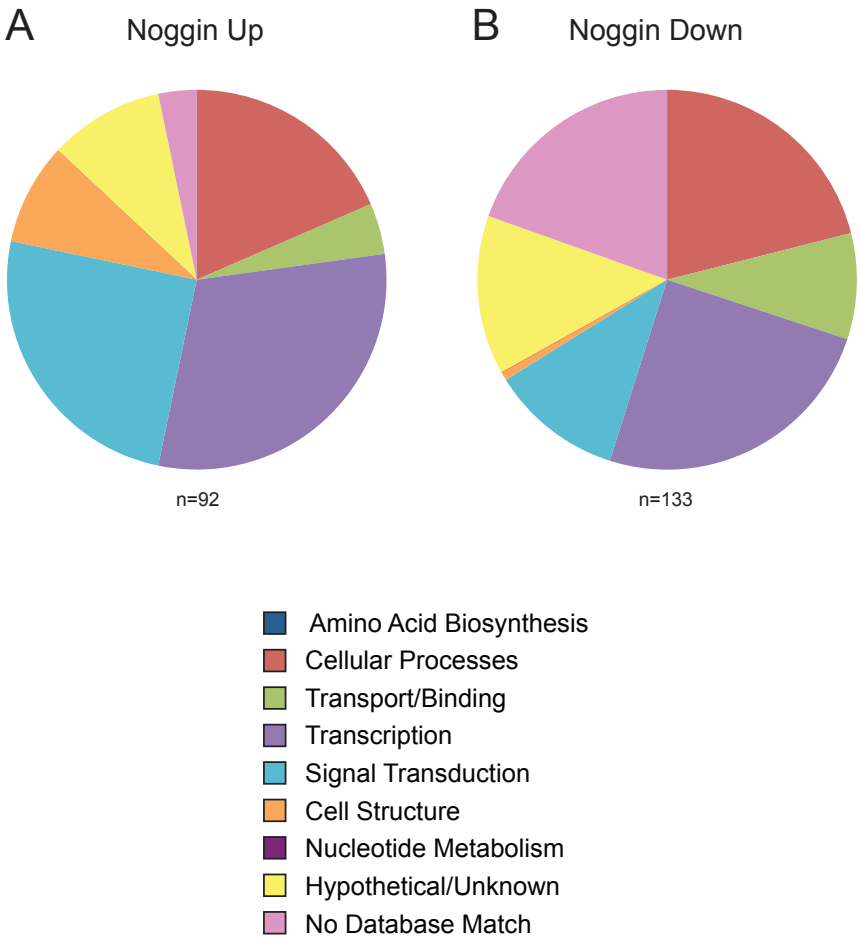

Figure 5.5 - Functional classification groupings of genes differentially expressed as a consequence of Noggin1 overexpression

Next the genes affected by Noggin were analysed. Noggin overexpression caused an upregulation of 92 genes; most belonged to three major groups: (1) transcription (30.4%); (2) signal transduction (23.0%) and (3) cellular processes (18.5%). *Noggin* overexpression caused 133 genes to be downregulated. The majority of them belonged to two main groups: (1) transcription (24.8%); (2) Cellular processes (21.1%), with a large number of hits having hypothetical roles (13.5%) or no database match (19.5%). Table 5.3 shows all of the numbers for the pie charts.

When taken together, the microarray data shows that Coco overexpression caused far more genes to be upregulated than were downregulated. Whilst Noggin overexpression caused more genes to be downregulated than were upregulated.

5.3 Results - ISH Screen

The initial aim from this chapter was to uncover possible downstream differences between Coco and Noggin. Bioinformatic analysis showed that Coco overexpression largely caused upregulation, whilst Noggin overexpression had the opposite effect. Having met the first aim, and knowing the genes that are up- and downregulated by overexpression of both genes, it was important to find novel expression patterns for genes downstream of Coco and Noggin.

In order to analyse genes either increased or decreased by *Coco and Noggin* an ISH screen was performed. Clones were chosen that represented genes that were up- or downregulated as consequence of either Coco or Noggin overexpression. Of the genes tested, eleven probes gave good expression patterns and were used to produce gene expression profiles (Table 5.4).

5.3.1 Genes with higher expression following Coco overexpression

5.3.1.1 Catalase

Catalase (*Cat2*) is a peroxisome related gene that converts Hydrogen Peroxide (H_2O_2) to water and molecular oxygen (Deisseroth and Dounce, 1970; Anand et al., 2009). *Cat2* had the highest fold (4.290) increase in expression following *Coco* overexpression. Using antibodies Catalase protein was shown to be localized to brain and dorso-anterior structures in late tadpole stages, but no early expression pattern was ever published (Cooper et al., 2007).

At blastula stage (9) *Cat2* appeared to be expressed in the animal pole (Figure 5.6A), but when looking at a section it was clear that the expression was mainly in the mesodermal cells from the marginal zone (Figure 5.6B). The reported dorsal localization seen at late tadpole stages was also seen at neurula stages. At stage 15 *Cat2* was expressed broadly in the anterior portion of the neural plate (Figure 5.6C), whilst a lateral view showed additional expression in lateral mesoderm, dorsally (Figure 5.6D). A sagittal section through a stage 15 embryo confirmed expression in the anterior neural plate and dorsal mesoderm (Figure 5.6E). At later neurula stages a similar pattern was seen. Strong *Cat2* expression was seen dorsally at stage 18 in both the spinal cord and dorsal mesoderm (Figure 5.6F), whilst a lateral view showed expression in the dorsal mesoderm (Figure 5.6G). There was no *Cat2* expression at tailbud stages (data not shown). The fact that *Cat2* is expressed just before gastrulation and at neurula stages, but not at later stages of development suggests a role for Catalase during gastrulation and early neural development in *Xenopus laevis*.

5.3.1.2 Tipin

Another gene that was significantly upregulated (2.872 fold) as a consequence of *Coco* overexpression was XTimeless Interacting Protein 1 (*Tipin*). *Tipin*,

Figure 5.6 – Catalase expression profile in *Xenopus laevis*. A) *Cat2* appears to be expressed in the animal pole of stage 9 embryos, B) *Cat2* expression is strongest around the blastocoel and surrounding marginal tissue. C-E) Expression is detected strongly in the anterior neural plate and the dorso-lateral mesoderm in stage 15 embryos. F-G) *Cat2* is expressed in dorsal neural and mesodermal tissue at stage 18.

A) Whole mount and B) section are lateral views orientated with animal up and vegetal down. C) Anterior view orientated with anterior up and dorsal down. D), G) Whole mount and E) Section are lateral views orientated with anterior right, posterior left, dorsal up and ventral up. F) Dorsal view orientated with anterior up and posterior down.

b, blastocoel, dml, dorsal midline, ant np, anterior neural plate, dlm, dorso-lateral mesoderm, a, archentron, eym, endoderm yolky mass, dm, dorsal mesoderm, sc, spinal cord, np, neural plate.

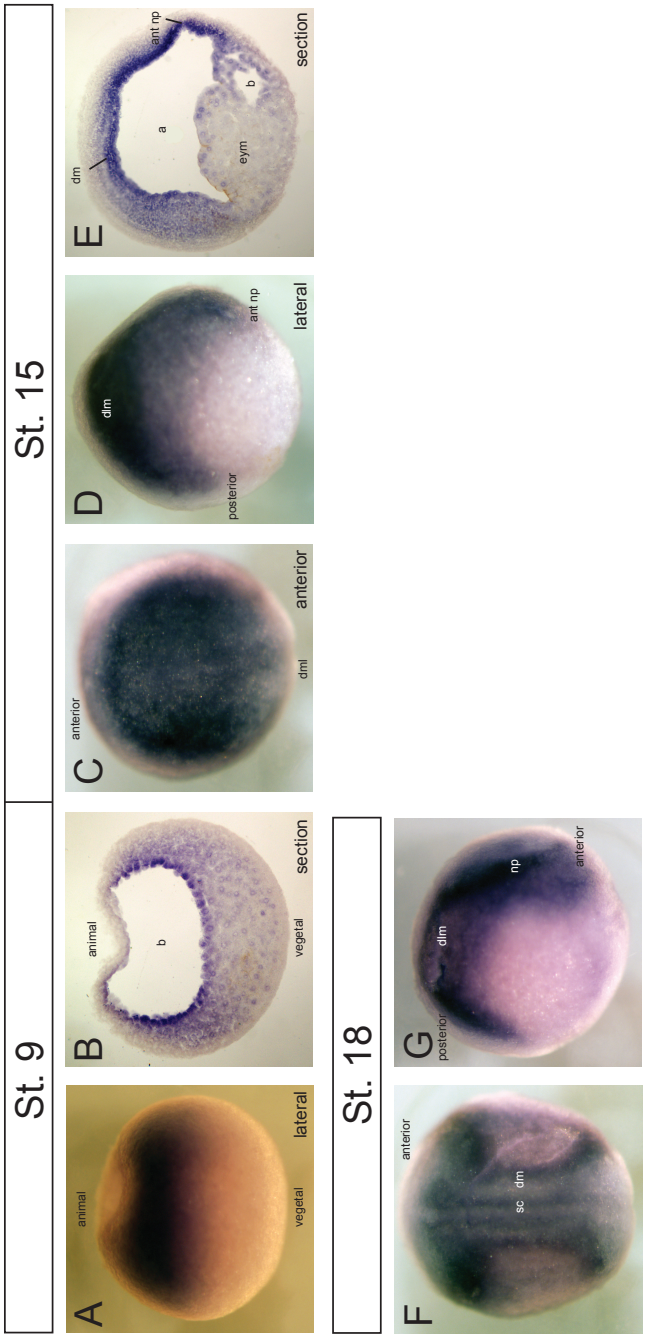

Figure 5.6 - Catalase expression profile in *Xenopus laevis*

originally identified in a 2-hybrid screen in yeast (Gotter, 2003) is required for stabilization of the replication fork during DNA damage control (Errico et al., 2007).

At early neurula stage (13) there was faint *Tipin* expression in the anterior portion of the presumptive neural plate (arrowheads, Figure 5.7A), however at stage 15 faint staining was only seen in the spinal cord (arrowhead, Figure 5.7B). At late neurula stages (18) a more defined expression pattern became clear. Expression was detected anteriorly in the presumptive midbrain and hindbrain (Figure 5.7C), with weaker expression throughout the spinal cord (Figure 5.7D). This anterior expression was dynamic as by stage 25 mid-/hindbrain expression was lost; instead strong expression was seen in the spinal cord and surrounding paraxial mesoderm (Figure 5.7E). By stage 27 the anterior expression had again returned, with staining throughout the brain (Figure 5.7F). The results suggest that there is a requirement for Tipin, presumably in DNA damage control, during early stages of development and the cyclic anterior/posterior expression patterns suggest that these requirements are dynamic.

5.3.1.3 Cellular Retinoic Acid Binding Protein 2

Cellular Retinoic Acid Binding Protein 2 (*Crabp2*) is a cytosolic protein that allows increased cellular responses to secreted Retinoic Acid (RA) and has also been shown to enhance the transcriptional activity of RA (Delva et al., 1999). Following overexpression of Coco there was a 2.457 fold increase of *Crabp2* expression levels.

The expression pattern of *Crabp2* has previously been reported (Dekker et al., 1994) and here we confirm their findings. At blastula stages there was expression in the animal half of the embryo (Figure 5.8A). At the earliest neurula stage (13) there was a more defined expression pattern. There was strong anterior expression bilaterally in the presumptive hindbrain (black arrowheads, Figure 5.8B) and a domain of staining in the forebrain (white arrowhead, Figure 5.8B). Also at stage

Figure 5.7 – Xtimeless Interacting Protein expression profile in *Xenopus laevis*. A) *Tipin* is expression anteriorly at stage 13, arrowheads mark anterior limit of expression. B) *Tipin* is expressed in the spinal cord at stage 15. C-D) Expression is detected in the midbrain, hindbrain and spinal cord at stage 18. E) *Tipin* is expressed in the spinal cord and surround mesoderm at stage 25. F) *Tipin* is expressed throughout the brain at stage 27.

A) and C) Anterior view orientated with Dorsal up and ventral down, B) and D) Dorsal views orientated with anterior up and posterior down, E-F) Lateral views orientated with anterior left, posterior right, dorsal up and ventral down.

sc, spinal cord, mb, midbrain, hb, hindbrain.

*ISH performed by L. Henshaw (MRC CDN, KCL), pictures and analysis performed by T. J. D. Bates.

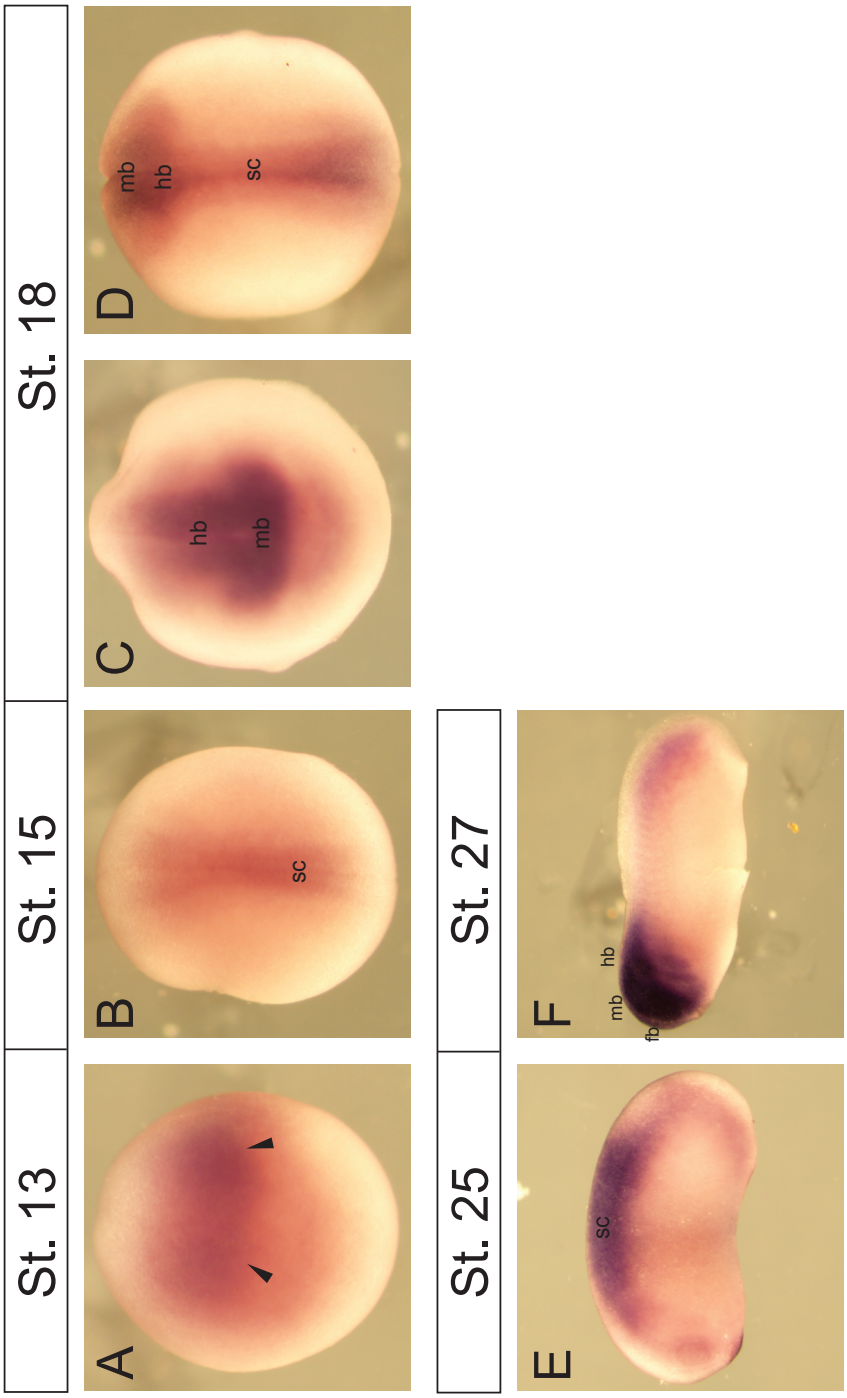

Figure 5.7 - Xtimeless Interacting Protein expression profile in *Xenopus laevis*

Figure 5.8 – Cellular Retinoic Acid Binding Protein 2 expression profile in *Xenopus laevis.* A) *Crabp2* is expressed in the animal half of a stage 9 embryo. B) *Crabp2* is expressed bilaterally in the presumptive midbrain (black arrowheads) and in a domain anterior of the forebrain (white arrowhead) at stage 13. C) *CRABP2* is expressed posteriorly surrounding the closing blastopore ring at stage 13. D-E) *CRABP2* is expressed in the forebrain (white arrowheads) and midbrain (black arrowheads), E) and faintly in the spinal cord (arrowheads) at stage 15.

A) Wholemount view orientated with animal up and vegetal down, B) and D) are anterior views orientated with dorsal up and ventral down, C) Posterior view orientated with dorsal up and ventral down, E) Dorsal view orientated with anterior up and posterior down.

b, blastocoel, fb, forebrain, mb, midbrain, hb, hindbrain, cbr, closing blastopore ring, sc, spinal cord.

*ISH performed by L. Henshaw (MRC CDN, KCL), pictures and analysis performed by T. J. D. Bates.

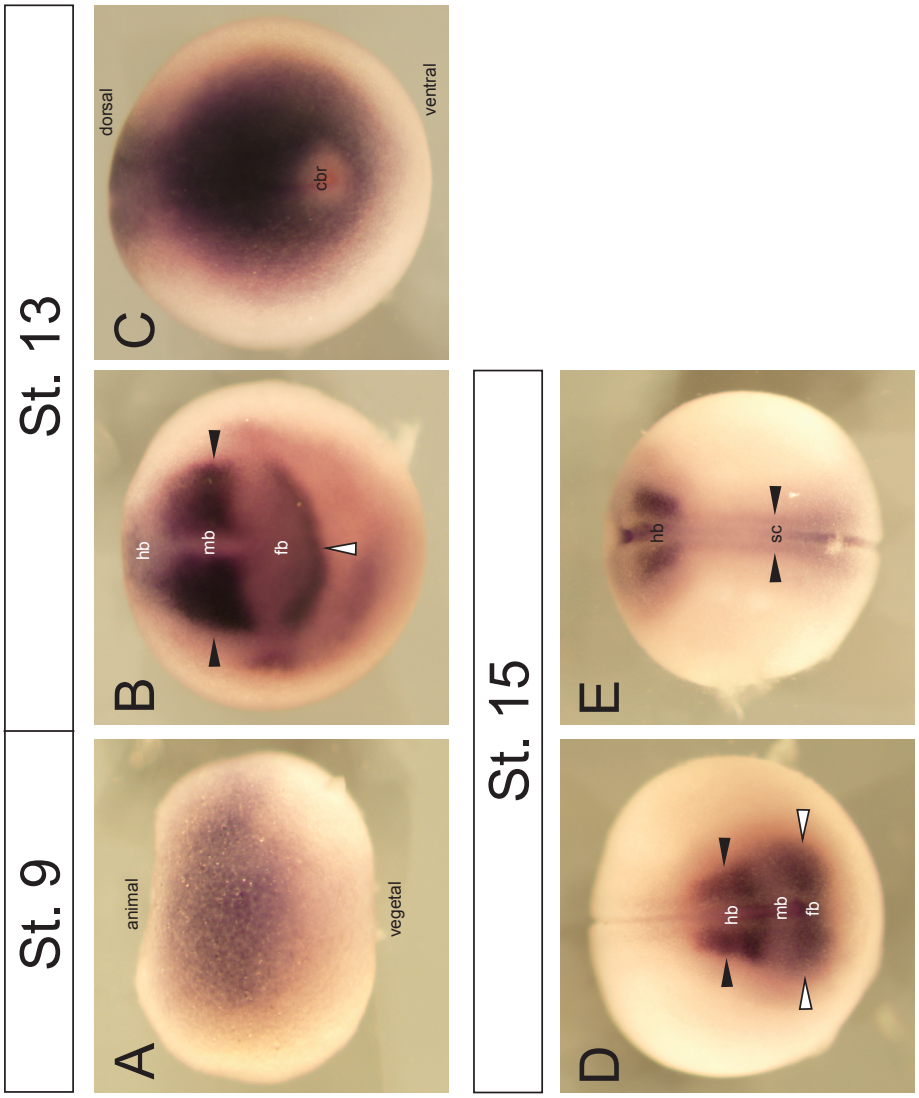

Figure 5.8 - Cellular Retinoic Acid Binding Protein 2 expression profile in *Xenopus laevis*

13 there was very strong expression posteriorly in the newly formed tailbud (Figure 5.8C). At stage 15, *Crabp2* was also expressed in the presumptive forebrain (white arrowheads, Figure 5.8D) and hindbrain (black arrowheads, Figure 5.8D), whilst there was also faint expression in the spinal cord and reduced expression posteriorly (black arrowheads, Figure 5.8E). These results confirm that *Crabp2* is expressed as previously described in the hindbrain and posteriorly in the tail bud (Dekker et al., 1994). The increase in *Crabp2* expression suggests a role for Coco in controlling levels of RA signalling.

5.3.1.4 ATPase Type 13A4

ATPase 13A4 (*Atp13a4*) is a previously uncharacterized P-type ATPase that had a 2.445 fold increase in expression following *Coco* overexpression. P-Type ATPase enzymes catalyse the decomposition of adenosine triphosphate (ATP) into adenosine diphosphate (ADP) releasing energy that drives transport of positive cations.

Atp13a4 was expressed faintly in the animal half of the embryos at blastula stages (Figure 5.9A), in marginal tissue (Figure 5.9B). At neurula stages there was faint expression in the anterior neural plate (Figure 5.9C), with staining also seen in dorsal mesoderm (Figure 5.9D). When sectioned, staining was seen within both dorsal neural and mesodermal tissue (Figure 5.9E). At stage 28 there was strong expression in the brain (Figure 5.9F). These results suggest that the previously uncharacterized ATPase 13A4, shown to be upregulated as a consequence of Coco overexpression, is required throughout dorsal tissue at neurula stages, and in the anterior portion of the embryo at tail bud.

5.3.1.5 Tolloid-like 2

Tolloid-like 2 (*Tll2*) is a *Xenopus laevis* homolog of the *Drosophila Tolloid* gene and had a 2.099 fold increase in expression following *Coco* overexpression. No *Tll2* expression pattern was observed in embryos younger than tail bud. At stage

Figure 5.9 - ATPase Type 13A4 expression profile in *Xenopus laevis*. A-B) *Atp13a4* is expressed in marginal tissue at stage 9. C-E) *Atp13a4* is expressed in the anterior neural plate and dorsal mesoderm at stage 15. F) *Atp13a4* is expressed in the brain at stage 26.

A) Wholemount and B) Section are lateral views orientated with animal up and vegetal down. C) Anterior view orientated with anterior up and dorsal down. D) Whole mount and E) Section are lateral views orientated with anterior right, posterior left, dorsal up and ventral down. F) Lateral view orientated with anterior left, posterior right, dorsal up and ventral down.

b, blastocoel, dml, dorsal midline, a, archenteron, dm, dorsal midline, ant np, anterior neural plate, yp, yolk plug, eym, endoderm yolky mass, cg, cement gland, fb, forebrain, mb, midbrain, hb, hindbrain, sc, spinal cord.

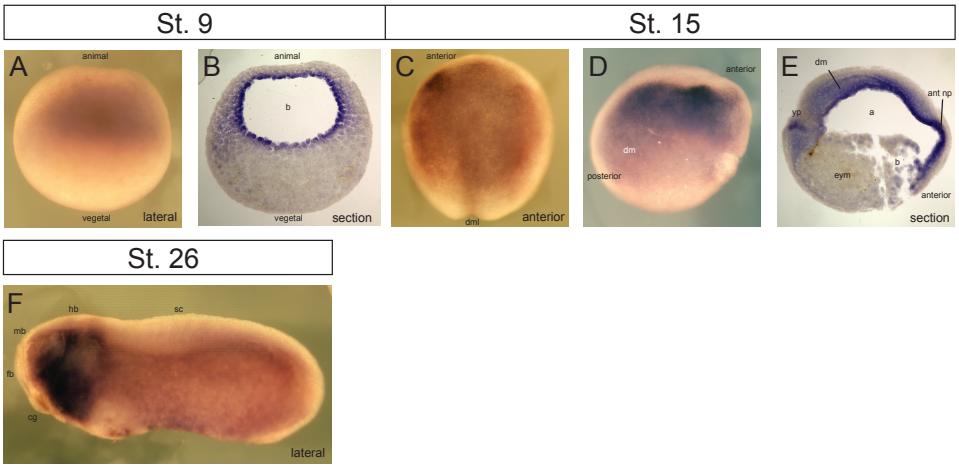

Figure 5.9 - ATPase Type 13A4 expression profile in *Xenopus laevis*

Figure 5.10 - Tolloid-like 2 expression profile in *Xenopus laevis*. A-C) *Tll2* is expressed faintly in the epidermis of the tail at stage 25. D-F) *Tll2* is expressed throughout the dorsal fin at stage 27.

A), D) Dorsal views orientated with anterior up and posterior down. B), E) Lateral views orientated with anterior left, posterior right, dorsal up and ventral down. C), F) Transverse section orientated with dorsal up and ventral down.

a, archenteron, nt, neural tube, n, notochord, m, mesoderm.

*ISH performed by L. Henshaw (MRC CDN, KCL), pictures and analysis performed by T. J. D. Bates.

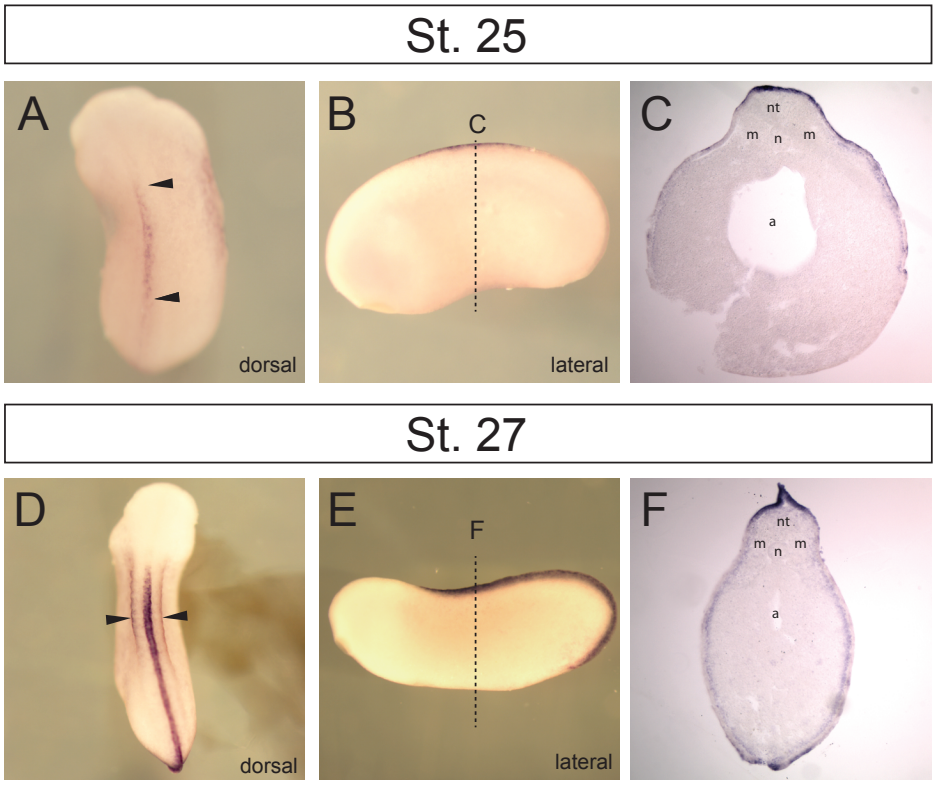

Figure 5.10 - Tolloid-like 2 expression profile in *Xenopus laevis*

25 *Tll2* was expressed in the dorsal most epidermis of the tail (Figure 5.10A-B) and this was confirmed in sections (Figure 5.10C). At stage 28 *Tll2* was expressed in the dorsal fin and neural crest populations (arrowheads) (Figure 5.10D-E), which could be seen in more detail when the embryo was sectioned (Figure 5.10F). These results suggest that *Tll2* has a very distinct expression pattern at tailbud stages during *Xenopus laevis* development, and therefore could play a role in dorsal development.

5.3.1.6 Caveolin 2

Caveolin 2 (*Cav2*), a scaffolding protein that is a major component of cavelae; small invaginations of the plasma membrane (Scherer et al., 1996), showed a 1.804 increase in expression following Coco overexpression.

At blastula stages *Cav2* was expressed in one portion of the marginal zone (black arrowheads, Figure 5.11A), which was also seen faintly at gastrula stage (black arrow heads, Figure 5.11B). At early neurula stage (13) there was faint *Cav2* expression anteriorly (black arrow heads, Figure 5.11C), which became more defined by stage 17 with staining throughout the midbrain and hindbrain (black arrow heads, Figure 5.11D). When looking laterally it seemed that *Cav2* was expressed in dorsal mesodermal tissue more posteriorly (Figure 5.11E), and this was clearer in a posterior view, where spinal cord expression was also seen (Figure 5.11F). Expression of *Cav2* seemed to be only within neural tissue at tailbud stages, with anterior staining throughout the forebrain, midbrain and hindbrain (Figure 5.11G) and more posteriorly in the spinal cord (Figure 5.11H), where the dorsal mesoderm expression continued. The increase of *Cav2* following *Coco* overexpression highlights a pathway including Coco that is required for membrane protein production, which functional studies could further elucidate.

5.3.1.7 NR13-Like Anti-Apoptotic Protein

Figure 5.11 – Caveolin 2 expression profile in *Xenopus laevis*. A) *Cav2* is expressed faintly in a portion of the marginal zone at stage 9, arrowheads mark limit of expression. B) Weak expression was detected in the dorsal marginal zone at stage 10.5. C) *Cav2* is expressed anteriorly in the presumptive neural plate at stage 13 (see arrowheads). D-F) *Cav2* is expressed in the midbrain, hindbrain, spinal cord and dorsal mesoderm at stage 17, arrowheads in D) mark anterior limits of expression. G-H) *Cav2* is expressed in the forebrain, midbrain, hindbrain, spinal cord and dorsal mesoderm at stage 23.

A-B) Lateral views orientated with animal up and vegetal down. C-D) Anterior views orientated with anterior down, and dorsal up. E) Lateral view orientated with anterior up, posterior down, dorsal left and ventral right. F) Dorsal view orientated with anterior up and posterior down. G) Lateral view orientated with anterior left, posterior right, dorsal up and ventral down. H) Dorsal view orientated with anterior left and posterior right.

dbl, dorsal blastopore lip, dml, dorsal midline, cg, cement gland, fb, forebrain, mb, midbrain, hb, hindbrain, sc, spinal cord, dm, dorsal mesoderm.

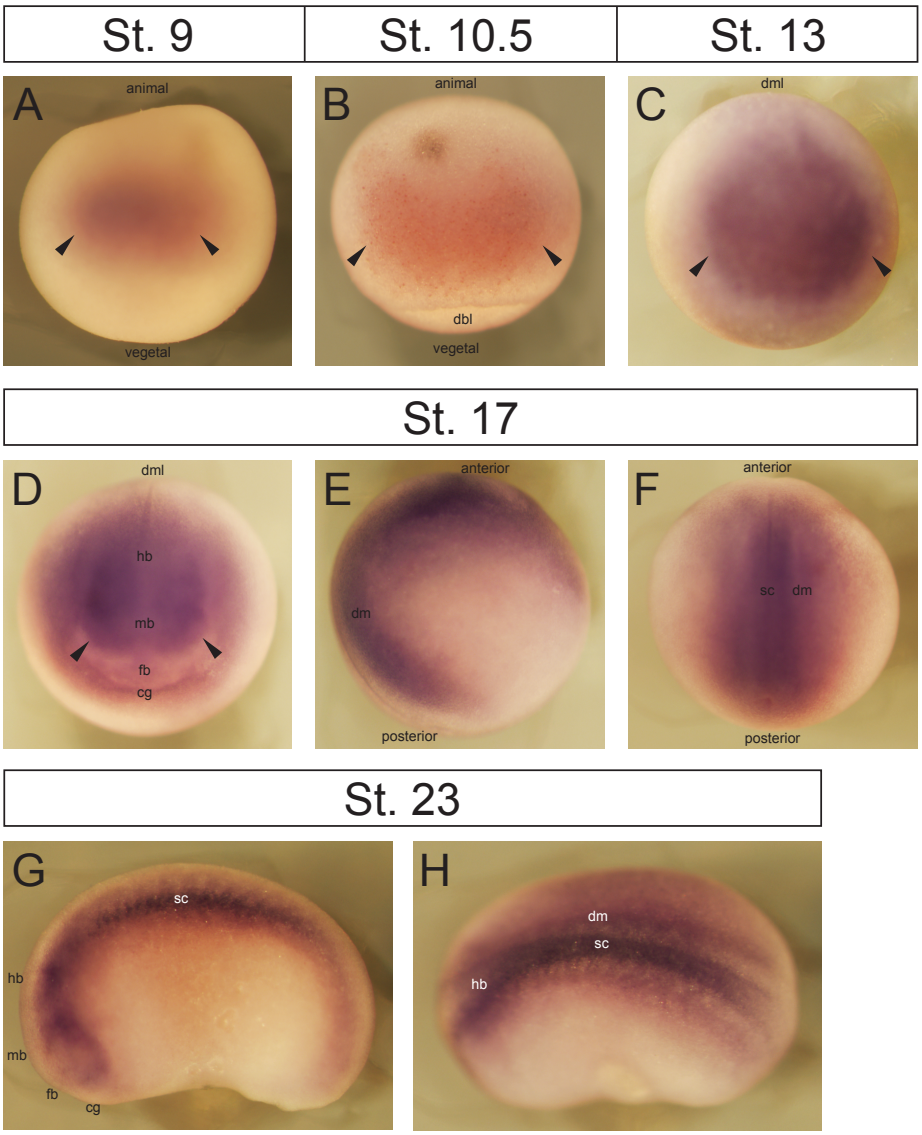

Figure 5.11 - Caveolin 2 expression profile in *Xenopus laevis*

NR13-Like Anti-Apoptotic Protein (*Nr13-l*) is an uncharacterized *Xenopus laevis* paralog of NR13, a potent apoptotic protein involved in the regulation of cell death in chick (Mangeney et al., 1996; Lee et al., 1999).

Nr13-l is expressed strongly throughout blastula and gastrula stages. Strong staining can be seen in the animal pole of a stage 9 embryo (Figure 5.12A), whilst there was no staining vegetally (Figure 5.12B). At gastrula, there was staining throughout the ectoderm (Figure 5.12C), but not within the endoderm (Figure 5.12D). There was no expression later than gastrulation stages. These results suggest that NR13-L is an anti-apoptotic protein specifically active during blastula and gastrula stages.

5.3.2 Genes upregulated as a consequence of Noggin overexpression

5.3.2.1 Cytochrome P450, Family 26, Subfamily C, Polypeptide 1

Cytochrome P450, Family 26, Subfamily C Polypeptide 1 (*Cyp26c1*) is a Retinoic Acid metabolising protein that has been shown to be involved in anterior *Xenopus laevis* development (Tanibe et al., 2008). *Cyp26c1* expression was increased 1.854 fold by *Noggin* overexpression.

At early neurula stages, there were two domains of *Cyp26C1* expression within presumptive neurectoderm (black arrowheads), with no expression at the midline (Figure 5.13A). During mid neurula stages (18/19) there was lateral expression in the presumptive hindbrain (black arrowheads, Figure 5.13B-C), and also expression in the future cement gland (cg) region of the embryo (white arrowheads, Figure 5.13B-C). At late neurula (21) the hindbrain expression of *Cyp26C1* had narrowed. More intense expression in the presumptive cement gland region was extended posteriorly by a stream of expression, which did not join up with the hindbrain expression (Figure 5.13D). *Cyp26C1* was also expressed posteriorly around the tail bud at stage 21 (Figure 5.13E). At mid neurula stage (25) hindbrain expression of *Cyp26C1* was maintained (

Figure 5.12 – Nr13-like Anti-apoptotic Protein expression profile in *Xenopus laevis*. A) *Nr13-l* is expressed throughout the ectoderm, B) but not vegetally, at stage 9. C-D) *NR13-L* is expressed thoughout the ectoderm at stage 11.

A) and C) Animal views, B) and D) Vegetal views.

dbl, dorsal blastopore lip, ecto, ectoderm, endo, endoderm.

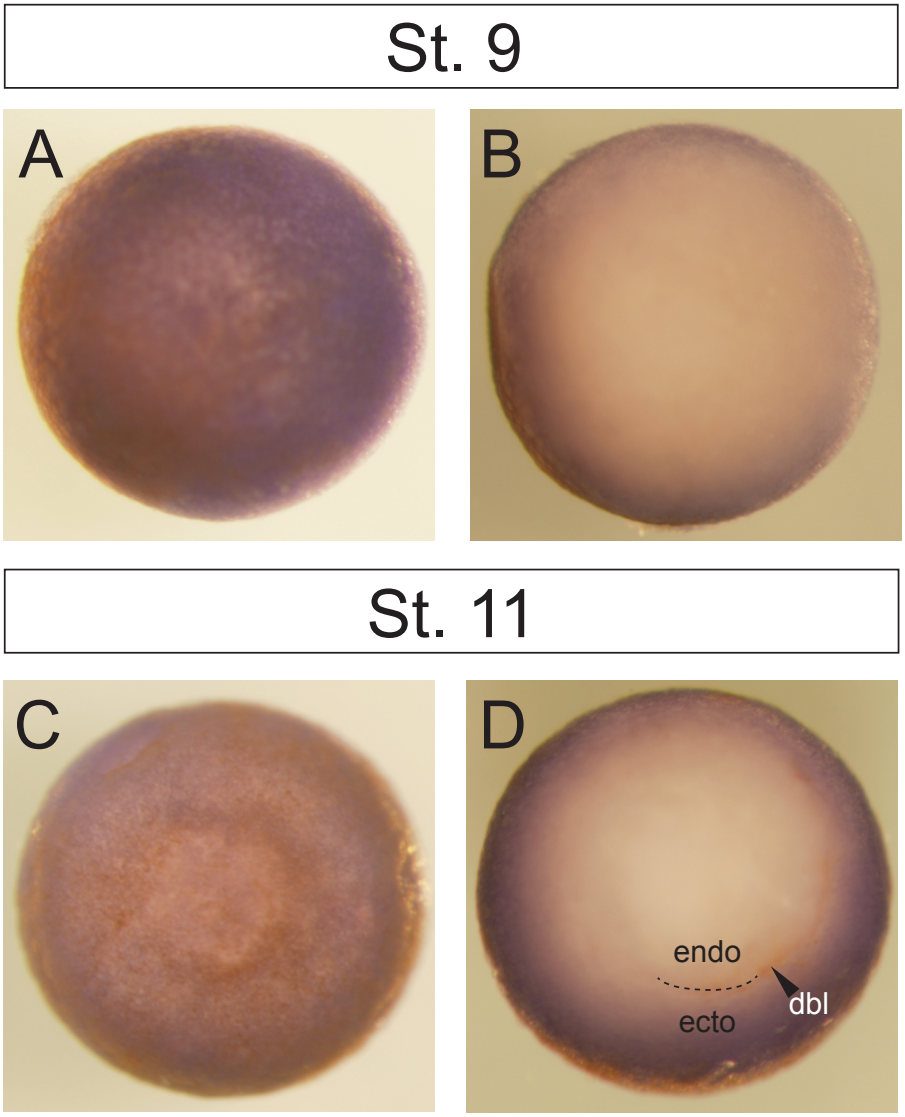

Figure 5.12 - Nr13-like Anti-apoptotic Protein expression profile in *Xenopus laevis*

Figure 5.13 - Cytochrome P450, Family 26, Subfamily C Polypeptide 1 expression profile in *Xenopus laevis*. A) *Cyp26c1* is expressed bilaterally in two domains of neurectoderm at stage 13 (arrowheads). B-C) *Cyp26c1* is expressed laterally in the presumptive hindbrain and in the cement gland region at both stage 18 and 19. In both cases black arrowheads mark hindbrain expression, and white arrowheads mark cement gland region expression. D-E) *Cyp26c1* is expressed in the cement gland region, the presumptive hindbrain and surrounding the tailbud at stage 21, arrowheads in D mark a stream of expression from the cement gland region. F-H) *Cyp26c1* is expressed in the cement gland, the presumptive hindbrain and surrounding the tailbud at stage 25, arrowheads in G mark a stream of expression from the cement gland region, that joins up with the hindbrain expression.

A-D), F) Anterior views orientated with anterior down and dorsal up. E), H) Posterior views orientated with dorsal up. G) Lateral view orientated with anterior left, posterior right, dorsal up and ventral down.

cg, cement gland, hb, hindbrain, tb, tailbud.

*ISH performed by L. Henshaw (MRC CDN, KCL), pictures and analysis performed by T. J. D. Bates.

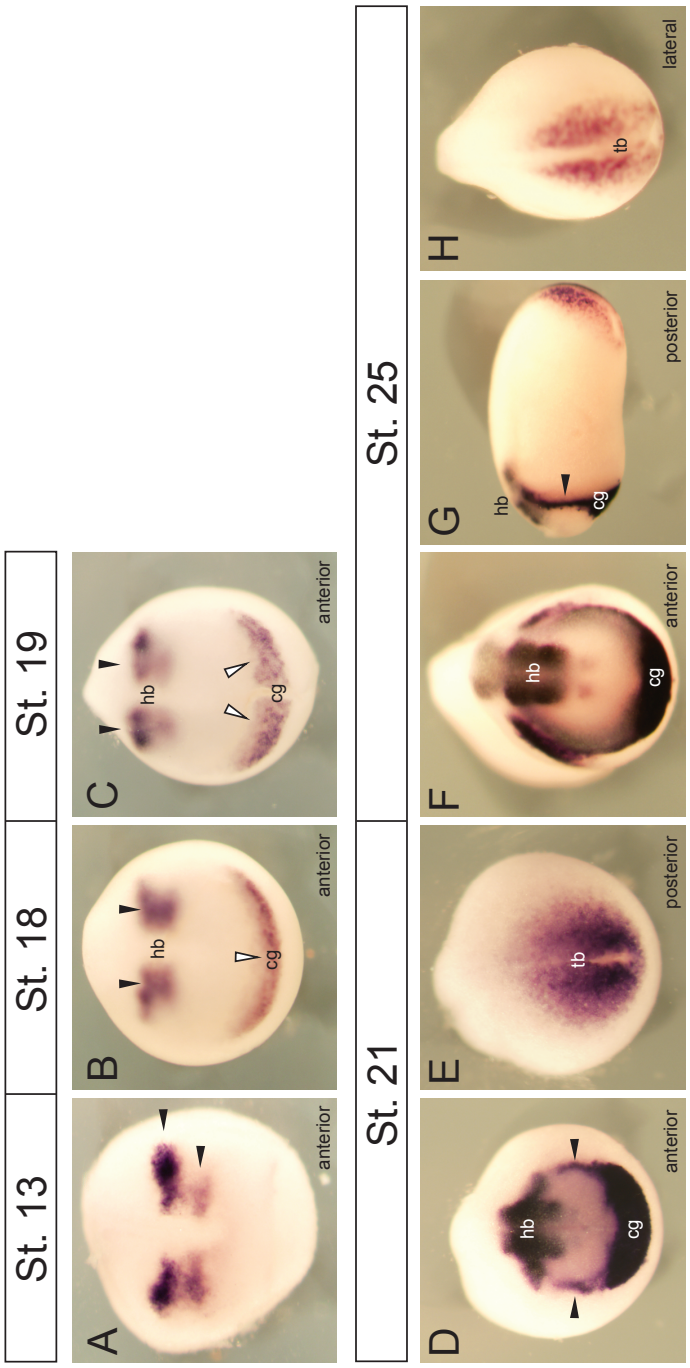

Figure 5.13 - Cytochrome P450, Family 26, Subfamily C Polypeptide 1 expression profile in *Xenopus laevis*

Figure 5.13F). When looking laterally it was clear that the stream of expression from the cement gland now joined up with the hindbrain region (arrow head, Figure 5.13G), whilst the previously unreported posterior expression was weaker at this stage (Figure 5.13H). In this study the expression pattern of *Cyp26c1* was confirmed, and posterior expression was described for the first time.

5.3.2.2 Hematopoietic Prostaglandin D Synthase

Hematopoietic Prostaglandin D Synthase (*Hpgds*) is also known as *Xenopus laevis* Isoenzyme of GST Sigma 1 (*XlGSTS1*), a Glutathione S-transferase that catalyses the antioxidant Glutathione (Carletti et al., 2003).

At stage 9 faint *Hpgds* staining was seen in the animal pole (Figure 5.14A) and whilst at stage 10.5 there was staining in the marginal zone (Figure 5.14B). When looking at neurula embryos, there was expression throughout all dorsal structures including the presumptive brain and spinal cord (Figure 5.14C), a pattern that was maintained up until stage 18 (data not shown/ Figure 5.14D). However, at late neurula stages (20) the posterior expression was not present. There was strong expression throughout the presumptive brain at stage 20 (Figure 5.14E) which continued into tailbud stages. At stage 24 there was expression of *Hpgds* throughout the fore-, mid- and hindbrain (Figure 5.14F) and faint expression in the neural crest stream that migrates dorso-ventrally towards the branchial arches (arrowhead, Figure 5.14F). The same expression domain was seen at stage 26, however *Hpgds* was expressed at a higher level (Figure 5.14G). This is the first expression data for *Hpgds*, and our data suggests a role for detoxifying enzymes downstream of BMP inhibition.

5.3.3 Genes with lowered expression following Coco overexpression

5.3.3.1 Zinc Finger 91-like

Figure 5.14 - Hematopoietic Prostaglandin D Synthase expression profile in *Xenopus laevis*. A) *Hpdgs* is expressed faintly in the animal pole at stage 9, B) and in the marginal zone at stage 10.5. C) At stage 17 there was *Hpdgs* throughout the forebrain (data not shown), midbrain, hindbrain and spinal cord. D) *Hpdgs* is expressed in the spinal cord and dorsal mesoderm at stage 18. E) *Hpdgs* is expressed throughout the forebrain, midbrain and hindbrain at stage 20, arrowheads mark anterior limit of expression. F) *Hpdgs* is expressed throughout the forebrain, midbrain and hindbrain, and in a stream of neural crest at stage 24; arrowhead marks neural crest stream. G) *Hpdgs* is expressed strongly throughout the forebrain, midbrain and hindbrain, and in a stream of neural crest at stage 26; arrowhead marks neural crest stream.

A) Lateral view orientated with animal up and vegetal down, B) Dorso-vegetal view, C) Dorsal view orientated with anterior up and posterior down, D) Posterior view orientated with posterior down and dorsal up, E) Anterior view orientated with anterior down and dorsal up, F-G) Lateral views orientated with anterior left, posterior right, dorsal up and ventral down.

dbl, dorsal blastopore lip, ecto, ectoderm, endo, endoderm, dm, dorsal mesoderm, cg, cement gland, fb, forebrain, mb, midbrain, hb, hindbrain, sc, spinal cord.

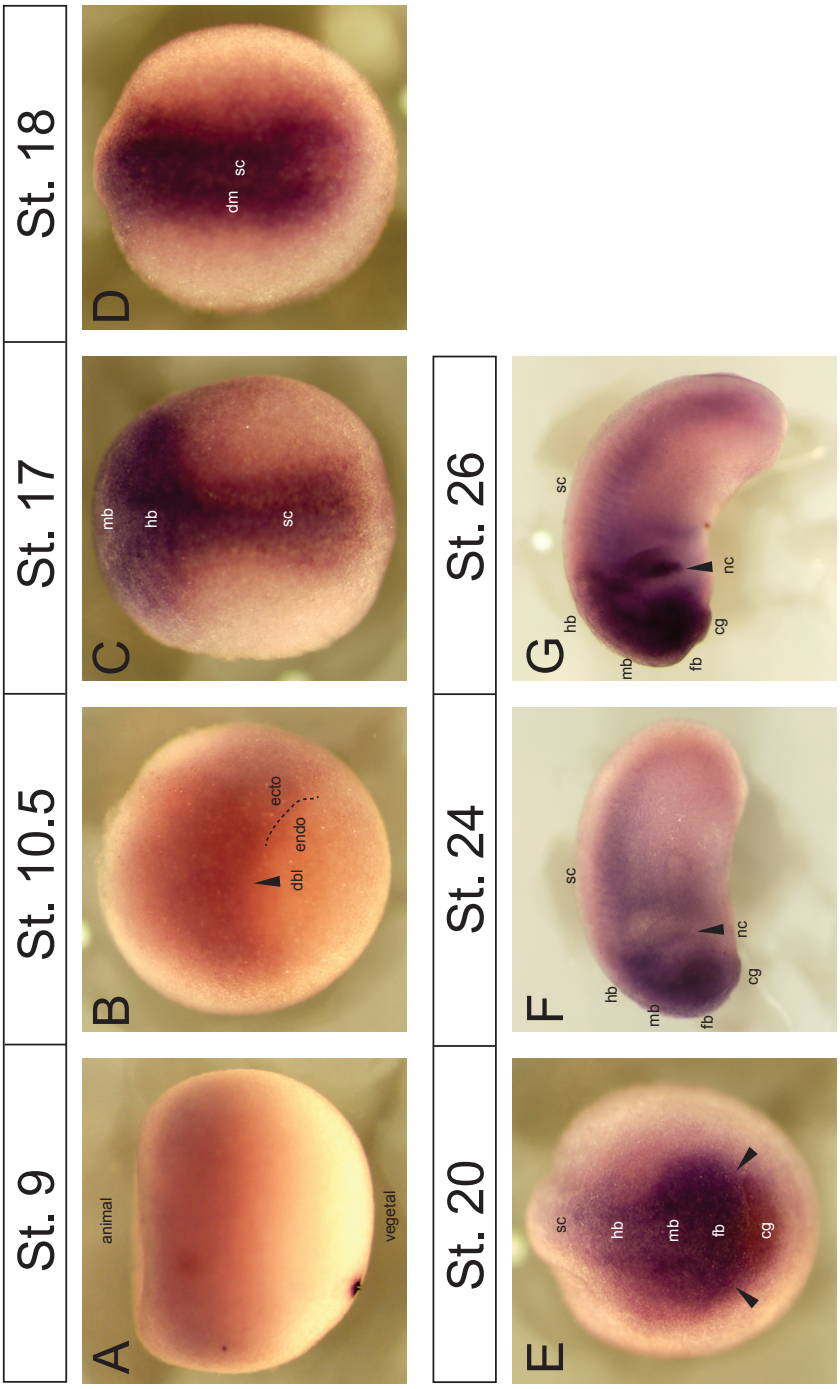

Figure 5.14 - Hematopoietic Prostaglandin D Synthase expression profile in *Xenopus laevis*

Zinc Finger 91-like (*Zfp91-l*), uncharacterized in *Xenopus laevis*, has been shown to be important for the non-canonical NF-κB pathway, a set of transcription factors that control various biological processes (Jin et al., 2010b). *Zfp91-l* is expressed strongly at blastula stage, in one half of the marginal zone (Figure 5.15A-B). At gastrula stage the staining is contralateral to the dorsal blastopore lip, in the ventro-lateral portions of the marginal zone (Figure 5.15C). The latest staining was seen at stage 13, when there was weak staining posteriorly (Figure 5.15D). This expression pattern highlights the possible role for ZFP91-like and the NF-κB pathway in a precise window of early development in *Xenopus laevis*.

5.3.4 Genes with lowered expression following Noggin overexpression

5.3.4.1 Transcription Elongation Factor A (SII) 3

Transcription Elongation Factor A (SII) 3 (*Tcea3*) is a transcription factor that facilitates transcription through sites of arrest (Plant et al., 1996). Biochemical expression studies have shown that *Tcea3* is expressed maternally and continues to be expressed throughout early development. Here its spatio-temporal mRNA expression pattern is described.

At blastula stage there was expression throughout the animal pole (Figure 5.16A), which continued into gastrula stages (Figure 5.16B). At stage 11 and stage 12 it was clear that *Tcea3* was expressed specifically in the ectoderm and not within the endoderm (Figure 5.16C-D). At early neurula stage there was faint expression anteriorly (arrowheads, Figure 5.16E) and strong expression posteriorly (arrowheads, Figure 5.16F). At later neurula stages there was a more defined anterior expression domain. Strong expression was detected in the presumptive forebrain and midbrain (arrowheads, Figure 5.16G) and throughout the spinal cord (Figure 5.16H) at stage 17, and strong expression anteriorly at stage 18 (arrowheads, Figure 5.16I). At tailbud there was strong expression

Figure 5.15 - Zfp91-like expression profile in *Xenopus laevis*. A-B) *Zfp91-l* is strongly expressed in one half on the marginal zone at stage 9, arrowheads in B) mark limits of expression. C) *Zfp91-l* is expressed in the ventral marginal zone at stage 10.5, arrowheads mark dorsal limit of expression. D) *Zfp91-l* is expressed in a small posterior domain at stage 13; arrowheads mark the limits of expression.

A) Lateral view orientated with animal up and vegetal down, B) Animal view, C) Lateral view orientated with animal up, vegetal down and dorsal left, D) Dorsal view orientated with anterior up and posterior down.

dbl, dorsal blastopore lip.

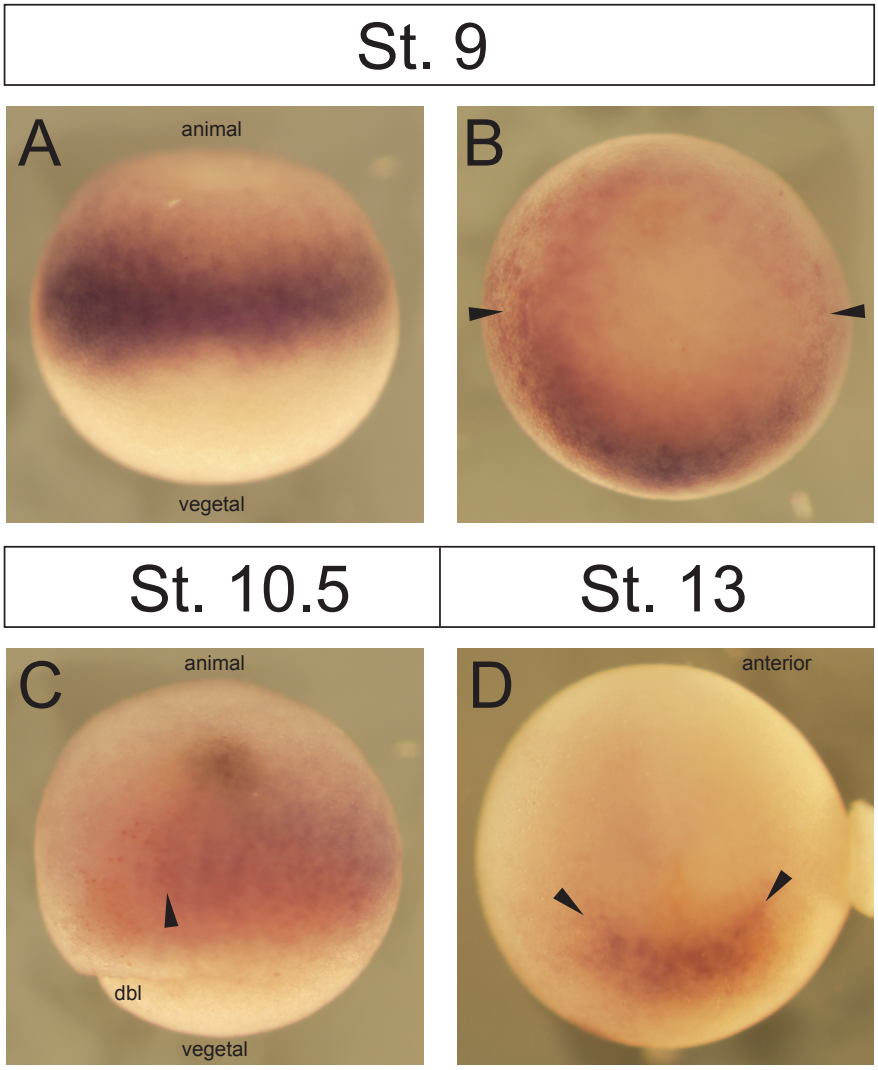

Figure 5.15 - Zfp91-like expression profile in *Xenopus laevis*

Figure 5.16 - Transcription Elongation Factor A (SII) 3 expression profile in *Xenopus laevis*. A) *Tcea3* is expressed faintly in the animal half of the embryo at stage 9. B-D) *Tcea3* is expressed in the ectoderm as gastrulation proceeds. E-F) *Tcea3* is expressed in a broad anterior domain and strongly posteriorly at stage 13, arrowheads in E) mark anterior limit of expression and in F) mark posterior expression. G) *Tcea3* is expressed throughout the forebrain, midbrain, hindbrain and spinal cord at stage 17, arrowheads mark anterior limit of expression. H) *Tcea3* is expressed strongly in the spinal cord and also in the dorsal mesoderm at stage 17. I) *Tcea3* is expressed throughout the forebrain, midbrain and hindbrain at stage 18, arrowheads mark anterior limit of expression. J-K) *Tcea3* is expressed throughout the forebrain, midbrain and hindbrain and in the somatic mesoderm at stage 23.

A-B) Lateral views orientated with animal up and vegetal down. C-D) Vegetal views. E), G), I) and J) anterior views orientated with dorsal up and ventral down. F) Posterior view orientated with dorsal up and ventral down. H) Dorsal view orientated with anterior up and posterior down. K) Lateral view orientated with anterior left, posterior right, dorsal up and ventral down.

dbl, dorsal blastopore lip, ecto, ectoderm, endo, endoderm, cg, cement gland, fb, forebrain, mb, midbrain, hb, hindbrain, sc, spinal cord, dm, dorsal muscle, sm, somitic mesoderm.

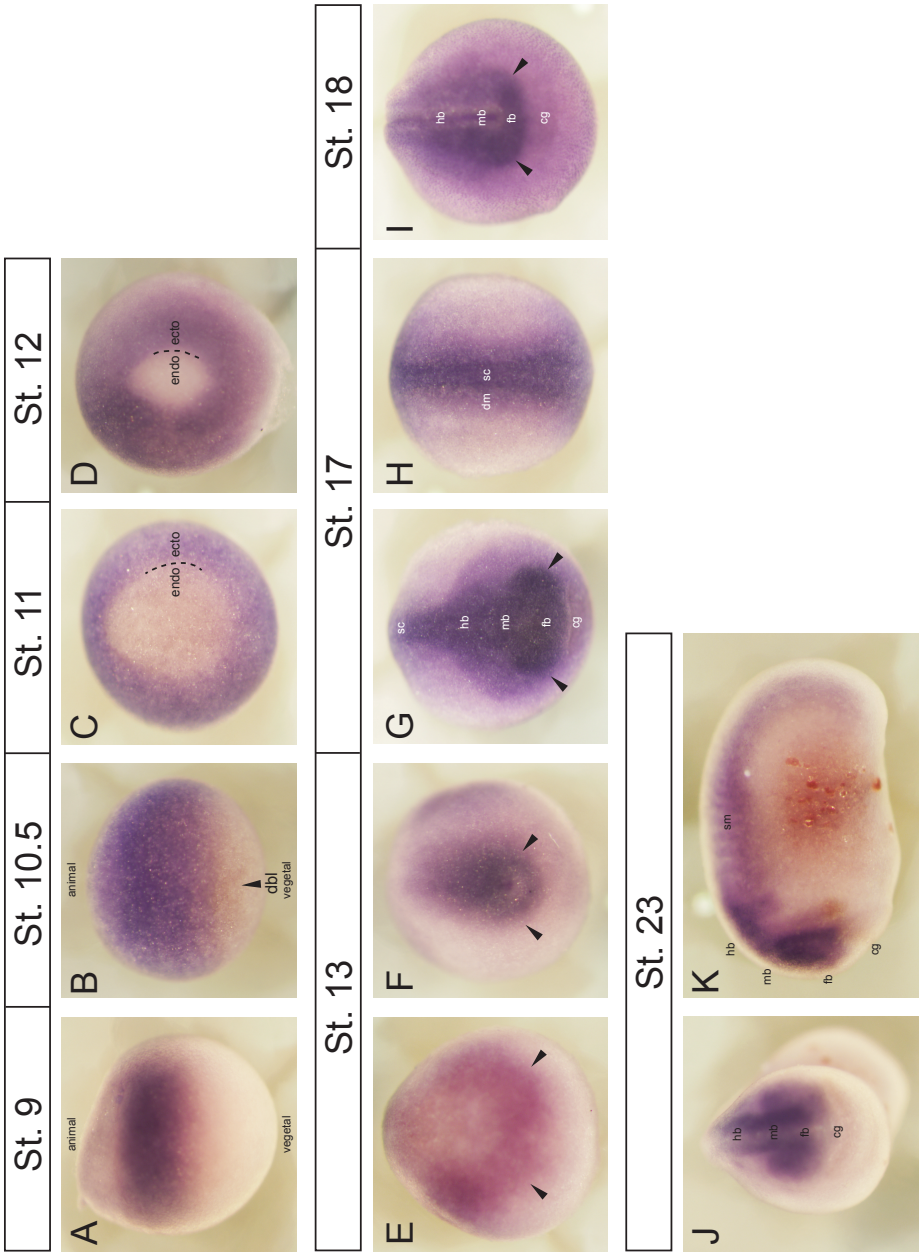

Figure 5.16 - Transcriptional Elongation Factor A (SII) 3 expression profile in *Xenopus laevis*

throughout the forebrain, midbrain and hindbrain (Figure 5.16J) and throughout the somitic mesoderm (Figure 5.16K).

5.4 Discussion

5.4.1 Chapter Summary

The first aim of this chapter was to use microarray analysis to investigate the differences between Coco, an inhibitor of BMP/Wnt/TGFβ signalling and Noggin, an inhibitor of only BMP signalling. Animal caps were cut from embryos injected with either Coco mRNA or Noggin mRNA and gene expression compared to uninjected controls. Fold increases or decreases were calculated for Coco and Noggin overexpression. The subsequent global analysis suggested there were differences between the two. This was confirmed statistically and when represented graphically it was clear that more genes were upregulated as a consequence of Coco overexpression, whilst Noggin overexpression caused more genes to be downregulated (Figures 5.1-5.3). Genes were also functionally classified (Figures 5.4-5.5), with groupings similar to previous publications (Altmann et al., 2001). Of the genes upregulated as a consequence of both Coco and Noggin overexpression most genes were involved in transcription and signal transduction.

The second aim of this chapter was to identify novel downstream targets of both Coco and Noggin signalling. A subset of the candidate downstream targets was chosen and ISH was performed in an attempt to highlight interesting expression patterns and to possibly gain insight into their function. Of the clones tested here eleven gave nice expression patterns; nine were novel expression profiles (*Cat2*, *Tipin*, *Atp13a4*, *Tll2*, *Cav2*, *Nr13-l*, *Hpgds*, *Zfp91-l* and *Tcea3*), whilst two previously published profiles were confirmed (*Crabp2* & *Cyp26c1*). The possible roles and interactions of these genes with Coco and Noggin will be discussed later.

5.4.2 Why do Coco and Noggin overexpression have such different effects?

Noggin1 initially discovered as an organizer mimicking factor (Smith and Harland, 1992) was shown to bind to BMP2/4 with a 'strikingly high' affinity (Zimmerman et al., 1996). Recent work describing the related Noggin2 claim that both Noggin proteins are able to inhibit BMP, Wnt and TGFβ signalling, and because of this induce ectopic heads (Bayramov et al., 2011). However, this was only possible for Noggin1 when replacing its endogenous 5' untranslated region (UTR) with synthetic sequence. When performing our microarray, the Noggin1 RNA was tested, and induced partial axes (at a concentration that Noggin2 would have induced ectopic heads). From these results we can assume that our microarray was performed with Noggin1 mRNA and therefore the differential expression that occurred was a consequence of the overexpression of a single BMP inhibitor.

Both Coco and Noggin1 act as extracellular inhibitors that bind ligands and stop them binding to their receptors and therefore inhibit downstream signalling. Because of this the global differences seen as a consequence of overexpression must be due to differences in efficiency of binding or downstream of the receptor.

Noggin1 only inhibits BMP2/4 ligands from binding to their receptors and therefore inhibits Smad 1/5/8/9 signalling (Zimmerman et al., 1996). Coco was shown to inhibit BMP ligands (Bell et al., 2003), but in addition also inhibits the Nodal related gene Xnr1, the TGFβ ligand Activin and Wnt ligand Wnt8. Inhibition of other extracellular ligands could cause large differences to overall gene expression levels following Coco and Noggin1 overexpression. In addition there could also be variations in affinity in the inhibition of BMP ligands between Coco and Noggin1 that affect the downstream signalling, again causing global differences between overexpression.

Lastly, it is thought one of the main effects of BMP inhibitors is induction of transcription factors (Shin et al., 2005). Large numbers of transcription factors were differentially expressed as a consequence of both Coco and Noggin1 overexpression. Interestingly there were different transcription factors

upregulated by Coco and Noggin1 presumably due to different intracellular activation. One other possible contributing factor is that Noggin1 overexpression downregulated nearly twice as many transcription factors than Coco, which could cause a large number of genes to be downregulated downstream of said transcription factors.

5.4.3 Genes that were upregulated but not included in screen

Having demonstrated global downstream differences between the effects of Coco and Noggin1 overexpression, it was interesting to see what types of genes were up- and downregulated, whether expected genes were seen, and if novel links between Coco, Noggin1 and other signalling pathways could be assumed.

As expected, both Coco and Noggin1 overexpression caused the upregulation of genes involved in anterior and neural pa2tterning. *Otx5*, a gene expressed in the Spemann organizer that is involved in anterior patterning (Kuroda et al., 2000); Msx2, essential for neural crest formation (Khadka et al., 2006) and Foxd5a, involved in neural ectoderm development (Sullivan et al., 2001) were all upregulated as a consequence of Coco overexpression. Zic4, essential for neural crest development (Fujimi et al., 2006); Zic1, essential for overall neural development (Nakata et al., 1998) and Six3, a gene required for anterior neural plate specification (Ghanbari et al., 2001; Gestri, 2005) were all upregulated as a consequence of Noggin overexpression. Patched 2, a Shh (Sonic Hedgehog) receptor expressed throughout neural tissue, was shown to be upregulated by Noggin1 in animal caps (Takabatake et al., 2000), and here was upregulated by Noggin1 overexpression. Shh has been shown to be involved in the initiation of L/R patterning by BMP inhibition (Katsu et al., 2012) and the upregulation by Noggin1 may be the result of a positive feedback loop.

In addition, Otx2, required for the specification of anterior fate (Pannese et al., 1995); Zic3, involved in specifying early neural fate (Nakata et al., 1997); Hes7, involved in midbrain/hindbrain patterning (Shinga et al., 2001); Irx1, a controller of neural plate formation (Gómez-Skarmeta et al., 1998); Hesx1, a gene

expressed in the anterior neural plate required for forebrain fate (Zaraisky et al., 1992; Andoniadou et al., 2011) and Chordin, a BMP inhibitor expressed in the Spemann organizer that is required for neural induction (Sasai et al., 1995) were all upregulated as a consequence of both Coco and Noggin overexpression.

In contrast there were also genes upregulated that might not have been expected. Cyp3a4, uncharacterized in *Xenopus*, is the most abundant P450 isoform. It is present in adult human liver tissue and is involved in steroid/drug metabolism (Dai et al., 2001). The increase in *Cyp3a4* expression could mean that following Coco overexpression there is a requirement for the breakdown of unwanted toxic molecules. A related gene Cyp27b1, a Vitamin D receptor (Li et al., 1997) was also upregulated, highlighting a possible increase in Vitamin D needs following Coco overexpression. Another gene to be upregulated as a consequence of Coco overexpression was C9, part of the immune response system. Initially expressed in early neural crest populations, C9 is expressed in the gut and associated organs in later development (McLIN et al., 2010). Its upregulation could be due to an increase of neural crest following Coco overexpression. Lastly and counter-intuitively, Smad3, a mediator of TGFβ signalling (Lagna et al., 1996) was upregulated. The increase of *Smad3* expression suggests a feedback loop with Coco possibly causing a downstream upregulation of TGFβ signalling.

Noggin1 overexpression caused the upregulation of two genes that highlighted links between itself and the Wnt pathway. *Frizzled4*, a Wnt receptor expressed in the neurectoderm (Shi and Boucaut, 2000) could well be involved in the dorsalization of the ectoderm via Noggin1 signals. Whilst Dickkopf1, also upregulated by Coco, is a secreted Wnt antagonist expressed in the Spemann organizer (Glinka et al., 1998). Noggin1 must therefore play a role in both promoting and inhibiting Wnt signalling dependent of the stage of development.

5.4.4 Genes that were downregulated but not included in screen

As expected, Noggin and Coco overexpression caused the downregulation of genes involved in ventral and non-neural patterning. Coco alone only

downregulated a few genes, but one of them was Vangl2. It is a component of the non-canonical Wnt pathway (Shafer et al., 2011), and its reduction would be expected by a Wnt inhibitor (Bell et al., 2003).

Sox17β, a TF involved in endoderm formation, (Hudson et al., 1997); BMP7, a TGFβ ligand that promotes ventral fates (Wang et al., 1997); Hes3, a negative regulator of neural differentiation (Sasai et al., 1992) and Smad9, an intracellular modulator of BMP4 activity (Nakayama et al., 1998) were all downregulated as a consequence of Noggin1 overexpression. Sox18, a gene required for cardiogenesis and ventral development (Zhang et al., 2005); Vent1, an antagonist of the Spemann organizer (V Gawantka, 1995); GATA5, a factor involved in endodermal specification (Afouda, 2005); Msx1, a mediator of epidermis development and neural inhibition (Suzuki et al., 1997); Cdx2 and Cdx4 transcription factors involved in posterior development (Isaacs et al., 1998; Faas and Isaacs, 2009) and Dlx3 an anti-neural factor (Feledy et al., 1999; Beanan and Sargent, 2000) were all downregulated by both Coco and Noggin1 overexpression.

Noggin1 and Coco overexpression also caused gene downregulations that were unexpected. Tsukushi, a BMP/FGF/Xnr inhibitor is involved in the control of germ layer specification (Morris et al., 2007) and Bambi, a silencer of TGFβ signalling (Onichtchouk et al., 1999) were downregulated as a consequence of Noggin1 overexpression and could highlight negative feedback loops to reduce inhibition of certain pathways. Sizzled, a secreted Wnt antagonist expressed ventrally (Salic et al., 1997) was downregulated by both Coco and Noggin1 expression, and could be the results of ventral Wnt signalling promotion, or just the reduction of a ventrally expressed gene in a dorsalized sample. Ras Association Domain Family 10 was the gene that was most downregulated as a consequence of Noggin1 overexpression and is uncharacterized in *Xenopus*. These factors have been shown to inhibit MAPK/Ras signalling, which promotes mesoderm induction (Cordenonsi et al., 2007). This upregulation would suggest that there is some positive regulation of MAPK/Ras signalling by Noggin1. Equally possible however is a role inhibiting proliferation, as other family

members have been shown to promote apoptosis (van der Weyden and Adams, 2007).

5.4.5 ISH analysis

The second aim of this chapter was to identify novel downstream targets of both Coco and Noggin signalling. Following bioinformatics analysis a set of candidate downstream targets were chosen. ISH was performed in an attempt to highlight interesting expression patterns.

5.4.5.1 Detoxification genes induced by Coco and Noggin

Catalase was chosen because it was the highest upregulated gene following Coco overexpression, and is thought to play a role in detoxification during early *Xenopus* development (Rizzo et al., 2007). When looking through the genes upregulated following Noggin overexpression, Hpgds, a gene that catalyses the antioxidant Glutathione was seen. Both expression profiles were produced in an attempt to see possible differences in requirements for detoxification downstream of Coco and Noggin.

Strong *Cat2* expression was seen in the animal pole at the blastula stage, whilst there was dorsal expression throughout neurula stages (Figure 5.6). Expression of *Hpgds* was very similar; weak expression was seen in the animal region of blastula and gastrula embryos, whilst there was strong expression dorsally through neurula stages and anteriorly at tailbud stages (Figure 5.14). These expression patterns suggest a requirement for detoxifying enzymes throughout dorsal and anterior development.

Catalase is a gene that degrades hydrogen peroxide (H_2O_2) into water and oxygen (Deisseroth and Dounce, 1970; Anand et al., 2009) and due to the large extent of the metabolism of anti-oxidants in early *Xenopus* development being Catalase dependent (Rizzo et al., 2007) one could assume that following Coco

overexpression there was a larger requirement for detoxifying enzymes. However, Catalase has been shown to be important for other aspects of development. Catalase has been shown not only to be required for correct gut development, but also that it could restore lost *Pax6* expression in the eye and reverse microcephaly (Peng et al., 2004). With control of H_2O_2 being involved in growth factor-mediated cell signalling (Sundaresan et al., 2005), these reports suggest that there could be many reasons why Catalase expression levels were increased by Coco overexpression. Although very little is known about the role of Hpgds during development, it seems that following Noggin1 overexpression there could be, as seen with Coco and Catalase, an increased requirement for a detoxification enzyme. Functional studies that investigate the requirement for detoxification following differed levels of Coco and Noggin1 changing could help increase understanding further.

5.4.5.2 Coco and Noggin could work together to control RA signalling

Retinoic Acid (RA) signalling is involved in regulation of diverse biological processes, including cellular proliferation, differentiation, and apoptosis, throughout embryonic development (Kumar and Duester, 2011). RA signalling has also been shown to be important for neural development, enhancing the expression of certain homeodomain transcription factors (Sirbu, 2005; Kiecker and Lumsden, 2005). Genes involved in the control of RA signalling were up- and downregulated as a consequence of both Coco and Noggin1 overexpression. Cyp26a is an RA metabolising enzyme that was shown to be involved in AP patterning (de Roos et al., 1999), and was upregulated following both Coco and Noggin1 overexpression. RXRB is an RA receptor that modulates the response to signalling acting as a ligand dependent transcription factor (Sharpe and Goldstone, 1997). Two other RA genes were analysed using ISH to try and understand spatial control of the signalling pathway by Coco and Noggin1.

Cellular Retinoic Acid Binding Protein 2, or *Crabp2*, expression was largely increased following Coco overexpression. Expression was seen in marginal tissue at blastula stages; whilst during neurula stages there was expression

throughout portions of the brain and strongly posteriorly surrounding the closing blastopore ring (Figure 5.8). Crabp2 is a binding protein that not only allows cells to receive but also enhances the transcription of Retinoic Acid (RA) signals (Dekker et al., 1994; Delva et al., 1999). I propose that it acts as a linker to other signalling pathways. Firstly RA signalling was shown to suppress BMP signalling through a reduction of pSmad1 stability (Sheng et al., 2010), and could be an indirect way to further increase BMP inhibition after Coco activity has reduced. However, the BMP pathway may not be the only link between Coco and RA. Crabp2 was also shown to be an indirect target of the canonical Wnt pathway, and could be a possible link between RA and Wnt signalling (Janssens et al., 2010). The increase of *Crabp2* expression could be due to a simple increase in RA signalling following Coco overexpression, however the reports described here suggest that there may be a higher complexity involved.

Noggin1 upregulated Cytochrome P450, Family 26, Subfamily C Polypeptide 1 (*Cyp26c1*), a Cyp26 enzyme that metabolises RA, degrading it and eliminating RA induced transcriptional activity (Sakai, 2001; Tanibe et al., 2008). The expression profile produced here, largely matches that of Tanibe et al. however, there was no mention of posterior expression, which was detected in stages 21 and 25 in this investigation (Figure 5.13). The levels of RA signalling are thought to be largely controlled by the opposing action of the RA catabolizing enzyme Raldh2 and the metabolizing Cyp26 enzymes (Swindell et al., 1999). Whilst expression analysis and loss of function studies offer evidence for Cyp26c1 being involved in hindbrain patterning (Tahayato et al., 2003; Reijntjes et al., 2004; Hernandez et al., 2007; Uehara et al., 2007), the expression profile suggests an additional general role in controlling RA levels both anteriorly and posteriorly. Cyp26c1 was upregulated by Noggin1 overexpression, a treatment that anteriorised embryos, so it is likely that Cyp26c1 both plays a role in reducing RA anteriorly (reducing the posteriorizing effect of RA) and also patterns the hindbrain. The results from the microarray and from the ISH screen show that Coco and Noggin1 play indirect roles in the control of RA signalling, something that loss of function experiments could help to elucidate.

5.4.5.3 DNA Damage control differently regulated by Coco and Noggin

Tipin, upregulated following *Coco* overexpression and Tcea3, downregulated by Noggin1 overexpression, are both genes involved in the control of DNA damage. Expression profiles were used here to see if there are spatio-temporal reasons for the difference in regulation by Coco and Noggin1.

Tipin's expression pattern was dynamic and suggested a neural specific role. Expression was shown anteriorly at stage 13, and dorsally at stage 15, whilst strong staining was seen in the midbrain, hindbrain and spinal cord at later neurula stages. At tailbud stages there were further changes with expression firstly in the spinal cord at stage 25 and then in the brain region at stage 27 (Figure 5.7). An extensive *Tcea3* expression profile was also compiled showing that expression was far less dynamic; there was strong expression throughout the ectoderm during blastula and gastrula stages and neural expression throughout neurula and tailbud stages (Figure 5.16).

Timeless Interacting Protein (*Tipin*) was originally identified in a 2-hybrid screen in yeast (Gotter, 2003) and is involved in checkpoint responses for replication block and also for stabilizing replication forks during DNA damage (Chou and Elledge, 2006; Errico et al., 2007). Tcea3 is a *Xenopus* transcription elongation factor that has the ability to suppress transcriptional pause (Natori et al., 1973; Sekimizu et al., 1979; Labhart and Morgan, 1998).

During neural development there are significant increases in cell number following proliferative signals, therefore it seems possible that an increase in *Tipin* expression following Coco overexpression, was a consequence of this and the cyclic expression pattern highlights a role in DNA damage control in specific portions of the embryo during development in *Xenopus laevis*. Interestingly the non-dynamic *Tcea3* expression was downregulated as a consequence of Noggin1 overexpression. These differences may highlight specific requirements for DNA damage control downstream of Coco and Noggin1 that could be based on the endogenous spatio-temporal expression patterns of both inhibitors.

5.4.5.4 The involvement of ATPases in neural development

Recently it was reported that antagonism of the neural specific Sarco/Endoplasmic Reticulum Ca^{2+}-ATPase 2 (*SERCA2*) increased the competency for neural differentiation (Lin et al., 2010; Pegoraro et al., 2011). Coco may also play a role in reducing the competency of the ectoderm for receiving mesoderm-inducing signals from the marginal zone. Because of this the expression of ATPase Type 13A4 was investigated to see if the expression profile offered any clues to an involvement in germ layer specification or neural development.

ATPase Type 13A4 is a probable P-Type Cation transporting ATPase protein. Members of this family are specific for pumping cations (positive), prominent examples of which are the Sodium/Potassium pump (Na^+/K^+-ATPase), the plasma membrane Proton pump (H^+-ATPase), the Proton-Potassium pump (H+/K+-ATPase) and the Calcium pump (Ca2+-ATPase). Expression was seen in marginal tissue at blastula stage, throughout dorsal neural and mesodermal tissue at neurula stages and throughout the brain at tailbud suggesting a role during neural tissue (Figure 5.16).

Ion regulation has long been associated with neural induction (Barth and Barth, 1969; Barth and Barth, 1972; Barth and Barth, 1974) and many groups have reported the requirement for ATPases during development. The Na^+/K^+-ATPase was shown to be involved in osmotic control of blastocoel formation (Slack and Warner, 1973), whilst both ionic manipulation and pharmacological inhibition of Na^+/K^+-ATPases disrupted development of the central nervous system (Messenger and Warner, 1979; Breckenridge and Warner, 1982; Messenger and Warner, 2000). The H^+-ATPase and Ca^{2+}-ATPase have also both been linked to neural development. The H^+-ATPase has also been linked to neural development. The *Xenopus laevis* H^+-ATPase Ac45LP was detected in developing neural tissue and linked to neural crest formation (Jansen et al., 2009).

However in *Xenopus* the H+/K+-ATPase has been shown to play a non-neural role. From as early as the 8-cell stage there is an asymmetric expression pattern, shown to be important for left/right (L/R) patterning (Levin et al., 2002). With *Coco* overexpression inducing ectopic neural tissue, loss of function showing an interaction with TGFβ signalling and L/R patterning being a later role of Coco, ATPases could play numerous roles in relation to Coco.

5.4.5.5 Tolloid-like 2: related, although not in function, to Tolloid-like1.

The *Drosophila* Tolloid protein, shown to be related to BMP1 (Shimell et al., 1991), cleaves Short Gastrulation (SOG), a protein involved in dorso-ventral patterning (Marqués et al., 1997). The vertebrate homolog of Tolloid, Tolloid-like 1 (*Tll1*) was shown to cleave the vertebrate homolog of SOG, Chordin (Piccolo et al., 1997). However, the role of its paralog Tolloid-like 2 (*Tll2*) remains unclear.

There was an increase of *Tll2* expression following overexpression of *Coco*, whilst *Tll1* was reduced by both Coco and Noggin. In order to investigate possible differences between the paralogs, the expression of *Tll2* was analysed.

As well as differences in their regulation by Coco and Noggin, there are also clear differences in gene expression that suggested diverse functions of the paralogs. *Tll1* is expressed in ventral/lateral sectors around the blastopore (Dale et al., 1992), and following ISH here it was clear that *Tll2* was expressed specifically in the mesenchyme of the dorsal fin at late tailbud stages (Figure 5.10). Tolloid-like 1 cleaves Chordin in *Xenopus*, however in mouse studies Tolloid-like 2 does not. Interestingly, *Tll2*(-/-) mutants exhibit an increase in muscle mass (Piccolo et al., 1997; Scott et al., 1999; Lee, 2008) highlighting different roles for Tolloid-like 2. Bearing in mind Tll2 is expressed in the mesenchyme of the tailbud, and *Tll2* (-/-) mice have an increase in muscle mass, I propose a role for Tolloid-like 2 in regulation of neural crest derived mesenchyme in the trunk, which gain and loss of function studies would help to investigate.

5.4.5.6 Does Coco inhibit ventral fate via inhibition of the NF-κB pathway

Many of the genes discussed here were upregulated as a consequence of *Coco* overexpression, however Zinc Finger 91-like (*Zfp91-l*) was chosen because it was one of the few genes downregulated as a consequence of *Coco* overexpression alone.

Zfp91-l is an uncharacterized *Xenopus* homolog of Zfp91. Following ISH analysis it was clear that at blastula stages there was asymmetric expression in the marginal zone, with latero-ventral expression at gastrulation stages, suggesting a role in ventral development (Figure 5.15).

Zfp91, an atypical E3 ligase involved in the NF-κB signalling pathway was originally discovered in a screen of acute myeloid leukaemia (AML) cells (Unoki et al., 2003; Jin et al., 2010b; Jin et al., 2010a). The NF-κB pathway has been shown to be important for aspects of axis formation and early patterning. Xrel2 a member of the NF-κB family of proteins is highly enriched ventrally prior to gastrulation in *Xenopus* whilst overexpression of Xrela, the homolog of NF-κB, disrupted gastrulation in *Xenopus* (Tannahill and Wardle, 1995; Kao and Lockwood, 1996). In slightly later development Xrel3 was shown to be required for head development and NF-κB signalling shown to be vital for correct axis formation (Lake et al., 2001; Armstrong et al., 2012). Coco overexpression caused a reduction in *Zfp91-l*, and it is likely that negative regulation of the NF-κB signalling via *Zfp91-l* is important for development.

5.4.5.7 Novel genes

The last two genes that will be discussed, Nr13-like and Caveolin 2, were picked for being completely novel, in relation to germ layer specification and neural development.

Anti-apoptotic protein Nr13-like (*NR13-l*) is an uncharacterized paralog of Nr13. Nr13 shares significant homology to the anti-apoptotic protein Bcl2, and was shown to inhibit Caspase-3 activity (Gillet et al., 1993; Moradi-Améli et al., 2002). Expression of *Nr13-l* was seen throughout the presumptive ectoderm during blastula and gastrula stages (Figure 5.12), areas that overlap with regions of cell death (Hensey and Gautier, 1998). It is possible that *Coco* overexpression increased proliferation throughout the ectoderm and therefore there was an increased need for anti-apoptotic factors at this stage of development.

Caveolin 2 (*Cav2*) is a scaffolding protein and is a major component of cavelae, small invaginations of the plasma membrane (Scherer et al., 1996) and although it was thought that Caveolin-2 was not expressed up until tadpole stage (Razani et al., 2002a) here expression was seen in the marginal zone during blastula and gastrula stages and strongly anteriorly in stage 13. At stage 17 *Cav2* was expressed throughout the presumptive brain and spinal cord and pan-neural expression was also seen at early tailbud stage (Figure 5.11). Although uncharacterized in *Xenopus*, mice lacking Caveolin 2 suffer from severe pulmonary dysfunction, whilst those deficient in Caveolin 1 have hyper-proliferation problems (Razani et al., 2001; Razani et al., 2002b).
There could be a role for Caveolin-2 in the circulation system, though the expression pattern suggests that Caveolin-2 has a neural role in *Xenopus laevis*.

Table 5-1 - Genes upregulated as a consequence of overexpression of Coco (Yellow), Noggin1 (Blue) or both (Red)

Gene Name	Role	Up Fold
Coco	TGFβ and Wnt Inhibitor	6.794
Complement Component 5	Immune Response	4.626
Catalase	H2O2 degradation	4.290
RING finger protein 213-like	-	4.098
Acetylcholine receptor gamma subunit precursor	Postsynaptic Membrane	4.030
Complement Component 5	Immune Response	3.953
Stromelysin-3	Extracellular Matrix Metalloprotease	3.794
RING finger protein 213-like	-	3.542
Orthodenticle Homeobox 2	Homeodomain Transcription Factor	3.482
Transcobalamin II precursor	Vitamin B Carrier Protein	3.476
Orthodenticle Homeobox 2	Homeodomain transcription factor	3.448
Orthodenticle Homeobox 2	Homeodomain Transcription Factor	3.448
Zic family member 4	Zinc Finger Transcription Factor	3.309
Xl2.57081	-	3.299
HES-3-like	-	3.259
Xl2.51791	-	3.170
Pleckstrin homology domain containing, family A	Intracellular signaling or / cytoskeleton.	3.021
Forkhead box D4-like 1	Forkhead transcription factor	3.003
Cytochrome P450, Family 26, Subfamily C Polypeptide 1	Retinoic Acid Metabolim Protein	2.961
XTimeless interacting protein	DNA Replication	2.872
Lipocalin cpl1	Choroid Plexus	2.856
Orthodenticle Homeobox 5	Homeodomain transcription factor	2.845
Orthodenticle Homeobox 5	Homeodomain transcription factor	2.727
Protein Kinase Domain Containing Homolog Gene 2	Serine/threonine protein kinase	2.654
Xl2.51791	-	2.643
Noggin	extracellular BMP antagonist	2.640
Hairy and Enhancer of Split 7	Helix-loop-helix transcription factor	2.609
Cytochrome P450, family 2, subfamily J, polypeptide 2	Cytochrome P450	2.524
Cytochrome P450, family 3, subfamily A, polypeptide 4	Cytochrome P450	2.522
Protein Kinase Domain Containing Homolog Gene 2	Serine/threonine protein kinase	2.519
Cytochrome P450, family 3, subfamily A, polypeptide 4	Cytochrome P450	2.510
Protease, serine, 12 (neurotrypsin)	Synaptic serine protease	2.489
Cellular Retinoic Acid Binding Protein 2	RA signalling	2.457
Beta-tubulin	Microtubule protein	2.456

ATPase type 13A4	ATP degradation	2.445
Family with sequence similarity 83	Lung Cancer Cell marker?	2.417
SH2 Domain Containing 3C	Regulation of B Cell Development	2.373
5'-nucleotidase, cytosolic III	Dephosphorylation of UMP and CMP	2.321
Solute carrier family 39	Metal ion transporter	2.310
Reticulon 1 (RTN1)	Neuroendocrine secretion or in membrane trafficking	2.303
Forkhead box D4-like 1	Forkhead domain transcription factor	2.298
Fez Family Zinc Finger Protein 2	Zinc Finger Transcription Factor	2.279
Protein kinase domain containing, cytoplasmic homolog, 2	Serine/threonine protein kinase	2.260
Msh homeobox 2	Transcription Factor	2.217
Annexin 4	Formation of pronephric tubules	2.210
Frizzled 4 Protein	Wnt Signaling Receptor	2.197
Forkhead-domain-containing protein 5	Transcription Factor	2.191
F-box only protein 32-like	Phosphorylation-dependent ubiquitination	2.184
HESX homeobox 1	Homeobox Trascription Factor	2.179
Chordin	BMP inhibitor	2.160
Dickkopf	Wnt Inhibitor	2.153
Jun D proto-oncogene	p53-dependent senescence and apoptosis	2.127
Orthodenticle Homeobox 5	Homeodomain transcription factor	2.121
Orthodenticle Homeobox 5	Homeodomain transcription factor	2.117
Xl2.57050	-	2.109
Cytochrome P450, family 27, subfamily B, polypeptide 1	Electron transport	2.106
Tolloid-like 2	BMP agonist	2.099
Xl2.57074	-	2.075
Xl2.1946	-	2.028
Galectin family xgalectin-VIa	Galactosidase binding	2.020
Anti-apoptotic protein NR13-like	Anti-apoptotic protein NR13-like	2.009
Xl2.28189	-	2.002
Xenopus laevis Orga02	-	2.001
Orthodenticle Homeobox 5	Homeodomain transcription factor	1.973
Xl2.56166	-	1.968
DENN/MADD domain containing 1C	RAS signaling inhibitor	1.959
Patched 2	Hedgehog Receptor	1.946
DENN/MADD domain containing 1C	RAS signaling inhibitor	1.943
Patched 2	Hedgehog Receptor	1.938
Cytochrome P450, family 26, subfamily A, polypeptide 1	Retinoic Acid hydroxylase	1.921
SIX homeobox 3	Homeodomain transcription factor	1.911
Xl2.1975	-	1.909
Proteasome 26S subunit, non-ATPase, 14	26S proteasome	1.895
Synapsin II	Synaptic Vesicle Protein	1.885
Zic family member 3	zinc finger, C2H2 type	1.882

Xl2.7783	-	1.875
Cytochrome P450, Family 26, Subfamily C Polypeptide 1	Retinoic Acid Metabolim Protein	1.854
Xl2.34447	-	1.848
Xl2.9682	-	1.846
Xl2.15788	-	1.845
Zic family member 3	Zinc Finger Transcription Factor	1.842
Zic family member 3	Zinc Finger Transcription Factor	1.842
Immunoglobulin Heavy Chain Precursor	Antigen binding	1.834
Thymopoietin	Muscle Contraction	1.808
Hairy and Enhancer of Split 7	Helix-loop-helix transcription factor	1.804
Caveolin-2	Plasma Membrane	1.804
Myosin light chain 2	Myosin regulation	1.792
Complement Component 5	Immune Response	1.782
Xl2.3695	-	1.776
Xl2.9023	-	1.773
LIM zinc finger	Protein Interactions	1.766
RNA polymerase II elongation		1.752
FK506 binding protein 9	Protein Folding and Trafficking	1.740
Solute Carrier Family 40	Iron transporter	1.727
Ubiquitin associated protein 1	Protein degradation	1.726
Lysophosphatidic acid receptor 6	G protein-coupled receptor	1.725
Exportin 1	Nuclear transport receptor CRM1/MSN5	1.719
Cannabinoid Receptor Interacting Protein 1	G-protein coupled receptor	1.717
Musashi Homolog 2	RNA binding	1.716
Xl2.1758	-	1.712
Sestrin 1	Regulation of cell growth and survival.	1.709
Matrix Metalloproteinase 14	ECM Degradation	1.696
Pleiotrophin	Neural Growth Factor	1.693
Cytochrome P450, Family 26, Subfamily A	Retinoic acid converting enzyme	1.665
Poly(U)-specific endoribonuclease-D	RNA degradation	1.661
Zic family member 4	Zinc Finger Transcription Factor	1.661
Xl2.3695	-	1.660
Heat Shock 22kDa protein 8	Programmed Cell Death Inhibitor	1.650
Cell Division Cycle 25 Homolog B	M-phase inducer phosphatase	1.649
Myosin HC	Muscle	1.642
Homeobox Iro Protein 1	Homeodomain transcription factor	1.632
Basic transcription protein 1 (gene 1)	Transcription Factor	1.622
Insulin-like Growth Factor 1	Growth Factor	1.622
Xl2.13334	-	1.620
Xl2.52258	-	1.618
Pinhead precursor	Head development	1.615
von Willebrand Factor C Domain-containing Protein	Coagulation Protein	1.608
Xl2.19235	-	1.580

StAR-related lipid transfer domain containing 4	Mediators of Intracellular Lipid Metabolism	1.578
Hypothetical Protein LOC100126657	-	1.573
Fgf Receptor2	FGF signaling	1.553
Complement component 9 precursor	Immune response	1.552
Hypothetical Protein MGC80829	-	1.537
Discoidin Domain receptor	Serine/threonine kinase	1.531
Hypothetical Protein MGC115585	-	1.530
Hypothetical Protein LOC100101306	-	1.530
Carboxypeptidase N, Polypeptide 1 precursor	Zinc carboxypeptidase	1.529
Matrix Metalloproteinase 14	ECM Degradation	1.528
ECM p1-I	ECM	1.512
Monocarboxylate transporter	-	1.501
Lecithin Retinol Acyltransferase	Retinol O-acyltransferase	1.499
UPF0632 protein C2orf89-like	-	1.499
Hematopoietic Prostaglandin D Synthase	Glutathione S-transferase	1.497
H2A histone family, member Y	DNA binding	1.488
Sestrin 1	Regulation of cell growth and survival.	1.483
Receptor Tyrosine Kinase-like Orphan Receptor 1	Serine/Threonine Kinase	1.483
Hairy Enhancer of Split 1	Helix-loop-helix Transcription factor	1.456
Angiotensin receptor related protein	hormone receptor	1.442
Microtubule-associated protein 1 3 alpha	Microtubule protein	1.440
Tankyrase	Wnt Inhibitor	1.428
Xl2.21725	-	1.427
Zic family member 1	Zinc Finger Transcription Factor	1.423
Elyp1	-	1.418
Alpha-2-HS-glycoprotein precursor	Cysteine Protease Inhibitor	1.417
Zic family member 1	Zinc Finger Transcription Factor	1.395
Poly (ADP-ribose) polymerase family, member 3	NAD+ ADP-ribosyltransferase	1.392
Xl2.47903	-	1.388
Homolog of rat pragma of Rnd2	Protein Kinase	1.388
Leucine-rich repeats and immunoglobulin-like domains 3	Membrane glycoprotein	1.386
TNF receptor-associated factor 4	Zinc Finger Transcription Factor	1.377
Encr-3	BTB/POZ and Kelch domains	1.374
Meis Homeobox 3	Homeodomain transcription factor	1.365
Internexin	Structural protein	1.362
Angiopoietin4	Ficolin and related extracellular proteins	1.356
Na(+)/K(+)-transporting ATPase	Membrane Protein	1.347
Angiomotin-like 2 (amotl2)	Growth-arrest-specific protein	1.345
Insulin-like Growth Factor 1	Growth Factor	1.343
Cell Division Cycle 25 Homolog B	M-phase inducer phosphatase	1.343
Cell Division Cycle 25 Homolog B	M-phase inducer phosphatase	1.342

Similar to gap junction protein	-	1.338
Crumbs Homolog 1-like	Structural Protein	1.330
Xl2.55575	-	1.305
SMAD family member 3	Signal transduction TGFβ	1.285
Shisa	Wnt and FGF Inhibitor	1.284
Hematopoietic Prostaglandin D Synthase	Glutathione S-transferase	1.284
Hematopoietic Prostaglandin D Synthase	Glutathione S-transferase	1.278
Complement component 9 precursor	Immune response	1.277
Membrane-associated ring finger (C3HC4) 8	Protein involved in mRNA turnover and stability	1.276
Rho GTPase-activating protein 6	Rho Signaling	1.275
RAB40B, member RAS oncogene family	Small GTPase	1.258
Tubulin, beta 6 class V	Microtubule protein	1.256
Zic family member 1	Zinc Finger Transcription Factor	1.252
Mannose receptor, C type 2	Sugar binding	1.240
E3 ubiquitin-protein ligase MARCH8	Protein involved in mRNA turnover and stability	1.229
Lysophosphatidic acid receptor 2	Transmembrane protein	1.215
Pyruvate dehydrogenase kinase 2	Glycolosis	1.213
Rho family GTPase 2	Rho family GTPase	1.204
RGM domain family, member A	Axon Guidance	1.204
RAB40B, member RAS oncogene family	Small GTPase	1.191
Xl2.13704	-	1.188
CD81-a	Membrane Protein	1.185
Similar to serum-inducible kinase	-	1.179
Schwannomin interacting protein 1	Links Membrane proteins and Cytoskeleton	1.174
Schwannomin interacting protein 1	Links Membrane proteins and Cytoskeleton	1.174
Iroquois Homeobox 1	Homeodomain transcription factor	1.172
Xl2.16421	-	1.168
Midkine-A precursor	Neurite growth factor	1.167
Fibroblast growth factor receptor-2	FGF signalling	1.162
heat shock protein 90kDa alpha (cytosolic)	Molecular chaperone	1.157
Angiotensin receptor-like 1b	Glycoprotein hormone receptor	1.156
Glucocorticoid-induced leucine zipper	Myosin class II heavy chain	1.155
Carbohydrate sulfotransferase 9-like	SO4 transfer	1.154
TCDD-inducible poly(ADP-ribose) polymerase	Nucleic Acid Binding	1.144
FAT tumour suppressor homolog 1	Cell adhesion/signal transduction	1.144
Basic Transcription Element Binding Protein 1	Zinc Finger Transcription Factor	1.138
Kruppel-like factor 9	Zinc Finger Transcription Factor	1.135

Table 5-2 - Genes downregulated as a consequence of overexpression of Coco (Yellow), Noggin1 (Blue) or both (Red)

Gene Name	Role	Down Fold
Ras Association Domain Family 10	Cell Growth/Differentiation Regulator	2.730
SRY Box 17 Beta	HMG-box transcription factor	2.455
XI2.3435.1.A1_at	-	2.432
Angiomotin-like 2	Growth-arrest-specific protein	2.078
BMP and Activin Membrane-bound Inhibitor	Negative Regulator of TGF-beta	2.054
Peroxiredoxin 3	Alkyl hydroperoxide reductase	2.036
Transcription Elongation Factor A (SII), 3	Transctiption Factor	1.952
Solute CarrierFamily 38, Member 2	-	1.949
Tumor Necrosis Factor Receptor Superfamily Member 12A	-	1.930
XI2.14536.1.A1_at	-	1.915
Oncoprotein Induced Transcript 1	Ca2+ Binding Protein	1.893
T-box 2	T-box transcription factor	1.877
Dynactic 3	Organelle Transport	1.849
Zinc Finger Protein 729-like	Zinc Finger Transcription Factor	1.848
X-epilectin	F-type Lectin	1.824
Lapl03	-	1.816
Tribbles Homolog 1	Serine/threonine protein kinase	1.801
Bone Morphogenetic Protein 7	TGF-beta related peptide growth factor	1.794
Cement Gland-specific Protein CGS	-	1.789
Tolloid-like 1	Metalloprotease	1.785
Anoctamin-9-like	-	1.767
Hairy and Enhancer of Split 3	Helix-loop-helix Transcription Factor	1.767
Xenopus laevis B2 keratin	-	1.759
XI2.6022.1.A1_at	-	1.737
XI2.16485.1.S1_at	-	1.735
Frizzled-related Protein 3	Secreted Wnt Antagonist	1.703
SMAD family member 9	TGF-beta pathway	1.702
XI2.41444.1.S1_at		1.682
SRY Box 18	HMG-box transcription factor	1.679
NHE3 Kinase A Regulatory Protein 2	Na+/H+ Exchanger Binding Protein	1.679
SMAD family member 9	TGF-beta pathway	1.674
Upstream Binding Protein 1	Transctiption Factor	1.673
XI2.4877.1.A1_a_at	-	1.672
Forkhead Box J1	Forkhead Domain Transcription Factor	1.646
Inhibitor of DNA Binding 4	Transcriptional Regulator	1.642
Glycerophosphodiester Phosphodiesterase 1	Glycerophosphoryl diester phosphodiesterase	1.641
Meso05 mRNA	-	1.636
Guanylate Nucleotide Binding Protein 2	Guanylate-binding protein	1.632
Transcription Factor AP-2 Alpha	Transctiption Factor	1.630

Xl2.15677.1.A1_at	-	1.617
Xl2.11400.1.A1_at	-	1.599
Xl2.21207.1.A1_at	-	1.593
Xl2.16336.1.A1_at	-	1.584
Frizzled Family Receptor 6	Wnt Receptor	1.511
Plakophilin-3	Neural Adherens Junction Protein	1.507
GATA binding protein 3	Zinc Finger TranscriptionFactor	1.505
Frizzled Family Receptor 3	Wnt Receptor	1.502
MSH Homeobox 1	Homeodomain Transcription Factor	1.502
Xl2.4877.1.A1_at	-	1.499
Xl2.22044.1.S1_at	-	1.496
S100 calcium binding protein A10	calcium binding	1.495
Xl2.51612.1.S1_at	-	1.491
Sizzled	CRD domain wnt inhibitor	1.485
GATA binding protein 5	Zinc Finger Transcription Factor	1.482
Phytanoyl-CoA Dioxygenase Domain Containing 1	Peroxisomal phytanoyl-CoA hydroxylase	1.478
Integrin Beta-3 Subunit	-	1.478
Growth Arrest and DNA-damage-inducible Gamma	-	1.460
Xl2.34274.1.A1_at	-	1.454
Xl2.21240.1.S1_at	-	1.451
SMAD Family Member 9	TGF-beta pathway	1.447
GATA binding protein 3	Zinc Finger Transcription Factor	1.442
GATA binding protein 3	Zinc Finger Transcription Factor	1.435
Zinc Finger Protein 91-like	Zinc Finger Transcription Factor	1.429
Caudal Type Homeo Box 4	Homeodomain Transcription Factor	1.421
Transposon Xmix-Xl-9	-	1.413
Glutamine Fructose-6-Phosphate Transaminase 1	Transaminase	1.408
Grainyhead-like Protein 3	Transctiption Factor	1.401
Vasorin	Slit-like Protein	1.400
VENT homeobox 1	Homeodomain Transcription Factor	1.397
Xl2.25006.1.A1_at	-	1.397
Forkhead Box I1	Forkhead Domain Transcription Factor	1.396
Distal-less Homeobox 2	Homeodomain Transcription Factor	1.395
Grainyhead-like Protein 3	Transctiption Factor	1.395
ATP/GTP Binding Protein-like 1	Zinc carboxypeptidase	1.394
Xl2.11187.1.A1_at	-	1.394
Ras-related C3 Botulinum Toxin Substrate 2	Small GTPase	1.388
Exportin 1	Nuclear transport receptor	1.382
Otogelin	Coagulation Protein	1.381
VENT Homeobox 3	Homeodomain Transcription Factor	1.377
Caudal Type Homeobox 2	Homeodomain Transcription Factor	1.369
Xl2.34452.2.A1_at	-	1.367

Heparan Sulfate 3-O-sulfotransferase	Sulfotransferases	1.366
Zinc Finger Protein 91-like	Zinc Finger Transcription Factor	1.366
Kin of IRRE-like 2	Immunoglobulin	1.361
VENT homeobox 1	Homeodomain Transcription Factor	1.360
Kringle Containing Transmembrane Protein 2	Dkk1 Receptor	1.350
Tripartite Motif Containing 29	Ubiquitin-protein Ligase	1.349
Transcription Factor AP-2 Alpha	Transctiption Factor	1.349
T-box 3	T-box transcription factor	1.343
Vang-like 2	Non-canonical wnt pathway signaling protein	1.342
Retinoid X Receptor Beta	Transcriptional Regulator	1.339
MSH Homeobox 1	Homeodomain Transcription Factor	1.336
Putative Wnt Inhibitor Frzb3	Secreted Wnt Antagonist	1.334
Transcription Factor AP-2 Alpha	Transctiption Factor	1.327
Heparan Sulfate 3-O-sulfotransferase	Sulfotransferases	1.320
XI2.2161.1.S1_at	-	1.316
MGC82879 protein	-	1.314
XI2.2941.1.A1_at	-	1.312
Tsukushi Small Leucine Rich Proteoglycan Homolog	Modulator of Nodal, Fgf, and BMP signaling	1.310
Beta 1,4-galactosyltransferase Polypeptide 3	Galactosyltransferase	1.309
Diacylglycerol Kinase Alpha	Diacylglycerol Kinase	1.307
Phosphorylase, Glycogen; Brain	Glycogen phosphorylase	1.304
tripartite motif containing 29	Ubiquitin-protein Ligase	1.302
Endothelin Converting Enzyme-like 1	M13 family peptidase	1.300
Prostaglandin-endoperoxide Synthase 2	Peroxidase	1.258
Riddle 4	Coagulation Protein	1.253
Cege01 mRNA	-	1.248
LIM domain only 4	Homeodomain Transcription Factor	1.246
7-Dehydrocholesterol Reductase	Ergosterol Biosynthesis	1.245
XI2.50552.1.S1_at	-	1.234
XI2.13436.2.S1_a_at	-	1.232
XI2.15173.1.A1_at	-	1.184
Albumin	Carrier Protein	1.183
B-cell translocation protein x	Anti-proliferation Factor	1.178
S100 Calcium Binding Protein A10	Ca2+ Binding Protein	1.164
AHNAK nucleoprotein	Multiple	1.157
LIM domain transcription factor	Transcription factor	1.155
MGC81570 protein	-	1.147
MGC81570 protein	-	1.147
S100 Related	-	1.146
Leucine Rich Repeat Neuronal 1	Ras suppressor protein	1.142
Cyclin O	Cyclin B related protein	1.133
XI2.3048.1.A1_at	-	1.133
Death-associated Protein Kinase 2	Calmodulin-dependent Protein Kinase	1.131
MGC80418 protein	-	1.125

Cyclin O	Cyclin B related protein	1.108
StAR-related lipid transfer (START) domain containing 13	Tumour Suppressor Protein	1.088
Syndecan Binding Protein	Beta Amyloid Precursor-binding Protein	1.085
Cyclin O	Cyclin B related protein	1.080
Nemo-like Kinase 2	Serine/Threonine Kinase	1.078
Xl2.55593.1.S1_at	-	1.077
Phosphorylase, Glycogen; Muscle	Glycogen phosphorylase	1.075
Zinc Finger BTB	-	1.066
Zinc Finger BTB	-	1.066
Forkhead Box J1	Forkhead Domain Transcription Factor	1.055
Alkaline Phosphatase, Liver/Bone/Kidney	Hydrolase	1.051
Xl2.50635.1.S1_at	-	1.044
Distal-less Homeobox 3	Homeodomain Transcription Factor	1.030
Anoctamin-9-like	Uncharacterized	1.012

	Coco Up	Coco Up %	Coco Down	Coco Down %	Noggin Up	Noggin Up %	Noggin Down	Noggin Down %
Amino Acid Biosynthesis	6	4.0%	0	0.0%	0	0.0%	1	0.7%
Cellular Processes	22	14.7%	3	7.9%	17	20.2%	29	21.3%
Transport/Binding	13	8.7%	4	10.5%	5	6.0%	11	8.1%
Transcription	28	18.7%	18	47.4%	24	28.6%	32	23.5%
Signal Transduction	26	17.3%	5	13.2%	22	26.2%	13	9.6%
Cell Structure	21	14.0%	0	0.0%	6	7.1%	6	4.4%
Nucleotide Metabolism	2	1.3%	0	0.0%	0	0.0%	0	0.0%
Hypothetical/Unknown	1	0.7%	8	21.1%	9	10.7%	18	13.2%
No Database Match	31	20.7%	0	0.0%	1	1.2%	26	19.1%

Gene Name	Symbol	Role	Up Fold	Figure
Catalase	*Cat2*	H2O2 degradation	4.290	5.6
XTimeless interacting protein	*Tipin*	DNA Replication	2.872	5.7
Cellular Retinoic Acid Binding Protein 2	*Crabp2*	RA signalling	2.457	5.8
ATPase type 13A4	*Atp13a4*	Probable Cation Transporter	2.445	5.9
Tolloid-like 2	*Tll2*	BMP agonist	2.099	5.10
Anti-apoptotic protein NR13-like	*Nr13-l*	Anti-apoptotic protein NR13-like	2.009	5.11
Caveolin-2	*Cav2*	Plasma Membrane	1.804	5.12
Cytochrome P450, Family 26, Subfamily C Polypeptide 1	*Cyp26c1*	Retinoic Acid Metabolim Protein	1.854	5.13
Hematopoietic Prostaglandin D Synthase	*Hpgds*	Glutathione S-transferase	1.497	5.14

Gene Name	Symbol	Role	Down Fold	Figure
Zinc Finger Protein 91-like	*Zfp91-l*	Zinc Finger Transcription Factor	1.429	5.15
Transcription Elongation Factor A (SII), 3	*Tcea3*	Transctiption Factor	1.952	5.16

Chapter 6 Discussion

6.1 Inhibition of TGFβ signalling is required for ectodermal specification

The TGFβ signalling factors Vg1, Activin and the Nodal-related genes are involved in germ layer specification. Maternal expression of the nodal related genes *Xnr5* and *Xnr6* are required for both endoderm formation and mesoderm induction (Luxardi et al., 2010). During endoderm formation, *Xnr5* and *Xnr6* are induced by Veg-T, signalling that is facilitated by Sox7 (Zhang, 2003; Zhang et al., 2005), and act redundantly to induce the closely related endoderm specifiers *Xnr1* and *Xnr2* (Yasuo and Lemaire, 1999). The Xnr genes induce downstream members of the Mix and GATA families of transcription factors, proteins involved in the acquisition of endodermal fate.

Xnr genes are also required for mesoderm induction. *Xnr* genes are enhanced by dorsally localized β-Catenin, leading to a dorso-ventral gradient of Xnr activity in the marginal zone. High levels of Nodal-related signal in combination with Vg1 and Wnt signalling act as the Nieuwkoop centre, a dorsalizing signal required for induction of the Spemann organizer. Lower levels of Nodal-related signalling induce *Bmp4* and *Wnt8* ventrally; these act synergistically to pattern ventral mesoderm. A reduction in Xnr signals during germ layer specification causes a drastic loss of the mesodermal marker *Xbra* (Luxardi et al., 2010).

The TGFβ ligand Activin is required for both endoderm and mesoderm formation (Hudson et al., 1997; Piepenburg, 2004). Activin causes the induction of both endodermal and mesodermal cell in both explants and cell cultures (Jones et al., 1993; Ninomiya et al., 1999; Kubo, 2004; Yasunaga et al., 2005; Gadue et al., 2006; D'Amour et al., 2006; Teo et al., 2012; Thomsen et al., 1990; Green et al., 1992).

The TGFβ factors that are involved in endoderm formation and mesoderm induction are secreted signals. Ectodermal specification requires TGFβ inhibitors that prevent these factors from being active in the animal portion of the embryo (Chang and Harland, 2007). Such inhibitors are expressed in the ectoderm. Xema is a gene that protects ectodermal fate via inhibition of both Nodal-related and FGF signalling, but more importantly can promote ectodermal specification by the induction of other ectodermally expressed genes (Suri, 2005; Mir et al., 2007; Mir et al., 2008). *Ectodermin* is expressed maternally and ubiquitinates Smad4, which indirectly inhibits the transcription of downstream mesodermal genes (Dupont et al., 2005). Norrin, is a secreted molecule that both protects ectodermal fate, via inhibition of Activin and BMPs, and also promotes neurectoderm specification by upregulating Wnt signalling (Xu et al., 2012). Coco is a distinct maternal factor that inhibits Activin, Wnt and BMP signalling (Figure 6.1). This investigation showed that Coco inhibits Activin during germ layer specification to control mesoderm and endoderm production.

6.2 Coco controls germ layer specification by inhibiting Activin

Coco loss of function, using morpholino knockdown, caused an animal shift of endoderm at the expense of dorsal mesoderm. Due to a requirement of TGFβ signalling for germ layer specification, it was thought that an over activation of one of the ligands might be causing the germ layer defects. Rescue experiments showed that an over activation of Activin was causing the Coco loss of function phenotype. These results suggest that in a wild type situation Coco is required to inhibit Activin signalling from becoming active in the animal portion of the embryo (Figure 6.2A), and that following CocoMO injection, there is a dorso-ventrally biased over activation of Activin signalling (Figure 6.2B). This over activation of Activin is therefore likely to be the cause of the loss of dorsal mesoderm (Figure 6.2C-D) and the shift of endoderm on the dorsal side of the embryo (Figure 6.2E-F). This data confirms Coco as a distinct, ectodermally expressed, inhibitor of BMP/Wnt/TGFβ signalling that plays a role in germ layer specification (Figure 6.2).

Figure 6.1 – Coco plays a distinct role during germ layer specification. Xema inhibits Nodal-related signals from the marginal zone, but more importantly promotes ectodermal fates. Ectodermin inhibits Nodal-related signals and Activin. Norrin inhibits BMP and Activin signalling, but promotes Wnt signalling dorsally. Coco inhibits Activin, BMP and Wnt signals to protect ectodermal fate.

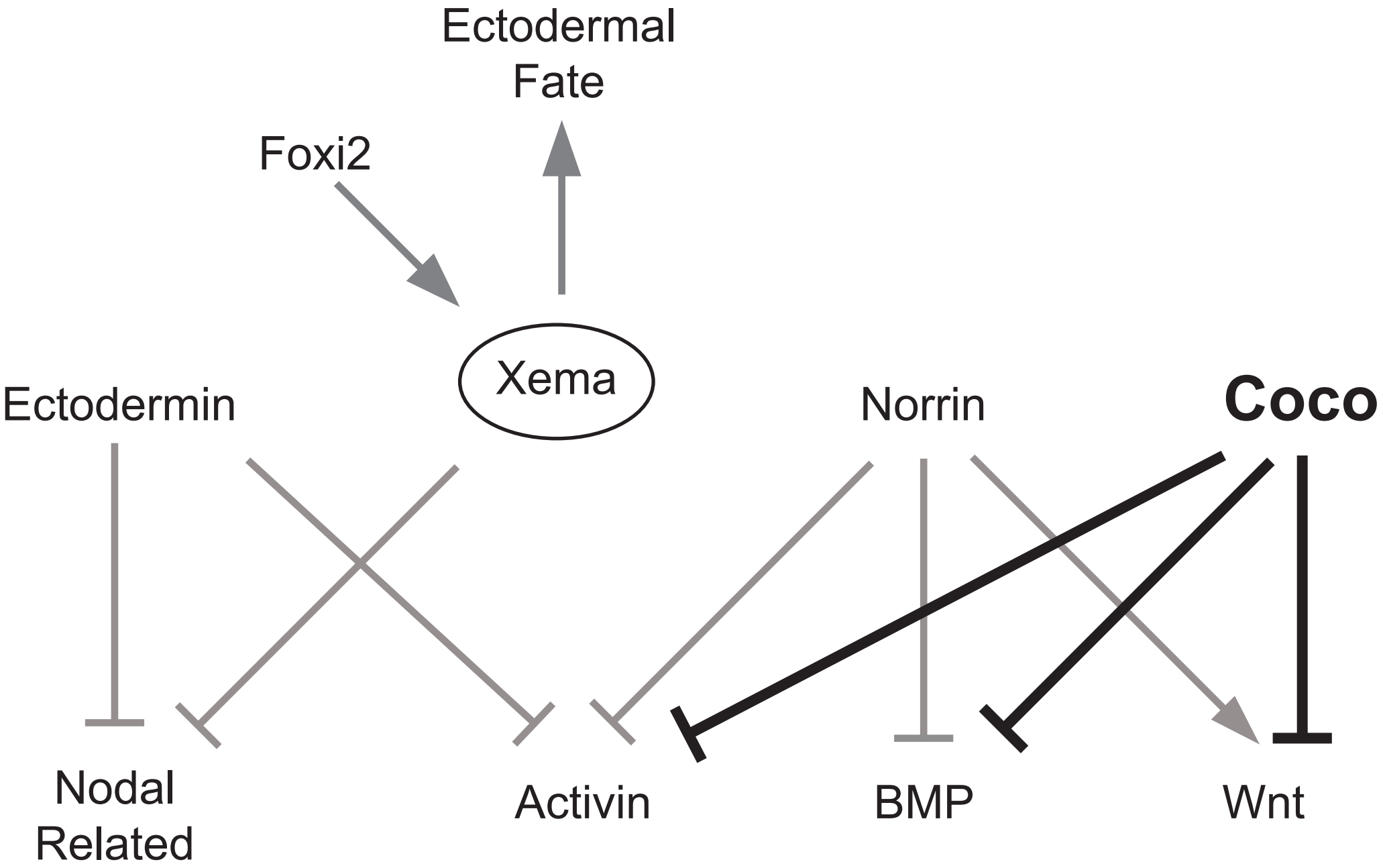
Ectodermal
Fate
Foxi2
Xema
Ectodermin
Norrin
Coco
Nodal
Related
Activin
BMP
Wnt

Figure 6.2 – Summary of phenotypes resulting from CocoMO injection in *Xenopus laevis*. A-B) Model of Coco inhibition of Activin in wild type and Coco MO injected embryos. C-F) Corresponding mesoderm and endoderm phenotypes in stage 9 embryos. A) In a wild type situation Coco (Blue) acts to inhibit the dorso-ventrally biased Activin signals from the marginal zone. B) Following knockdown of Coco there is an asymmetric over activation of the Activin signals dorsally. C) Representation of wild type *Xbra* expression (a marker of mesoderm), D) Representation of *Xbra* expression in embryo injected with CocoMO globally at the one-cell stage. CocoMO induced loss of *Xbra*, most severe dorsally. E) Representation of wild type *Sox17β* expression (a marker of endoderm), F) Representation of *Sox17β* expression in embryo injected with CocoMO globally at the one-cell stage, showing animal shift of endoderm dorsally.

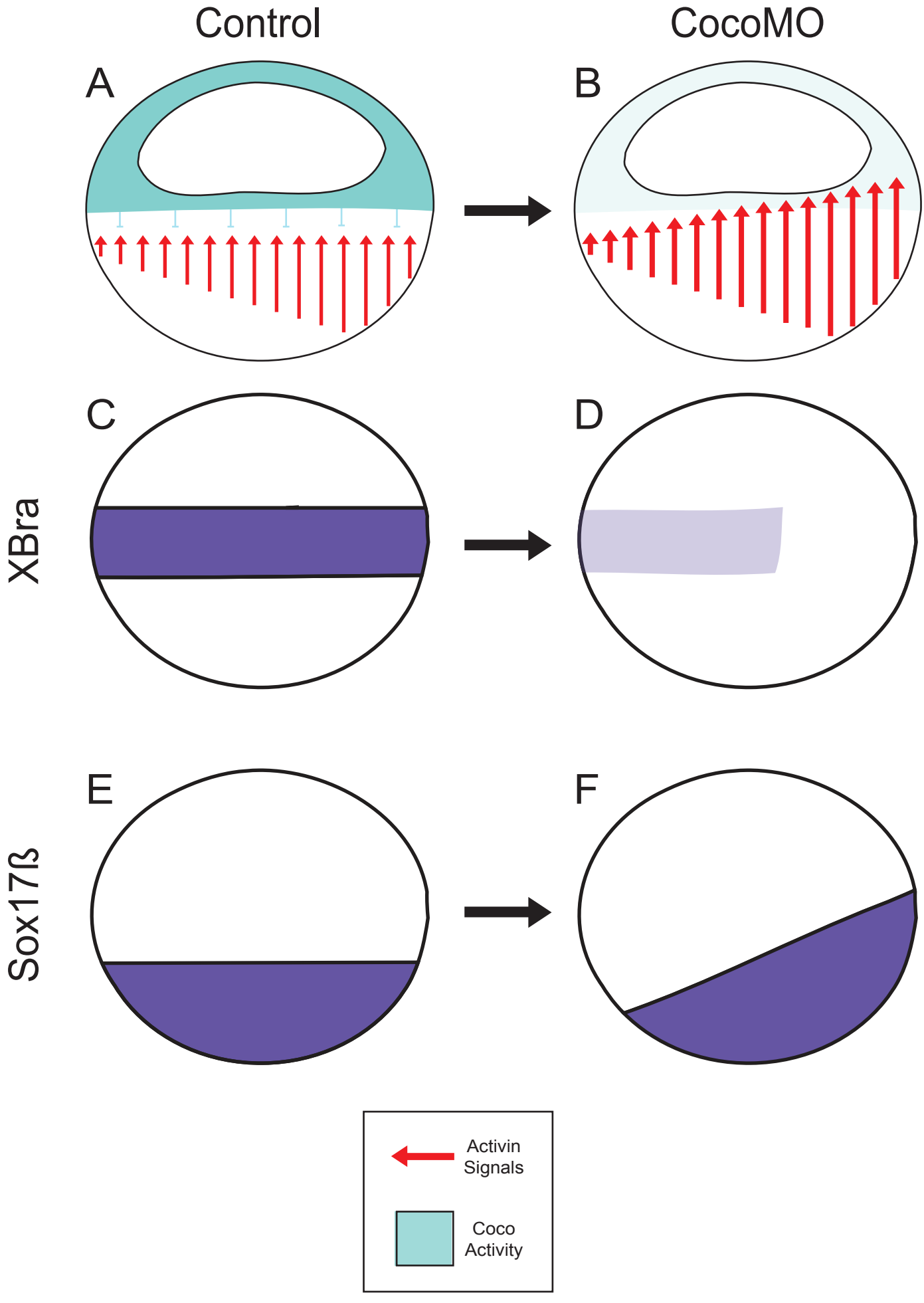
Control
CocoMO
A
B
C
D
E
F
XBra
Sox17ß
Activin Signals
Coco Activity

Not only has this investigation uncovered an early endogenous role of Coco; it has given further insight into the role of Activin during development. Previously published *Xenopus* gain of function studies that highlighted an induction of endoderm by Activin were performed using ectodermal explants (Jones et al., 1993; Ninomiya et al., 1999) whilst other evidence came from *in vitro* cell culture (Kubo, 2004; Yasunaga et al., 2005; Gadue et al., 2006; D'Amour et al., 2006; Teo et al., 2012).

The results from this investigation provide *in vivo* evidence that an over activation of Activin causes the induction of endoderm at the expense of mesoderm. In addition there is experimental evidence for a dorso-ventral bias of Activin during development, with the over activation of Activin causing germ layer defects on the dorsal side of the embryo (Thomsen et al., 1990; Green et al., 1992).

6.3 Coco is involved in competency of the ectoderm

In this investigation it was clear that Coco inhibits Activin during germ layer specification, a results that agrees with work from the original publication. In 2003 it was suggested that Coco might play a role in reducing the competence of the ectoderm to Activin signals (Bell et al., 2003), a result that was confirmed by results here.

6.4 Coco in other species

After gastrulation, the expression levels of Coco drop, and there is a shift in role from germ layer specification to L/R patterning (Vonica and Brivanlou, 2007; Schweickert et al., 2010). The mouse homologue Cerl-2, the zebrafish homologue Charon and the chick homologue Cer1 all act to restrict Nodal signalling to the left side of the embryo during the initiation of the L/R specification, with loss of function causing randomisation of the axis (Hashimoto, 2004; Marques et al., 2004; Tavares et al., 2007).

The role Coco plays in germ layer specification is likely to be *Xenopus* specific, and there could be a few reasons for an additional role in germ layer specification when compared to the mouse. Coco acts as a maternal signal to protect animal and then ectodermal fate during development (Bell et al., 2003), opposing other maternal signals from becoming active in the animal region for five-six hours before the onset of zygotic transcription (Newport and Kirschner, 1982). In contrast, in mouse, zygotic transcription starts from the two-cell stage (Schultz, 1993), meaning maternal signals play less of a role.

In *Xenopus*, Activin and Nodal-related signals are required for the formation of endoderm and the induction of mesoderm (Luxardi et al., 2010; Piepenburg, 2004), and Coco plays a role inhibiting Activin from becoming active in the animal half of the *Xenopus* embryo. However in mouse, Activin mutant mice develop normally (Schrewe et al., 1994), whilst the Nodal knockout causes drastic defects in gastrulation and a lack of axial development (Conlon et al., 1994). It is likely therefore that Coco plays a role in inhibiting Activin signalling in *Xenopus* germ layer specification, which it is not required to do in mouse, because of the divergent function that Activin plays.

6.5 Microarray findings: Gain of function does not offer insight into endogenous role

When performing the microarray, Coco overexpression was compared to a control situation. Overexpression of Coco caused an upregulation to genes involved in anterior and neural patterning, which matches the overexpression phenotypes described in 2003. With Coco playing a role in germ layer specification it might be thought that overexpression would cause a reduction in the expression of genes involved in endoderm formation and mesoderm induction, however this is not the case. Only *GATA5*, a transcription factor involved in endoderm specification (Afouda, 2005) was downregulated, with the large majority of genes downregulated as a consequence of Coco overexpression

are involved in ventral and non-neural development, again presumably a consequence of Coco's overexpression phenotype.

6.6 Coco as a tool for investigating the levels of BMP inhibition

Although investigation into the requirements of BMP inhibition downstream of Coco overexpression offered little insight into the endogenous role of Coco, it did highlight Coco overexpression as a tool for understanding how levels of BMP inhibition affect development. The clear induction of ectopic heads can be both morphologically and molecularly analysed, and here, showed clearly that Coco requires the BMP inhibitors Follistatin, Chordin and Noggin downstream to induce ectopic heads that contain forebrain and midbrain (Figure 6.3). When Coco mRNA was coinjected with combinations of MOs against the BMP inhibitors, it was also clear that redundancy exists for BMP inhibitors, even downstream of Coco overexpression.

6.7 Future experiments

This thesis has outlined the early endogenous role of Coco in *Xenopus laevis*, but there are future experiments that could further confirm the results from this investigation.

Following Coco knockdown, rescue experiments suggested that an over activation of Activin signalling caused the animal shift of the endoderm and loss of dorsal mesoderm. Biochemical analysis would confirm it was specifically an over activation of Activin signalling, and not an indirect effect. The use of α-PSmad2, an antibody that marks the activated form of Activin's downstream initiator, has been used to show the endogenous pattern of signalling in *Xenopus* development (Faure et al., 2000). α-PSmad2 could be utilised in relation to this investigation, highlighting dorsal increases in Activin. In addition, to draw conclusions about germ layers we need to assess CocoMO's affect on ectoderm.

Figure 6.3* – Coco as a tool for investigating the levels of BMP inhibition. A) Representation of ectopic tissue induced by Coco overexpression, which contained forebrain (blue) and midbrain tissue (red). B) Representation of ectopic tissue induced following coinjection of Coco and single/double MOs, which contained forebrain (blue), midbrain tissue (red) and hindbrain tissue (yellow). C) Representation of ectopic tissue induced following coinjection of Coco and triple MOs, which contained midbrain tissue (red), hindbrain tissue (yellow) and spinal cord tissue (green). *This is a reproduction of Figure 3.8 that is being used to discuss future experiments.

A

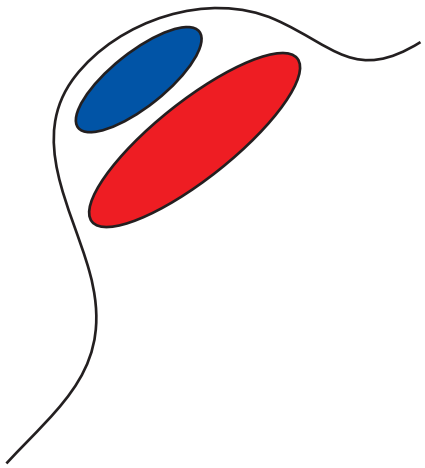

FB

MB

HB

Coco mRNA

B

SC

Coco mRNA
+ Single /
Double MOs

C

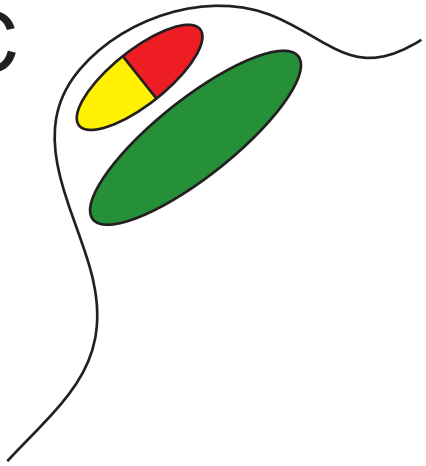

Coco mRNA
+ Triple MOs

Experiments using ISH analysis to assess ectoderm have been unsuccessful; an alternative approach is using RT-PCR. Primers will be designed for endodermal (*Sox17β*), mesodermal (*Xbra*) and ectodermal markers (*Norrin*/*Xema*), and cDNA from embryos injected with CocoMO will be compared to that of control uninjected embryos.

Coco expression overlaps with maternal *Bmp4* (Bell et al., 2003) and presumably acts to inhibit maternal signalling prior to epidermal specification. Animal activation of Wnt signalling is required for neurectoderm specification, and Coco may play a role in delaying this during germ layer specification.
Experiments should be performed that investigate an endogenous requirement for an inhibition of BMP and Wnt signalling by Coco during germ layer specification. CocoMO/BMP4MO and CocoMO/Wnt8MO would highlight possible roles for Coco in preventing ventral patterning signals from acting in the animal portion of the embryo.

The microarray performed in this study, analysed Coco gain of function, whilst work from other labs have used loss of function arrays to assess downstream gene signalling (Ramis et al., 2007). In order to investigate global endogenous requirements for Coco a study that assessed differential expression following CocoMO injection may well offer better insights into downstream requirements during development. The timing of the microarray would be important, with blastula readings highlighting possible germ layer specific downstream targets.

The requirement for BMP inhibition downstream of Coco overexpression was clearly shown in this investigation, however the roles of Wnt and Nodal-related signals were not. To address this, coinjections of Coco mRNA with MOs against other Wnt and Nodal ligands could be performed, which could highlight the possible contributions from the respective pathways.

References

Afouda, B. A. (2005). GATA4, 5 and 6 mediate TGF maintenance of endodermal gene expression in Xenopus embryos. *Development* **132**, 763–774.

Albano, R., Godsave, S. and Huylebroeck, D. (1990). A mesoderm-inducing factor produced by WEHI-3 murine myelomonocytic leukemia cells is activin A. *Development* **110**, 435-443.

Altmann, C. R., Bell, E., Sczyrba, A., Pun, J., Bekiranov, S., Gaasterland, T. and Brivanlou, A. H. (2001). Microarray-Based Analysis of Early Development in Xenopus laevis. *Dev. Biol.* **236**, 64–75.

Altschul, S. F., Gish, W., Miller, W., Myers, E. W. and Lipman, D. J. (1990). Basic local alignment search tool. *J. Mol. Biol.* **215**, 403–410.

Alvarez, I. S., Araujo, M. and Nieto, M. A. (1998). Neural induction in whole chick embryo cultures by FGF. *Dev. Biol.* **199**, 42–54.

Amaya, E., Musci, T. J. and Kirschner, M. W. (1991). Expression of a dominant negative mutant of the FGF receptor disrupts mesoderm formation in Xenopus embryos. *Cell* **66**, 257–270.

Anand, P., Kwak, Y., Simha, R. and Donaldson, R. P. (2009). Hydrogen peroxide induced oxidation of peroxisomal malate synthase and catalase. *Archives of Biochemistry and Biophysics* **491**, 25–31.

Anderson, R. M., Lawrence, A. R., Stottmann, R. W., Bachiller, D. and Klingensmith, J. (2002). Chordin and noggin promote organizing centers of forebrain development in the mouse. *Development* **129**, 4975–4987.

Andoniadou, C. L., Signore, M., Young, R. M., Gaston-Massuet, C., Wilson, S. W., Fuchs, E. and Martinez-Barbera, J. P. (2011). HESX1- and TCF3-mediated repression of Wnt/ -catenin targets is required for normal development of the anterior forebrain. *Development* **138**, 4931–4942.

Armstrong, N. J., Fagotto, F., Prothmann, C. and Rupp, R. A. W. (2012). Maternal Wnt/β-Catenin Signaling Coactivates Transcription through NF-κB Binding Sites during Xenopus Axis Formation. *PLoS ONE* **7**, e36136.

Asashima, M., Nakano, H., Uchiyama, H., Sugino, H., Nakamura, T., Eto, Y., Ejima, D., Nishimatsu, S., Ueno, N. and Kinoshita, K. (1991). Presence of activin (erythroid differentiation factor) in unfertilized eggs and blastulae of Xenopus laevis. *Proc. Natl. Acad. Sci. U.S.A.* **88**, 6511–6514.

Bachiller, D., Klingensmith, J., Kemp, C., Belo, J. A., Anderson, R. M., May, S. R., McMahon, J. A., McMahon, A. P., Harland, R. M., Rossant, J., et al. (2000). The organizer factors Chordin and Noggin are required for mouse forebrain development. *Nature* **403**, 658–661.

Baker, J. C., Beddington, R. S. and Harland, R. M. (1999). Wnt signaling in Xenopus embryos inhibits bmp4 expression and activates neural development. *Genes & Development* **13**, 3149–3159.

Bally-Cuif, L. and Boncinelli, E. (1997). Transcription factors and head formation in vertebrates. *Bioessays* **19**, 127–135.

Barth, L. G. and Barth, L. J. (1969). The sodium dependence of embryonic induction. *Dev. Biol.* **20**, 236–262.

Barth, L. G. and Barth, L. J. (1972). 22 Sodium and 45 calcium uptake during embryonic induction in Rana pipiens. *Dev. Biol.* **28**, 18–34.

Barth, L. G. and Barth, L. J. (1974). Ionic regulation of embryonic induction and cell differentiation in Rana pipiens. *Dev. Biol.* **39**, 1–22.

Bayramov, A. V., Eroshkin, F. M., Martynova, N. Y., Ermakova, G. V., Solovieva, E. A. and Zaraisky, A. G. (2011). Novel functions of Noggin proteins: inhibition of Activin/Nodal and Wnt signaling. *Development* **138**, 5345–5356.

Beanan, M. J. and Sargent, T. D. (2000). Regulation and function of Dlx3 in vertebrate development. *Dev. Dyn.* **218**, 545–553.

Bell, E., Muñoz-Sanjuán, I., Altmann, C. R., Vonica, A. and Brivanlou, A. H. (2003). Cell fate specification and competence by Coco, a maternal BMP, TGFbeta and Wnt inhibitor. *Development* **130**, 1381–1389.

Birsoy, B. (2006). Vg1 is an essential signaling molecule in Xenopus development. *Development* **133**, 15–20.

Blitz, I. L. and Cho, K. W. (1995). Anterior neurectoderm is progressively induced during gastrulation: the role of the Xenopus homeobox gene orthodenticle. *Development* **121**, 993–1004.

Bouwmeester, T., Kim, S., Sasai, Y., Lu, B. and De Robertis, E. M. (1996). Cerberus is a head-inducing secreted factor expressed in the anterior endoderm of Spemann's organizer. *Nature* **382**, 595–601.

Breckenridge, L. J. and Warner, A. E. (1982). Intracellular sodium and the differentiation of amphibian embryonic neurones. *J. Physiol. (Lond.)* **332**, 393–413.

Brivanlou, A. H. and Thomsen G. H. (1995). Ventral mesodermal patterning in Xenopus embryos: Expression patterns and activities of BMP-2 and BMP-4 - Developmental Genetics - **17**, 78-89.

Carletti, E., Luca, A. D., Urbani, A., Sacchetta, P. and Ilio, C. D. (2003). Sigma-class glutathione transferase from Xenopus laevis: molecular cloning, expression, and site-directed mutagenesis. *Archives of Biochemistry and Biophysics* **419**, 214–221.

Carnac, G., Kodjabachian, L., Gurdon, J. B. and Lemaire, P. (1996). The homeobox gene Siamois is a target of the Wnt dorsalisation pathway and triggers organiser activity in the absence of mesoderm. *Development* **122**, 3055–3065.

Casey, E. S., Tada, M., Fairclough, L., Wylie, C. C., Heasman, J. and Smith, J. C. (1999). Bix4 is activated directly by VegT and mediates endoderm formation in Xenopus development. *Development* **126**, 4193–4200.

Cha, S. W., Tadjuidje, E., Tao, Q., Wylie, C. and Heasman, J. (2008). Wnt5a and Wnt11 interact in a maternal Dkk1-regulated fashion to activate both canonical and non-canonical signaling in Xenopus axis formation. *Development* **135**, 3719–3729.

Cha, S.-W., McAdams, M., Kormish, J., Wylie, C. and Kofron, M. (2012). Foxi2 Is an Animally Localized Maternal mRNA in Xenopus, and an Activator of the Zygotic Ectoderm Activator Foxi1e. *PLoS ONE* **7**, e41782.

Cha, S.-W., Tadjuidje, E., White, J., Wells, J., Mayhew, C., Wylie, C. and Heasman, J. (2009). Wnt11/5a Complex Formation Caused by Tyrosine Sulfation Increases Canonical Signaling Activity. *Curr. Biol.* **19**, 1573–1580.

Chambers, D. and Lumsden, A. (2008). Profiling gene transcription in the developing embryo: microarray analysis on gene chips. *Methods Mol. Biol.* **461**, 631–655.

Chang, C. and Harland, R. M. (2007). Neural induction requires continued suppression of both Smad1 and Smad2 signals during gastrulation. *Development* **134**, 3861–3872.

Chang, C., Holtzman, D. A., Chau, S., Chickering, T., Woolf, E. A., Holmgren, L. M., Bodorova, J., Gearing, D. P., Holmes, W. E. and Brivanlou, A. H. (2001). Twisted gastrulation can function as a BMP antagonist. *Nature* **410**, 483–487.

Chou, D. M. and Elledge, S. J. (2006). Tipin and Timeless form a mutually protective complex required for genotoxic stress resistance and checkpoint function. *Proc. Natl. Acad. Sci. U.S.A.* **103**, 18143–18147.

Christian, J., McMAHON, J. and McMahon, A. (1991). Xwnt-8, a Xenopus Wnt-1/int-1-related gene responsive to mesoderm-inducing growth factors, may play a role in ventral mesodermal patterning during embryogenesis. *Development* **111(4)**, 1045-1055.

Conlon, F. L., Lyons, K. M., Takaesu, N., Barth, K. S., Kispert, A., Herrmann, B. and Robertson, E. J. (1994). A primary requirement for nodal in the formation and maintenance of the primitive streak in the mouse. *Development* **120**, 1919–1928.

Cooke, J., Smith, J. C., Smith, E. J. and Yaqoob, M. (1987). The organization of mesodermal pattern in Xenopus laevis: experiments using a Xenopus

mesoderm-inducing factor. *Development* **101**, 893–908.

Cooper, C. A., Walsh, L. A. and Damjanovski, S. (2007). Peroxisome biogenesis occurs in late dorsal-anterior structures in the development ofXenopus laevis. *Dev. Dyn.* **236**, 3554–3561.

Cordenonsi, M., Montagner, M., Adorno, M., Zacchigna, L., Martello, G., Mamidi, A., Soligo, S., Dupont, S. and Piccolo, S. (2007). Integration of TGF- and Ras/MAPK Signaling Through p53 Phosphorylation. *Science* **315**, 840–843.

Cornell, R. A. and Kimelman, D. (1994). Activin-mediated mesoderm induction requires FGF. *Development* **120**, 453–462.

D'Amour, K. A., Bang, A. G., Eliazer, S., Kelly, O. G., Agulnick, A. D., Smart, N. G., Moorman, M. A., Kroon, E., Carpenter, M. K. and Baetge, E. E. (2006). Production of pancreatic hormone–expressing endocrine cells from human embryonic stem cells. *Nat Biotechnol* **24**, 1392–1401.

Dai, D., Tang, J., Rose, R., Hodgson, E., Bienstock, R. J., Mohrenweiser, H. W. and Goldstein, J. A. (2001). Identification of variants of CYP3A4 and characterization of their abilities to metabolize testosterone and chlorpyrifos. *Journal of Pharmacology and Experimental Therapeutics* **299**, 825–831.

Dale, L., Howes, G., Price, B. M. and Smith, J. C. (1992). Bone morphogenetic protein 4: a ventralizing factor in early Xenopus development. *Development* **115**, 573–585.

Davis, S., Miura, S., Hill, C., Mishina, Y. and Klingensmith, J. (2004). BMP receptor IA is required in the mammalian embryo for endodermal morphogenesis and ectodermal patterning. *Dev. Biol.* **270**, 47–63.

de Roos, K., Sonneveld, E., Compaan, B., Berge, ten, D., Durston, A. J. and van der Saag, P. T. (1999). Expression of retinoic acid 4-hydroxylase (CYP26) during mouse and Xenopus laevis embryogenesis. *Mech. Dev.* **82**, 205–211.

Deisseroth, A. and Dounce, A. (1970). Catalase: Physical and chemical properties, mechanism of catalysis, and physiological role. *Physiological reviews* **50**, 319–375.

Dekker, E. J., Vaessen, M. J., van den Berg, C., Timmermans, A., Godsave, S., Holling, T., Nieuwkoop, P., Geurts van Kessel, A. and Durston, A. (1994). Overexpression of a cellular retinoic acid binding protein (xCRABP) causes anteroposterior defects in developing Xenopus embryos. *Development* **120**, 973–985.

Delaune, E. (2005). Neural induction in Xenopus requires early FGF signalling in addition to BMP inhibition. *Development* **132**, 299–310.

Delva, L., Bastie, J. N., Rochette-Egly, C., Kraïba, R., Balitrand, N., Despouy, G., Chambon, P. and Chomienne, C. (1999). Physical and

functional interactions between cellular retinoic acid binding protein II and the retinoic acid-dependent nuclear complex. *Mol. Cell. Biol.* **19**, 7158–7167.

Demartis, A., Maffei, M., Vignali, R., Barsacchi, G. and De Simone, V. (1994). Cloning and developmental expression of LFB3/HNF1 beta transcription factor in Xenopus laevis. *Mech. Dev.* **47**, 19–28.

Dohrmann, C. E., Hemmati-Brivanlou, A., Thomsen, G. H., Fields, A., Woolf, T. M. and Melton, D. A. (1993). Expression of activin mRNA during early development in Xenopus laevis. *Dev. Biol.* **157**, 474–483.

Dupont, S., Zacchigna, L., Cordenonsi, M., Soligo, S., Adorno, M., Rugge, M. and Piccolo, S. (2005). Germ-Layer Specification and Control of Cell Growth by Ectodermin, a Smad4 Ubiquitin Ligase. *Cell* **121**, 87–99.

Ecochard, V., Cayrol, C., Rey, S., Foulquier, F., Caillol, D., Lemaire, P. and Duprat, A. (1998). A novel Xenopus mix-like gene milk involved in the control of the endomesodermal fates. *Development* **125**, 2577–2585.

Errico, A., Costanzo, V. and Hunt, T. (2007). Tipin is required for stalled replication forks to resume DNA replication after removal of aphidicolin in Xenopus egg extracts. *Proc. Natl. Acad. Sci. U.S.A.* **104**, 14929.

Esteban, C. R., Capdevila, J., Economides, A. N., Pascual, J., Ortiz, A. and Izpisua-Belmonte, J. (1999). The novel Cer-like protein Caronte mediates the establishment of embryonic left-right asymmetry. *Nature* **401**, 243–251.

Faas, L. and Isaacs, H. V. (2009). Overlapping functions of Cdx1, Cdx2, and Cdx4 in the development of the amphibian Xenopus tropicalis. *Dev. Dyn.* **238**, 835–852.

Fainsod, A., Deissler, K., Yelin, R., Marom, K., Epstein, M., Pillemer, G., Steinbeisser, H. and Blum, M. (1997). The dorsalizing and neural inducing gene follistatin is an antagonist of BMP-4. *Mech. Dev.* **63**, 39–50.

Faure, S., Lee, M. A., Keller, T., Dijke, ten, P. and Whitman, M. (2000). Endogenous patterns of TGFbeta superfamily signaling during early Xenopus development. *Development* **127**, 2917–2931.

Feledy, J. A., Sargent, T. D., Morasso, M. I. and Jang, S. I. (1999). Transcriptional activation by the homeodomain protein distal-less 3. *Nucleic Acids Research* **27**, 764–770.

Fujimi, T. J., Mikoshiba, K. and Aruga, J. (2006). Xenopus Zic4: Conservation and diversification of expression profiles and protein function among the Xenopus Zicfamily. *Dev. Dyn.* **235**, 3379–3386.

Gadue, P., Huber, T. L., Paddison, P. J. and Keller, G. M. (2006). Wnt and TGF-β signaling are required for the induction of an in vitro model of primitive streak formation using embryonic stem cells. *Proc. Natl. Acad. Sci. U.S.A.* **103**, 16806–16811.

Gestri, G., Carl, M., Appolloni, I., Wilson, S., Barsacchi, G., Andreazzoli, M. (2005). Six3 functions in anterior neural plate specification by promoting cell proliferation and inhibiting Bmp4 expression. *Development* **132**, 2401–2413.

Ghanbari, H., Seo, H. C., Fjose, A. and Brändli, A. W. (2001). Molecular cloning and embryonic expression of Xenopus Six homeobox genes. *Mech. Dev.* **101**, 271–277.

Gillet, G., Michel, D., Crisanti, P., Guerin, M., Herault, Y., Pessac, B., Calothy, G., Brun, G. and Volovitch, M. (1993). Serum factors and v-src control two complementary mitogenic pathways in quail neuroretinal cells in culture. *Oncogene* **8**, 565–574.

Gimlich, R. L. and Gerhart, J. C. (1984). Early cellular interactions promote embryonic axis formation in Xenopus laevis. *Dev. Biol.* **104**, 117–130.

Glinka, A., Wu, W., Delius, H., Monaghan, A. P., Blumenstock, C. and Niehrs, C. (1998). Dickkopf-1 is a member of a new family of secreted proteins and functions in head induction. *Nature* **391**, 357–362.

Glinka, A., Wu, W., Onichtchouk, D., Blumenstock, C. and Niehrs, C. (1997). Head induction by simultaneous repression of Bmp and Wnt signalling in Xenopus. *Nature* **389**, 517–519.

Gotter, A. L. (2003). Tipin, a Novel Timeless-Interacting Protein, is Developmentally Co-expressed with Timeless and Disrupts its Self-association. *J. Mol. Biol.* **331**, 167–176.

Gómez-Skarmeta, J. L., Glavic, A., La Calle-Mustienes, de, E., Modolell, J. and Mayor, R. (1998). Xiro, a Xenopus homolog of the Drosophila Iroquois complex genes, controls development at the neural plate. *EMBO J.* **17**, 181–190.

Gómez-Skarmeta, J., La Calle-Mustienes, de, E. and Modolell, J. (2001). The Wnt-activated Xiro1 gene encodes a repressor that is essential for neural development and downregulates Bmp4. *Development* **128**, 551–560.

Graff, J. M., Thies, R. S., Song, J. J., Celeste, A. J. and Melton, D. A. (1994). Studies with a Xenopus BMP receptor suggest that ventral mesoderm-inducing signals override dorsal signals in vivo. *Cell* **79**, 169–179.

Green, J. B. and Smith, J. C. (1990). Graded changes in dose of a Xenopus activin A homologue elicit stepwise transitions in embryonic cell fate. *Nature* **347**, 391–394.

Green, J. B., New, H. V. and Smith, J. C. (1992). Responses of embryonic Xenopus cells to activin and FGF are separated by multiple dose thresholds and correspond to distinct axes of the mesoderm. *Cell* **71**, 731–739.

Green, J. B., Smith, J. C. and Gerhart, J. C. (1994). Slow emergence of a multithreshold response to activin requires cell-contact-dependent

sharpening but not prepattern. *Development* **120**, 2271–2278.

Grunz, H. and Tacke, L. (1989). Neural differentiation of Xenopus laevis ectoderm takes place after disaggregation and delayed reaggregation without inducer. *Cell differentiation and development* **28**, 211–217.

Hansen, C. S., Marion, C. D., Steele, K., George, S. and Smith, W. C. (1997). Direct neural induction and selective inhibition of mesoderm and epidermis inducers by Xnr3. *Development* **124**, 483–492.

Hashimoto, H. , Rebagliati, M., Ahmad, N., Muraoka, O., Kurokawa, T., Hibl, M., Suzuki, T. (2004). The Cerberus/Dan-family protein Charon is a negative regulator of Nodal signaling during left-right patterning in zebrafish. *Development* **131**, 1741–1753.

Hawley, S. H., Wünnenberg-Stapleton, K., Hashimoto, C., Laurent, M. N., Watabe, T., Blumberg, B. W. and Cho, K. W. (1995). Disruption of BMP signals in embryonic Xenopus ectoderm leads to direct neural induction. *Genes & Development* **9**, 2923–2935.

Heasman, J., Crawford, A., Goldstone, K., Garner-Hamrick, P., Gumbiner, B., McCrea, P., Kintner, C., Noro, C. Y. and Wylie, C. (1994). Overexpression of cadherins and underexpression of beta-catenin inhibit dorsal mesoderm induction in early Xenopus embryos. *Cell* **79**, 791–803.

Heasman, J., Kofron, M. and Wylie, C. (2000). βCatenin Signaling Activity Dissected in the Early Xenopus Embryo: A Novel Antisense Approach. *Dev. Biol.* **222**, 124–134.

Hemmati-Brivanlou, A., Kelly, O. G. and Melton, D. A. (1994). Follistatin, an antagonist of activin, is expressed in the Spemann organizer and displays direct neuralizing activity. *Cell* **77**, 283–295.

Hemmati-Brivanlou, A., Wright, D. A. and Melton, D. A. (1992). Embryonic expression and functional analysis of a Xenopus activin receptor. *Dev. Dyn.* **194**, 1–11.

Henry, G. L. and Melton, D. A. (1998). Mixer, a homeobox gene required for endoderm development. *Science* **281**, 91–96.

Hensey, C. and Gautier, J. (1998). Programmed cell death during Xenopus development: a spatio-temporal analysis. *Dev. Biol.* **203**, 36–48.

Hernandez, R. E., Putzke, A. P., Myers, J. P., Margaretha, L. and Moens, C. B. (2007). Cyp26 enzymes generate the retinoic acid response pattern necessary for hindbrain development. *Development* **134**, 177–187.

Holley, S. A., Jackson, P. D., Sasai, Y., Lu, B., De Robertis, E. M., Hoffmann, F. M. and Ferguson, E. L. (1995). A conserved system for dorsal-ventral patterning in insects and vertebrates involving sog and chordin. *Nature* **376**, 249–253.

Hoppler, S. and Moon, R. T. (1998). BMP-2/-4 and Wnt-8 cooperatively pattern the Xenopus mesoderm. *Mech. Dev.* **71**, 119–129.

Hoppler, S., Brown, J. D. and Moon, R. T. (1996). Expression of a dominant-negative Wnt blocks induction of MyoD in Xenopus embryos. *Genes & Development* **10**, 2805–2817.

Horb, M. E. and Thomsen, G. H. (1997). A vegetally localized T-box transcription factor in Xenopus eggs specifies mesoderm and endoderm and is essential for embryonic mesoderm formation. *Development* **124**, 1689–1698.

Huber, W., Heydebreck, von, A., Sültmann, H., Poustka, A. and Vingron, M. (2002). Variance stabilization applied to microarray data calibration and to the quantification of differential expression. *Bioinformatics* **18 Suppl 1**, S96–104.

Hudson, C., Clements, D., Friday, R. V., Stott, D. and Woodland, H. R. (1997). Xsox17alpha and -beta mediate endoderm formation in Xenopus. *Cell* **91**, 397–405.

Iemura, S., Yamamoto, T. S., Takagi, C., Uchiyama, H., Natsume, T., Shimasaki, S., Sugino, H. and Ueno, N. (1998). Direct binding of follistatin to a complex of bone-morphogenetic protein and its receptor inhibits ventral and epidermal cell fates in early Xenopus embryo. *Proc. Natl. Acad. Sci. U.S.A.* **95**, 9337–9342.

Irizarry, R. A., Hobbs, B., Collin, F., Beazer-Barclay, Y. D., Antonellis, K. J., Scherf, U. and Speed, T. P. (2003). Exploration, normalization, and summaries of high density oligonucleotide array probe level data. *Biostatistics* **4**, 249–264.

Isaacs, H. V., Pownall, M. E. and Slack, J. M. (1998). Regulation of Hox gene expression and posterior development by the Xenopus caudal homologue Xcad3. *EMBO J.* **17**, 3413–3427.

Jansen, E. J. R., Bakel, N. H. M., Coenen, A. J. M., Dooren, S. H., Lith, H. A. M. and Martens, G. J. M. (2009). An isoform of the vacuolar (H+)-ATPase accessory subunit Ac45. *Cell. Mol. Life Sci.* **67**, 629–640.

Janssens, S., Denayer, T., Deroo, T., Van Roy, F. and Vleminckx, K. (2010). Direct control of Hoxd1 and Irx3 expression by Wnt/beta-catenin signaling during anteroposterior patterning of the neural axis in Xenopus. *Int. J. Dev. Biol.* **54**, 1435–1442.

Jin, H. R., Jin, X. and Lee, J. J. (2010a). Zinc-finger protein 91 plays a key role in LIGHT-induced activation of non-canonical NF-ÎºB pathway. *Biochem. Biophys. Res. Commun.* **400**, 581–586.

Jin, X., Jin, H. R., Jung, H. S., Lee, S. J., Lee, J. H. and Lee, J. J. (2010b). An Atypical E3 Ligase Zinc Finger Protein 91 Stabilizes and Activates NF- B-

inducing Kinase via Lys63-linked Ubiquitination. *Journal of Biological Chemistry* **285**, 30539–30547.

Jones, C. M., Kuehn, M. R., Hogan, B. L., Smith, J. C. and Wright, C. V. (1995). Nodal-related signals induce axial mesoderm and dorsalize mesoderm during gastrulation. *Development* **121**, 3651–3662.

Jones, C. M., Lyons, K. M., Lapan, P. M., Wright, C. V. and Hogan, B. L. (1992). DVR-4 (bone morphogenetic protein-4) as a posterior-ventralizing factor in Xenopus mesoderm induction. *Development* **115**, 639–647.

Jones, E. A., Abel, M. H. and Woodland, H. R. (1993). The possible role of mesodermal growth factors in the formation of endoderm in Xenopus laevis. *Dev. Genes Evol.* **202**, 233–239.

Joseph, E. M. and Melton, D. A. (1997). ScienceDirect.com - Developmental Biology - Xnr4: A Xenopus Nodal-Related Gene Expressed in the Spemann Organizer. *Developmental Biology* **184,** 367-372.

Joseph, E. M. and Melton, D. A. (1998). Mutant Vg1 ligands disrupt endoderm and mesoderm formation in Xenopus embryos. *Development* **125**, 2677–2685.

Kao, K. and Lockwood, A. (1996). Negative regulation of dorsal patterning in early embryos by overexpression of XrelA, a Xenopus homologue of NF-[kappa] B. *Mech. Dev.* **58**, 129–139.

Katsu, K., Tokumori, D., Tatsumi, N., Suzuki, A. and Yokouchi, Y. (2012). BMP inhibition by DAN in Hensen's node is a critical step for the establishment of left–right asymmetry in the chick embryo. *Dev. Biol.* **363**, 15–26.

Khadka, D., Luo, T. and Sargent, T. D. (2006). Msx1 and Msx2 have shared essential functions in neural crest but may be dispensable in epidermis and axis formation in Xenopus. *Int. J. Dev. Biol.* **50**.

Khokha, M. K., Yeh, J., Grammer, T. C. and Harland, R. M. (2005). Depletion of three BMP antagonists from Spemann's organizer leads to a catastrophic loss of dorsal structures. *Dev. Cell* **8**, 401–411.

Kiecker, C. and Lumsden, A. (2005). Compartments and their boundaries in vertebrate brain development. *Nat. Rev. Neurosci.* **6**, 553–564.

Kimelman, D. (2006). Mesoderm induction: from caps to chips. *Nat Rev Genet* **7**, 360–372.

Kofron, M., Wylie, C., Heasman, J. (2004). The role of Mixer in patterning the early Xenopus embryo. *Development* **131**, 2431–2441.

Kofron, M., Demel, T., Xanthos, J., Lohr, J., Sun, B., Sive, H., Osada, S., Wright, C., Wylie, C. and Heasman, J. (1999). Mesoderm induction in Xenopus is a zygotic event regulated by maternal VegT via TGFbeta growth

factors. *Development* **126**, 5759–5770.

Kondo, M., Tashiro, K., Fujii, G., Asano, M., Miyoshi, R., Yamada, R., Muramatsu, M. and Shiokawa, K. (1991). Activin receptor mRNA is expressed early in Xenopus embryogenesis and the level of the expression affects the body axis formation. *Biochem. Biophys. Res. Commun.* **181**, 684–690.

Kroll, K. L. and Amaya, E. (1996). Transgenic Xenopus embryos from sperm nuclear transplantations reveal FGF signaling requirements during gastrulation. *Development* **122**, 3173–3183.

Kubo, A. (2004). Development of definitive endoderm from embryonic stem cells in culture. *Development* **131**, 1651–1662.

Kumar, S. and Duester, G. (2011). SnapShot: Retinoic Acid Signaling. *Cell* **147**, 1422–1422.e1.

Kuroda, H., Hayata, T., Eisaki, A. and Asashima, M. (2000). Cloning a novel developmental regulating gene, Xotx5: its potential role in anterior formation in Xenopus laevis. *Dev Growth Differ* **42**, 87–93.

Kuroda, H., Wessely, O. and Robertis, E. M. D. (2004). Neural Induction in Xenopus: Requirement for Ectodermal and Endomesodermal Signals via Chordin, Noggin, β-Catenin, and Cerberus. *PLoS Biol* **2**, e92.

Labhart, P. and Morgan, G. T. (1998). Identification of novel genes encoding transcription elongation factor TFIIS (TCEA) in vertebrates: conservation of three distinct TFIIS isoforms in frog, mouse, and human. *Genomics* **52**, 278–288.

LaBonne, C. and Whitman, M. (1994). Mesoderm induction by activin requires FGF-mediated intracellular signals. *Development* **120**, 463–472.

Lagna, G., Hata, A., Hemmati-Brivanlou, A. and Massagué, J. (1996). Partnership between DPC4 and SMAD proteins in TGF-beta signalling pathways. *Nature* **383**, 832–836.

Lake, B. B., Ford, R. and Kao, K. R. (2001). Xrel3 is required for head development in Xenopus laevis. *Development* **128**, 263–273.

Larabell, C. A., Torres, M., Rowning, B. A., Yost, C., Miller, J. R., Wu, M., Kimelman, D. and Moon, R. T. (1997). Establishment of the dorso-ventral axis in Xenopus embryos is presaged by early asymmetries in beta-catenin that are modulated by the Wnt signaling pathway. *J. Cell Biol.* **136**, 1123–1136.

Lee, R. M., Gillet, G., Burnside, J., Thomas, S. J. and Neiman, P. (1999). Role of Nr13 in regulation of programmed cell death in the bursa of Fabricius. *Genes & Development* **13**, 718–728.

Lee, S.-J., Shinozaki, K., Shannon, J., Kouskoff, V., Kennedy, M., Woo, S.,

Fehling, H. J., Keller, G. (2008). Genetic Analysis of the Role of Proteolysis in the Activation of Latent Myostatin. *PLoS ONE* **3**, e1628.

Lemaire, P., Darras, S., Caillol, D. and Kodjabachian, L. (1998). A role for the vegetally expressed Xenopus gene Mix. 1 in endoderm formation and in the restriction of mesoderm to the marginal zone. *Development* **125**, 2371–2380.

Levin, M., Thorlin, T., Robinson, K. R., Nogi, T. and Mercola, M. (2002). Asymmetries in H+/K+-ATPase and cell membrane potentials comprise a very early step in left-right patterning. *Cell* **111**, 77–89.

Leyns, L., Bouwmeester, T., Kim, S. H., Piccolo, S. and De Robertis, E. M. (1997). Frzb-1 is a secreted antagonist of Wnt signaling expressed in the Spemann organizer. *Cell* **88**, 747–756.

Li, Y. C., Bergwitz, C., Jüppner, H. and Demay, M. B. (1997). Cloning and characterization of the vitamin D receptor from Xenopus laevis. *Endocrinology* **138**, 2347–2353.

Lin, H.-H., Bell, E., Uwanogho, D., Perfect, L. W., Noristani, H., Bates, T. J. D., Snetkov, V., Price, J. and Sun, Y.-M. (2010). Neuronatin Promotes Neural Lineage in ESCs via Ca2+ Signaling. *STEM CELLS* **28**, 1950–1960.

Luxardi, G., Marchal, L., Thomé, V. and Kodjabachian, L. (2010). Distinct Xenopus Nodal ligands sequentially induce mesendoderm and control gastrulation movements in parallel to the Wnt/PCP pathway. *Development* **137**, 417–426.

Maéno, M., Ong, R. C., Suzuki, A., Ueno, N. and Kung, H. F. (1994). A truncated bone morphogenetic protein 4 receptor alters the fate of ventral mesoderm to dorsal mesoderm: roles of animal pole tissue in the development of ventral mesoderm. *Proc. Natl. Acad. Sci. U.S.A.* **91**, 10260–10264.

Mangeney, M., Schmitt, J. R., Leverrier, Y., Thomas, J., Marvel, J., Brun, G. and Gillet, G. (1996). The product of the v-src-inducible gene nr-13 is a potent anti-apoptotic factor. *Oncogene* **13**, 1441–1446.

Marques, S., Borges, A.-C., Silva, A. C., Freitas, S., Cordenonsi, M. and Belo, J. A. (2004). The activity of the Nodal antagonist Cerl-2 in the mouse node is required for correct L/R body axis. *Genes & Development* **18**, 2342–2347.

Marqués, G., Musacchio, M., Shimell, M. J., Wünnenberg-Stapleton, K., Cho, K. W. Y. and O'Connor, M. B. (1997). Production of a DPP activity gradient in the early Drosophila embryo through the opposing actions of the SOG and TLD proteins. *Cell* **91**, 417–426.

Mathews, L., Vale, W. W. (1991). ScienceDirect.com - Cell - Expression cloning of an activin receptor, a predicted transmembrane serine kinase. *Cell*.

65, 973-982

McLIN, V. A., Hu, C. H., Shah, R. and Jamrich, M. (2010). Expression of complement components coincides with early patterning and organogenesis in Xenopus laevis. *Int. J. Dev. Biol.* **52**, 1123.

Messenger, E. A. and Warner, A. E. (1979). The function of the sodium pump during differentiation of amphibian embryonic neurones. *J. Physiol. (Lond.)* **292**, 85–105.

Messenger, N. J. and Warner, A. E. (2000). Primary Neuronal Differentiation in Xenopus Embryos Is Linked to the β3 Subunit of the Sodium Pump. *Dev. Biol.* **220**, 168–182.

Mir, A., Kofron, M., Heasman, J., Mogle, M., Lang, S., Birsoy, B. and Wylie, C. (2008). Long- and short-range signals control the dynamic expression of an animal hemisphere-specific gene in Xenopus. *Dev. Biol.* **315**, 161–172.

Mir, A., Kofron, M., Zorn, A. M., Bajzer, M., Haque, M., Heasman, J. and Wylie, C. C. (2007). FoxI1e activates ectoderm formation and controls cell position in the Xenopus blastula. *Development* **134**, 779–788.

Molenaar, M., van de Wetering, M., Oosterwegel, M., Peterson-Maduro, J., Godsave, S., Korinek, V., Roose, J., Destrée, O. and Clevers, H. (1996). XTcf-3 transcription factor mediates beta-catenin-induced axis formation in Xenopus embryos. *Cell* **86**, 391–399.

Moradi-Améli, M., Lorca, T., Ficheux, D., di Pietro, A. and Gillet, G. (2002). Interaction between the Antiapoptotic Protein Nr-13 and Cytochrome c. Antagonistic Effect of the BH3 Domain of Bax †. *Biochemistry* **41**, 8540–8550.

Morgan, R. and Sargent, M. G. (1997). The role in neural patterning of translation initiation factor eIF4AII; induction of neural fold genes. *Development* **124**, 2751–2760.

Morgan, R., Hooiveld, M. H. and Durston, A. J. (1999). A novel guanine exchange factor increases the competence of early ectoderm to respond to neural induction. *Mech. Dev.* **88**, 67–72.

Morris, S. A., Almeida, A. D., Tanaka, H., Ohta, K. and Ohnuma, S.-I. (2007). Tsukushi Modulates Xnr2, FGF and BMP Signaling: Regulation of Xenopus Germ Layer Formation. *PLoS ONE* **2**, e1004.

Mukhopadhyay, M., Shtrom, S., Rodriguez-Esteban, C., Chen, L., Tsukui, T., Gomer, L., Dorward, D. W., Glinka, A., Grinberg, A. and Huang, S. P. (2001). Dickkopf1 is required for embryonic head induction and limb morphogenesis in the mouse. *Dev. Cell* **1**, 423–434.

Muñoz-Sanjuán, I. and Brivanlou, A. H. (2002). Neural induction, the default model and embryonic stem cells. *Nat. Rev. Neurosci.* **3**, 271–280.

Nakamura, T., Takio, K., Eto, Y., Shibai, H., Titani, K. and Sugino, H. (1990). Activin-binding protein from rat ovary is follistatin. *Science* **247**, 836–838.

Nakata, K., Nagai, T., Aruga, J. and Mikoshiba, K. (1997). Xenopus Zic3, a primary regulator both in neural and neural crest development. *Proc. Natl. Acad. Sci. U.S.A.* **94**, 11980–11985.

Nakata, K., Nagai, T., Aruga, J. and Mikoshiba, K. (1998). Xenopus Zic family and its role in neural and neural crest development. *Mech. Dev.* **75**, 43–51.

Nakayama, T., Snyder, M. A., Grewal, S. S., Tsuneizumi, K., Tabata, T. and Christian, J. L. (1998). Xenopus Smad8 acts downstream of BMP-4 to modulate its activity during vertebrate embryonic patterning. *Development* **125**, 857–867.

Natori, S., Takeuchi, K., Takahashi, K. and Mizuno, D. (1973). DNA Dependent RNA Polymerase from Ehrlich Ascites Tumor Cells. *Journal of Biochemistry* **73**, 879–888.

Newport, J. and Kirschner, M. (1982). A major developmental transition in early Xenopus embryos: I. characterization and timing of cellular changes at the midblastula stage. *Cell* **30**, 675.

Nieto, M. and Bradley, L. (1991). Conserved segmental expression of Krox-20 in the vertebrate hindbrain and its relationship to lineage restriction. *Development*.

Ninomiya, H., Takahashi, S., Tanegashima, K., Yokota, C. and Asashima, M. (1999). Endoderm differentiation and inductive effect of activin-treated ectoderm in Xenopus. *Dev Growth Differ* **41**, 391–400.

Nishimatsu, S. and Thomsen, G. H. (1998). Ventral mesoderm induction and patterning by bone morphogenetic protein heterodimers in Xenopus embryos. *Mech. Dev.* **74**, 75–88.

Nishimatsu, S., Suzuki, A., Shoda, A., Murakami, K. and Ueno, N. (1992). Genes for bone morphogenetic proteins are differentially transcribed in early amphibian embryos. *Biochem. Biophys. Res. Commun.* **186**, 1487–1495.

Onichtchouk, D., Chen, Y. G., Dosch, R., Gawantka, V., Delius, H., Massagué, J. and Niehrs, C. (1999). Silencing of TGF-beta signalling by the pseudoreceptor BAMBI. *Nature* **401**, 480–485.

Otte, A. P. and Moon, R. T. (1992). Protein kinase C isozymes have distinct roles in neural induction and competence in Xenopus. *Cell* **68**, 1021–1029.

Pannese, M., Lupo, G., Kablar, B., Boncinelli, E., Barsacchi, G. and Vignali, R. (1998). The Xenopus Emx genes identify presumptive dorsal telencephalon and are induced by head organizer signals. *Mech. Dev.* **73**, 73–83.

Pannese, M., Polo, C., Andreazzoli, M., Vignali, R., Kablar, B., Barsacchi, G. and Boncinelli, E. (1995). The Xenopus homologue of Otx2 is a maternal homeobox gene that demarcates and specifies anterior body regions. *Development* **121**, 707–720.

Pearce, J. J. H., Penny, G. and Rossant, J. (1999). A mouse cerberus/Dan-related gene family. *Dev. Biol.* **209**, 98–110.

Pegoraro, C., Pollet, N. and Monsoro-Burq, A. H. (2011). Tissue-specific expression of Sarcoplasmic/Endoplasmic Reticulum Calcium ATPases (ATP2A/SERCA) 1, 2, 3 during Xenopus laevis development. *Gene Expression Patterns* **11**, 122–128.

Peng, Y., Yang, P.-H., Guo, Y., Ng, S. S. M., Liu, J., Fung, P. C. W., Tay, D., Ge, J., He, M.-L., Kung, H.-F., et al. (2004). Catalase and peroxiredoxin 5 protect Xenopus embryos against alcohol-induced ocular anomalies. *Invest. Ophthalmol. Vis. Sci.* **45**, 23–29.

Piccolo, S., Agius, E., Leyns, L., Bhattacharyya, S., Grunz, H., Bouwmeester, T. and De Robertis, E. (1999). The head inducer Cerberus is a multifunctional antagonist of Nodal, BMP and Wnt signals. *Nature* **397**, 707.

Piccolo, S., Agius, E., Lu, B., Goodman, S., Dale, L. and De Robertis, E. M. (1997). Cleavage of Chordin by Xolloid metalloprotease suggests a role for proteolytic processing in the regulation of Spemann organizer activity. *Cell* **91**, 407–416.

Piepenburg, O. (2004). Activin redux: specification of mesodermal pattern in Xenopus by graded concentrations of endogenous activin B. *Development* **131**, 4977–4986.

Plant, K. E., Hair, A. and Morgan, G. T. (1996). Genes encoding isoforms of transcription elongation factor TFIIS in Xenopus and the use of multiple unusual RNA processing signals. *Nucleic Acids Research* **24**, 3514–3521.

Pohl, B. S., Rossner, A. and Knochel, W. (2005). The Fox gene family in Xenopus laevis:FoxI2, FoxM1 and FoxP1 in early development. *Int. J. Dev. Biol.* **49**, 53–58.

Ramis, J. M., Collart, C. and Smith, J. C. (2007). Xnrs and Activin Regulate Distinct Genes during Xenopus Development: Activin Regulates Cell Division. *PLoS ONE* **2**, e213.

Razani, B., Engelman, J. A., Wang, X. B., Schubert, W., Zhang, X. L., Marks, C. B., Macaluso, F., Russell, R. G., Li, M., Pestell, R. G., et al. (2001). Caveolin-1 null mice are viable but show evidence of hyperproliferative and vascular abnormalities. *J. Biol. Chem.* **276**, 38121–38138.

Razani, B., Park, D. S., Miyanaga, Y., Ghatpande, A., Cohen, J., Wang, X.

B., Scherer, P. E., Evans, T. and Lisanti, M. P. (2002a). Molecular cloning and developmental expression of the caveolin gene family in the amphibian Xenopus laevis. *Biochemistry* **41**, 7914–7924.

Razani, B., Woodman, S. E. and Lisanti, M. P. (2002b). Caveolae: from cell biology to animal physiology. *Pharmacol. Rev.* **54**, 431–467.

Rebagliati, M. R., Weeks, D. L., Harvey, R. P. and Melton, D. A. (1985). Identification and cloning of localized maternal RNAs from xenopus eggs. *Cell* **42**, 769–777.

Reijntjes, S., Gale, E. and Maden, M. (2004). Generating gradients of retinoic acid in the chick embryo:Cyp26C1 expression and a comparative analysis of the Cyp26 enzymes. *Dev. Dyn.* **230**, 509–517.

Rizzo, A. M., Adorni, L., Montorfano, G., Rossi, F. and Berra, B. (2007). Antioxidant metabolism of Xenopus laevis embryos during the first days of development. *Comparative Biochemistry and Physiology Part B: Biochemistry and Molecular Biology* **146**, 94–100.

Roël, G., Hamilton, F. S., Gent, Y., Bain, A. A., Destrée, O. and Hoppler, S. (2002). Lef-1 and Tcf-3 transcription factors mediate tissue-specific Wnt signaling during Xenopus development. *Curr. Biol.* **12**, 1941–1945.

Sakai, Y. (2001). The retinoic acid-inactivating enzyme CYP26 is essential for establishing an uneven distribution of retinoic acid along the anterio-posterior axis within the mouse embryo. *Genes & Development* **15**, 213–225.

Salic, A. N., Kroll, K. L., Evans, L. M. and Kirschner, M. W. (1997). Sizzled: a secreted Xwnt8 antagonist expressed in the ventral marginal zone of Xenopus embryos. *Development* **124**, 4739–4748.

Sasai, Y., Kageyama, R., Tagawa, Y., Shigemoto, R. and Nakanishi, S. (1992). Two mammalian helix-loop-helix factors structurally related to Drosophila hairy and Enhancer of split. *Genes & Development* **6**, 2620–2634.

Sasai, Y., Lu, B., Piccolo, S. and De Robertis, E. M. (1996). Endoderm induction by the organizer-secreted factors chordin and noggin in Xenopus animal caps. *EMBO J.* **15**, 4547–4555.

Sasai, Y., Lu, B., Steinbeisser, H. and De Robertis, E. M. (1995). Regulation of neural induction by the Chd and Bmp-4 antagonistic patterning signals in Xenopus. *Nature* **377**, 757.

Sasai, Y., Lu, B., Steinbeisser, H., Geissert, D., Gont, L. K. and De Robertis, E. M. (1994). Xenopus chordin: a novel dorsalizing factor activated by organizer-specific homeobox genes. *Cell* **79**, 779–790.

Scherer, P. E., Okamoto, T., Chun, M., Nishimoto, I., Lodish, H. F. and Lisanti, M. P. (1996). Identification, sequence, and expression of caveolin-2 defines a caveolin gene family. *Proc. Natl. Acad. Sci. U.S.A.* **93**, 131–135.

Schier, A. F. (2003). Nodal signaling in vertebrate development. *Annu. Rev. Cell Dev. Biol.* **19**, 589–621.

Schohl, A. and Fagotto, F. (2002). Beta-catenin, MAPK and Smad signaling during early Xenopus development. *Development* **129**, 37–52.

Schrewe, H., Gendron-Maguire, M., Harbison, M. L. and Gridley, T. (1994). Mice homozygous for a null mutation of activin β B are viable and fertile. *Mech. Dev.* **47**, 43–51.

Schultz, R. M. (1993). Regulation of zygotic gene activation in the mouse. *Bioessays* **15**, 531–538.

Schweickert, A., Vick, P., Getwan, M., Weber, T., Schneider, I., Eberhardt, M., Beyer, T., Pachur, A. and Blum, M. (2010). The Nodal Inhibitor Coco Is a Critical Target of Leftward Flow in Xenopus. *Curr. Biol.* **20**, 738–743.

Scott, I. C., Blitz, I. L., Pappano, W. N., Imamura, Y., Clark, T. G., Steiglitz, B. M., Thomas, C. L., Maas, S. A., Takahara, K. and Cho, K. W. Y. (1999). Mammalian BMP-1/Tolloid-related metalloproteinases, including novel family member mammalian Tolloid-like 2, have differential enzymatic activities and distributions of expression relevant to patterning and skeletogenesis. *Dev. Biol.* **213**, 283–300.

Sekimizu, K., Nakanishi, Y., Mizuno, D. and Natori, S. (1979). Purification and preparation of antibody to RNA polymerase II stimulatory factors from Ehrlich ascites tumor cells. *Biochemistry* **18**, 1582–1588.

Servetnick, M. and Grainger, R. M. (1991). Changes in neural and lens competence in Xenopus ectoderm: evidence for an autonomous developmental timer. *Development* **112**, 177–188.

Shafer, B., Onishi, K., Lo, C., Colakoglu, G. and Zou, Y. (2011). Vangl2 Promotes Wnt/Planar Cell Polarity-like Signaling by Antagonizing Dvl1-Mediated Feedback Inhibition in Growth Cone Guidance. *Dev. Cell* **20**, 177–191.

Sharpe, C. and Goldstone, K. (1997). Retinoid receptors promote primary neurogenesis in Xenopus. *Development* **124**, 515–523.

Sharpe, C., Fritz, A., De Robertis, E. and Gurdon, J. (1987). A homeobox-containing marker of posterior neural differentiation shows the importance of predetermination in neural induction. *Cell* **50**, 749.

Shen, M. (2007). Nodal signaling: developmental roles and regulation. *Development* **134**, 1023-1034.

Sheng, N., Xie, Z., Wang, C., Bai, G., Zhang, K., Zhu, Q., Song, J., Guillemot, F., Chen, Y. G. and Lin, A. (2010). Retinoic acid regulates bone morphogenic protein signal duration by promoting the degradation of phosphorylated Smad1. *Proc. Natl. Acad. Sci. U.S.A.* **107**, 18886–18891.

Shi, D. L. and Boucaut, J. C. (2000). Xenopus frizzled 4 is a maternal mRNA and its zygotic expression is localized to the neuroectoderm and trunk lateral plate mesoderm. *Mech. Dev.* **94**, 243–245.

Shi, Y. B. and Hayes, W. P. (1994). Thyroid hormone-dependent regulation of the intestinal fatty acid-binding protein gene during amphibian metamorphosis. *Dev. Biol.* **161**, 48–58.

Shimell, M. J., Ferguson, E. L., Childs, S. R. and O'Connor, M. B. (1991). The Drosophila dorsal-ventral patterning gene tolloid is related to human bone morphogenetic protein 1. *Cell* **67**, 469–481.

Shin, Y., Kitayama, A., Koide, T., Peiffer, D. A., Mochii, M., Liao, A., Ueno, N. and Cho, K. W. Y. (2005). Identification of neural genes usingXenopus DNA microarrays. *Dev. Dyn.* **232**, 432–444.

Shinga, J., Itoh, M., Shiokawa, K., Taira, S. and Taira, M. (2001). Early patterning of the prospective midbrain-hindbrain boundary by the HES-related gene XHR1 in Xenopus embryos. *Mech. Dev.* **109**, 225–239.

Simpson, E. H., Johnson, D. K., Hunsicker, P., Suffolk, R., Jordan, S. A. and Jackson, I. J. (1999). The mouse Cer1 (Cerberus related or homologue) gene is not required for anterior pattern formation. *Dev. Biol.* **213**, 202–206.

Sinner, D. (2006). Global analysis of the transcriptional network controlling Xenopus endoderm formation. *Development* **133**, 1955–1966.

Sirbu, I. O. (2005). Shifting boundaries of retinoic acid activity control hindbrain segmental gene expression. *Development* **132**, 2611–2622.

Slack, C. and Warner, A. E. (1973). Intracellular and intercellular potentials in the early amphibian embryo. *J. Physiol. (Lond.)* **232**, 313–330.

Smith, J. C., Price, B. M., Green, J. B., Weigel, D. and Herrmann, B. G. (1991). Expression of a Xenopus homolog of Brachyury (T) is an immediate-early response to mesoderm induction. *Cell* **67**, 79–87.

Smith, W. C. and Harland, R. M. (1992). Expression cloning of noggin, a new dorsalizing factor localized to the Spemann organizer in Xenopus embryos. *Cell* **70**, 829.

Smith, W. C., Knecht, A. K., Wu, M. and Harland, R. M. (1993). Secreted noggin protein mimics the Spemann organizer in dorsalizing Xenopus mesoderm. *Nature* **361**, 547–549.

Smyth, G. K. (2004). Linear models and empirical bayes methods for assessing differential expression in microarray experiments. *Statistical applications in genetics and molecular biology* **3**, 3.

Sokol, S., Christian, J. L., Moon, R. T. and Melton, D. A. (1991). Injected Wnt RNA induces a complete body axis in Xenopus embryos. *Cell* **67**, 741.

Spemann, H. and Mangold, H. (1924). Über induktion von Embryonalanlagen durch Implantation artfremder Organisatoren. *Dev. Genes Evol.* **100**, 599–638.

Stennard, F., Carnac, G. and Gurdon, J. (1996). The Xenopus T-box gene, Antipodean, encodes a vegetally localised maternal mRNA and can trigger mesoderm formation. *Development* **122**, 4179–4188.

Streit, A. and Stern, C. D. (1995). L5: A carbohydrate epitope involved in neural development. *Biology of the Cell* **84**, 63–67.

Streit, A., Berliner, A. J., Papanayotou, C., Sirulnik, A. and Stern, C. D. (2000). Initiation of neural induction by FGF signalling before gastrulation. *Nature* **406**, 74–78.

Streit, A., Lee, K. J., Woo, I., Roberts, C., Jessell, T. M. and Stern, C. D. (1998). Chordin regulates primitive streak development and the stability of induced neural cells, but is not sufficient for neural induction in the chick embryo. *Development* **125**, 507–519.

Streit, A., Sockanathan, S., Pérez, L., Rex, M., Scotting, P. J., Sharpe, P. T., Lovell-Badge, R. and Stern, C. D. (1997). Preventing the loss of competence for neural induction: HGF/SF, L5 and Sox-2. *Development* **124**, 1191–1202.

Sullivan, S. A., Akers, L. and Moody, S. A. (2001). foxD5a, a Xenopus Winged Helix Gene, Maintains an Immature Neural Ectoderm via Transcriptional Repression That Is Dependent on the C-Terminal Domain. *Dev. Biol.* **232**, 439–457.

Sun, B. I., Bush, S. M., Collins-Racie, L. A., LaVallie, E. R., DiBlasio-Smith, E. A., Wolfman, N. M., McCoy, J. M. and Sive, H. L. (1999). derrière: a TGF-beta family member required for posterior development in Xenopus. *Development* **126**, 1467–1482.

Sundaresan, N. R., Ahmed, K. A., Saxena, V. K., Sastry, K. V. H., Saxena, M., Pramod, A. B., Nath, M., Singh, K. B., Rasool, T. J., DevRoy, A. K., et al. (2005). Differential expression of inducible nitric oxide synthase and cytokine mRNA in chicken lines divergent for cutaneous hypersensitivity response. *Veterinary Immunology and Immunopathology* **108**, 373–385.

Suri, C. (2005). Xema, a foxi-class gene expressed in the gastrula stage Xenopus ectoderm, is required for the suppression of mesendoderm. *Development* **132**, 2733–2742.

Suzuki, A., Thies, R. S., Yamaji, N., Song, J. J., Wozney, J. M., Murakami, K. and Ueno, N. (1994). A truncated bone morphogenetic protein receptor affects dorsal-ventral patterning in the early Xenopus embryo. *Proc. Natl. Acad. Sci. U.S.A.* **91**, 10255–10259.

Suzuki, A., Ueno, N. and Hemmati-Brivanlou, A. (1997). Xenopus msx1

mediates epidermal induction and neural inhibition by BMP4. *Development* **124**, 3037–3044.

Swindell, E. C., Thaller, C., Sockanathan, S., Petkovich, M., Jessell, T. M. and Eichele, G. (1999). Complementary domains of retinoic acid production and degradation in the early chick embryo. *Dev. Biol.* **216**, 282–296.

Tada, M., Casey, E., Fairclough, L. and Smith, J. (1998). Bix1, a direct target of Xenopus T-box genes, causes formation of ventral mesoderm and endoderm. *Development* **125**, 3997–4006.

Tahayato, A., Dollé, P. and Petkovich, M. (2003). Cyp26C1 encodes a novel retinoic acid-metabolizing enzyme expressed in the hindbrain, inner ear, first branchial arch and tooth buds during murine development. *Gene Expression Patterns* **3**, 449–454.

Takabatake, T., Takahashi, T. C., Takabatake, Y., Yamada, K., Ogawa, M. and Takeshima, K. (2000). Distinct expression of two types of Xenopus Patched genes during early embryogenesis and hindlimb development. *Mech. Dev.* **98**, 99–104.

Takahashi, S., Yokota, C., Takano, K., Tanegashima, K., Onuma, Y., Goto, J. and Asashima, M. (2000). Two novel nodal-related genes initiate early inductive events in Xenopus Nieuwkoop center. *Development* **127**, 5319–5329.

Tanibe, M., Michiue, T., Yukita, A., Danno, H., Ikuzawa, M., Ishiura, S. and Asashima, M. (2008). Retinoic acid metabolizing factor xCyp26c is specifically expressed in neuroectoderm and regulates anterior neural patterning in Xenopus laevis. *Int. J. Dev. Biol.* **52**, 893–901.

Tannahill, D. and Wardle, F. C. (1995). Control of axis formation in Xenopus by the NF-kappa B-I kappa B system. *Int. J. Dev. Biol.* **39**, 549–558.

Tao, Q., Yokota, C., Puck, H., Kofron, M., Birsoy, B., Yan, D., Asashima, M., Wylie, C. C., Lin, X. and Heasman, J. (2005). Maternal Wnt11 Activates the Canonical Wnt Signaling Pathway Required for Axis Formation in Xenopus Embryos. *Cell* **120**, 857–871.

Tashiro, K., Yamada, R., Asano, M., Hashimoto, M., Muramatsu, M. and Shiokawa, K. (1991). Expression of mRNA for activin-binding protein (follistatin) during early embryonic development of Xenopus laevis. *Biochem. Biophys. Res. Commun.* **174**, 1022–1027.

Tavares, A. T., Andrade, S., Silva, A. C. and Belo, J. A. (2007). Cerberus is a feedback inhibitor of Nodal asymmetric signaling in the chick embryo. *Development* **134**, 2051–2060.

Teo, A. K. K., Ali, Y., Wong, K. Y., Chipperfield, H., Sadasivam, A., Poobalan, Y., Tan, E. K., Wang, S. T., Abraham, S., Tsuneyoshi, N., et al. (2012). Activin and BMP4 Synergistically Promote Formation of

Definitive Endoderm in Human Embryonic Stem Cells. *STEM CELLS* **30**, 631–642.

Thomsen, G. H. and Melton, D. A. (1993). Processed Vg1 protein is an axial mesoderm inducer in xenopus. *Cell* **74**, 433–441.

Thomsen, G., Woolf, T., Whitman, M., Sokol, S., Vaughan, J., Vale, W. and Melton, D. A. (1990). Activins are expressed early in Xenopus embryogenesis and can induce axial mesoderm and anterior structures. *Cell* **63**, 485–493.

Uehara, M., Yashiro, K., Mamiya, S., Nishino, J., Chambon, P., Dollé, P. and Sakai, Y. (2007). CYP26A1 and CYP26C1 cooperatively regulate anterior–posterior patterning of the developing brain and the production of migratory cranial neural crest cells in the mouse. *Dev. Biol.* **302**, 399–411.

Unoki, M., Okutsu, J. and Nakamura, Y. (2003). Identification of a novel human gene, ZFP91, involved in acute myelogenous leukemia. *Int. J. Oncol.* **22**, 1217–1223.

V Gawantka, Delius, H., Hirschfeld, K., Blumenstock, C., Niehrs, C. (1995). Antagonizing the Spemann organizer: role of the homeobox gene Xvent-1. *EMBO J.* **14**, 6268.

Vale, W., Rivier, J., Vaughan, J., McClintock, R., Corrigan, A., Woo, W., Karr, D. and Spiess, J. (1986). Purification and characterization of an FSH releasing protein from porcine ovarian follicular fluid. *Nature* **321**, 776–779.

van der Weyden, L. and Adams, D. J. (2007). The Ras-association domain family (RASSF) members and their role in human tumourigenesis. *Biochimica et Biophysica Acta (BBA) - Reviews on Cancer* **1776**, 58–85.

Vonica, A. and Brivanlou, A. H. (2007). The left–right axis is regulated by the interplay of Coco, Xnr1 and derrière in Xenopus embryos. *Dev. Biol.* **303**, 281–294.

Wang, S., Krinks, M., Lin, K., Luyten, F. P. and Moos, M. (1997). Frzb, a secreted protein expressed in the Spemann organizer, binds and inhibits Wnt-8. *Cell* **88**, 757–766.

Weber, H., Symes, C. E., Walmsley, M. E., Rodaway, A. and Patient, R. K. (2000). A role for GATA5 in Xenopus endoderm specification. *Development* **127**, 4345–4360.

Weinstein, D. C. and Hemmati-Brivanlou, A. (1997). Neural induction in Xenopus laevis: evidence for the default model. *Current opinion in neurobiology* **7**, 7–12.

Wilkinson, D. G., Bhatt, S. and Herrmann, B. G. (1990). Expression pattern of the mouse T gene and its role in mesoderm formation. Nature **343**, 657-659.

Wills, A. E., Choi, V. M., Bennett, M. J., Khokha, M. K. and Harland, R. M. (2010). BMP antagonists and FGF signaling contribute to different domains of the neural plate in Xenopus. *Dev. Biol.* **337**, 335–350.

Wilson, P. A. and Hemmati-Brivanlou, A. (1995). Induction of epidermis and inhibition of neural fate by Bmp-4. *Nature* **376**, 331–333.

Wright, C. V., Schnegelsberg, P. and De Robertis, E. M. (1989). XlHbox 8: a novel Xenopus homeo protein restricted to a narrow band of endoderm. *Development* **105**, 787–794.

Wright, C., Morita, E. and Wilkin, D. (1990). The Xenopus XIHbox 6 homeo protein, a marker of posterior neural induction, is expressed in proliferating neurons. *Development*.

Wylie, C., Kofron, M., Payne, C., Anderson, R., Hosobuchi, M., Joseph, E. and Heasman, J. (1996). Maternal beta-catenin establishes a "dorsal signal" in early Xenopus embryos. *Development* **122**, 2987–2996.

Xu, S., Cheng, F., Liang, J., Wu, W. and Zhang, J. (2012). Maternal xNorrin, a Canonical Wnt Signaling Agonist and TGF-β Antagonist, Controls Early Neuroectoderm Specification in Xenopus. *PLoS Biol* **10**, e1001286.

Yan, B. and Moody, S. A. (2007). The competence of Xenopus blastomeres to produce neural and retinal progeny is repressed by two endo-mesoderm promoting pathways. *Dev. Biol.* **305**, 103–119.

Yang, J., Tan, C., Darken, R. S., Wilson, P. A. and Klein, P. S. (2002). Beta-catenin/Tcf-regulated transcription prior to the midblastula transition. *Development* **129**, 5743–5752.

Yasunaga, M., Tada, S., Torikai-Nishikawa, S., Nakano, Y., Okada, M., Jakt, L. M., Nishikawa, S., Chiba, T., Era, T. and Nishikawa, S.-I. (2005). Induction and monitoring of definitive and visceral endoderm differentiation of mouse ES cells. *Nat Biotechnol* **23**, 1542–1550.

Yasuo, H. and Lemaire, P. (1999). A two-step model for the fate determination of presumptive endodermal blastomeres in Xenopus embryos. *Curr. Biol.* **9**, 869–879.

Zaraisky, A., Lukyanov, S., Vasiliev, O., Smirnov, Y., Belyavsky, A. and Kazanskaya, O. (1992). A novel homeobox gene expressed in the anterior neural plate of the Xenopus embryo. *Dev. Biol.* **152**, 373–382.

Zhang, C. (2003). The -catenin/VegT-regulated early zygotic gene Xnr5 is a direct target of SOX3 regulation. *Development* **130**, 5609–5624.

Zhang, C., Basta, T. and Klymkowsky, M. W. (2005). SOX7 and SOX18 are essential for cardiogenesis in Xenopus. *Dev. Dyn.* **234**, 878–891.

Zhang, J. and King, M. L. (1996). Xenopus VegT RNA is localized to the vegetal cortex during oogenesis and encodes a novel T-box transcription

factor involved in mesodermal patterning. *Development* **122**, 4119–4129.

Zhang, J., Houston, D. W., King, M. L., Payne, C., Wylie, C. and Heasman, J. (1998). The role of maternal VegT in establishing the primary germ layers in Xenopus embryos. *Cell* **94**, 515–524.

Zimmerman, L. B., De Jesús-Escobar, J. M. and Harland, R. M. (1996). The Spemann organizer signal noggin binds and inactivates bone morphogenetic protein 4. *Cell* **86**, 599–606.